Chemical and optical aspects of appearance changes in oil paintings from the 19th and early 20th century

Yoshiko Shimazu

The work described in this volume was performed as part of the 'De Mayerne' programme funded by the Dutch Organisation for Scientific Research (NWO), in the project MM19 (Materials and Methods in the 19th Century) at Instituut Collectie Nederland (ICN) (now Rijksdienst voor het Cultureel Erfgoed: RCE, Hobbemastraat 22, 1071 ZC Amsterdam) and the FOM Institute for Atomic and Molecular Physics (AMOLF), Molecular Paintings Research Group, Kruislaan 407, 1098 SJ Amsterdam, The Netherlands.

Cover: Verdigris and yellow lake paints from the paint modeling tests
Designed by Michiko Koga and Yoshiko Shimazu

Chemical and optical aspects of appearance changes in oil paintings from the 19th and early 20th century

ACADEMISCH PROEFSCHRIFT

ter verkrijging van de graad van doctor
aan de Universiteit van Amsterdam
op gezag van de Rector Magnificus
prof. dr. D.C. van den Boom
ten overstaan van een door het college voor promoties
ingestelde commissie,
in het openbaar te verdedigen in de Agnietenkapel
op donderdag 5 februari 2015, te 12:00 uur

door

Yoshiko Shimazu

geboren te Yamanashi, Japan

Promotiecommissie

Promotor:	Prof. dr. J.J. Boon
Co-promotor:	Dr. K.J. van den Berg
Overige commissieleden:	Prof. dr. C.G. de Koster
	Prof. dr. P.J. Schoenmakers
	Dr. A.G.A. van Grevenstein-Kruse
	Dr. J.H. Townsend
	Dr. K. Keune

Faculteit der Natuurwetenschappen, Wiskunde en Informatica

MOLART Reports

This volume is the fifteenth in the series of MOLART reports. The MOLART reports summarize research results obtained in the course of the MOLART and De Mayerne research programs supported by the Netherlands Organization for Scientific Research (NWO).

1. Molecular studies of fresh and aged triterpenoid varnishes, Gisela A. van der Doelen, 1999.
   ISBN 90-801704-3-7

2. A mathematical study on craquelure and other mechanical damage in paintings, Petri de Willigen, 1999.
   ISBN 90-407-1946-2

3. Solvent extractable components of oil paint films, Kenneth R. Sutherland, 2001.
   ISBN 90-801704-4-5

4. Molecular changes in egg tempera paint dosimeters as tools to monitor the museum environment, Oscar F. van den Brink, 2001.
   ISBN 90-801704-6-1

5. Discoloration in Renaissance and Baroque oil paintings, Margriet van Eikema Hommes, 2004.
   Archetype Publications, London.

6. Analytical chemical studies on traditional linseed oil paints, Jorrit D.J. van den Berg, 2002.
   ISBN 90-801704-7-X

7. Microspectroscopic analysis of traditional oil paint, Jaap van der Weerd, 2002.
   ISBN 90-801704-8-8

8. Laser desorption mass spectrometric studies of artist's organic pigments, Nicolas Wyplosz, 2003.
   ISBN 90-77209-02-6

9. Molecular studies of Asphalt, Mummy and Kassel earth pigments: their characterization, identification and effect on the drying of traditional oil paint, Georgina M. Languri, 2004.
   ISBN 90-77209-07-7

10. Analysis of diterpenoid resins and polymers in paint media and varnishes; with an attached atlas of mass spectra, Klaas Jan van den Berg, 2003.

11. Binding medium, pigments and metal soaps characterized and localized in paint cross-sections, Katrien Keune, 2005.
ISBN 90-77209-10-7

12. Paints quantified: image analytical studies of preparatory grounds used by Van Gogh, Beatrice Marino, 2006.
ISBN-10 90-77209-19-6, ISBN-13 978-90-77209-19-6

13. Reporting highlights of the De Mayerne Program, research program on molecular studies in conservation and technical studies in art history, Jaap J. Boon and Ester S.B. Ferreira (editors), 2006.
ISBN 90-77875-14-X

14. Color changes and chemical reactivity in seventeenth-century oil paintings, Annelies van Loon, 2008.
ISBN/EAN 978-90-77209-17-2

15. Chemical and optical aspects of appearance changes in oil paintings from the 19th and early 20th century, Yoshiko Shimazu, 2015.

PDF versions of the reports except for 2, 3, 5, and 10 can be downloaded from www.amolf.nl. MOLART 10 is only available as PDF from www.jaap-enterprise.com and the RCE website, via
http://wiki.collectiewijzer.nl/index.php?title=Bestand%3AMolart_Report_10.pdf

Contents

Abbreviations

AMOLF:	FOM Institute for Atomic and Molecular Physics
BSE:	Back scattered electron
DTMS:	Direct temperature resolved mass spectrometry
FOM:	Fundamenteel Onderzoek der Materie
FTIR:	Fourier transfer infrared spectrometry
HPLC:	High performance liquid chromatography
ICN:	Instituute Collectie Nederland (currently RCE)
LM	Light microscopy/microscope
MOLART:	Molecular aspects of ageing in painted art
MS:	Mass spectrometry
NWO:	Nederlandse Organisatie voor Wetenschappelijk Onderzoek
Py-GCMS:	Pyrolysis gas chromatography mass spectrometry
RCE:	Rijsdienst voor het Cultureel Erfgoed / Cultural Heritage Agency of the Netherlands
RI:	Refractive Index/Indices
SEM-EDX:	Scanning electron microscope- energy dispersive X-ray analyser
TIC:	Total ion current
TMAH:	Tetramethylammonium hydroxide
UVf :	Ultra violet fluorescence image with a light microscope
VIS:	Visible light image with a light microscope

INTRODUCTION

Appearance and its change with time in paintings

The appearance of paintings is the most important factor that determines their aesthetic value. Appearance articulates the artists' intentions and is an integral part of the composition. It supports the spatial depiction and illusion, the expression of color and surfaces, in short the meaning expressed by the colored materials i.e. the paints. Painting details such as a delicate line, a fluid or textured brush stroke together with unique color combination make it possible to appreciate the painting's appearance and meaning. Therefore appearance changes in paintings not only lead to change of the aesthetic aspects of the works but also to differences and changes of the original meaning [Van de Wetering 1999]. We know that various causes such as the effects of the natural aging of materials, unpredicted or unappreciated chemical reactions, and also less successful interventions during conservation treatment can lead to significant appearance changes [Feller 1954; Todd *et al*. 1990; Heydenreich 1994].

Oil medium as well as varnish will yellow over time, which in some cases severely affects the color of pictures [Kirsh and Levenson 2000: 214-241; Carlyle 2001: 23-29; Townsend *et al*. 2011]. Discoloration or fading of pigments such as smalt, indigo, and red lakes are now well-known causes of a distinct color change [Plesters 1969; Townsend 1993; White *et al*. 2006; Van Bommel *et al*. 2005; Van Eikema Hommes 2004: 95-170]. Apart from color, changes in the physical conditions of paintings such as loss of paint or deformation of the surface lead to appearance changes as well. This is because appearance is also associated with gloss, transparency, texture etc. Although these do not directly relate to color, they certainly have an influence on color appearance [Hunter 1975: 7-17]. A familiar phenomenon is varnishing, which does not only provide surface gloss but also increases color contrast and saturation [Berns and De la Rie 2002].

From the eighteenth century onwards, painting materials and techniques have drastically changed. Industrially produced modern materials increasingly became available, and are now predominantly used in contemporary paintings. Paint components were produced as industrial products, and some traditional shades were adjusted by mixing several types of pigments [Pey 1987; Carlyle 2001:147-164]. Adulteration, which is an industrial practice adding (supposedly) ineffective materials to products, further changed paint compositions [Carlyle 1993; Townsend *et al*. 1995]. At the same time, artists rapidly explored the new materials, and often mixed several pigments or commercial paints to achieve a desired effect. Some of these homemade paints appeared to be stable but some turned out to be disastrously inferior [Gettens and Sterner 1941]. Moreover, over the nineteenth century, the apprenticeship system of traditional painting

practice was also lost in continental Europe, with the UK breaking with the traditional training first, and a growing emphasis on originality and individuality evolved gradually [Bomford *et al*. 1990; Wallert *et al*. 1995].

During the 19th century, painting techniques and materials were much different from those in earlier times, and also became more diverse [Hermens *et al*. 2002; Townsend 2002; Kirby *et al*. 2007]. The industrially produced materials in addition to the painter's non-traditional working methods have contributed to the complex condition of nineteenth century paintings. It could be because of this background that the causes of paint defects or damages in paintings of the 19th century are often sought in the materials, which artists are assumed to have used, such as bituminous materials [Willoughby 1987; Carlyle and Southall 1993; Pozsgai and Erdohalmi-Torok 1988; Erhardt *et al*. 1990]. Although analytical evidence does not indicate that these blamed particular materials are actually the cause [Wittmann 1988; Carlyle and Townsend 1990; Jones *et al*. 1999], severely cracked surface, illogical colors or extremely dark appearance are rarely accepted as representing the original surface [Kirsh and Levenson 2000: 152-160; Van den Berg *et al*. 2002]. It is obvious that no artist wanted his paintings cracked, completely darkened or dripping as it would be impossible to convey his intentions properly.

Physiological effects

The introduction of modern color theory in the nineteenth century had a strong influence on some artists [Gage 1999; Derefeldt 1999]. Some artists realised the importance of the light source and visual perception [Bomford *et al*. 1990: 76-90; Mayer and Myers 1999; Kirby *et al*. 2003]. Although visual perception is outside the scope of this thesis, some common physiological phenomena are briefly mentioned in order to distinguish physical properties of paint from physiological response in visual perception [Gouras 1991].

Human color vision is provided by cone cells, which are photoreceptors, and the wavelengths they detect are then processed within the brain. Color adaptation is a common physiological response: cone sensitivity adjusts within a given contrast. For instance, the longer you look at a color, the more this color will appear less vivid than at the first glance as the eye adapts to the given color.

Also, the contrast, which is created by two surfaces reflecting at a different light intensity is not always perceived as having the same degree of difference [Li and Gilchrist 1999]. This may lead to a different color appearance of a given color depending on the surrounding colors, known as simultaneous contrast. Darker color or darkness appears more intense when the surrounding is lighter. In practical terms, two uniform colors on the same plate next to each other tend to appear higher in contrast than their actual difference. This function is important when we observe paintings [Werner and Ratliff 1999].

Color constancy is another physiological response influencing appearance, which may conflict with color adaptation [Wright 1968]. Color constancy is the phenomenon whereby we tend to perceive the same (recognizable) object as always having the same color, even though the actual light received by the eye varies considerably if the illuminating light source is changed. In other words color changes due to difference of the light source (illuminant) are compensated for by human vision.

It is not only the color or the surface conditions, but also the viewing conditions and visual perception that play an important role in understanding the current appearance of paintings [Child 2003; Villers and Hedley 1993]. Indeed depending on how we look at paintings they may appear differently. As we have gained much knowledge of both physics and visual perception in the twentieth century, people in the 19th century must have seen paintings without being able to rationalize the observer's physiological responses. Changes in any one's 'seeing' conditions may even emphasize a small change. It is noted that these physiological responses in perception are one of reasons that it is difficult to objectively evaluate a painting's appearance. Therefore it is not realistic to rule out the visual perception system when we discuss appearance. At some point we need to accept that our visual perception might be the cause of "appearance changes" [Willmer 1953; Eastaugh 1990].

Focuses of the thesis

A painting's appearance is very subjective and sometime inconsistent from one viewer to another. It is as yet not possible to objectively and systematically evaluate what we see [Feller 1967; Hunter 1975: 191-284; Bergstrom 2004]. On the other hand, we are now able to find details of paint condition from the chemical point of view that can be associated with the appearance. This thesis therefore aims to fill some gaps between actual observations and theoretical explanations. We may be able to find micro level changes in paint that can suggest a significant discrepancy between the current and original appearance, regardless of viewing conditions on display or in storage.

Previous studies of paintings have already revealed many aspects of painting techniques and materials in non-traditional paintings [Bomford *et al*. 1990; Townsend 2002; Townsend *et al*. 2004; Leone *et al*. 2005]. Extensive studies, especially in the MOLART and de Mayerne projects have demonstrated that saponification of white pigments is a common chemical change in an oil paint system [Boon *et al*. 2002; Van der Weerd *et al*. 2002; 2003; and 2005; Higgitt *et al*. 2003; Noble *et al*. 2005; Keune and Boon 2007]. Besides chemical aspects of the reaction having been studied, the examples and theoretical treatments of optical effects have already been given [Van Loon 2008: 205-239]. This thesis further discusses the optical effects of chemical changes, mainly saponification of white pigments, how this influences visually on paintings, especially in relation to appearance changes in nineteenth century paintings that were intended to be more traditional in appearance.

Short description of the chapters

In order to understand how changes in an oil paint system would affect the appearance, Chapter 1 briefly reviews optical theories relating to paint appearance. It focuses on light behavior, especially how the light interacts with pigment particles. It also describes the importance of white pigments as light reflectors, and optical effects due to changes in their distribution. This chapter aims at assisting understanding of the link between our observation and optical theories, and also is expected to be a theoretical background on why chemical changes in an oil paint system could become perceptible.

Chapters 2 and 3 report two case studies of late 19th century paintings at Tate (London, UK). Both depict dark subjects – interiors lit by artificial light sources – and their depiction of shadows and gradations of lighting are integral to their meaning. Both are difficult to appreciate now, and were assumed to show appearance changes due to metal soap formation, which were indeed demonstrated. However the metal soaps were found not only in the area where the appearance changes were suspected but also in 'visually intact' areas. Reasons for local area changes in the appearance are suggested. Chapter 3 also includes experiments with paint, which show how metal soap containing paint would appear.

Chapter 4 deals with appearance changes due to a decrease of light absorption. Examination of the self-portrait by F.H. Verster in 1921 (De Lakenhal, Leiden,The Netherlands) suggests that there is a color contrast change. Metal soap formation and fading of red lake were confirmed, and these are assumed to have led to decrease in reflectance. Fading of lake pigments is a well-known phenomenon, although usually the impact of color change is the main focus. From an optical point of view, fading also leads to a decrease of light absorption which means a relative increase of transparency. Optical effects on color contrast changes by combination with the fading and metal soap formation are discussed.

In Chapter 5, results of the examination of an extremely dark painting with surface deformation, '*La Descente des Vaches*' (Museum Mesdag, The Hague, The Netherlands) are reported. The painting was once prized because of the richness of its green color, which can no longer be seen today. Once it was thought that the use of bituminous materials caused the alteration. Materials analysis found little evidence for the use of bituminous materials in this painting. Instead, it was observed that extremely thick brown paint in some areas was a package of several light absorbing green and brown paint layers. Eventually the main cause was revealed to be due to the decomposition of emerald green pigment, which had turned brown. Disappearance of the pigment particles caused a loss of selective light absorption and deeper penetration of light accompanied by a relative decrease of light reflection.

This thesis includes the following publications.

Chapter 2: Shimadzu, Y. and Van den Berg, K.J. 2006. On metal soap related colour and transparency changes in a 19th C painting by Millais. In: J.J. Boon and E.S.B. Ferreira, eds. Reporting Highlights of the De Mayerne Program. The Hague: NWO, pp. 43-52.

Chapter 3: Shimadzu, Y., Keune, K., Van den Berg, K.J., Boon J.J., and Townsend, J.H. 2008. The effects of lead and zinc saponification on surface ap-pearance of paint. In: J. Bridgland, ed. ICOM Committee for Conservation 15th Triennial Meeting, Preprints. New Delhi: Allied Publishers Ltd., pp.626-632.

Chapter 5: Keune, K., Boon, J.J., Boitelle, R., and Shimadzu, Y. 2012. Degradation of Emerald green in oil paint and its contribution to the rapid change in colour of the Descente des vaches (1834–1835) painted by Théodore Rousseau. Studies in Conservation, 58 (3), 199-210.

References

Bergstrom, B. 2004. Aspects of colour communication between different paint materials. In: *AIC 2004 Color and Paints, Interim Meeting of the International Color Association, Proceedings*. pp. 295-298.

Berns, R.S. and De la Rie, R. 2002. The relative importance of surface roughness and refractive index in the effects of varnishes on the appearance of paintings. In: R. Vontobel, ed. *ICOM Committee for Conservation 13th Triennial Meeting, Preprints.* London: James & James, pp. 211-216.

Bomford, D., Kirby, J., Leighton, J., Roy, A., White, R., and Williams, L. 1990. *Art in the making: Impressionism*. National Gallery: London.

Boon, J.J., Van der Weerd, J., Keune, K., Noble, P., Wadum, J. 2002. Mechanical and chemical changes in old master paintings: dissolution, metal soap formation and remineralization processes in lead pigmented ground/intermediate paint layers of 17th century paintings. In: R. Vontobel, ed. *ICOM Committee for Conservation 13th Triennial Meeting, Preprints*. London: James & James, pp. 401- 406.

Carlyle, L. 1993. Authenticity and Adulteration: What Materials were 19th Century Artists Really Using?. *The Conservator*, 17, 56-60.

Carlyle, L. 2001. *The Artist's Assistant*. London: Archetype Publications Ltd.

Carlyle, L. and Southall, A. 1993. No Short Mechanic Road to Fame -The Implications of Certain Artists' Materials for the Durability of British Painting: 1770-1840. In: *Robert Vernon's Gift: British Art for the Nation 1847*. London: Tate Gallery, pp. 21-26.

Carlyle, L. and Townsend, J.H. 1990. An investigation of lead sulphide darkening of nineteenth century painting materials. In: V. Todd, S. Hackney, J. Townsend, N. Eastaugh, eds. *Dirt and Pictures Separated*. London: United Kingdom Institute of Conservation, pp. 40-43.

Child, R.E. 2003. Colour Co-ordinated; The Physics of Seeing. *The Picture Restorer*, vol. 12, Autumn, 10-13.

Derefeldt, G. 1999. Colour Appearance Systems. In: *Colour and Culture: Practice and Meaning from Antiquity to Abstraction*. University of California Press, pp. 218-261.

Eastaugh, N. 1990. The visual effects of dirt on paintings. In: V. Todd, S. Hackney, J. Townsend, N. Eastaugh, eds. *Dirt and Pictures Separated*. London: United Kingdom Institute of Conservation, pp. 19-23.

Erhardt, D., Von Endt, D., and Tsang, J. 1990. Condition, Change, and Complexity: The Media of Albert Pinkham Ryder. In: *Postprints of The Paintings Specialty Group Annual*. AIC, pp. 28-35.

Feller, R.L. 1954. Color Change in Oil Paintings. *Carnegie Magazine*, Oct, 1-6.

Feller, R.L. 1967. Problems in Spectrophotometry. In: *Conference on Museum Climatology.* London: IIC, pp. 257-269.

Gage, J. 1999. Colour under Control: The Reign of Newton. In: *Colour and Culture: Practice and Meaning from Antiquity to Abstraction*. University of California Press, pp. 153-176.

Gettens, R.J., Sterner, F.W. 1941. Notes: The compatibility of pigments in artists' oil paints. *Technical Studies in the Field of the Fine Arts*, 10 (1), 18-28.

Gouras, P. (Ed.). 1991. *The Perception of Colour (Vision and Visual Dysfunction. Vol. 6*). UK: Macmillan Press.

Hermens, E., Kwakernaak, A., Van den Berg, K.J., and Geldof, M. 2002. A travel experience –The Corot Painting Box –Matthijs Maris and 19th century tube paints. *Art Matters, Netherlands Technical Studies in Art*, 1, 104-121.

Heydenreich, G. 1994. Removal of a wax-resin lining and colour changes: A case study. *The Conservator*, 18 (1), 23-27.

Higgitt, C., Spring, M., Saunders, D. 2003. Pigment-medium interactions in oil paint films containing red lead or lead-tin yellow. *National Gallery Technical Bulletin*, 24, 75-95.

Hunter, R. S. 1975. *The Measurement of Appearance*. John Wiley & Sons.

Jones, R., Townsend, J.H., and Boon, J.J. 1999. A technical assessment of eight portraits by Reynolds being considered for conservation treatment. In: J. Bridgland, ed. *ICOM Committee for Conservation 12th Triennial Meeting, Preprints*. London: James & James, pp. 375-380.

Keune K. and Boon, J.J. 2007. Analytical Imaging Studies of Cross-Sections of Paintings Affected by Lead Soap Aggregate Formation. *Studies in Conservation*, 52, 161-176.

Kirby, J., Stonor, K., Roy, A., Burnstock, A., Grout, R., and White. R. 2003. Seurat's Painting Practice: Theory, Development and Technology. *National Gallery Technical Bulletin*, 24, 4-37.

Kirby, J., Spring, M., and Higgitt, C. 2007. The Technology of Eighteenth- and Nineteenth-Century Red Lake Pigments. *National Gallery Technical Bulletin*, 28, 69-95.

Kirsh, A., and Levenson, R. S. 2000. *Seeing Through Paintings: Physical Examination in Art Historical Studies Vol. 1*. Yale University Press.

Leone, B., Burnstock, A., Jones, C., Hallebeek, P., Boon, J.J., and Keune, K. 2005. The deterioration of cadmium sulphide yellow artists' pigments. In: I. Verger, ed. *ICOM Committee for Conservation 14th Triennial Meeting, Preprints*. London: James & James, pp. 803-813.

Li, X., and Gilchrist, A. L. 1999. Relative area and relative luminance combine to anchor surface lightness values. *Perception & Psychophysics*, 61 (5), 771-785.

Mayer, L., and Myers, G. 1999. Bierstadt and other 19th-century American Painters in Context. *Journal of American Institute for Conservation*, 38, 55-67.

Noble, P., van Loon, A., and Boon, J.J. 2005. Chemical changes in old master paintings II: darkening due to increased transparency as a result of metal soap formation. In: I. Verger, ed. *ICOM Committee for Conservation 14th Triennial Meeting, Preprint*s. London: James & James, pp. 496-503.

Pey, E.B.F. 1987. The Hafkenscheid Collection: a collection of pigments and painting materials dating from the first half of the 19th century. *Maltechnik Restauro*, 93 (2), 23-33.

Plesters, J. 1969. A Preliminary Note on the Incidence of Discolouration of Smalt in Oil Media. *Studies in Conservation,* 14, 62-74.

Pozsgai, I. and Erdohalmi-Torok, K. 1988. Electron beam microanalytical examination of samples from the painting. In: *2nd international conference on non-destructive testing, microanalytical methods and environment evaluation for study and conservation of works of art, Istituto Centrale Per Il Restauro--Associazione Italiana Prove Non Distruttive*. IV/16.1- 16.5.

Todd, V., Booth, P., Carlyle, L., Davies, M., Sitwell, C.L., Kalinsky, N., Southall, A., and Townsend, J. (eds.). 1990. *Appearance, Opinion, Change: Evaluating the Look of Paintings*. United Kingdom Institute for Conservation.

Townsend, J. 1993. Changes in Appearance with Time. In: *Turner's Painting Techniques*. Tate Gallery, pp. 67-78.

Townsend, J.H., Carlyle, L., Khandekar, N., and Woodcock, S. 1995. Later Nineteenth Century Pigments: Evidence for Additions and Substitutions. *The Conservator*, 19, 65-78.

Townsend, J.H. 2002. The materials used by British oil painters throughout the nineteenth century. *Reviews in Conservation*, 3, 46-55.

Townsend, J.H., Ridge, J., and Hackney, S. 2004. *Pre-Raphaelite Painting Techniques*. Tate Publishing.

Townsend, J.H., Carlyle, L., Cho, J.H., and Campos, M.F. 2011. The yellowing/bleaching behaviour of oil paint: further investigations into significant colour change in response to dark storage followed by light exposure. In: J. Bridgland, ed. *ICOM Committee for Conservation 16th Triennial Meeting, Preprints*. London: James & James.

Van Bommel, M.R., Geldof, M., and Hendriks, E. 2005. An investigation of organic red lake pigments used by Vincent Van Gogh (November 1885 to February 1888). *Art Matters, Netherlands Technical Studies in Art*, 3, 111-137.

Van Eikema Hommes, M. 2004. *Changing Pictures –Discolouration in 15th to 17th Century Oil Paintings*. London: Archetype Publications Ltd.

Van de Wetering, E. 1999. Conservation-restoration Ethics and the problem of modern art. In: IJ. Hummele and D. Sille, eds. *Modern Art: Who Cares?*. Amsterdam: The Foundation for the Conservation of Modern Art and the Netherlands Institute for Cultural Heritage, pp. 247-249.

Van den Berg, K.J., Geldof, M., De Groot, S., and Van Keulen, H. 2002. Darkening and surface degradation in 19th- and early 20th-century paintings: an analytical study. In: R. Vontobel, ed. *ICOM Committee for Conservation 13th Triennial Meeting, Preprints*. London: James & James, pp. 464-472.

Van der Weerd, J., Boon, J.J., Geldof, M., Heeren, R.M.A., and Noble, P. 2002. Chemical Changes in Old Master Paintings—Dissolution, Metal Soap Formation and Remineralisation Processes in lead Pigmented Paint Layers of 17th Century Paintings. *Zeitschrift fur Kunsttechnologie und Konservierung*, 16, 36-51.

Van der Weerd, J., Geldof, M., Van der Loeff, L.S., Heeren, R.M.A., and Boon, J.J. 2003. Zinc Soap Aggregate Formation in 'Falling Leaves (Les Alyscamps)' by Vincent van Gogh. *Zeitschrift fur Kunsttechnologie und Konservierung*, 17(2), 407-416.

Van der Weerd, J., Van Loon, A., and Boon, J.J. 2005. FTIR Studies of the Effects of Pigments on the Aging of Oil. *Studies in Conservation*, 50, 3-22.

Van Loon, A. 2008. *Color changes and chemical reactivity in seventeenth-century oil paintings*. PhD dissertation, University of Amsterdam.

Villers, C. and Hedley, G. 1993. Evaluating colour change: intention, interpretation and lighting. In: *Measured Opinions: collected papers on the conservation of paintings*. London: IIC, pp. 145-148.

Wallert, A., Hermens, E., and Peek, M. eds. 1995. *Historical Painting Techniques, Materials, and Studio Practice*. Getty Trust Publications.

Werner, J.S. and Ratliff, F. 1999. Some origins of the lightness and darkness of colors in the visual arts and in the brain. *Technè*, 9-10, 61-72.

White, R., Phillips, M.R., Thomas, P., and Wuhrer, R. 2006. In-situ investigation of discolouration processes between historic oil paint pigments. *Microchimica acta*, 155 (1-2), 319-322.

Willmer, E.N. 1953. The Physiology of the Perception of Surface Colours. *Journal of the Perception of Surface Colours*, 36, 491-499.

Willoughby, C. 1987. Search for Permanence—Materials and Methods of G.F. Watts, In: Heinz Althöfer (Hrsg.), *Das 19, Janhrhundert und die Restaurierung; Beiträge zur Malerei, Maltechnik und Konservierung*. pp. 203-216.

Wittmann, Z., Bélafi-Réti, K., Décsy, Z., Erdöhalmi-Török, K., Kiss-Bendefy, M., Vassányi, I., and Velledits, L. 1988. Examination of painting materials used by Mihály Munkácsy for his painting Studio. In: *Archaeometrical research in Hungary*, pp. 201-215.

Wright, W.D. 1968. Adaptation and contrast. In: *The Measurement of Colour,* 3rd ed. London: Adam Hilger Ltd., pp.47-51.

Chapter 1

Appearance of oil paint and its changes

1.1 Introduction

The appearance of a painting is determined mainly by the original paints, which consist of colorants, extenders and binding media. The selections of the materials and the techniques with which they are applied create the appearance that expresses the intention of the artist. In the course of time, the materials used in the painting undergo natural aging, as a result of chemical and physical changes that may become visually discernable. Apart from discoloration of pigments, increased transparency and darkening of oil paintings are also classified as appearance changes [Van den Berg *et al*. 2002]. Such changes in paints are commonly accepted as unavoidable, but they are in part caused by the use of inappropriate materials [Kühn 1963; Willoughby 1987; Carlyle 1993; Keune and Boon 2007], and might be accelerated by the environmental or treatment history of the work. These aspects could be studied in future, building on the research presented here.

Recent research of a number of oil paintings has demonstrated that saponification of certain pigments can lead to appearance changes [Noble *et al*. 2005 and 2007; Van Loon 2008]. That reactivity was already noticed in the late nineteenth century in relation to the nature of the drying oil and the use of common pigments [Church 1890: 258-259]. Eibner [1909: 120-121] suggested that lead white paint becomes more translucent due to the saponification of lead white with fatty acids in oil. Later Laurie [1926] proposed that it was caused by an increase of the refractive index of oil binding media, on the basis of refractive index measurements on a very few extremely old samples which might not have contained oil alone [Townsend 1993]. Some paintings, which show the underpaint or *pentimenti* are often assumed to be examples of transparency changes, for instance, the paintings *A Woman Drinking with Two Men* by Pieter de Hooch (National Gallery, London, UK), and *Asparagus* by Adriaen Coorte (Rijksmuseum, The Netherlands) [Laurie 1967: 140-155 and Plate 22, Van Eikema Hommes 2004: 116-119].

In the seventeenth century, it had already been noted that a dark ground color would gradually become more apparent on the paint surface [Bouvier 1828; Massing 1998]. In the nineteenth century, Church [1890: 43] stated that pigments (which must have meant a paint) in time lessen in opacity as a result of ‘the more complete interpenetration of the oil between the particles’. He continued that yellow ochre and raw sienna, for example, darken in color because they become more translucent. Laurie [1926] did not agree with Church’s explanation originally and tried to explain ‘a

lowering tone' (which seems to refer to the same phenomenon Church observed) with his theory of changing refraction index (RI) of an oil binder (see 1.3.1).

The two explanations by Eibner and Laurie are widely accepted as causes of an increase in transparency of oil paints [Hall 1992a; Ruhemann 1995; Nicolaus 1999; Callen and Gallimore 2000], while optical theories underpinning these explanations are not always understood well [Kirsh and Levenson 2000: 160-161; Van Eikema Hommes 2004: 116-119]. Little consideration is given to define what these transparency changes are and in what way or on what time scale these changes could become visible.

Identifying such changes is still technically difficult, because the original appearance can never be exactly known. However, evaluation of the current appearance of such paintings and understanding of chemical and physical conditions of the paint may help to explain the reasons of their current appearance. For this purpose, this chapter will review basic optical theories regarding the appearance of paintings and paint, and discuss relationships between appearance and possible causes for its change over time.

1.2 Appearance-determining factors in oil paint

The appearance of an object is an end result of a series of optical and physiological events. The light illuminates the object and the reflected light stimulates human eyes and brain (Figure 1.1). What we 'see' depends on how the reflected light stimulates our sight system [Gouras 1991]. Light reflection is a key factor that enables us to perceive appearance. In principle, when we say 'light' it means 'white light' which contains all visible wavelengths, like daylight. Depending on the light source, the same object can be perceived to have a different color, although in most cases color differences are corrected by our perception system [Pokorny *et al*. 1991]. An extreme example of this phenomenon is known as metamerism where two colors appear to be the same color under a certain illumination but the same pair of colors would appear different under another light source [Johnston-Feller 2001: 40-49]. Strictly speaking, the appearance of an object seen by two people, even though it is observed under the same conditions, cannot be compared since the mental construction of appearance involves human visual perception and processing. This chapter will only deal with optical properties of paint and will exclude

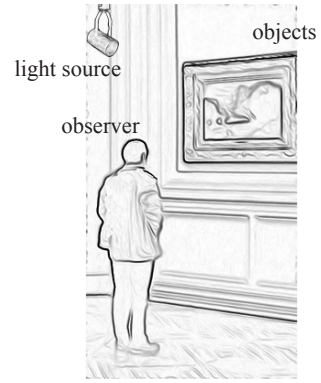

Figure 1.1 Appearance is constructed from three factors: light source, object and observer.

differences due to individuals and also specific effects from light sources. However, we should keep in mind that appearance involves these three factors.

1.2.1 Appearance attributes

Color and surface geometry are two aspects or attributes of appearance [Hunter 1975: 6-14]. Color attributes are divided in three components being 1) hue, 2) chroma (saturation), and 3) value (lightness) according to the Munsell definition [Hunter 1975: 3-12]. The hue is specified by the wavelength distribution of a light source and the characteristic light absorption of an object, and the wavelength of absorbed and reflected light. Saturation is vividness or purity of hue. In a spectrum, when the reflectance curve is broader, the vividness of the color is low, namely it is low in chromaticity [Zollinger 1991: 13-14]. When a colorant is mixed with other colorants, the mixture may be perceived a distinct color from all the colorants, because it now includes the selective light absorptions of the individual colorants [Evans 1948: 286-289]. Mixing colors can make paint dull, and eventually leads to the paint being perceived as from gray/brown to visually black because of homogenous light reflection or absorption throughout the visible wavelengths. The lightness refers to intensity of reflectance, which is described as light and dark. High intensity in light reflection throughout the visible wavelengths is perceived as white, and low intensity appears black. The two colors are achromatic colors without any wavelength selectivity.

These three color attributes relate to each other. For instance, light colors such as white or yellow, have an absorption in the shorter wavelengths, while dark colors such as blue or green absorb most of their light at longer wavelengths (Figure 1.2). When comparing two typical spectra of blue and yellow it is apparent that the yellow reflects more light than the blue in the total amount of reflection. It means that blue is naturally low in lightness, and therefore highly saturated light blue is not possible [Evans 1948:

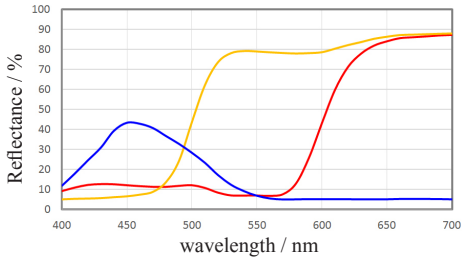

	red	yellow	blue
L*	51	87	42
a*	52	-7	-5
b*	17	85	-43

Figure 1.2 Reflectance spectra of red, yellow, and blue, corresponding L*a*b* data and reconstructed color with Photoshop® software using L*a*b* data. Because yellow reflects most of visible light, the yellow show the highest lightness (L*). A straight line for 100% reflectance would represent pure white.

129-130]. This indicates that lightness changes are accompanied by saturation changes, since the maximum reflection is inextricably linked to the selective absorption.

Geometric attributes such as gloss, texture, and transparency are determined by the distribution of light (see below) [Hunter 1975: 12-17]. They also relate to the color attributes. For instance, a white surface tends to give an opaque or matte impression, while a smooth dark blue surface tends to give a glossy deep impression. In addition, the physical state of the paint such as surface roughness would certainly affect the saturation and lightness.

In an oil paint system, pigments and lakes strongly determine the color of the paint, while a binding medium has a strong influence on the geometric attributes. Thus, a combination of pigments and binding medium will create the optical properties of paint, which can differ from the optical properties of each of these materials separately.

1.2.2 Surface reflection

Light that reaches an object will be divided into two portions at the surface (Figure 1.3). One part reflects and returns directly while the other part enters the object. The entering light will be transmitted through the object and is then absorbed and/or reflected. Since we see paints or a painting from the same side as the light source, integrated light reflection from the object is the most crucial component for us to see when viewing the object, whereas transmitted light, which goes beyond the object, does not contribute to the appearance (Figure 1.4). This view is illustrated in a simple way in Figure 1.3 but in reality there are many interactions between the light and materials that create a rich and varied appearance.

The first reflection occurs at the interface between air and the paint, more precisely the interface between air and oil binding medium (Figure 1.5). When the

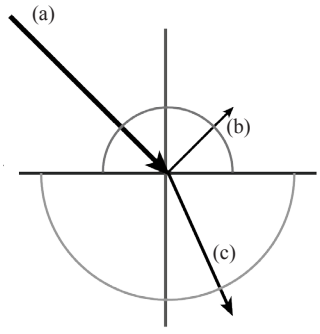

Figure 1.3 Light behavior at the interface of two media
(a) Incident light
(b) Reflection
(c) Refraction: Insident light will be bent when it enters a different matter. Refractive index is a ratio of the velocities of the light in vacuum and a matter (see 1.2.4).

The arrows indicate specular components, while the semicircles indicate diffuse components.

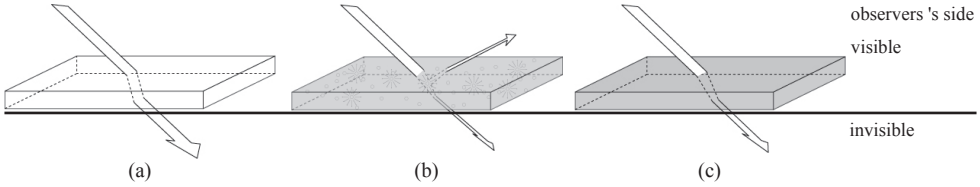

Figure 1.4 Three types of light paths
(a) Transmission: light transmit through the object, (b) Reflection, absorption, and transmission, (c) Absorption, transmission.

surface is smooth, the incident light from one direction will reflect in a single direction, a phenomenon known as specular reflection. In most cases however paint reflects the light diffusely since the paint surface is not completely smooth. What we see mostly at the surface is diffuse reflection from the paint body. When we see specular reflection together with the diffuse reflection from paint, the surface appears glossy [Evans 1948: 47-50; Hunter 1975: 12-17]. Depending on the degree of surface roughness, the surface looks glossy or matte.

The size of pigment particles and the relative amount of binding medium have an influence on surface roughness and therefore on the gloss. When the particle size is relatively large, the surface becomes rough [Elm 1959]. This may be compensated by a large relative amount or "skin" of binding medium covering the particles protruding from the surface. A common practice that makes effective use of this behavior of light is varnishing [De la Rie 1987]. Since a varnish layer more or less moderates the surface roughness, the painted surface becomes smoother than before varnishing, and so colors become more saturated (see 1.2.4.2 Internal reflection). On the other hand, degradation of the binding medium may create a surface roughness known as chalking, where the pigment particles protrude above the retreated binding medium. This effect is most common in painted surfaces exposed to direct sun light.

The more light reflected at the surface, the less light enters the paint. A glossy area where the specular reflection is dominant, or a very rough surface, will prevent further light transmission. As a consequence less color information from the paint becomes available to the eye. It should be noted that reflection in general is not dependent on the wavelength. Therefore the light reflected

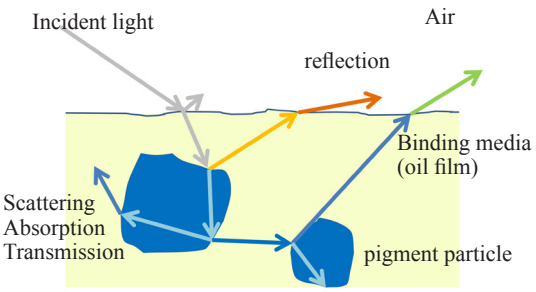

Figure 1.5 Detail light paths in an oil paint
Blue light is reflected after the light is scattered at the pigment particles.

at the surface will show the same spectral distribution as the incident light. The hue of reflected light will be the same as the incident light. When the incident light is daylight, the reflection will be white, while the reflection will be red when the incident light is red.

1.2.3 Absorption and scattering

The light that was not reflected at the surface, will enter the paint. In an imaginary micro-view of the paint inside, the light is absorbed by a slightly yellow oil medium during travelling. The oil will absorb part of the blue light, thus creating a transmitted light that is slightly yellow. When it interacts with pigment particles, the remaining yellow light will be reflected. Because the particles are generally small, the light will be reflected radially at the particle surface. This type of reflection is called scattering [Evans 1948: 65-67]. The remaining light enters the pigment particles absorbing another group of wavelengths (see Figure 1.5). Non-absorbed light is transmitted and enters back into the medium. This light has the color of the pigment. Furthermore, the scattered and transmitted light will encounter other particles and will be scattered and absorbed again. In other words, the light is repeatedly scattered and absorbed in the paint until it leaves the system or is absorbed completely. This process is called multiple scattering and it plays an important role in determining the appearance.

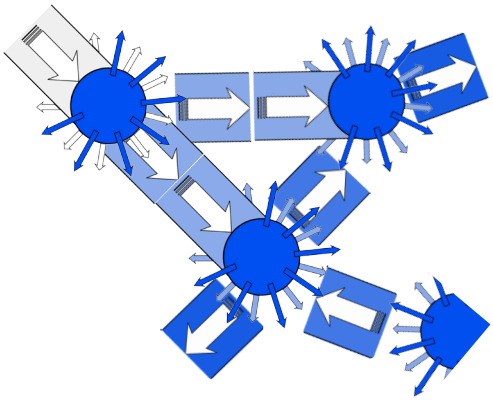

Figure 1.6 Image of multiple scattering and absorption by pigment particles.
The surface of the particle, which receive the incident light at first will reflect almost white light (as only very little amount of light is absorbed by binder), while the rest of the incident light is partially absorbed, and scatters the color of pigment (here it is blue). The blue light will encounter other particles nearby, and this time the particles' surface will reflect blue light. Therefore the blue light is enhanced when the layer is thick and contains many particles in a 'stack', all of them successively scattering the light.

Obviously, the key factor involved in scattering and absorption is pigment (or extender) particles [Mitton 1973]. Light will also scatter at any boundary or interface of two phases in a paint system. The most effective boundaries are borders between pigment particles and binding media. As we have seen and will describe below, the difference in refractive index (RI) plays a crucial role here. White pigments with only scattering ability have a significant effect on the reflectance. Other boundaries, which are microcracks, small voids, and separation between a pigment particle and a binding medium, two adjacent layers, or the texture of pigment particles, act as a white pigment as well [Feller and Kunz 2002]. For instance, the white appearance of a suspension such as milk, is only caused by the scattering at boundaries created by two non-miscible materials (water and fat).

Black pigments scatter light only at the surface and the remainder of any wavelength of light is absorbed, and as a result reflection is largely suppressed. Colored pigment particles scatter both the incident light and transmitted light. For instance, a red pigment particle at first scatters white light, and at the same time scatters red light (Figure 1.6). If the particle has a rough surface, the surface scattering becomes relatively large, thus reducing the scattering from the other particles. Smaller particles look generally whiter. This is explained in the same manner as a relative increase of scattering at the surface due to an increase in surface area and a decrease of absorption because of the smaller volume of particles [Hunter 1975: 30-33]. It should be noted that particles that are smaller than approximately half the wavelength (about 0.2~0.3 μm) no longer scatter light but selective absorption would remain [Stearns 1953].

1.2.4 Refractive index

Refractive index (RI) is an optical material property. The definition is a ratio of the velocities of the light in vacuum and matter. This means that light travels slower in a higher RI medium. This is based on the law of conservation of energy. Light entering an oil film from air will slow down since the oil film (RI ca.1.5) is denser than air (RI 1.0). At this point, some part of the incident light cannot go into the film and is reflected into the air while the light entering into the film is refracted, which means it changes direction. In general, light is reflected more at an interface of two media of which one possesses the larger RI difference.

It should be noted that RI is wavelength dependent, weakly dependent on temperature, and also is influenced by the angle of incident light. For instance, it is possible that two individual materials that have the same RIs at a certain wavelength, have different RI at another wavelengths [Hecht 1987: 61-63]. Therefore the prediction of RI-effects on paint appearance is extremely complicated. Further detailed discussions of this issue can be found in other references on optics [Hecht 1987]. Effects of interfacial RI differences on systems; pigment/oil binding medium, air/varnish or air/oil binding medium, are described briefly in the following section.

1.2.4.1 RI of pigment in oil binding media

A pigment with a relatively high RI will reflect more light at the pigment/binding medium interface following the general light behavior of refraction and reflection, as has been described above. For instance, titanium oxide paint (Rutile RI 2.76) reflects a larger amount of light than lead white (basic lead carbonate RI 1.94-2.09) [Judd and Wyszecki 1963: 385]. Before c.1850, lead white was the only white pigment useable in oil paint, because it had a high light reflectance and appropriate particles size (greater than the wavelength of visible light) [Gettens *et al*. 1993]. The RI of lead white is the highest of the white pigments available at that time, for instance in comparison to chalk (calcium carbonate RI 1.66).

Under most conditions where a single type of white pigment with an RI relatively close to that of the binder is used, the less light is reflected. However, sometimes other factors play a role. For example, industrially-produced zinc oxide, which was introduced as a pigment c.1850 was inferior to lead white in hiding power initially, even though its RI (2.02) is close to the RI of lead white (1.94-2.09). Later, the development in production methods must have improved for controlling particle size of zinc oxide [Eastaugh *et al*. 2014].

Unlike a relatively smooth interface between an oil film and air, pigment/binding media interfaces are rather complicated. Light behavior of paint with smaller particle sizes differs from surfaces [Judd and Wyszecki 1963]. Reflection from particles is not only governed by the RI difference but also is greatly affected by scattering and absorption (see below 1.3).

1.2.4.2 Internal reflection

As pointed out above, paint with a relatively large amount of binding medium or varnished surface would have a saturated appearance [Feller 1957; Thomson 1957; Berns and De la Rie 2002]. Such saturated color can be obtained when pure pigments are placed in water. This phenomenon is observed when light travels from a higher RI medium to a lower RI medium.

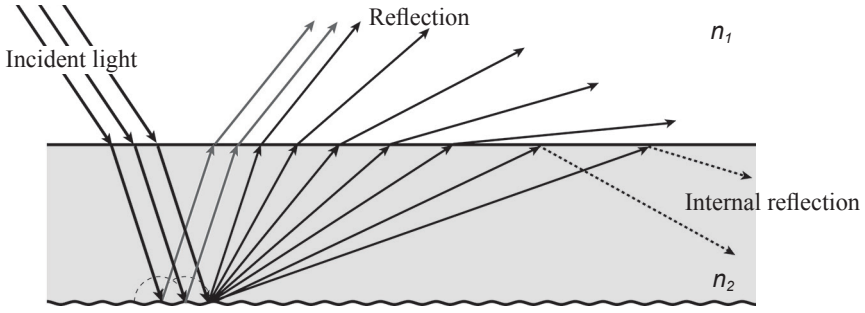

Figure 1.7 Internal reflection. When the light encounters from a higher RI phase (n_2) to another lower RI phase (n_1) ($n_1 < n_2$), a certain amount of light is reflected back into the phase of n_2.

After scattering-absorption interactions between light and paint, the remaining light hits the interface of the oil binder and air. Some portion of the light can pass this interface, which is observed as the reflection, but some portion "reflects" back into the paint again. This is known as total internal reflection (Figure 1.7) [Hecht 1987: 104-108; Johnston-Feller 2001: 86-88]. It means that some portion of the light is trapped in the paint system. As consequence a considerable decrease of light reflection occurs.

1.3 Opacity and transparency

The term 'transparency' in the context of the appearance of paints or a painting may mean different things to different people. This is partially because there is no specific method for its quantification [Hunter 1975: 77]. It is also known that recognition of 'transparency' can be created by certain conditions or color combinations [Metelli 1974; Eastlake 1960: 349-352].

In optics, transparency simply means that light can or can't be transmitted. In this way, opaque and transparent are clearly defined as terms [Johnston-Feller 2001: 114-116]. Opaque means no light transmission; either complete absorption or complete reflection, and transparent means the opposite. Based on this definition, combinations of absorption-scattering inside paint can be classified into three types earlier illustrated in Figure 1.4;

(a) no absorption nor scattering,
(b) absorption and scattering,
(c) absorption but no scattering.

When these conditions meet over the visible light wavelength range, for example, a material with the class (a) characteristic is transparent (and colorless), a class (b) material looks translucent from gray to white (depending on scattering power of the achromatic material), and a class (c) material can only be black. Depending on which wavelength of light is absorbed or reflected, materials will look differently and give various color impressions as discussed in the following section (1.3.1).

The optical definitions of transparency and opacity seem to be unconventional in some descriptions of the appearance of painting. For instance, the colorman Field [1841: 51-52], author of the influential book *Chromatography*, stated that the transparency of paint belongs to shades and blackness. Laurie wrote 'the pigments [he must have meant a paint] are growing deeper in tone and more translucent' [Laurie 1967: 140-144]. Considering these descriptions, 'transparency' means little scattering in a darker color, in other words, less scattering but high in optical saturation. In this way, the phenomenon 'lowering tone' observed by Laurie must have been 'a loss or decrease of scattering'.

1.3.1 Effects of the light reflector and absorber

Opacity of paint is determined by scattering and absorption, and can be evaluated more practically as hiding power. For white paint this merely relies on the scattering ability of the pigment in oil binding media, i.e. the greater the scattering the greater the hiding power. For colored paints, absorption is the main factor determining the opacity.

As discussed before, major factors determining the scattering are RI of pigments, particle size distribution, and pigment volume concentration (PVC). For hiding power, the thickness of the paint layer is an essential factor as well. The hiding power of white paint can be improved with smaller particle sizes or/and mixing two different sizes of particles resulting in better packing [Stieg 1973], as well as by increasing the thickness of the paint layer. In this way, it is possible to compensate somewhat for the disadvantage of a low RI difference between pigment and binding media. For example, a lead white (RI 1.94-2.09) paint with barium sulfate (RI 1.64) can have almost the same hiding power as a paint with only lead white.

An addition of a colored pigment to a white paint increases the hiding power drastically [Mitton 1973]. White pigments in an oil paint scatter not only white light coming directly from the surface but also scatter the transmitted light passing through the colored pigments much more (Figure 1.6). Depending on the mixing ratio of white and colored pigments, the color of a pigment can be enhanced without much white light scattering. In case an appropriate amount of lead white is added, the paint would look reasonably saturated (Figure 1.8) [Schäfer and Wallisch 1981].

As expected, an addition of black pigment, which is a strong light absorber, will severely reduce the light reflectivity. Since black pigments absorb light over all visible wavelengths, the maximum reflectance of any colored pigments will be lowered. Consequently, the paint becomes darker.

As described above, the balance of scattering and absorption largely determines the transparency/opacity of paints. Some of the factors were tested with paint reconstruction shown in the appendix to this chapter. When the scattering dominates, the paint appearance of paint approaches opaque or appears matte. Such paint is insensitive to a change in scattering but is sensitive to absorption. On the other hand, when paint hardly scatters, an addition of a small amount of a light reflector could affect the appearance, especially the transparency.

1.3.2 Effects of the layer structure on paint appearance

In oil paintings, paint layers are often translucent and not thick enough to completely cover and thus hide underlying layers [Tilliard and Bullett 1953]. If there is no light reflection from an underlying material, the transmitted light would be lost (see Figure 1.4). Examples given are when the underlayers are either black (or extremely dark), or transparent (or air). In other words, when the underlying layers are dark colored

Figure 1.8
Translucent Verdigris paints: from left to right, without additives, with 5% lead acetate by weight, with 5% and 10% of basic lead carbonate by weight.

All the paints on the white substrate do not show apparent differences. The paints with basic lead carbonate appear blue in color on the black substrate due to the scattering power of basic lead carbonate.

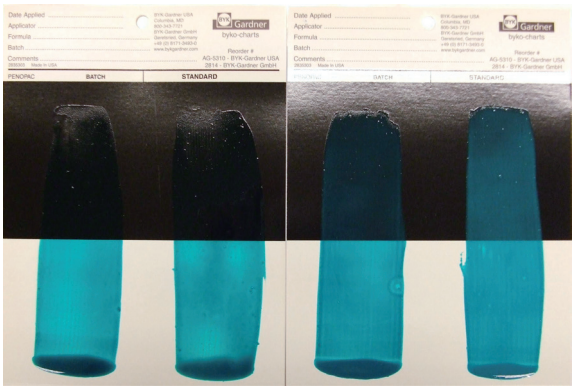

or translucent the reflection of the transmitted light is reduced. When the absorption wavelengths differ between upper and lower layers, the color of the upper paint layer would be severely affected by the color of the lower paint [Evans 1948: 291-294]. In the practice of glazing, it is logical that a translucent glaze paint is recommended to be painted over an underlying layer with a similarly colored paint, so that the brilliant saturation of the upper paint will not be disturbed by the reflection from the underlying paint [Hall 1992b; Van Eikema Hommes 2004: 41].

In summary, what we see is a total reflection from a paint system, which comprises of the following reflections (Figure 1.9):

1) Surface reflection at the interface of air-binding media or air-pigment surface directly
2) Reflection (scattering and transmission) from a paint that is not affected by the color of the underlying layers
3) Surface reflection at the interface of paint and underlayers

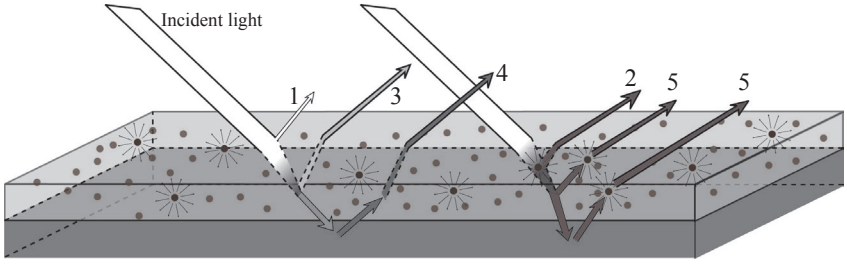

Figure 1.9 Illustrated image of paint reflection
1) Surface reflection at interface of air-binding media or -directly pigment surface
2) Reflection (scattering and transmission) from the paint which is not affected by color of the underlying material
3) Surface reflection at interface of the paint-underlying material
4) Reflection from the underlying material
5) Reflection from the paint which is affected by color of the underlying material.

4) Reflection from underlayers
5) Reflection from the paint, which is affected by the color of the underlying layers

The reduced light reflection is a consequence of the larger light transmission. Furthermore, the greater light transmission allows paint layers to absorb more light, which results in a relative decrease of reflection from the paint [Evans 1948: 291-294]. A change of reflection (including scattering) in a layer, which is situated closer to the surface, will affect the appearance more, yet any changes in these processes have a potential to cause an appearance change.

1.4 Theoretical factors that change appearance

1.4.1 RI increase of oil binding media

The most commonly accepted explanation even today for the typical slight a transparency increase of oil paint is the idea of an RI increase of oil binding media proposed by Laurie [1926]. He realized that the RI of linseed oil films slowly but continuously increased even after curing. This increase of RI of oils would reduce the RI difference between the oil medium and the pigment and thus would lead to lowering of the light scattering, as a consequence an increase in transparency. Experiments aimed at visualizing this phenomenon demonstrated that a higher RI medium with lead white (RI 2.01), or with ultramarine blue (RI 1.51) [Feller and Kunz 2002] indeed shows a lower reflectance. However, these results cannot simply be applied to actual paints since a few essential aspects regarding paint appearance had not been considered. In addition to the refractive indices of binding media, the other factors are the color effect of pigments and the relative amount of coloring pigments. As mentioned earlier these two factors will affect the paint transparency. With respect to the first aspect, both Laurie and Feller used media with a RI higher than 1.60 in their experiments, based on the Laurie's RI measurement of 1.60 in an old oil painting [Laurie 1937]. But is this assumption realistic?

The RI of a fresh drying oil varies and depends on the type of oil producing plant, the weather, the area of growth, the oil preparation method, etc. but is generally near 1.48 at a temperature between 15 and 20°C [Kanthack and Goldsmith 1921; Gardner and Sward 1962: 424]. A China wood oil has an RI that varies between 1.515 and 1.520, which is higher than any other vegetable oil [Toch 1925]. The RI of polymers is basically dependent on chemical constituents and molecular structure [Groh and Zimmermann 1991]. The longer a hydrocarbon chain, the higher the RI. This suggests that the increase of RI in oil binding media was due to polymerization of the polyunsaturated triglycerides [Caldwell and Mattiello 1932; Hutchinson 1973]. In addition, carbon conjugated bonds contribute to a higher RI as well [Xu *et al*. 2004]. Therefore an increase of the RI of oils will eventually hit a ceiling and is then expected to decrease due to deterioration or decomposition of the cross-linked network structure.

Laurie's observation of that dried oil medium could reach RI 1.60 [Laurie 1937], seems to be incorrect; indeed, other RI measurements point out that an RI of drying oil seldom goes beyond 1.55 and such a small increase of RI would not be visible in the appearance of the paint nor a painting [Townsend 1993].

1.4.2 Effects of discoloration of binding media on paint appearance

Artists thought that oil paint with lead white tends to yellow significantly in the course of time [Carlyle 2001: 258-261, 513]. This problem seems to be greater when paintings are kept in the dark [O'Neill *et al*. 1962; Levison 1985], and was understood by the mid 19th century [Carlyle *et al*. 2002]. Fresh drying oils are slightly yellow owing to their chromophores [Cast and Hamilton 1999] but these disappear in the course of time due to cross linking and oxidation. Since lead white can scatter the yellow light strongly due to its high RI, the yellowness is much more enhanced. Yellowing has always been interpreted as a medium-related phenomenon but in older paints the binding medium analytical data only point to diacids and saturated monocarboxylic acids, neither of which have light absorbing optical centers [Boon *et al*. 1997; Boon 2006].

In the case of darkening of lead white paint, the yellowing could also be interpreted as a lead phase organic metallic phenomenon rather than a medium phenomenon (Boon Pers. Comm. 2013). A molecular level understanding of "yellowing oil paint" remains to be established.

In colored pigments, the effect is rather small although blue paint can be affected. The blue pigment absorbs the red and yellow part of the spectrum while surface scattering is yellow because oil absorbs blue light. As a result of subtractive color mixing, green light would remain. On the other hand, when paint contains yellow or red pigment, the paint is affected less. Since the pigments anyway absorb blue light significantly, the yellowness of an oil binder would become scarcely visible.

1.4.3 Metal soap formation in paint appearance

Saponification is a chemical reaction with acid oil constituents and metals from pigments that leaves both components no longer in their original forms. The sharp distinction in the boundaries between binding media and pigment particles will therefore be reduced, or even disappear. From an optical point of view, the saponification of pigments leads to a decrease of scattering factors that causes a reduction in the light reflected. Possible physical changes along with saponification, such as reorientation of particles, disintegration or re-crystallization might also contribute to appearance changes. Furthermore, disintegration of pigment particles would increase the reactivity by providing a larger surface area for reaction with fatty acid groups from the binding

medium.

When paint contains only white pigments, a reduction in reflected light lowers the lightness of paint, which equals a decrease of hiding power. This could be perceived as a transparency change of the paint depending on the relative amount of metal soaps and the thickness of the layer. On the other hand, if there is still intact white pigment remaining that can scatter light, the decrease of scattering may not have a significant effect visually. Moreover, if the achromatic contrast can be adjusted by our visual perception, it would not be visible.

In another case of a colored paint with a relatively small amount of white pigments, both the white pigment and colored pigment are light reflecting, while at the same time the colored pigment is a light absorber of certain wavelengths. If the white pigment is saponified, the paint loses some of its scattering capability. Since the color of pigment is enhanced owing to multiple scattering of the white pigment (see 1.2.3), a decrease in the scattering from the white pigment is expected to lead to a relative increase of light absorption by the colored pigment and of light transmission. Consequently a reduction in light reflected at the surface is expected. This could result in an appearance change of the paint without discoloration of the colored pigment.

Thirdly, when colored pigments are saponified, the paint will lose both lightness and absorption together. The resulting decrease in reflectance may not be very apparent visually, since the impact of color loss is expected to be greater. The loss of colored pigment may however lead to considerable light transmission. The overall effect of saponification should thus not be underestimated.

1.5 Conclusions

Appearance-determining factors and light behavior in an oil paint system on the appearance of paint and paintings are briefly reviewed. The importance of light reflectivity and how pigments play a role in the appearance are also re-evaluated. Optical theories confirm that certain chemical and physical changes could lead to appearance changes in paint. Such changes may become visible as a result of more than one optical factor, while some factors may be cancelled out due to compensation by other factors.

The three explanations for the increase of transparency of oil paint have a foundation in theory. Whether changes are perceptible is another matter. In this respect, Laurie's explanation [Laurie 1926] can be ruled out. Considering that any optical interface can reflect light, the explanation by Church is logical when voids such as small air pockets or spatial inconsistencies exist around pigment particles at the early stage of execution of a painting. Saponification of pigments can lead to a decrease of light reflection or/and a decrease of light absorption. These changes may appear as an increase of paint transparency or a reduction of light reflectivity. As Eibner suggested, paint with only lead white would increase in transparency through the saponification

of the lead white because the hiding power is lowered. The function of white pigments in terms of paint appearance is not only to provide whiteness, but specially to act as light reflectors to for all wavelengths of light. White pigments can thus make the light reflection of paint higher, while their reduced concentration due to saponification will result in a decrease of lightness.

References

Berns, R.S. and De la Rie, R. 2002. The relative importance of surface roughness and refractive index in the effects of varnishes on the appearance of paintings. In: R. Vontobel, ed. *ICOM Committee for Conservation 13th Triennial Meeting, Rio de Janeiro, Preprints*. London: James & James, pp. 211-216.

Boon, J.J., Peulve, S.L., Van den Brink, O.F., Duursma, M.C., and Rainford, D. 1997. Molecular aspects of mobile and stationary phases in ageing tempera and oil paint films. In: E.T. Bakkenist, R. Hoppenbrouwers and H. Dubois, eds. *Early Italian Paintings: Techniques and Analysis*. Maastricht: Limburg Conservation Institute (SRAL), pp. 35-56.

Boon, J.J. 2006. Processes inside paintings that affect the picture: chemical changes at, near and underneath the paint surface. In: J.J. Boon and E.S.B. Ferreira, eds. *Reporting Highlights of the De Mayerne Program*. The Hague: NWO, pp.21-32.

Bouvier, M.B.L. 1828. *Vollständige Anweisung zur Öhlmahlerei für Künstler und Kunstfreunde.* Halle: Hemmerde und Schwetschke, pp. 423-424.

Caldwell, B.P. and Mattiello, J. 1932. Linseed oil: Changes in physical and chemical properties during heat-bodying. *Industrial and Engineering Chemistry*, 24, 158-162.

Callen, A. and Gallimore, K. 2000. Grounds for oil painting (Chapter 4). In: *The Art of Impressionism: Painting Technique & the Making of Modernity*. Yale University Press, pp. 50-61.

Carlyle, L. 1993. Authenticity and Adulteration: What Materials were 19th Century Artists Really Using?. *The Conservator*, 17, 56-60.

Carlyle, L. 2001. *The Artist's Assistant*. Archetype Publications.

Carlyle, L., N. Binnie, E. Kaminska, and A. Ruggles. 2002. The yellowing/bleaching of oil paintings and oil paint samples, including the effect of oil processing, driers and mediums on the colour of lead white paint. In: R. Vontobel, ed. *ICOM-CC 13th Triennial Meeting Preprints*. London: James and James, pp. 328–337.

Cast, J. and Hamilton, R.J. 1999. Introduction. In: R.J., Hamilton, ed. *Spectral Properties of Lipids (The Chemistry and Technology of Oils and Fats)*. Sheffield Academic Press, pp. 1-18.

Church, A.H. 1890. *The Chemistry of Paints and Painting*. London: Seeley and Co. Limited.

De la Rie, R. 1987. The Influence of Varnishes on the Appearance of Paintings. *Studies in Conservation*, 32, 1-13.

Eastaugh, N., Nadolny, J., and Swiech, W. 2014. Interpretaioni of documentary sources for the industrial preparation of 'zinc white' in the 19th century. In: H. Dubois, J.H. Townsend, S. Eyb-Green, J. Nadolny, S. Neven and S. Kroustallis. Eds. *Making and transforming art: changes in artists' materials and practice*. London: Archetype, pp.102-108.

Eastlake, S.C.L. 1960. *Methods and materials of painting of the great schools and masters (Vol. 2)*. Dover Publications.

Eibner, A. 1909. *Malmaterialienkunde –als Grundlage der Maltechnik*. Berlin: Verlag von Julius Springer.

Elm, A.C. 1959. Size and shape properties of representative white hiding and extender pigments. *Official Digest*, June, 720-735.

Evans, R.M. 1948. *An Introduction to Color*. New York: John Wiley and Sons, Inc.

Feller, R. L. 1957. Factors Affecting the Appearance of Picture Varnish. *Science*, 125 (7), 1143-1144.

Feller, R.L. and Kunz, N. 2002. The Effect of Pigment Volume Concentration on the Lightness or Darkness of Porous Paints. In: *Contributions to Conservation Science*. Pittsburgh: Carnegie Mellon University Press, pp. 66-74.

Field, G. 1841. *Chromatography; Or, A Treatise on Colours and Pigments: And of Their Powers in Painting*. London: Tilt and Bogue. [First published 1835 in London.]

Gardner, H.A., Sward, G.G. 1962. *Paint Testing Manual: Physical and Chemical Examination [of] Paints, Varnishes, Lacquers, and Colors*. ASTM International.

Gouras, P. (Ed.). 1991. *The Perception of Colour (Vision and Visual Dysfunction. Vol. 6)*. UK: Macmillan Press.

Groh, W. and Zimmermann, A. 1991. What is the lowest refractive index of an organic polymer?. *Macromolecules*, 24 (25), 6660-6663.

Hall, M.B. 1992a. The influence of time and restoration. In: *Color and Meaning: Practice and Theory in Renaissance Painting*. Cambridge University Press, pp. 1-13.

Hall, M.B. 1992b. Alberti, Flemish technique, and the Introduction of Oil. In: *Color and meaning; Practice and Theory in Renaissance Painting*. Cambridge University Press, pp. 52-56, 69-74.

Hecht, E. 1987. *Optics*. Massachusetts: Addison-Wesley.

Hunter, R. S. 1975. *The Measurement of Appearance*. John Wiley & Sons.

Hutchinson, G.H. 1973. Some aspects of drying oils technology. *Journal of the Oil and Colour Chemists' Association*, 56, 44-53.

Johnston-Feller, R. 2001. *Color Science in the Examination of Museum Objects: Nondestructive procedures, Tools for Conservation*. The J. Paul Getty Trust.

Judd, D.B. and Wyszecki, G. 1963. Physics and Psychophysics of Colorant Layers. In: *Color in Business, Science, and Industry*. New York: John Wiley & Sons, Inc.

Kanthack, R. and Goldsmith, J.N. 1921. *Tables of refractive indices*. Hilger.

Kirsh, A., and Levenson, R. S. 2000. *Seeing through Paintings: Physical examination in art historical studies Vol. 1*. Yale University Press.

Keune K. and Boon, J.J. 2007. Analytical Imaging Studies of Cross-Sections of Paintings Affected by Lead Soap Aggregate Formation. *Studies in Conservation*, 52, 161-176.

Kühn, H. 1963. Aspects of Panel-Painting. *Ciba Review*, 1, 3-36.

Gettens, R.J., Kühn, H., and Chase, W.T. 1993. Lead White. In: A. Roy, ed. *Artists' Pigments: a Handbook of their History and Characteristics*, *vol. 2*. Oxford University Press, pp. 67-81.

Laurie, A.P. 1926. On the Change of Refractive Index of Linseed Oil in the Process of Drying and its Effect on the Deterioration of Oil Paintings. *Proceedings of the Royal Society of London*, 112, 176-181.

Laurie, A.P. 1937. The Refractive Index of a Solid Film of Linseed Oil Rise in Refractive Index with Age. *Proceedings of the Royal Society of London*, 156, 123-133.

Laurie, A.P. 1967. *The Painter's Methods and Materials*. New York: Dover Publications.

Levison, H.W. 1985. Yellowing and Bleaching of Paint Films. *Journal of American Institute for Conservation*, 24, 69-76.

Massing, A. 1998. French painting technique in the Seventeenth and early Eighteenth centuries and De la Fontaine's Academie dela Peinture (Paris 1679). In: E. Hermens, ed. *Looking through Paintings*. Archetype Publications Ltd., pp. 334-353.

Metelli, F. 1974. The Perception of Transparency. *Science American*, 230 (4), 90-98.

Mitton, P.B. 1973. Opacity, Hiding Power, and Tinting Strength. In: T.C. Patton, ed. *Pigment Handbook III: Characterization Physical Relationships*. Wiley, pp. 289-339.

Nicolaus, K. 1999. Loss of opacity. In: C. Westphal, ed. *The Restoration of Paintings*. Könemann, pp. 162-163.

Noble, P., van Loon, A., and Boon, J.J. 2005. Chemical changes in old master paintings II: darkening due to increased transparency as a result of metal soap formation. In: I. Verger, ed. *ICOM Committee for Conservation 14th Triennial Meeting, Preprints*. London: James & James, pp. 496-503.

Noble, P. and Boon, J.J. 2007. Metal soap degradation of oil paintings: aggregates, increased transparency and efflorescence. In: H.M. Parkin, ed. *AIC paintings specialty group postprints of the 19th annual meeting*. AIC, pp. 1-15.

O'Neill, L.A., Rybicka, S.M., and Robey, T. 1962. Yellowing of Drying Oil Films. *Chemistry and Industry*, 1796-1797.

Pokorny, J., Shevell, S.K., Smith, V.C. 1991. Colour appearance and colour constancy. In: P. Gouras, ed. *The Perception of Colour*. UK: Macmillan Press, pp. 43–61.

Ruhemann, H. 1995. Technical Analysis of an Early Painting by Botticelli. *Studies in Conservation*, 2 (1), 17-40.

Schäfer, H. and Wallisch, G. 1981. Obtaining opacity with organic pigments in paint. *Journal of Oil and Colour Chemists' Association*, 64, 405-414.

Stearns, E.I. 1953. Principles underlying the color and appearance of coatings, *Official Digest*, 336, 55-69.

Stieg, F.B. 1973. Pigments/Binder Geometry; Interparticulate relationships. In: T.C. Patton, ed. *Pigment Handbook III: Characterization Physical Relationships*. Wiley, pp. 203-217.

Thomson, G. 1957. Some picture varnishes. *Studies in Conservation*, 3, 64-78.

Tilliard, D.L. and Bullett, T.R. 1953. Optical properties of paints: the basis of instrument measurement. *Journal of the Oil and Color Chemists' Association*, 36, 545-568.

Toch, M. 1925. Analysis of Paint Materials; Refractometry. In: *The Chemistry and Technology of Paints (3rd Ed)*. D.Van Nostrand Company, pp. 389-393.

Townsend, J.H. 1993. The refractive index of 19th-century paint media: A preliminary study. In: J. Bridgland, ed. *ICOM Committee for Conservation 10th Triennial Meeting, Preprints*. London: James & James, pp.586-592.

Van den Berg, K.J., Geldof, M., De Groot, S., and Van Keulen, H. 2002. Darkening and surface degradation in 19th- and early 20th-century paintings: an analytical study. In: R. Vontobel, ed. *ICOM Committee for Conservation 13th Triennial Meeting, Preprints*. London: James & James, pp. 464-472.

Van Eikema Hommes, M. 2004. *Changing Pictures –Discolouration in 15th to 17th Century Oil Paintings*. London: Archetype Publications Ltd.

Van Loon., A. 2008. *Color changes and chemical reactivity in seventeenth-century oil paintings*. PhD dissertation, University of Amsterdam.

Willoughby, C 1987. Search for Permanence–Materials and Methods of G.F. Watts. In: Heinz Althöfer (Hrsg.), *Das 19, Janhrhundert und die Restaurierung; Beiträge zur Malerei, Maltechnik und Konservierung*. , pp. 203-216.

Xu, J., Chen, B., Zhang, Q., Guo, G. 2004. Prediction of refractive indices of linear polymers by a four-descriptor QSPR model. *Polymer*, 45, 8651-8659.

Zollinger, H. 1991. *Color Chemistry: Syntheses, Properties and Applications of Organic Dyes and Pigments*, 2nd ed. Weinheim.

Appendix to Chapter 1

Testing factors affecting the appearance of paint

This appendix shows the results of various experiments to demonstrate how formulation of the paint, and also thickness of a paint layer can change the paint appearance. The optical effects of certain factors on the appearance of paint can be shown by creating suitable experimental conditions and by manipulating the paint formulation. Opacity is presented as a key issue here and this is evaluated by determination of the hiding power of paint layers with a fixed thickness using colorimetric measurements.

The thickness of paint layers, applied with brushes for instance, will vary at each area. Paints would rarely have been homogenous prior to the later or at the earliest mid 19th century when they were produced on an industrial scale. The following experiments are meant to give some idea how a range of formulations affects opacity.

Oil paints were made by mixing pigment(s) and medium by hand using a glass slab and muller and were applied to black and white charts (Byko-charts, coated type, BYK-Gardner GmbH) with a paint applicator (4-Sided Applicator[1], BYK-Gardner GmbH). Color measurements (Minolta CM-2600d, illuminant D65 and a 10° observer, 8mm diameter aperture using CIELAB1976 color space) were carried out on three or more spots on a dried paint on each black and white substrate. The data are shown as reflectance spectra and with a mean value of L*a*b* for each sample, excluding the specular component and UV component of the illuminant. ΔL* was obtained by subtracting the L* value of the paint on the black substrate (L*b) from the L* value of the paint on the white substrate (L*w), which is one of the indications of hiding power of the paint. Δa* and Δb* were calculated in the same manner. Color images were created by inputting the L*a*b* data in 'color picker tool' in Photoshop® to give a visual impression. Therefore color accuracy of the images were not taken into account.

1A.1 Pigment Volume Concentration

Experiment A:

Different volume concentrations of basic lead carbonate paint were made in order to investigate the effect of the volume concentration (PVC) on hiding power of the paints. PVCs were set at 40, 50, and 60 (Table 1A.1). As a pigment, basic lead carbonate (Fluka) was used. The paints were applied with a wet film thickness of 30 μm.

1: Gap clearance are 30, 60, 90, and 120 μm, film width is 60 mm, the material is stainless steel.

Result:

In general a higher concentration of pigment should result in a higher hiding power. As expected, the paint with the lowest PVC, PVC 40, has the lowest hiding power (Figure 1A.1, Table 1A.2). However, the reflectance spectra of the paints of PVCs 50 and 60 were found to be almost the same. This result is explained as follows: above a certain concentration some particles are too close to scatter as an independent particle, so they act as a larger particle. PVC is an important factor to the opacity but the effect may not be significant when the paint contains a large number of particles [Balfour 1994: 76-88].

Table 1A.1 Model paint formulations in Experiment A

sample name	Basic lead carbonate weight/g (volume/cm^3)	Oil weight/g (volume/cm^3)
PVC40	2.70 (0.4)	0.56 (0.6)
PVC50	3.40 (0.5)	0.47 (0.5)
PVC60	4.10 (0.6)	0.37 (0.4)

Table 1A.2 L*a*b* data of the model paints in Experiment A

sample code	On white substrate			On black substrate			Differences		
	L*	a*	b*	L*	a*	b*	ΔL*	Δa*	Δb*
PVC40	92	-1	6	75	-2	1	22	1	5
PVC50	94	-1	5	85	-2	-2	9	1	7
PVC60	94	-1	4	85	-2	-3	9	1	7

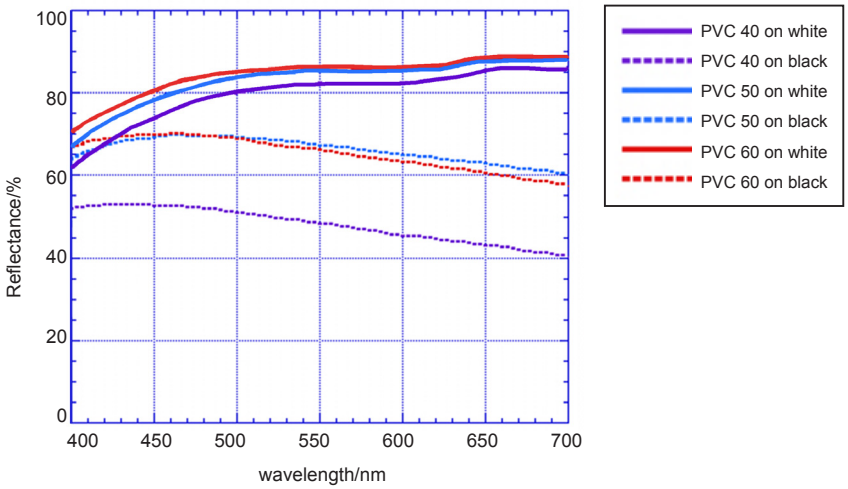

Figure 1A.1 Reflectance spectra of basic lead carbonate paints

1A.2 Opacity of white paint with two types of pigments

Experiment B:

White paints were made containing mixtures of basic lead carbonate and barium sulfate. PVC was set at 40%. Mixed ratios of basic lead carbonate to barium sulfate were 100, 75, 50, 25, and 0% in volume (Table 1A.3). The paints were applied with a wet thickness of 60 μm.

Result:

The paints B-a (pure lead white) and B-c (50% lead white) gave very similar reflectance spectra despite the fact their formulations are different, while B-b has the greatest hiding power (Table 1A.4, Figure 1A.2), though by a margin that is hardly visually perceptible.

The reason is that the scattering power is not only determined by refractive index but also by particle size distribution. If the scattering were determined by an RI difference between the pigment and binding medium only, then increasing the volume of barium sulfate would lead to a reduction of the hiding power since basic lead carbonate has a higher RI than barium sulfate. In practice, the particle size influences the packing geometry of the paint, which in turn has a strong effect on the scattering. If lead white and barium sulfate had a different particle size distribution, the particles would be packed better and this would be more important than the effect of RI. However, in an over-packed condition the closest particles behave as larger particles and consequently

Table 1A.3 Model paint formulations in Experiment B

Sample name	Basic lead carbonate weight/g (volume/cm^3)	Barium sulfate weight/g (volume/cm^3)	Oil weight/g (volume/cm^3)
B-a	2.7 (0.4)	———	0.56 (0.6)
B-b	2.0 (0.3)	0.4 (0.1)	
B-c	1.4 (0.2)	0.9 (0.2)	
B-d	0.7 (0.1)	1.3 (0.3)	
B-e	———	1.8 (0.4)	

Table 1A.4 L*a*b* data of the model paints in Experiment B

Sample code	On white substrate			On black substrate			Differences		
	L*	a*	b*	L*	a*	b*	ΔL*	Δa*	Δb*
B-a	93	-2	7	84	-2	-1	9	0	8
B-b	94	-1	4	87	-2	-1	7	1	5
B-c	93	-1	5	84	-2	-2	9	1	7
B-d	93	-2	6	78	-2	-3	15	0	9
B-e	93	-2	7	54	-2	-5	39	0	12

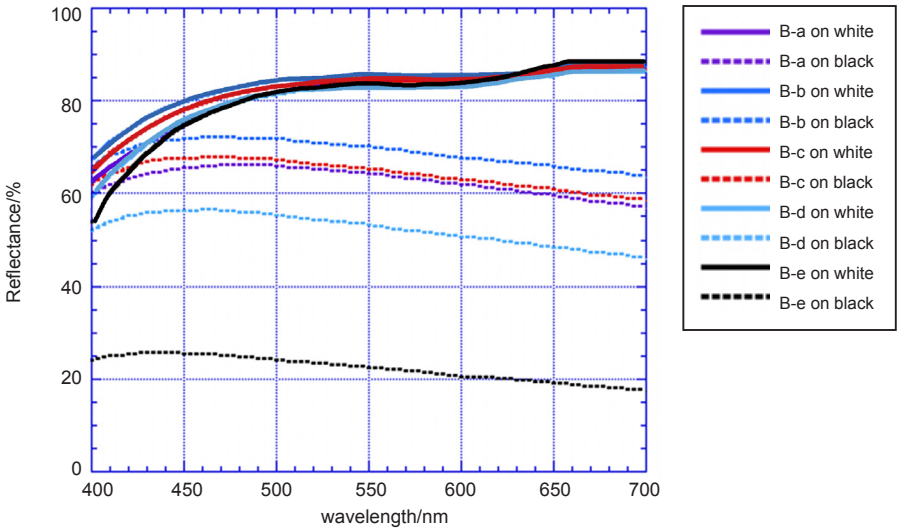

Figure 1A.2 Reflectance spectra of paints of experiment B

would scatter less than the particles would independently [Stieg 1959; Doroszkowski 1994: 45-50]. It can be concluded that in the present experiments the relatively low RI of barium sulfate was compensated by the small particle size, for this batch.

1A.3 Opacity with a light absorber

Experiment C:

A small amount of red paint (red iron oxide paint with PVC 30) was added to the white paints of experiment B. By adding the red paint, the total volume increased about 7%. The PVC of the red pigment was less than 2% (Table 1A.5). The application thickness was 60 μm.

Result:

The red pigment is a light absorber in these paints, and that made all white paints mostly cover the contrast of the black and white substrates shown in the reflectance spectra and the Δ-values of L*a*b* (Figure 1A.3, Table 1A.6).

The result shows that opacity of a colored paint in general is much higher than a white paint owing to absorption by the colored pigment. This experiment also demonstrates that lightness relates to saturation. Despite the fact that all paints contain the same amount of red pigment, the a* differs one from the others which indicates that different strength of the scattering of the white pigments caused the tone differences.

Table 1A.5 Model paint formulations in Experiment C

Sample name	Basic lead carbonate weight/g (volume/cm^3)	Barium sulfate weight/g (volume/cm^3)	Oil weight/g (volume/cm^3)	Red paint
C-a	2.7 (0.4)	——	0.56 (0.6)	0.14 g (red iron oxide (d=5.0): 0.02cm^3 and oil 0.05 cm^3) [PVC of red pigment in total < 0.02]
C-b	2.0 (0.3)	0.4 (0.1)		
C-c	1.4 (0.2)	0.9 (0.2)		
C-d	0.7 (0.1)	1.3 (0.3)		
C-e	——	1.8 (0.4)		

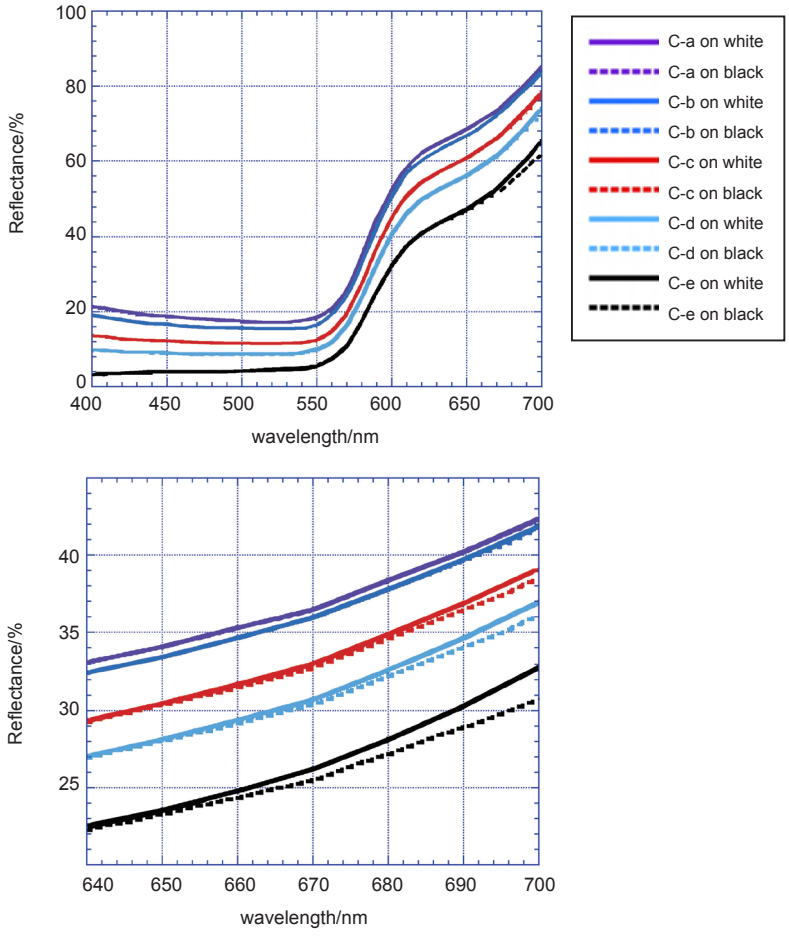

Figure 1A.3 Reflectance spectra of paints of experiment C
(upper) from 400 nm to 700 nm
(bottom) Details; from 640 nm to 700 nm

Table 1A.6 L*a*b* data of the model paints in Experiment C

Sample code	On white substrate			On black substrate			Differences		
	L*	a*	b*	L*	a*	b*	ΔL*	Δa*	Δb*
C-a	44	27	14	44	27	13	0	0	1
C-b	43	28	15	43	28	15	0	0	0
C-c	40	30	18	40	30	17	0	0	1
C-d	37	31	20	37	31	20	0	0	0
C-e	31	34	28	31	33	28	0	1	0

1A.4 Addition of a small amount of light absorbers

Experiment D:

The effect of an addition of a small amount of light absorbing material was tested by making a green paint with a very small amount of copper monoxide (CuO). Copper monoxide can be an alteration product from copper containing pigments causing an increase of light absorption because it is a black material [Kühn 1970] [1]. Malachite, although rarely used in the nineteenth century paintings, was chosen since it reasonably reflects green light. Copper monoxide was added to mimic a possible conversion of only a small i.e. 1wt% conversion of the green copper pigment in the paint. The 1wt% corresponds to about 0.4% in volume of the total paint mass. Barium sulfate was added to make the paint less light reflective. The PVC of the paints was set at 40% (Table 1A.7). The application thickness was 60 µm.

Table 1A.7 Paint formulation of the malachite green paint

Sample (sample code)	Malachite weight/g (volume/cm^3)	CuO weight/g (volume/cm^3)	Barium sulfate weight/g (volume/cm^3)	Oil weight/g (volume/cm^3)	PVC
Malachite paint (McBy)	0.78 (0.20)	n.a.	0.88 (0.20)	0.56 (0.60)	0.40
Malachite paint with a small amount of CuO added (McBy-CuO)	0.74 (0.19)	0.03 (0.004)	0.88 (0.20)	0.56 (0.60)	0.39

2: The selection of copper monoxide may not mimic the deterioration of a real paint film [Cartechini *et al.* 2008], but the presence of a strong light absorber was key for experiment.

Table 1A.8 Result of colour measurement (L*a*b*)

Sample code	On white substrate			On black substrate			Differences		
	L*	a*	b*	L*	a*	b*	ΔL*	Δa*	Δb*
McBy	53	-20	20	42	-14	10	11	6	10
McBy-CuO	42	-15	14	37	-12	9	5	3	5

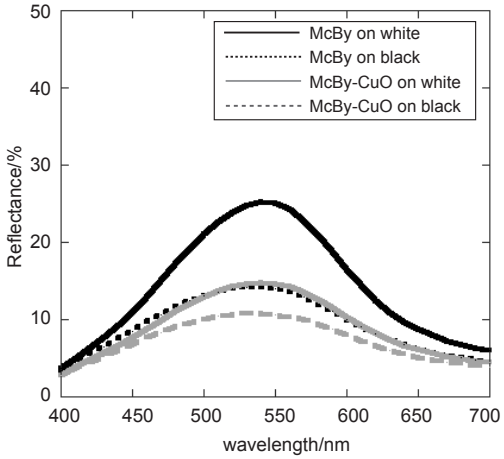

Figure 1A.4 Reflectance spectra of the malachite and copper monoxide containing paints

Result:

The reflectance was reduced by about 10% at 540 nm, which is the maximum reflection wavelength (Table 1A.8, Figure 1A.4). The transparency of paint was decreased due to the increased light absorption by copper monoxide. This result demonstrates that the presence of a light absorbing compound in a paint system drastically reduces the lightness and increases the hiding power.

1A.5 Addition of a small amount of light reflectors

Experiment E:

The scattering ability of lead white was compared with a lead acetate containing paint. In order to better visualize the scattering effect, a set amount of lead white or lead acetate was added into translucent green and yellow paints. The green paint was made with verdigris (Kremer Pigmente GmbH & Co. KG) and the yellow paint was made with a yellow lake (Reseda: Kremer). These two pigments create paints with a relatively high translucency.

PVC of the verdigris (specific gravity 1.88) paint was set at 25% and the yellow

lake paint was set at 20%. The PVC of the yellow lake was calculated using the specific gravity of the substrate compound i.e. potash alum ($KAl(SO_4)_2$), 1.75. The PVCs were different because of the consistency of the paints. Basic lead carbonate (Fluka) as lead white and lead acetate trihydrate (Sigma-Aldrich) were added to these green and yellow paints, respectively. The amount of lead added was set at 10% by weight of the paint. The corresponding volume concentration in the paint is about 2% in the lead white containing samples and about 6% in the lead acetate containing samples (Table 1A.9).

Result:

Visual observations and color measurements of the paints demonstrated that addition of about 2 vol% of lead white made the paints appear distinctly different from the paint with lead acetate (Figure 1A.5). The appearance difference is noticeable when the underlying support was black. Both the yellow and green paint containing lead white (YPbW, GPbW respectively) on the black substrate, have c.10% higher reflectance at the maximum wavelength compared to the corresponding paints with lead acetate (YPbAc, GPbAc respectively) (Table 1A.10, Figures 1A.6 and 1A.7). Owing to the presence of light reflectors in YPbW and GPbW, yellow and green hues are recognized even when the paints are on the black substrate.

On the other hand, YPbAc, GPbAc on the black substrate appeared almost black. Because there are few reflectors in the paints, the light is absorbed by both the paint itself and the black substrate. The PVCs of lead acetate in the paint are around 6% in the yellow paint, and 7% in the green paint, which are both higher than the lead white PVCs. This demonstrates that lead acetate has a small optical effect. This is already

Table 1A.9 Formulation of yellow and green paints with lead compounds

	Pigment		Oil		PVC
	weight/g	volume/cm^3	weight/g	volume/cm^3	
Yellow paint (Reseda)	0.32	0.18	0.68	0.73	0.20
Green paint (Verdigris)	0.40	0.21	0.60	0.64	0.25

Sample code	Formulation	Amount of lead compound		Volume concentration of lead compound to paint	Weight concentration of Pb to oil
		weight/g	volume/cm^3		
YPbW	Yellow paint 1g + 10wt% Pb as lead white	0.125	0.018	0.019	0.147
YPbAc	Yellow paint 1g + 10wt% Pb as lead acetate	0.157	0.061	0.063	0.147
GPbW	Green paint 1g + 10wt% Pb as lead white	0.125	0.018	0.021	0.167
GPbAc	Green paint 1g + 10wt% Pb as lead acetate	0.157	0.061	0.067	0.167

Table 1A.10 Result of color measurement (L*a*b* and C*)

Sample code	On white substrate				On black substrate				Differences			
	L*	a*	b*	C*	L*	a*	b*	C*	ΔL*	Δa*	Δb*	ΔC*
YPbW	76	1	83	83	35	-7	26	27	41	8	57	56
YPbAc	80	-1	80	80	19	-1	4	4	61	0	76	76
GPbW	48	-59	14	61	27	-22	3	22	21	-37	11	39
GPbAc	51	-57	13	58	19	-3	0	3	32	-54	13	55

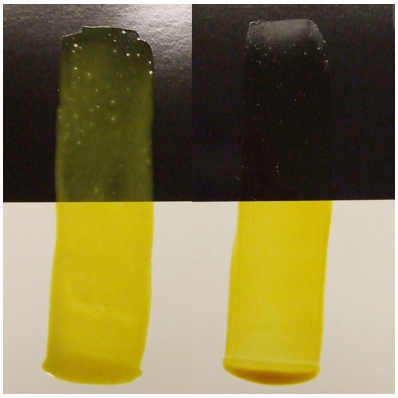

(a) YPbW YPbAc

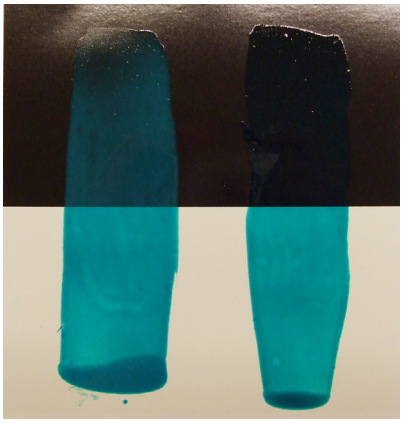

(b) GPbW GPbAc

Figure 1A.5 Photograph of the model paints
(a) yellow paint
(b) green paint

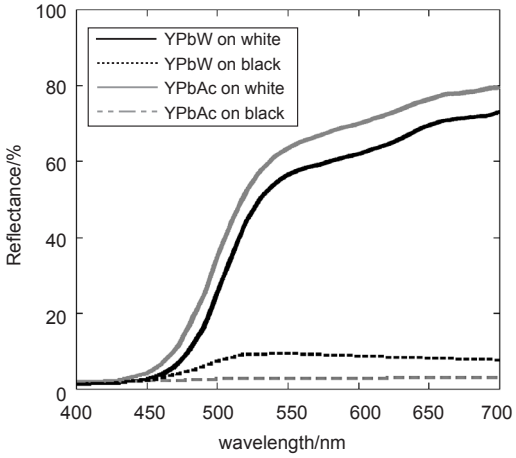

Figure 1A.6 Reflectance curves of YPbW and YPbAc

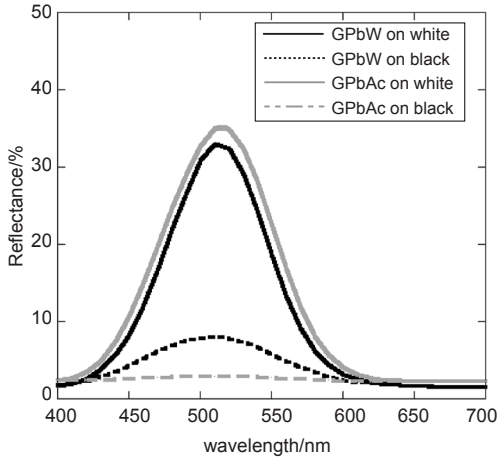

Figure 1A.7 Reflectance curves of GPbW and GPbAc

expected since lead acetate is colorless and has a refractive index (around 1.6) closer to the oil (around 1.5) than that of lead white (around 2.0).

The paints on the white substrates barely show any appearance differences. Light absorption by the paints and reflection from the white substrate dominates the appearance and the scattering of lead white is too small to be effective. Because of the strong light reflection from the white substrate, scattering in the paints were almost completely offset. Although it is a small difference, a reverse effect is noted showing that lightness (L*) of YPbW and GPbW is slightly lower than of YPbAc and GPbAc's. Because there are few light scattering particles in the lead acetate containing paints the incident light passes through the paints and reflects at the white substrate without much decrease of the light intensity by light absorption. In YPbW and GPbW, lead white reflects the light within the paint layer, which increases the light path. A longer light path gives more chances for absorption or scattering of the light. In this condition, the light absorption was more effective than scattering; as a consequence, the lightness diminished somewhat.

1A.6 Optical effects of superimposing yellow and green translucent paint layers

Experiment F:

For experimentally visualization of the surface appearance from two superimposed light absorbing paints, the green and yellow glaze-like paint prepared in experiment E were painted over one another. Two types of the yellow and green paints were painted on each other to make eight combinations (Table 1A.11).

Result:

When the yellow paints were on top, the surface tended to appear lighter than when green paints were on top. The strong light absorbent property of the green paints made all combinations show a green hue regardless of the order of application.

A small amount of lead white in both yellow and green paints (YPbW and GPbW) (Table 1A.12) had an important influence on the appearance when the paints were applied on the black substrate. On the other hand, the paints on the white substrates showed no difference due to illumination of the paints by the reflection from the substrate.

This result also demonstrates the importance of reflection from the underlying layers on the surface appearance in translucent paints. This is obvious in samples YG1 and GY1. Since there were almost no light reflectors in both combinations, they appear very dark, nearly visually black (Figure 1A.8). YG4 and GY4 show the highest lightness in each group as expected (Figure 1A.9).

The presence of the highly translucent paints of YPbAc and GPbAc had a smaller effect on the surface appearance when they were placed between the top layer and the

Table 1A.11 List of superimposed paint samples

Sample code	Top paint	Underlying paint
YG1	YPbAc	GPbAc
YG2	YPbAc	GPbW(a)
YG3	YPbW	GPbAc
YG4	YPbW	GPbW(a)
GY1	GPbAc	YPbAc
GY2	GPbAc	YPbW
GY3	GPbW(b)	YPbAc
GY4	GPbW(b)	YPbW

*Two GPbW (a) and (b) are the same composition but because they were applied separately the reflectance were a little different.

Table 1A.12 Result of color measurement (L*a*b*)

Sample code	On black substrate		
	L*	a*	b*
YG1	17	-5	7
YG2	30	-16	20
YG3	38	-7	19
YG4	41	-16	22
GY1	18	-11	3
GY2	26	-26	11
GY3	35	-28	1
GY4	37	-34	5
YPbW	35	-7	26
GPbW(a)	27	-22	3
GPbW(b)	32	-26	1

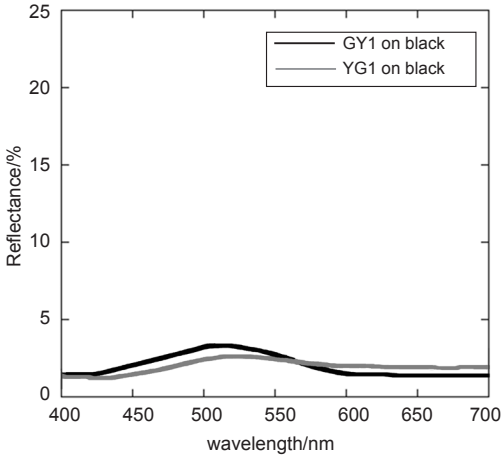

Figure 1A.8 Reflectance curves of YG1 and GY1 on black substrate

black substrate (compare YG3 to YPbW and GY3 to GPbW) (Figure 1A.10). YG3 and GY3 were a little lighter which was an effect due to the interface reflection at the boundary of two paint layers.

When YPbAc and GPbAc were applied over the light reflecting paints GPbW and YPbW respectively (YG2 and GY2), their optical contribution to the surface was certainly apparent. In YG2, the yellow component was added and the lightness was

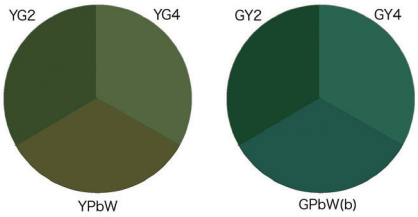

Figure 1A.9 Illustrated colour images of superimposed paints [YG2/YG4/YPbW] and [GY2/GY4/GPbW(b)] (all on black substarte).

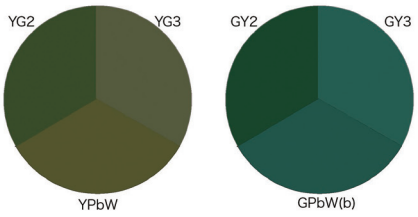

Figure 1A.10 Illustrated colour images of superimposed paints [YG2/YG3/YPbW] and [GY2/GY3/GPbW(b)] (all on black substarte).

smaller (Figure 1A.10). In GY2, the upper green paint absorbed the yellow light from the lower YPbW paint and the surface became darker than GPbW.

From an optical point of view, placing more than two glaze-like paints of different colors on top of each other is not a logical practice. For an effective set of paint layers, the light transmitted through the glaze paint needs to be reflected by the underlying layer.

References

Balfour, J.C. 1994. Titanium Dioxide pigments. In: R. B. Mackay, ed. *Technological Applications of Dispersions*. Marcel Dekker, Inc., pp. 69-104.

Cartechini, L., Miliani, C., Brunetti, B. G., Sgamellotti, A., Altavilla, C., Ciliberto, E., and D'acapito, F. 2008. X-ray absorption investigations of copper resinate blackening in a XV century Italian painting. *Applied Physics A*, 92 (1), 243-250.

Doroszkowski, A. 1994. Paints. In: R.B. Mackay, ed. *Technological Applications of Dispersions*. Marcel Dekker, Inc. pp. 1-67.

Kühn, H. 1970. Verdigris and copper resinate. *Studies in Conservation*, 15 (1), 12-36.

Stieg, F.B. 1959. The Relationship of Pigment Packing Patterns and C.P.V.C. to Film Characteristices and Hiding Power. *Official Digest,* 31 (6), 736-751.

Chapter 2

On metal soap related transparency changes in a late 19th-century painting by J.E. Millais (Tate N01584, 1895)

The painting 'Speak! Speak!' by John Everett Millais at Tate shows severe loss of detail in certain areas, apparently due to darkening of the paint. Analytical microscopic data showed the extensive saponification of the top lead white and zinc white containing paint layers, with evidence of the formation of aggregates of zinc carboxylates. Consumption of the white pigments for the saponification leads to reduction in the light scattering properties, as a consequence opacity of the top layers is reduced, allowing the underpaint layers to become more prominent. The apparent degree of darkening of the paint areas is not only dependent on the degree of saponification of the top layer but also has a relationship to the color of the affected paint layer and the paint underneath. The partial darkening can thus be explained by a reduction of the light reflected from white paints associated with the saponification of the white pigments.

2.1 Introduction

Oil paints can become more translucent with time and may reveal underpaint layers to an extent that exposes the underdrawing and even the artists' *pentimenti* [Kühn 1963; Laurie 1967: 140-155; Van Eikema Hommes 2004: 38]. This has been interpreted as a darkening of the painting as well as a change in perceived intent and the appearance of the picture. Explanations for the phenomenon were suggested in the early literature: increasing transparency in oil paintings would be caused by incomplete interpenetration between binding media and pigments [Church 1890: 43], the "saponification of lead white pigment" as suggested by Eibner [1909: 120-121] or an alteration of the refractive index of the oil media [Laurie 1926].

Townsend [1993] pointed out that a refractive index change of the oil binding medium is in fact small and unlikely to have any influence in the appearance of paintings, which rejects Laurie's proposed explanation. Support for the second

hypothesis is found in the many recent reports on lead soap formation and aggregation [Boon *et al*. 2002; Van der Weerd *et al*. 2002; 2003; and 2005; Higgitt *et al*. 2003; Keune *et al*. 2007], the observed dissolution of lead white in underpaints [Keune and Boon 2007] and the changes in transparency in a panel painting of Van der Neer [Noble *et al*. 2005]. In the latter painting specific areas in the painting have a darker appearance, which is related to a severe loss of light reflectivity due to replacement of lead white by lead soaps as a function of the thickness of the ground and the nature of the wood underneath.

The saponification of lead white, red lead, and zinc oxide in oil paint has been described in the paint industry literature from the beginning of the 20th century. Although these pigments were considered to be beneficial for the rheology and drying properties of the industrial paint [Heaton 1928: 80; Tumosa and Mecklenburg 2005], they were often associated with a surface haziness called 'seeding' [Jacobsen and Gardner 1941; Elm 1957]. This defect was thought to result from the reaction of the acid components in oil with basic pigments. A similar phenomenon was also observed in oil paintings a short while after drying [Ordonez and Twilley 1997].

These studies have shown that the saponification of lead and zinc containing oil paints is not uncommon. It is also pointed out that the interaction of metals from pigments and driers with compounds derived from the oxidation of oil, form an essential part of the development into a stable polymer network in paints [Verhoeven *et al*. 2006; Boon 2006]. On the other hand, especially monocarboxylic acids can develop into metal soap aggregates that may threaten the stability of the painting. Therefore metal soap formation could be a cause of appearance changes in terms of both optical and chemical aspects. It is however unclear why not all paints containing the pigments mentioned have (yet) developed surface efflorescence observed as haziness or alteration in paint appearance.

In this study, optical effects due to metal soap formation are taken into account. The painting '*Speak! Speak!*' in 1895 by John Everett Millais (English; 1829-1896) (Tate N01584) (Figure 2.1) shows partial darkening that is thought to relate to metal soap formation. The examination focuses on an area where the white and yellow fur cover in the foreground is painted over the dark shadows under the bed. Additionally, Millais' late working technique and the materials he used are examined.

2.2 Examination of the painting

2.2.1 Current appearance

The painting is a night scene with the man crying out at the appearance – or imagined form – of his lost love, who is wearing a white dress and white or glittering jewels. According to the exhibition catalogue [Spielmann 1898: 119-120], the letter on the floor is a well worn letter from her that he had been reading through the night. The artist

Figure 2.1 *Speak! Speak!* (1895) by John Everett Millais (Tate N01584: 1676 × 2108 mm) ©Tate 2015

intentionally left uncertainty whether she is a real or an illusion.

As the painting is a night scene, everything is illuminated by candlelight. The candlelit atmosphere was created with warm-toned paints of orange and brown. The bright colors of the tablecloth are painted in bright opaque orange and several shades (or tones with white) of opaque yellow paint. The man's flesh is depicted in the opaque orange paint to reflect the candlelit environment. Thus, flesh-toned paint is hardly present anywhere. Other opaquely painted areas, such as the white dress and the jewels, which are made with impasted white paint, have a transparent wash of thinned paint on top of rather translucent brown paint.

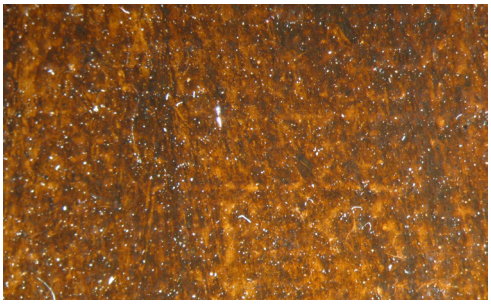

Figure 2.2 Thinly applied brown paint. The texture of the canvas is visible through the translucent brown paint. ©Tate 2015

Mostly the paints are thinly applied (Figure 2.2). The man's hair and the bed curtains at upper right are fairly thinly painted. There is now visible some evidence for a six-inch grid marked in pencil, applied to the priming prior to paint application. Five vertical lines are visible at the top edge, the rightmost 56 cm in from the stretcher, and two horizontal ones are visible coming from the lower left. In the dress, the paint on top failed to wet the line, leaving graphite pencil visible. Elsewhere, paint covers the lines completely.

The most thinly-painted part, where the area has lost details and appears dark, corresponds to the fur cover, where it is hanging over the bed. The veil-like appearance of the yellow fur is suspected to be caused by loss of light reflectivity due to saponification of certain pigments. An increase in transparency of the upper paint layers may have led to the darkening around this area. In addition, many of the warm-toned areas include brown and orange pigments. Any change in the lighter toned paint components would therefore lead to a darker appearance.

2.2.2 Condition of the painting

The paint condition is rather stable with no severe cracking, the result of the thin application of the paint. The painting is unlined. The ground has a regular stippled texture. There is no evidence that priming or paint has been absorbed through to the back of the canvas. The canvas is neither badly deteriorated nor discolored for its age. It is very fine, closely-woven, with prominent slubs, with about 25 threads/cm. The tacking margins are covered with non-original tape so the canvas fixings are not visible. Original tacks may be present. The stretcher is quite well keyed out, and could be original.

According to the conservation records at Tate, there have been some treatment campaigns. Surface cleaning and varnishing at the National Gallery in 1897 was reported in 1898. A very patchy appearance of varnish, though it is uncertain whether it is the varnish from 1897, was reported in 1975. In 1988, flaking at the lower left corner and low centre right was secured from the front with wax-resin. In addition, Vinamul (polyvinyl acetate) was used to consolidate paint along the lower edge, behind the tape. The latest conservation treatment is reported in 1993 as varnishing with Ketone-N cyclohexanone resin.

2.2.3 Samples and methodology

Eight samples including one sample from the suspected darkening area were taken (Figure 2.3, Table 2.1). Each sample was first examined with a ZEISS Stemi SV1 binocular microscope using an optic illumination source (ZEISS KL1500LCD) at Tate conservation laboratory. Then the paint cross-sections were examined with a ZEISS

Axioplan 2 light microscope at ICN (presently RCE), and Fourier transform infrared spectrometry imaging technique (img-FTIR) was performed with Bio-Rad FTS-6000 FTIR spectrometer connected to an IR microscope Bio-Rad UMA-500 at AMOLF. This technique is particularly useful for identification and localization of metal soaps in cross-sections, by means of the characteristic absorption at around 1530 cm^{-1} of the metal-carboxylate group. Further study of the layer structure, the identification and distribution of elements was performed with a JEOL JSM-5910LV scanning electron microscope (SEM) using a backscattered electron (BSE) detector and an energy dispersive X-ray detector (EDX) (ThermoNoran) operated by Vantage software.

Figure 2.3 Sampling areas (sample number 10 to 17) ©Tate 2015

Table 2.1 Sample list

Sample No	Sampling area	Surface apperance
s10	lower edge, above tape in middle of the foreground	grayish brown
s11	haze on stairs, left of the foreground	hazy white on brown paint
s12	train of the woman's dress on left side	whitish gray
s13	wooden door on left side	dark brown
s14	near consolidated area on the lower edge	yellowish brown
s15	near consolidated area, above tape, on the lower edge	yellowish brown
s16	white dress over graphite pencil line on priming, that the paint is failing to wet	off-white
s17	fur in 'disappearing' area where the fur overlies the edge of the bed	brownish yellow

The paint cross-sections from s16 and s17 were further polished with a Cross-section Polisher CP® (JEOL) [Boon and Asahina 2006] for a more detailed morphological examination. The polisher employs an argon ion beam to fine polish the surface of cross-sections with the objective to maintain the microstructure.

2.2.4 Layer build-up and used materials

All cross-sections have a common build-up with a "double" priming: a white layer underneath a light brown priming layer (Figures 2.4 and 2.5). The first priming layer (layer 1) contains mainly calcium carbonate with some lead white whereas the second one (layer 2) is a thinner lead white containing layer tinted with red ochre. The relatively intense red color of this layer suggests that the second priming was by the artist or done to his request by the manufacturer (Witlox Pers. Comm. 2006).

The paint layer build-up is simple and most of the layers are thinly applied. The samples s10, s11, and s14, which were taken from the floor, depict areas in the foreground and show a similar layer build-up. After the priming, gray, dark brown, and yellow paint layers are found. The gray paint layer appears uneven, while the dark brown layer was applied evenly (Figures 2.6 and 2.7). The brown paint contains iron and manganese indicating the use of umber. A UV-fluorescent layer between the brown and yellow layers is indicative of a resin containing layer (Figure 2.8).

Sample s12 was taken from the train of the woman's white dress, which was slightly more grayish than the white dress itself. Judging from the surface it is not certain if the paint of the train was applied over the floor paint. A lead white paint layer was found on top of the tinted priming (Figure 2.9), and the next application of gray paint toned down the whiteness and harmonizes the surroundings. The paint layer build-up clearly shows the artist's intention to paint the grayish train. Sample s13, which was taken from depicting the wooden door with less candle light, has a dark brown paint thickly applied on the priming (Figure 2.10). Thinly applied gray and warm colored glazing layers create the wood texture. These cross-sections show a systematic paint layer build-up to achieve dark and light appearance.

Sample s17 was taken from the supposedly darkened yellow fur area. Sample s16 was removed from the woman's white dress for comparison. In this area no significant darkening is observed.

In sample s16, a very thin layer 3 with lead white, umber and bone black was applied on the priming (Figure 2.11a, Table 2.2). On top of it, two thin layers; layer 4 with lead white and bone black, and layer 5 with a formulation similar to layer 3, are observed. The layer 6 contains lead white, vermilion and chrome yellow. This layer contains aluminum and shows reddish UV fluorescence suggesting the use of red lakes (Figure 2.11b). EDX analysis detected zinc in this layer suggesting zinc oxide. Finally, a translucent brown glaze, is thinly applied presumably to obtain a "candle-lit" effect (layer 7). This thin glaze will not have significant hiding power and the surface appearance of

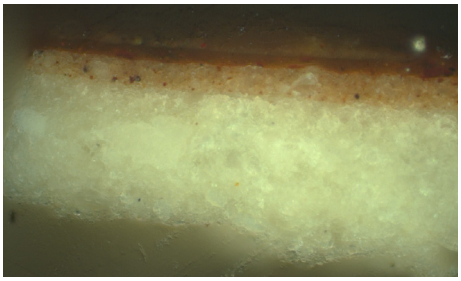

Figure 2.4 Visible light image (VIS) of s11 in cross-section. The bottom white paint layer is the first priming.

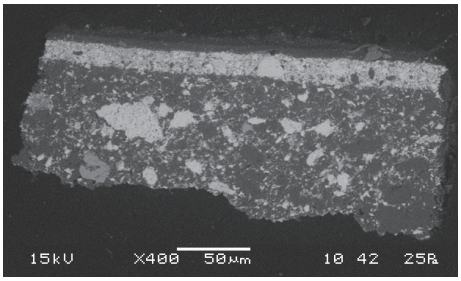

Figure 2.5 SEM-backscattered electron (BSE) image of s11.

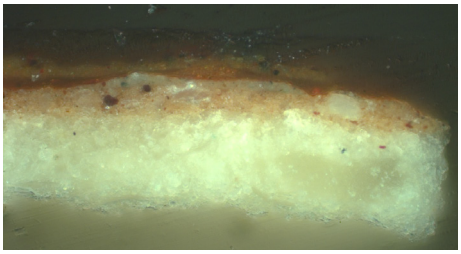

Figure 2.6 VIS of s10 in cross-section, showing the similar layer build-up as seen in the other cross-sections (see also Figures 2.4 of s11 and 2.7 of s14).

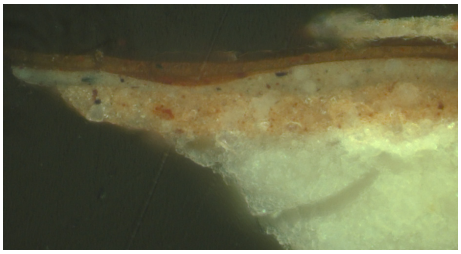

Figure 2.7 VIS of s14 in cross-section.

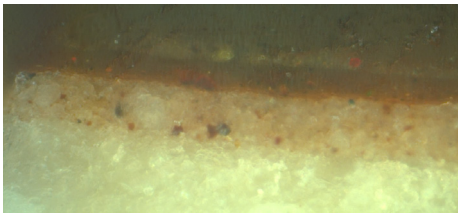

(a)

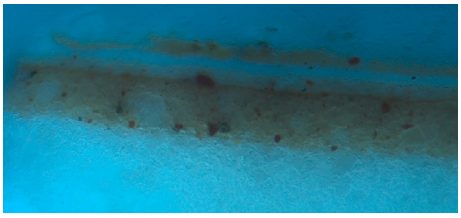

(b)

Figure 2.8 Detailed of s11. (a) VIS, (b) UVf showing the intermediate UV fluorescing layer without visible pigment particles.

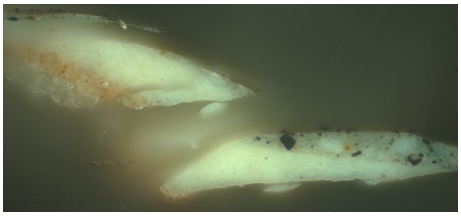

Figure 2.9 Detailed VIS of s12 showing the lead white paint on top of the second tinted priming.

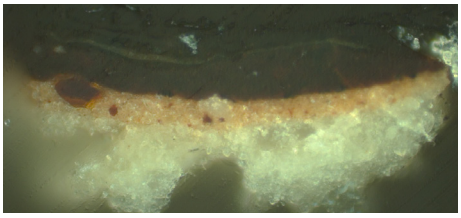

Figure 2.10 Detailed VIS of s13 showing the thickly applied brown paint layer.

this area is in part determined by layer 6.

Sample s17 is a dark brown paint (layer 3) containing umber and lead white, on top of the second priming (Figure 2.12a, Table 2.3). The subsequent layer 4 contains lead white, vermilion and bone black. There are few pigment particles in layer 5, which could be interpreted as an oiling out layer. The layer 6 corresponds to the light yellow paint depicting the fur cover, which consists mainly of chrome yellow, lead white, and

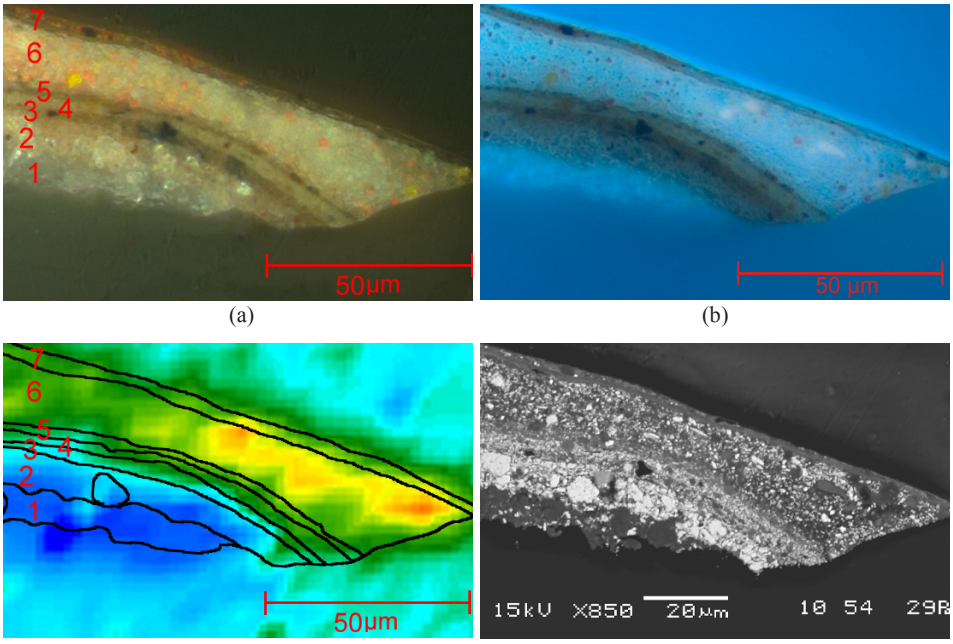

(a) (b)

(c) (d)

Figure 2.11 (a) VIS image of the s16 cross-section from the white dress showing seven layers, (b) under UV light, (c) infrared absorption image at 1531 cm^{-1} representing the relative concentration of metal carboxylates. There is a high carboxylate absorption in layer 6 (Red-yellow-green-blue corresponds from high to low intensity), (d) the corresponding SEM-BSE image.

Table 2.2 Layer build-up and identified pigments in s16 taken from the women's white dress

Layer No	Appearance in cross-section	Identified pigments
7	Thinly applied brown glaze	lead white, red ochre
6	Reddish white	lead white, zinc oxide, vermilion, Al substrate (possibly red lakes), chrome yellow
5	translucent light brown	umber, lead white
4	gray	lead white, bone black
3	translucent light brown	lead white, umber, bone black
2	brown second priming	lead white, red ochre, barium sulfate
1	white first priming	calcium carbonate, lead white

zinc oxide. The top paint is a thinly applied brown glaze. A thin varnish layer with UV fluorescence is observed, but an intermediate resinous layer in this sample is absent (Figure 2.12b).

In summary, red and brown colors were intentionally used to create a candle-lit effect. Iron and manganese detected by EDX demonstrate the use of red ochre and umber. Shades are adjusted by addition of white pigments and/or bone black. Gray paint in s12 contains cobalt blue. Warm toned glaze paints contain red ochre as the main color source. Vermilion is also found in s10. Yellow pigments in the glaze paints are cadmium yellow in s10 and chrome yellow in s14. In the paints, chrome yellow and vermilion are found in s16 and s17, but not in the other cross-sections. The presence of a red lake is indicated in the paint of s16.

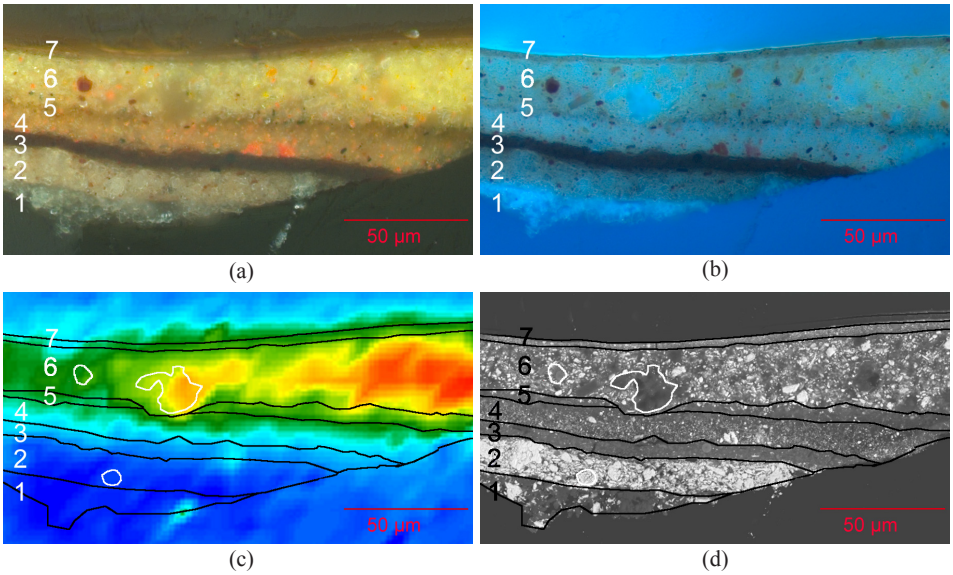

Figure 2.12 (a) VIS image of s17 cross-section from the yellow fur showing seven layers, (b) under UV light, (c) infrared absorption image at 1530 cm^{-1} representing metal carboxylates with a high absorption in layer 6, (d) the corresponding SEM-BSE image.

Table 2.3 Layer build-up and identified pigments in s17 taken from the fur overlying the bed

Layer No	Appearance in cross-section	Identified pigments
7	Thinly applied brown glaze	lead white, red ochre
6	orange-yellow	lead white, zinc oxide, chrome yellow, vermilion, red ochre
5	translucent yellow layer	(oiling out?)
4	red	lead white, vermilion, bone black
3	dark brown	umber, lead white
2	brown second priming	lead white, red ochre, barium sulfate
1	white first priming	calcium carbonate, lead white

2.2.5 Organic component analysis

Millais' purchases of Roberson's medium (oil, mastic and copal resins mixture), and also a quick or slow-drying copal medium in his (early) pre-Raphaelite period are recorded in the account book of the artists' colorman Roberson [Hackney *at el*. 2004]. According to Reid [1909: 164-165], Millais seems to have continued using copal containing binding media. The organic component analysis aimed to clarify whether he used resinous binding media.

Direct temperature resolved mass spectrometry (DTMS) and pyrolysis and thermally assisted hydrolysis and methylation gas chromatography/mass spectrometry (Py-TMAH-GCMS) analyses were performed on samples s10 and s15. A drying oil, Ketone N, beeswax, colophony, dammar, and mastic were discovered (spectra not shown). Lead azelate (C9-lead soap) in the white priming was indicated by DTMS. P/S ratios of the priming of s10 and the paint of s15 were about 1 in the DTMS results suggesting the use of linseed oil. Ketone N is from the later applied varnish, beeswax and colophony are most probably from the wax-resin treatment. These materials used in the past conservation treatments hinder a detailed interpretation of results of the binding medium. The use of resinous binder has not been confirmed.

2.3 Saponification and the darkening

The darkening is inferred to be caused by the loss of light due to the saponification of the white pigments, especially lead white. Zinc oxide, whose presence is implied by EDX analysis, can also react away to the corresponding metal soaps. It has been established that both lead white and zinc white react with carboxylate groups from oil derived constituents in the paint forming metal carboxylates (metal soaps) [Boon *et al*. 2002; Van der Weerd *et al*. 2002; 2003; and 2005; Higgitt *et al*. 2003; Keune 2005; Keune and Boon 2007]. Because metal carboxylates have a lower scattering power than the original white pigments, metal carboxylate formation in oil paint causes lowering the hiding power and thus the whiteness of paint. Therefore, it was crucial to demonstrate presence of metal soaps in the samples to explain the darkened appearance of parts of the painting.

Identification and localization of metal soaps in the cross-sections were performed with FTIR microscopy by imaging the metal carboxylate absorption peak at around 1530 cm^{-1}. The carboxylate absorption from lead carboxylates appears between 1540 cm^{-1} and 1510 cm^{-1}, while zinc carboxylates appears from 1550 cm^{-1} to 1530 cm^{-1}. The distinction between zinc carboxylates and lead carboxylates is therefore uncertain on the basis of FTIR data only. SEM-EDX elemental mapping is useful in this respect as it provides the distribution of the elements of zinc and lead.

FTIR analysis was performed to the sample s10, s11, s16 and s17. The presence of lead soap was suggested in s10 by DTMS analysis. Some areas in the priming of

s10 and s11 show low reflectivity to both light and X-rays. It was difficult however to localize the metal soap in both cross-sections, since the paint layers are too thin to obtain a significant IR absorption. No obvious carboxylate absorption was indicated in the priming either, possibly due to the broad absorption of carbonate ions in calcium carbonate and lead white, obscuring the carboxylate absorption.

Samples s16 and s17 were examined by imaging FTIR and SEM-EDX. The sample s16 was taken from the area of the woman's dress, which does not show any obvious darkening. The sample s17 was taken from an area with clear darkening.

It was established that metal carboxylates are present in layer 6 of sample s16 (Figure 2.11c), and also in layer 6 of sample s17 (Figure 2.12c). The intense absorption indicated as red and yellow areas in the figures correspond to translucent areas in the light microscope images (Figures 2.11 and 2.12) thus supporting the formation of metal soaps [Keune and Boon 2007; Higgitt *et al*. 2003]. The SEM backscattered electron images of s16 and s17 also show a lower BSE density of the layers 6 in both cross-sections (Figures 2.11d and 2.12d). In general, lead white pigments in paint layer appear bright in SEM backscattered images (see for example the lead white pigment particles in layer of s17 in Figure 2.12d). In contrast, metal soaps appear darker due to their low degree of crystallinity and higher organic content [Keune and Boon 2007]. These dark areas in the SEM images overlap with areas that have translucent appearance in light microscope (Figures 2.11d and 2.12d) and are rich in metal carboxylates according to the imaging FTIR results. The edges of the pigment particles are not very well defined and suggest an interface area where the reaction between the binding medium acid groups and pigment has occurred, therefore further supporting the formation of metal soaps.

Interestingly, samples s16 and s17 both have other lead white containing layers where there would be potential for lead soap formation, but metal soaps were only found in the upper layers. A crucial difference between metal soap containing layers and those that show no evidence of metal soap formation is the presence of zinc. The EDX mapping of sample s17 reveals that a relatively higher amount of zinc was detected in the layer 6, which shows a high intensity of metal carboxylate absorption. The dark area indeed is rich in carbon and zinc (Figure 2.13). Although the dark spots, especially the marked area in layer 6 seems to be mainly consisting of zinc soap according to the EDX data, we cannot exclude the presence of lead in these agglomerates. According to experimental studies, it seems that free monocarboxylic acids from hydrolysis of acylglycerol moieties in oil paint are required for the saponification of lead white (Hoogland and Boon Pers. Comm. 2006). Further, it has been reported that zinc oxide paint has a high moisture sorption behavior [Dunn 1954].

Therefore, it is reasonable to assume that zinc oxide containing paints would be more reactive than those with lead white only since the capacity of moisture sorption could increase the hydrolysis of the oil network in the paint and thus lead to subsequent saponification of zinc and lead pigments.

The most significant optical effect of saponification is the partial disappearance

of the white pigments. Since white pigment particles are good light reflectors [Hunter 1975: 155-159], a loss of the interfaces of binding medium and pigment due to the interaction -would contribute to a decrease in total light reflectance. This allows the incident light to transmit through the upper layers and reach the lower paint layers. In other words it results in a relative increase of light absorption, i.e. a decrease in reflected light and as a consequence one expects an optical darkening, especially when upper paints are lighter than underlying paints. It is evident in the study of '*Speak! Speak!*', where both samples collected from a darkened area (s17) and from an apparently

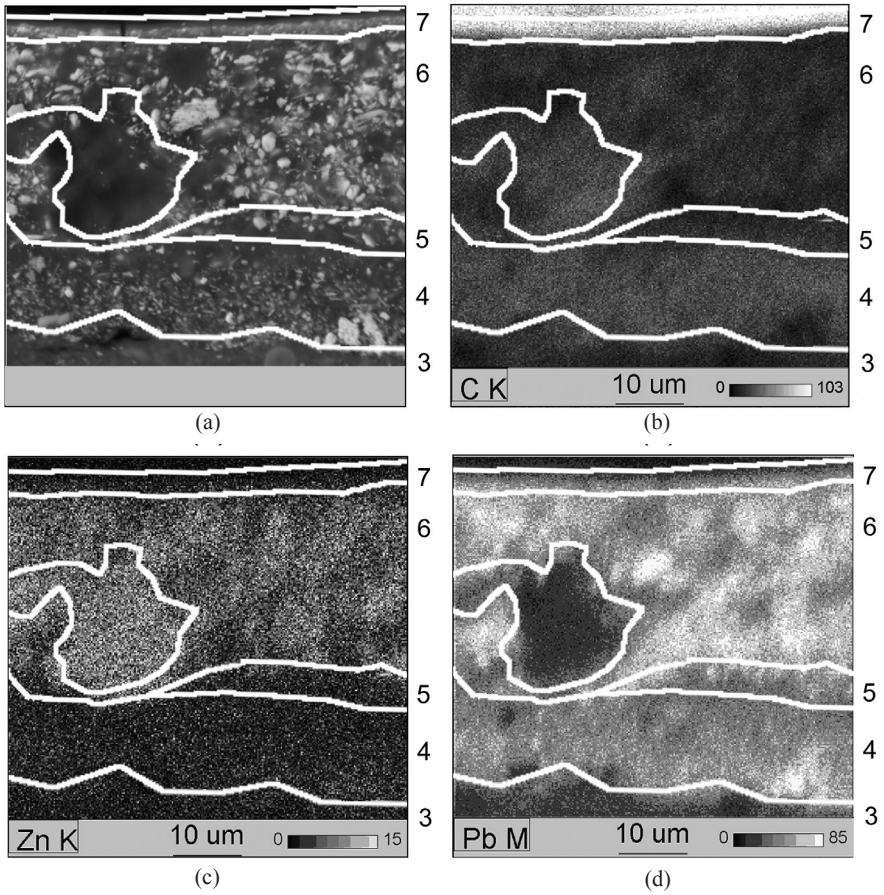

Figure 2.13 EDX mapping of s17 showing the elements distribution. (a) SEM BSE image of analysed area. (b) Mapping of carbon distribution showing relative high concentration of carbon in the marked area, layer 6. (c) Mapping of zinc distribution showing zinc is present mainly in layer 6. (d) Mapping of lead distribution showing lead is present in layer 6 as well as in layers 4 and 5.

optically unaltered area (s16) are highly saponified. Here only the s17 has darker paints underneath as well as a high amount of chrome yellow in the upper layer therefore it develops a darker appearance upon dissolution of the white pigments.

2.4 Conclusion

The combination of chemical analysis and detailed examination of the darkened areas in *Speak! Speak!* demonstrates that the relative light absorption of the paint layers is increased due to saponification of white pigments. The overall effect causes a darkening of the painting. On the other hand, the saponification by itself might not produce an appreciable optical darkening effect. The saponification of white pigments causes an increase in light penetration. Therefore, in the case of light reflecting from saponified paint layers or underlaying paint layers, the increase of light penetration has little effect. However, saponification in the upper paint layers painted over dark paint layers can lead to a severe optical effect as was demonstrated here. The critical factor is the color of the remaining paint and the color of the underlying paint. The presence of zinc white seems to more actively promote saponification compared to lead white alone because of its zinc white's hygroscopicity. This aspect needs to be further investigated [Shimadzu and Van den Berg 2006].

References

Boon, J.J., Van der Weerd, J., Keune, K., Noble, P., Wadum, J. 2002. Mechanical and chemical changes in old master paintings: dissolution, metal soap formation and remineralization processes in lead pigmented ground/intermediate paint layers of 17th century paintings. In: R. Vontobel, ed. *ICOM Committee for Conservation 13th Triennial Meeting, Preprints*. London: James & James, pp. 401- 406.

Boon, J.J. 2006. Processes inside paintings that affect the picture: chemical changes at, near and underneath the paint surface. In: J.J. Boon and E. Ferreira eds. *Reporting Highlights of the De Mayerne Program*. The Hague: NWO, pp.21-32.

Boon, J.J. and Asahina, S. 2006. Surface preparation of cross sections from traditional and modern paint using the Argon ion milling polishing CP system. *Microscopy and Microanalysis*, 12(S02), 1322-1323.

Church, A.H. 1890. *The Chemistry of Paints and Painting*. London: Seeley and Co. Limited.

Eibner, A. 1909. *Malmaterialienkunde –als Grundlage der Maltechnik*. Berlin: Verlag von Julius Springer.

Elm, A.C. 1957. Reevaluation of the Function of Pigments in Paints. *Official Digest*, 20, 351-385.

Dunn, Jr. E.J. 1954. Moisture Resistance of Paint Films. *Official Digest*, 26, 387-407.

Hackney, S., Townsend, J.H., and Ridge, J. 2004. Pre-Raphaelite Methods and Materials. In: Townsend, J.H., Ridge, J., and Hackney, S. eds. *Pre-Raphaelite Painting Techniques 1848-56*. Tate Publishing.

Heaton, N. 1928. *Outline of Paint Technology*. London: Charles Griffn & Co.

Higgitt, C., Spring, M., Saunders, D. 2003. Pigment-medium interactions in oil paint films containing red lead or lead-tin yellow, *National Gallery Technical Bulletin*, 24, 75-95.

Hunter, R. S. 1975. *The Measurement of Appearance*. John Wiley & Sons.

Jacobsen, A.E. and Gardner, W.H. 1941. Zinc Soaps in Paints: zinc oleates. *Industrial and Engineering Chemistry*, 33, Oct., 1254-1256.

Keune, K. 2005. *Binding medium, pigments and metal soaps characterized and localized in paint cross-sections*. PhD Dissertation. University of Amsterdam, Amsterdam, The Netherlands.

Keune K. and Boon, J.J. 2007. Analytical Imaging Studies of Cross-Sections of Paintings Affected by Lead Soap Aggregate Formation. *Studies in Conservation*, 52, 161-176.

Keune K., Kirsch, K., and Boon, J.J. 2007. Lead soap effluorescence in a 19th C painting: appearance, nature and sources of materials. In: Parkin, H.M. ed. *AIC paintings specialty group postprints of the 19th annual meeting*. AIC, pp. 145-149.

Kühn, H. 1963. Aspects of Panel-Painting. *Ciba Review*, 1, 3-36.

Laurie, A.P. 1926. On the Change of Refractive Index of Linseed Oil in the Process of Drying and its Effect on the Deterioration of Oil Paintings. *Proceedings of the Royal Society of London*, 112, 176-181.

Laurie, A.P. 1967. *The Painter's Methods and Materials*. New York: Dover Publications.

Noble, P., van Loon, A., and Boon, J.J. 2005. Chemical changes in old master paintings II: darkening due to increased transparency as a result of metal soap formation. In: I. Verger, ed. *ICOM Committee for Conservation 14th Triennial Meeting, Preprints*. London: James & James, pp. 496-503.

Ordonez, E. and Twilley, J. 1997. Clarifying the Haze; Efflorescence on Works of Art. *Analytical Chemistry*, 69, 416A-422A.

Reid, J.E. 1909. *Sir J.E. Millais, P.R.A*. Walter Scott Publishing Company, Limited.

Shimadzu, Y. and Van den Berg, K.J. 2006. On metal soap related colour and transparency changes in a 19th C painting by Millais. In: J.J. Boon and E.S.B. Ferreira, eds. *Reporting Highlights of the De Mayerne Program*. The Hague: NWO, pp. 43-52.

Spielmann, M.H. 1898. *Millais and his works, with special reference to the exhibition at the Royal Academy 1898: With a chapter "Thoughts on our art of to-day"*. Royal Academy of Arts (Great Britain).

Townsend, J.H. 1993. The refractive index of 19th-Century paint Media: A preliminary study. In: J. Bridgland, ed. *ICOM Committee for Conservation 10th Triennial Meeting, Preprints*. London: James & James, pp.586-592.

Tumosa, C.S. and Mecklenburg, M.F. 2005. The influence of lead ions on the drying of oils. *Reviews in Conservation*, 6, 39-47.

Van der Weerd, J., Boon, J.J., Geldof, M., Heeren, R.M.A., and Noble, P. 2002. Chemical Changes in Old Master Paintings—Dissolution, Metal Soap Formation and Remineralisation Processes in lead Pigmented Paint Layers of 17th Century Paintings. *Zeitschrift fur Kunsttechnologie und Konservierung*, 16, 36-51.

Van der Weerd, J., Geldof, M., Van der Loeff, L.S., Heeren, R.M.A., and Boon, J.J. 2003. Zinc Soap Aggregate Formation in 'Falling Leaves (Les Alyscamps)' by Vincent van Gogh. *Zeitschrift fur Kunsttechnologie und Konservierung*, 17(2), 407-416.

Van der Weerd, J., Van Loon, A., and Boon, J.J. 2005. FTIR Studies of the Effects of Pigments on the Aging of Oil. *Studies in Conservation*, 50, 3-22.

Van Eikema Hommes, M. 2004. *Changing Pictures –Discolouration in 15th to 17th Century Oil Paintings*. London: Archetype Publications Ltd.

Verhoeven, M.A., Carlyle, L., Reedijk, J., and Haasnoot, J.G. 2006. Exploring the application of solid-state Nuclear Magnetic Resonance to the study of the deterioration of paintings. In: J.J. Boon and E. Ferreira eds. *Reporting Highlights of the De Mayerne Program*. The Hague: NWO, pp. 33-42.

Chapter 3

Effects of lead and zinc white saponification on the surface appearance of a late 19th-century painting by Luke Fildes (Tate N01522 exh. 1891)

Changes in appearance due to metal soap formation in a late 19th century painting The Doctor by Luke Fildes (Tate N01522 exhibited in 1891) were investigated. Preferential saponification of zinc white in lead and zinc white containing paints was found in both light and dark areas. SEM-BSE imaging of an amorphous area of zinc soap suggests that this leads to a reduction in reflectance from the surface. Paint reconstructions demonstrate that saponification of white pigments causes a significant decrease in light reflection. The optical effects of saponification are perceptible, and depend on the color and hiding power of both the surface and underlying paints. This explains why the appearance of the painting can be altered to differing extents in different areas.

3.1 Introduction

The late 19th century painting '*The Doctor*' at Tate (Tate N01522) painted by Luke Fildes (English; 1843-1927) and exhibited in 1891 (Figure 3.1) was selected for scientific research to investigate a possible correlation between appearance changes and chemical changes. The main focus of the research was to verify whether its dark appearance today was the artist's intention or had been caused by transparency changes of the paint layers after completion of the work.

The figure of the father among the four figures: a girl, a doctor and the girl's parents in the painting is thought to be 'disappearing'. As the background of the figure is dark in appearance, merging of the father's figure into the dark background is also described as 'darkening'. This means that the color shades of the background and the figure have become so similar that there is little distinction between these two pictorial elements.

Examination of cross-sections prepared from sampling points where the appearance changes were observed indicates a presence of metal soaps in lower paint layers. Apparently unaffected paint layers are also present in both upper and lower layers within the same sample. Since the paint layer build-up is an important factor determining the surface appearance, the position of the paint layer where saponification takes place must be considered. The results of a technical examination of *The Doctor* are put into perspective through paint reconstructions applied to substrates of different colors, where optical effects on surface appearance due to saponification of whites in different stratigraphies are studied.

3.2 History of the painting

The first record of this painting is a sketch of Fildes working on the framed painting in his studio published in *The Art Journal*, 1891 (Figure 3.2) [Holden 1982]. After the first exhibition at the Royal Academy in 1891, the painting was purchased by Sir Henry Tate. The first conservation treatment recorded took place in 1921. The original varnish was removed. Conservation treatments have been carried out several times. Removal of blanching materials, revarnishing with synthetic resins, lining with beeswax, dammar and gum elemi heated to 65°C, and retouching with Paraloid B67 have been recorded.

Figure 3.1 '*The Doctor*' by Luke Fildes, exhibited in 1891 (Tate: N01522, 1664 × 2420 mm) ©Tate 2015

The original blind stretcher with four panels is in place. During one conservation treatment, a CHARLES ROBERSON stamp on the reverse was found, which is no longer visible due to the lining canvas. The stretcher has very thick members, to accommodate the considerable weight of the blind stretcher. The white ground, presumably preprimed, appears to be highly textured. It is noted in the conservation record that it matches the texture of samples from a Roberson No 2 or No 3, medium-fine 'stippled ground' [Holden 1982]. According to the surface examination, the paint was not thinned. Even heavy brushstrokes skip across the textured surface and leave a discontinuous paint film.

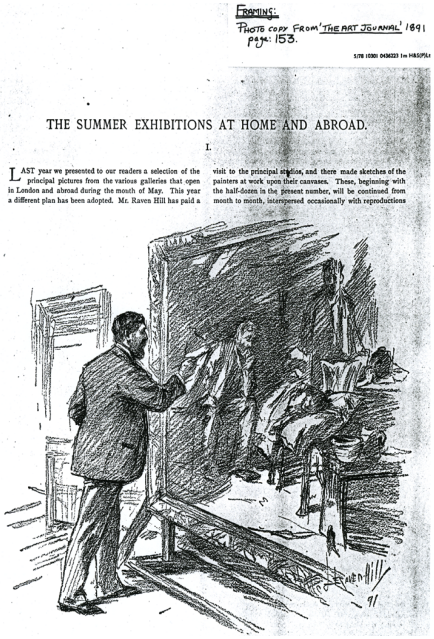
FRAMING:
PHOTO COPY FROM 'THE ART JOURNAL' 1891
PAGE: 153.

THE SUMMER EXHIBITIONS AT HOME AND ABROAD.

I.

LAST year we presented to our readers a selection of the principal pictures from the various galleries that open in London and abroad during the month of May. This year a different plan has been adopted. Mr. Raven Hill has paid a visit to the principal studios, and there made sketches of the painters at work upon their canvases. These, beginning with the half-dozen in the present number, will be continued from month to month, interspersed occasionally with reproductions

Figure 3.2 Sketch published in *The Art Journal* ©Tate 2015 [Holden 1982]

3.3 Identification of the painting materials

Fourteen samples were taken for examination of the materials used and their present chemical condition (Figure 3.3). All samples were examined using a stereo microscope and a light microscope. Identification of the pigment was mainly done by SEM in electron backscattered mode (BSE) combined with energy dispersive X-ray analysis (EDX) for elemental analysis, using the instruments in Appendix at the end of this volume. Mass analysis to examine organic components was performed on samples s4, s5, and s6. Results are listed in Table 3.1.

3.3.1 Identification of the pigment

Sample s1 was taken in the foreground of the left bottom corner. A brown paint is present over the priming, which consists of two white paints at the bottom of the cross-section (Figure 3.4). The first layer consists of calcium carbonate, lead white, and a small amount of barium sulfate. The main component of the second priming (layer 2) is lead white. A small amount of calcium carbonate and barium sulfate is also found.

In the paints, lead white and zinc oxide are the major white pigments used. The presence of zinc oxide was confirmed by the characteristic UV fluorescence of the

Figure 3.3 Sampling areas in '*The Doctor*' ©Tate 2015

Table 3.1 List of samples

Sample number	Surface color	Sample number	Surface color	Sample number	Surface color
s1	dark brown	s6	dark brown	s11	pale yellow
s2	white	s7	dark blue	s12	brown
s3	yellow	s8	bright red	s13	green
s4	dark brown	s9	deep yellow	s14	greenish blue
s5	dark blue	s10	mid yellow		

Table 3.2 EDX results of unembedded samples

Sample number	Surface appearance	Detected elements
s5	dark blue and red	Si, Al, Pb, S, Na, Ca, Fe, Hg, Zn
s7	dark blue	Al, Co, Pb, Si, Ca, (P, Na)
s8	bright red	Pb, S, Hg, Al, (Si, Ba)
s9	deep yellow	Pb, Fe, Si, AL, (Ca)
s10	mid yellow	Pb, Si, Al , Ba, Fe
s11	pale yellow	Pb, Zn, (Si, Fe)
s13	green	Pb, Cr, Zn, Si, Al, (Ca)
s14	greenish blue	As, Cu, S, (Al, Ca, Cl)

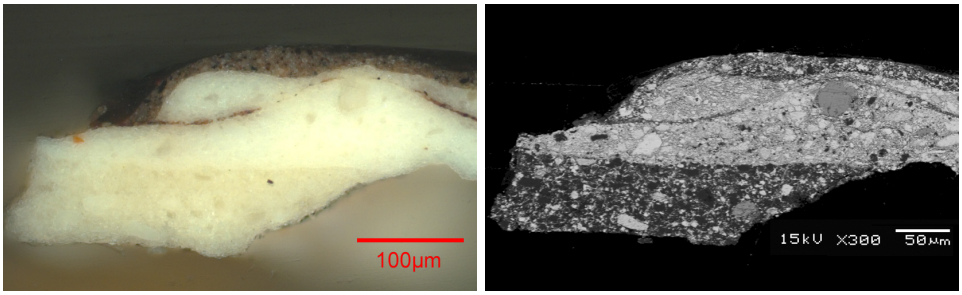

Figure 3.4 Two white priming layers in s1. *Left*: Visible light image in cross-section (VIS), *right*: SEM-backscattered electron (BSE) image.

pigment and zinc detection with EDX. Detection of iron in yellow and brown areas indicates the use of ochre as pigment (Table 3.2). Some brown paints also contain manganese suggesting the presence of umber. Cadmium yellow (CdS) was identified in samples s2 and s3. Sample s8 from a bright red area contains vermilion and possibly a red lake on an aluminum-based substrate. Reddish UV fluorescence in layer 10 of s2 and layer 13 of s3 was observed. EDX detected aluminum (Al) and phosphorus (P) from the area, which indicates an alumina substrate which was often used for Kopp's purpurin [Van Bommel *et al.* 2005].

Samples s4 and s7 contain cobalt blue and ultramarine blue. Dark areas of the background and shadow areas in the foreground were painted with these blue pigments. Bone black was also found in both samples.

The green lampshade on the wooden table at the right-hand side was painted with viridian (s13). The greenish highlight on the hanging lamp in the background (s14) was painted with emerald green. Emerald green was also found in the other samples.

3.3.2 Results of organic mass spectrometric analysis

Direct temperature resolved mass spectrometry (DTMS) and thermally assisted hydrolysis and methylation gas chromatography/mass spectrometry in combination with Curie Point pyrolysis (Py-TMAH-GCMS) were performed to examine the binding media. DTMS was applied to samples s2 to s6, while Py-TMAH-GCMS was applied to samples s4 to s6. The results are almost the same in all samples (Table 3.3). Drying oil components were detected in both DTMS and Py-TMAH-GCMS analyses. Ion fragments from saturated fatty acids in DTMS are stearic acid at *m/z* 284 (C16) and palmitic acid at *m/z* 256 (C18) (Figure 3.5). Py-TMAH-GCMS detected azelaic acid (2C9) in relatively high intensity.

All samples contain beeswax, which is due to the lining process during a past conservation treatment. The ion fragment at *m/z* 257, which is known as the ion fragment of the palmitic acid moiety from beeswax, was detected in a relatively

Table 3.3 Results of mass spectrometric analyses

	Detection components	s2	s3	s4	s5	s6
DTMS	FA:C16	++	++	++	++	++
	FA:C18	++	++	++	++	++
	Beeswax	+++	+	++	++	+
	Acrylate	++	+++	+++	+++	+++
	Triterpenoid resin	-	trace	trace	-	trace
	Lead	+++	+	+++	+++	++
	Zn/SO_2	++	+	+	+	
	Arsenate	-	+	trace	+	+
Py-TMAH-GCMS	FA:C16			++	++	++
	FA:C18			++	++	+
	FA:2C9			+++	+	++
	Acrylate			+++	+++	+++++

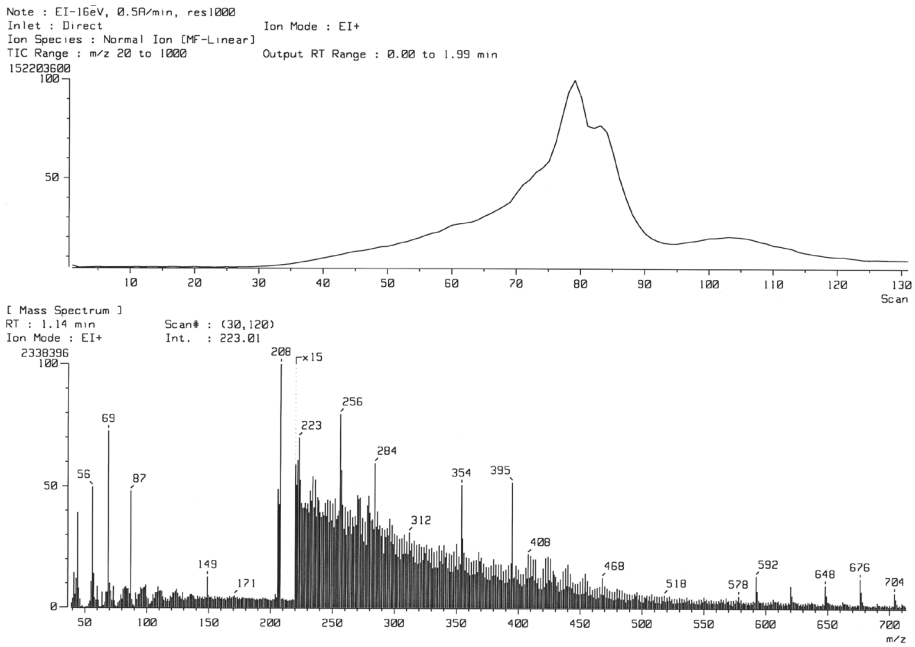

Figure 3.5 DTMS result of s6. Upper: total ion current chromatogram (TIC), Lower: summed spectrum of scan between 30 and 120. In addition to ion fragments from drying oil (*m/z* 256, 284), beeswax (*m/z* 592 etc.) and acrylate (*m/z* 69) ion fragments were detected.

high intensity in the DTMS analysis [Boon and Van Och 1996]. Series of wax ester molecular ions (C16FA~C24(+nCH_2)$_2$Alc) at *m/z* 592 620, 648, 676, and 704 are also observed in the spectra. The detection of beeswax in s3, s4, s5, and s6, which were taken from the middle-ground of the painting, indicates that the wax fully impregnated the paint layers.

An ion fragment detected at *m/z* 69 in DTMS originate from the acrylate Paraloid B67, which is another conservation material. A marker for this acrylate was also detected by Py-TMAH-GCMS. A trace of triterpenoid resin can be seen in DTMS spectra. It is not clear whether it is a remaining original varnish, a later varnish, or dammar resin from the wax-resin lining.

Besides the organic components, some inorganic components were detected with DTMS. Lead (*m/z* 208) was detected in the high temperature part of analysis. Zinc (*m/z* 64, 66, 68) or/and sulfate (as SO_2: *m/z* 64) and arsenate (III) (As_4O_6 *m/z* 395) were also detected. These components correspond to pigments found in the paints.

3.4 Examination of the paint layer build-up and saponification

The focus of the research in '*The Doctor*' is the figure of the father standing in the background. This figure appears to be sinking into the dark background and is fading away. Four samples among six paint cross-sections were taken to closely investigate this issue. The paint samples of s12 from the father's figure, s4 from the dark area, and s2 and s3 from light colored areas were examined in detail.

Specular reflection imaging FTIR of s2, s3 and s12 was used for the identification of metal soaps [Van der Weerd *et al.* 2003; 2005]. The argon ion polishing technique [Boon and Van der Horst 2008] was applied to s3 and s12 to investigate micro-structural features of the saponified paint layers.

Sample s2

Sample s2 was taken from the white cloth on the table on the left-middle edge side. This paint sample consists of eleven layers (Figure 3.6, Table 3.4). Layer 1 and 2 are priming layers discerned on the basis of the composition and the contrast in the SEM-BSE image. A thinly applied dark brown paint (layer 3) contains lead white, zinc white, red ochre, umber, and calcium carbonate or calcium sulfate. A brown paint (layer 4) is observed containing lead white, zinc white, red ochre, and bone black. A thin dark brown paint layer (5) is partially visible. On top a white paint layer (6) was applied. This paint consists of lead white and zinc white, which is apparent by light microscopic examination with UV light. A yellow paint (layer 7) on layer 6 contains

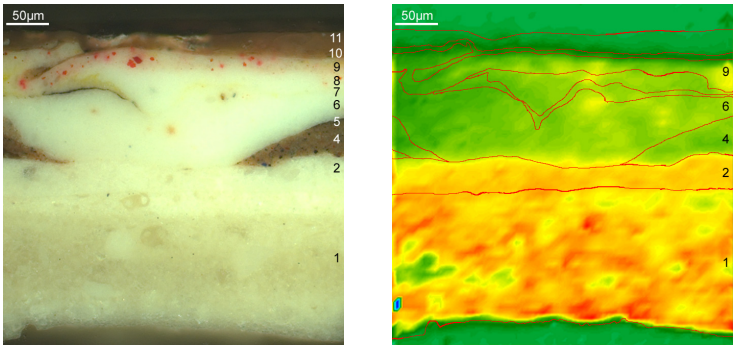

Figure 3.6 Cross-section s2 from the reddish white paint area (a) VIS, (b) UV fluorescence (UVf), (c) Image of 1404 cm^{-1} representing carbonate absorption from calcium carbonate and lead white (d) image of 1536 cm^{-1} representing metal carboxylate

Table 3.4 Layer build-up of s2 taken from the reddish white paint area

Layer	Thickness (µm)	Color in cross-section	Interpretation of light microscopic images and SEM-EDX
11	10		varnish (and retouch)
10	10	warm brown	red lake on aluminum based substrate
9*	10	reddish white	lead white, vermilion, lead soap
8*	10	white	lead whtie, zinc oxide, zinc soap
7*	3	yellow	lead white, zinc oxide, zinc soap, cadmium yellow
6*	10-30	white	lead whtie, zinc oxide, zinc soap
5*	2	dark brown	(no EDX was performed)
4*	10-15	brown	red ochre, bone black, lead white, zinc oxide, zinc soap
3*	3	dark brown	red ochre, umber, lead white, zinc oxide, calcium carbonate or sulfate
2	10-20	white	lead white, calcium carbonate, barium sulfate
1	>120	white	calcium carbonate, lead white, barium sulfate

The marked layers with '*' are affected by saponification.

cadmium yellow identified by EDX. The layer also contains lead white and zinc white. The detection of zinc by EDX is not only from zinc white but could originate also an impurity in cadmium yellow. The next layer (8) is again a white paint consisting of lead white and zinc white. Layer 9 is a reddish white paint layer over a white one with lead white, vermilion, and a small amount of red ochre. Specular reflection imaging FTIR detected absorption at around 1536 cm^{-1} from zinc- or lead- carboxylate in layer 3 to 9 (Figure 3.7). SEM back-scattered images corresponding to these areas show many dark, small dots supporting metal soap formation in these layers (see 3.5.2. below). Finally a warm translucent brown paint (layer 10) was thinly applied. Reddish UV florescence from this layer and detection of aluminum and phosphorous by EDX suggest the presence of a red lake. Layer 11 is the new varnish and shows retouching materials.

Sample s3

Sample s3 was taken from the yellow pillow in the middle ground where no significant appearance change was visible. Paint layer build-up of s3 consists of fourteen layers (Table 3.5). Layer 1 consists of lead and zinc whites, which are affected by saponification. Layer 2 is a lead white layer. Two brown paint layers (layer 3 and 5) out of four brown paint layers (layer 3 to 6) with ochre and umber are partially affected by zinc soap formation (Figure 3.7). Layer 4 contains aluminum implying the use of a red lake, a conclusion supported by a slightly reddish UV fluorescence. Layer 6 contains lead white, calcium carbonate, barium sulfate, and bone black. These four brown paint layers are presumably the painted shadow of the pillow. On layer 6 a thin lead white layer (layer 7) and a relatively thick white paint containing lead and zinc (layer 8) were applied. Zinc detected by EDX in combination with greenish UV fluorescence from some particles in layer 8 suggests a presence of zinc oxide (zinc white). Specular reflection imaging FTIR detected strong metal carboxylate absorption at around 1530 cm^{-1} in this layer indicating that saponification has taken place. Layer 9 is a slightly yellow paint containing mainly lead white. Partially visible is a purplish blue paint in layer 10. Subsequently a pale yellow paint (11) consisting of lead white, yellow ochre, cadmium yellow and calcium carbonate was applied. Layer 12 consists of mainly lead white and layer 13 is a thin top paint layer with a warm brown tone. Aluminum and phosphorous detected by EDX in layer 13 suggests a presence of red lake. Layer 14 is a thin varnish layer.

Sample s4

Sample s4 was taken in the middle-ground from a leg of one of the two chairs, on which the girl is lying. The surface color is dark brown. The cross-section shows indeed dark brown paint and also blue paints (Figure 3.8, Table 3.6). The first layer (layer 1) in the sample is identified as the second priming. On top there are eleven layers, which were not applied with an even thickness making the paint stratigraphy very complex.

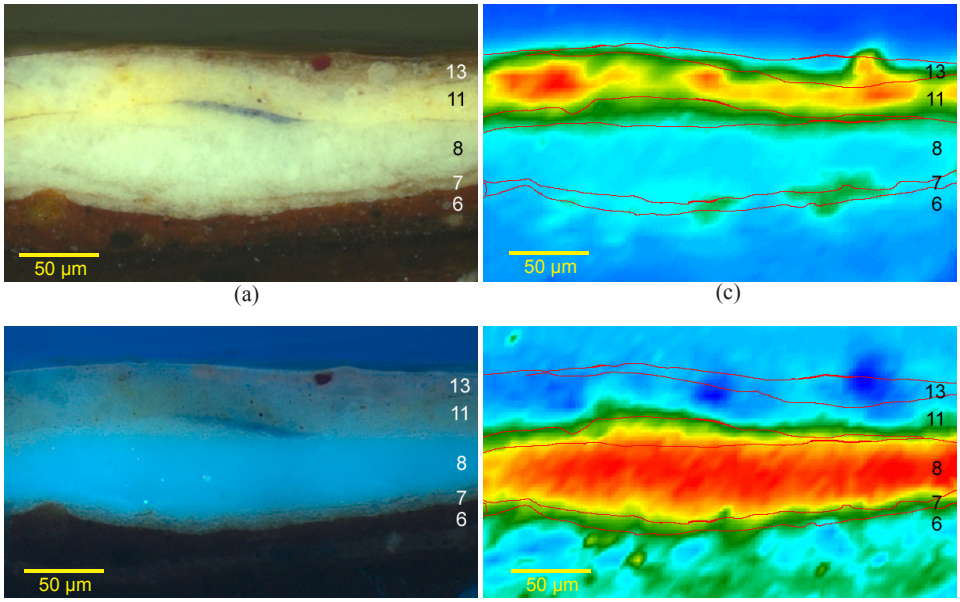

Figure 3.7 Cross-section s3 from the pale yellow paint area (a) VIS, (b) UVf, (c) image of IR absorption at 1409 cm^{-1} representing carbonate absorption from calcium carbonate and lead white (d) image of IR absorption at 1530 cm^{-1} representing metal carboxylates.

Table 3.5 Layer build-up of s3 taken from the pale yellow paint area

Layer	Thickness (µm)	Color in cross-section	Interpretation of light microscopic images and SEM-EDX
14	5		varnish
13	5-10	red	lead white, vermilion, red lake
12	10-25	white	lead white
11	10-25	pale yellow	lead white, yellow ochre, cadmium orange or yellow
10	5	purplish blue	(no EDX was performed)
9	10	white	lead white
8*	20-40	white	lead white, zinc soap, zinc oxide
7	10	white	lead white
6	15-25	brown	ochre, calcium carbonate, umber, lead white, bone black, barium sulfate
5*	10-15	brown	ochre, umber, lead white, zinc soap
4	10-20	brown	ochre, umber, aluminium compound as a lake substrate
3*	15-25	brown	ochre, lead white, zinc soap, bone black, calcium carbonate, umber, ultramarine blue
2	10	white	lead white
1*	>15	white	lead white, zinc soap

The marked layers with '*' are affected by saponification.

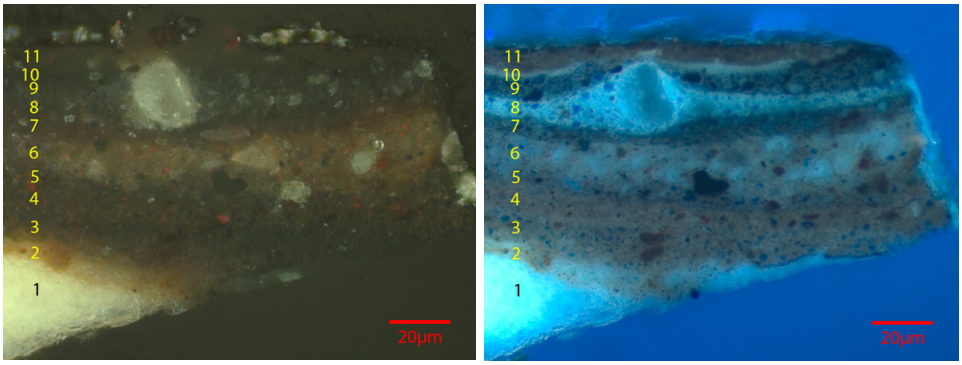

Figure 3.8 Cross-section s4 from the brown paint area. *Left*: VIS, *right*: UVf. Superimposed dark paint of blue and brown layers are observed.

Table 3.6 Layer build-up of s4 taken from the brown paint area

Layer	Thickness (µm)	Color in cross-section	Interpretation of light microscopic images and SEM-EDX
11	5-12	warm brown	red ochre, red lake, lead white
10	2-5	translucent	organic layer
9	5-10	blue	lead white, ultramarine blue, cobalt blue, bone black
8	5	blue	lead white, ultramarine blue
7	5	blue	lead white, cobalt blue, red ochre
6	10-20	brown	ultramarine blue, red ochre, lead white, bone black, dispersed zinc
5	5-10	violet	cobalt blue, red ochre, lead white
4	5-20	violet	ultramarine blue, red ochre, lead white
3	5-13	dark brown	ultramarine blue, red ochre, lead white
2	<10	light brown	lead white, red ochre
1	>40	white	lead white

It seems that the artist built up the dark and deep color appearance by applying several layers on top of each other. In general a blue paint consists of lead white and zinc oxide with cobalt blue or/and ultramarine blue (layer 7 to 9). Brown paints contain vermilion, red ochre, umber, and possibly a red lake (layer 2, 3 and 6). A mixture of blue and red particles presumably for violet/purple paint can be seen in layer 4 and 5. Lead white and zinc oxide were commonly present in almost all layers. Bright particles in SEM-BSE images confirm the presence of lead white pigment, whereas zinc was detected by EDX in a dispersed form suggesting the presence of zinc soaps. An organic layer (layer 10), which is evident by a light microscopic examination with UV light was applied on top of the deep blue paint (layer 9). A warm brown glaze consisting of a red lake on an aluminum based substrate was found in this sample as well (layer 11).

Sample s12

Sample s12 was taken from the left ear of the father. The paint layer build-up of s12 consists of nine layers (Figure 3.9, Table 3.7). Layer 1 consists of lead white, calcium carbonate, and barium sulfate, which must be a second ground when compared with other samples. Layer 2 is a thinly applied gray paint containing some black particles. A relatively thick light brown paint (layer 3) contains lead white, minium and zinc white reacting into zinc soaps. A strong metal-carboxylate absorption at 1530 cm^{-1} was detected in layer 3 to 5 by FTIR microscopy, although it was less intense in layer 3 and 4. Layer 4 is a brown paint containing lead white, minium, ochre, and dispersed zinc in metal soap form. Layer 5 is a yellowish brown paint containing ochre, lead pigments and dispersed zinc as metal soap (Figure 3.10). A few very thin layers, which are within about 5 µm in total (layer 6), were applied on layer 5. Layer 7 is an organic presumably resin varnish layer as suggested by strong UV fluorescence, poorly IR reflected, EDX (only C and O) and low back scatter electron reflectivity. The next layer (8) is a thinly applied translucent brown paint. The top paint (9) contains several pigments including lead white, vermilion, emerald green, and possibly madder lake. In addition dispersed zinc suggesting metal soap was detected by EDX in layer 9.

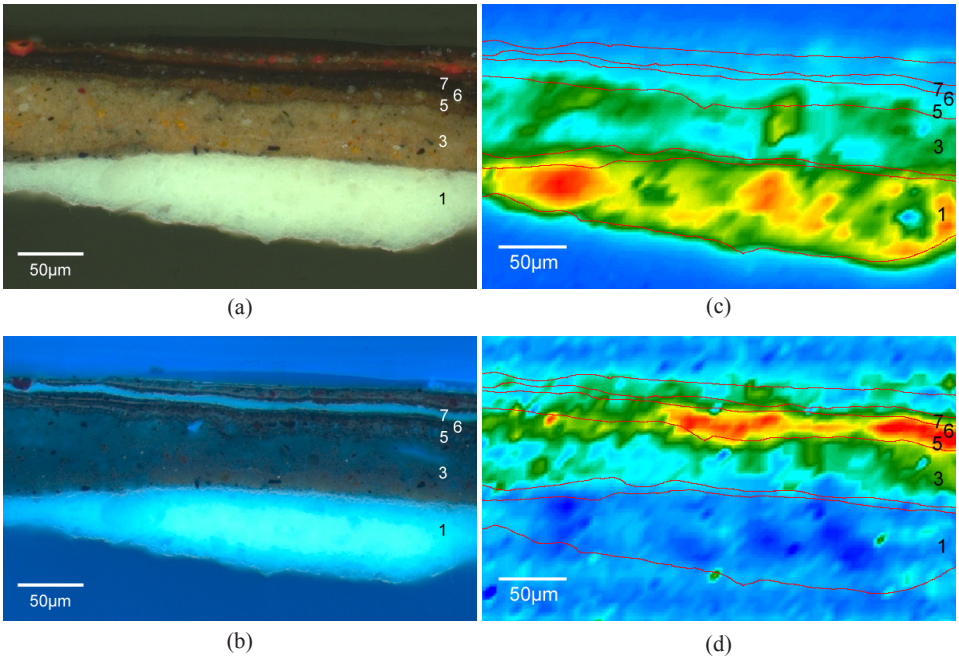

Figure 3.9 Cross-section s12 from the area of suspected appearance change. (a) VIS, (b) UVf, (c) image of IR absorption at 1428 cm^{-1}, representing carbonate absorption from calcium carbonate and lead white (d) image of of IR absorption at 1530 cm^{-1} representing metal carboxylates.

Table 3.7 Layer build-up of s12 taken from the fur cover painted area where appearance change suspected

Layer	Thickness (μm)	Color in cross-section	Interpretation of light microscopic images and SEM-EDX
9	3-5	reddish-brown	lead white, vermilion, zinc soap, emerald green, barirum sulfate, ochre, calcium carbonate, bone black
8	3-5	brown	calcium carbonate, lead white, ochre or/and umber
7	10	(organic layer)	strong UV fluorescence
6	5	dark brown(?)	(thinly applied 2-3 layers) ochre, lead white,
5*	5-15	brown	lead white, minium, zinc soap, lead soap, yellow ochre, umber, calcium carbonate
4*	10-15	translucent brown	lead white, minium, zinc soap, lead soap, ochre, calcium carbonate, cadmium
3*	50-60	light brown	lead white, minium, zinc soap, lead soap, zinc oxide barirum sulfate, ochre
2	5-15	gray	very thin layer containing black particles
1	>60	white	lead white, calcium carbonate, barirum sulfate

The marked layers with '*' are affected by saponification.

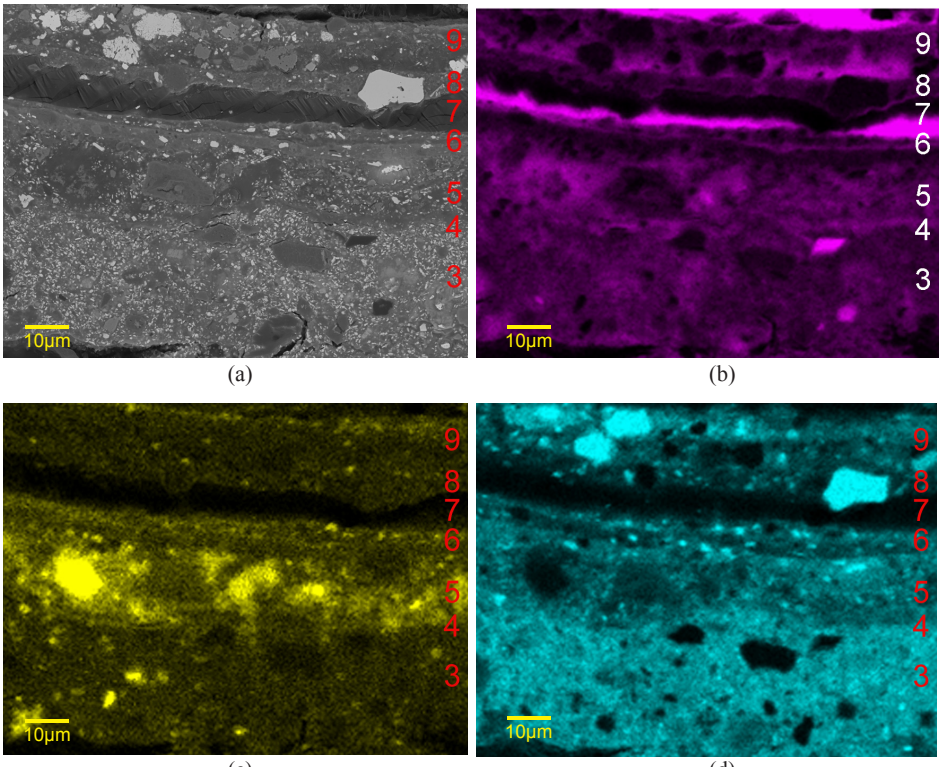

Figure 3.10 EDX mapping result of s12. (a) EDX mappeingn performed area, BSE image of layer 3 to layer 9 in s12, (b) carbon, (c) zinc, and (d) lead distribution

The data from all samples indicate that some of the paint layers are saponified. Large amorphous patches suggest zinc soaps in those layers where dispersed zinc could be detected by EDX. The saponifications are not confined to one paint layer but reflect a metal soap forming regime throughout the painting. The most strongly saponified layer in s3 is a white paint and is situated underneath intact lead white containing layers (11 and 12). The layers most notably affected by saponification in s12 are the brown paints, which are situated below the thin brown surface paint layers with some zinc soap and the organic intermediate layer (7).

3.5 Discussion

3.5.1 The artist's painting technique from the layer build-up

The layer build-up in the cross-sections point to possible working procedures, or how the artist could have painted the painting. The paint build-up of s2, for instance, shows that the white tablecloth (layer 6 to 8) was painted over the wooden table that was painted with brown paint (layer 3 to 5) (Figure 3.6). The surface was modified with reddish and translucent brown paint layers (layer 9 and 10) presumably to give a candle-lit effect. The same approach can be seen in s3 (Figure 3.7). At first the brownish dark blue shadow was painted and then the yellowish-white pillow paint was applied on top of this layer.

A similar practice was also observed in the dark colored areas. After the second white priming, in the case of s4, several blue and brown layers were applied building up a deep blue shade, which presumably depicts the dark shadow area of the background (Figure 3.8). Applying an extensive number of layers in s4 and s12 is a common feature of the dark areas (Figure 3.9). This suggests the artist's intention of making the dark color deeply dark. Layer 14, which is warm brown with a red lake, is possibly the one depicting the leg of the chair. In s12 mainly brown shades can be seen instead of blue as in s4. The application sequence of the paint – from the background towards the front – is the same as the one seen in s2 and s3.

3.5.2 Micro-structural features of metal soap forming paint layers

The relationship between the carboxylate absorption identified by the imaging FTIR technique and the morphology of the paint layers observed in the SEM-BSE image is discussed in this section.

All three samples analyzed (s2, s3, and s12) show the metal carboxylate absorption at around 1530 cm^{-1}. A relatively intense IR absorption at 1535 cm^{-1} was detected in layer 3 to 9 of s2 (Figure 3.6) which are the upper part of the paint layers; in layer 6 and 7 of s3 which are middle layers (Figure 3.7); and in layers above the second

priming of s12 (Figure 3.8). These areas can be brown, pale yellow and white in color suggesting there is no color association with the saponified layers. The presence of zinc white and lead white is a common feature supporting lead and/or zinc soap formation in these layers (see the identified pigments, Tables 3.4-3.7).

Lead carboxylate absorption from lead stearate or palmitate appears at around 1510 cm^{-1} and in paint samples will usually appear at around 1510-1540 cm^{-1} [Robinet and Corbeil 2003; Keune 2005:144-150]. Zinc-carboxylate absorption appears at 1530-1550 cm^{-1}. Therefore when both metal soaps are possible, identification of which metal soap has formed is barely possible using only FTIR and requires elemental analysis.

Detection of dispersed zinc by EDX and amorphous features in SEM-BSE in the layers with metal-carboxylate IR absorption strongly suggest formation of zinc soaps. Close observation of the ion polished cross-sections by SEM-BSE reveals the detailed micro-structural features of these layers. All layers with metal carboxylates show comparable SEM-BSE images (Figures 3.11-3.13). The most noticeable feature is dark

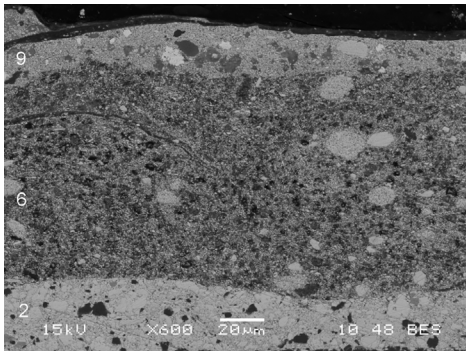

Figure 3.11 BSE image of the saponified layer in s2

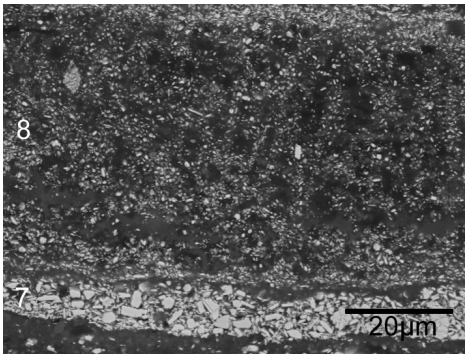

Figure 3.12 BSE image of the saponified layer in s3

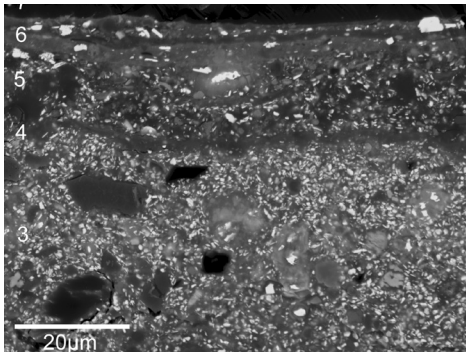

Figure 3.13 BSE image of the saponified layer in s12

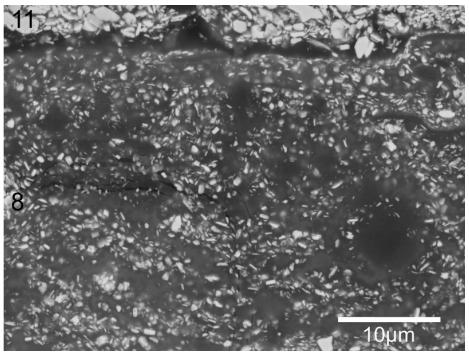

Figure 3.14 Micro-structural feature of saponified paint layer 8 and intact lead white containing layer 11 in s3.

patches (ca. 10-20 μm in diameter) due to low electron reflectance in layer 8 of s3 and layer 3 to 5 of s12. In these areas zinc is detected by EDX but zinc containing particles are indistinct. Similar dark patches in the SEM-BSE images have been recognized before and the patches were identified as aggregates of zinc-soap in other late 19th century oil paintings [Keune and Boon 2007].

Some greenish UV fluorescence particles in zinc carboxylate rich layers are likely remaining zinc white, suggesting that the source of zinc in the painting was the zinc oxide. Although zinc can be present in other pigments (notably zinc sulfide) or driers (such as zinc sulfate) or even as an additive to tube paint (zinc stearate, though not necessarily at his date), EDX results exclude possible other zinc containing pigments as no metals correlating with other zinc containing pigments were detected. A zinc source as drier cannot be excluded. However, a drier added by a manufacturer should have been there in a limited amount (typically 1-5%) and addition of a drier by the artist is also less expected since the paint is white. Furthermore, the reactivity of zinc oxide to fatty acid was noted in the past and its reactive tendency towards zinc soap formation has been proven [Jacobsen and Gardner 1941; Kühn 1986].

In contrast, lead white particles (ca. 0,5-2 μm in diameter) are found in the saponified layers (eg. layer 8 in s3). The high electron reflectivity of the particles and the sharp borders of the crystals indicate that lead white crystals are intact. The lead white crystals are oriented around the zinc soap rich areas and clearly outline their circumference (Figure 3.14). On the other hand, formation of lead soaps is also indicated in the paint layers that contain lead containing pigments dominantly such as layer 3 in s12 and layer 9 in s2. A close SEM examination combined with light microscopic examination in s12 reveals that both lead white and minium (lead tetroxide) were very likely saponified (Figure 3.15). Some minium particles may be present as a result of recrystallization from lead soaps [Van der Weerd 2002], rather than because they were chosen by the artist. Lead soap appears hazy in the SEM-BSE image (Figure 3.16) owing to new formation of nanocrystals of lead carbonate, a phenomenon

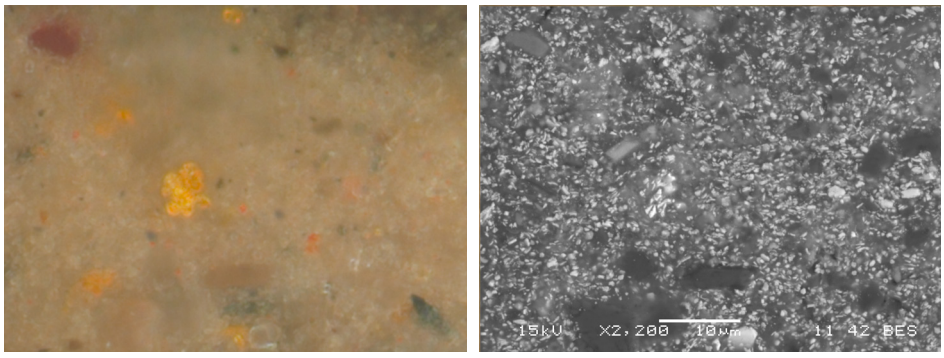

Figure 3.15 (a) VIS of layer 3 in s12 where possible lead soap were formed (b) BSE image corresponding to the image (a)

that has been seen often, most clearly in lead soap aggregates in the *Anatomy lesson of Doctor Nicolaes Tulp* of Rembrandt van Rijn in 1632 (Mauritshuis, The Hague, The Netherlands) [Noble *et al.* 1998; Boon *et al.* 2002].

It is known independently that zinc oxide is more reactive to fatty acid components than lead white [O'Neill and Brett 1969]. A relatively large amount of reactive fatty acids must be available in this painting considering the wide spread formation of metal soaps based on both zinc and lead.

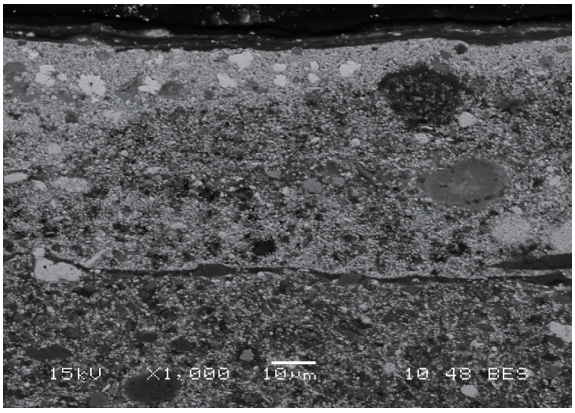

Figure 3.16 Contrast difference between lead and zinc soap aggregates in s2. Two metal soap mass at the right-hand side. The dark mass corresponds to zinc soap, the hazy mass below the dark mass corresponds to lead soap suggested by EDX.

In summary, the results of the FTIR and SEM examination indicate that layers with zinc oxide and lead containing pigments have saponified. The saponified areas tend to appear dark or translucent in light microscopic images because their refractive indices are near that of oil. In addition, extremely fine particles, less than half of the shortest wavelength of visible light, which corresponds to about 0,4 µm diameter, will no longer reflect light regardless of their refractive index [Stieg 1962]. Particle sizes of zinc oxide are known to be small and sometimes approach the limit of light scattering ability [Heaton 1928: 80]. Fully transparent zinc whites are even commercially available. The low BSE contrast and hazy area in the SEM-BSE images not only point to saponification of the original pigments, but could also indicate disintegration of original particles or remineralisation processes [Boon *et al.* 2007]. Moreover mixing lead white and zinc white might have made the situation worse. Lead white and zinc white mixtures were commonly produced in the contemporary paint industry in the 19th century to improve paint properties such as opacity and workability: it is quite possible that the artist used these mixtures unconscously. However, it becomes clear that the beneficial aspects could become a disadvantage in course of time. Opacity improvement by mixing two different types of pigment is largely due to an increase complexity in scattering ability [Stieg 1973]. However, smaller particles sizes will be easily affected by saponification. Furthermore, the smaller particle sizes of zinc white must have resulted in a higher absorption of oil than only lead white pigmented paint thus leading to an extra amount of reactive fatty acids forming carboxylates. All these changes on the microscopic level influence the optical properties of the aged paints and are expected to result in macroscopically noticeable appearance changes.

3.5.3 Experiments testing the optical effects of saponification

The optical effects of saponification were modeled using various relative concentrations of zinc white and zinc stearate. This approach was taken since saponification of pigments in oil paint is difficult to achieve in a controlled way (Hoogland and Boon Pers. Comm. 2006). In addition, a key aspect in saponification of the white pigments from an optical point of view is not the formation of metal soaps alone but loss of the original white pigments, if we ignore the volume changes due to the metal soaps formed.

A refractive index (RI) of commercial zinc stearate 1.48-1.50 measured by refractometry at room temperature is close to the RI of oil film at ca. 1.49-1.51 [Townsend 1993]. Although strictly speaking metal soaps are not transparent in oil, it is assumed here that metal soaps are effectively transparent. As an actual paint formulation is extremely complicated, model paints were simplified and designed containing barium sulfate (Blanc fix: De Kat), which was a common extender (as natural or synthetic) in the 19th century. Zinc oxide was chosen as the main white in this study.

The model paints were applied to a black and white chart (Byko-charts, BYK-Gardner GmbH) with a wet thickness 60 μm using the paint applicator describe in chapter 1. Colors were measured by a spectrophotometer (Minolta, CM-2600d, illuminant D65 and a 10° observer, using CIELAB1976 color space) after drying. The color measuring area was 8 mm in diameter, and more than three spots were measured on each black and white substrate, and averaged.

The results are shown with CIELAB1976 (L*, a*, b*) color space and some with spectral reflectance graphs. Each mean L*a*b* data, both specular component and UV component of the illuminant excluded, was used to create the color images in Photoshop® (color picker tool) and illustrated in Figures 3.17-3.19 and 3.21. These images were made to provide an impression of how the color change might be seen while the accuracy was not questioned. ΔL* was obtained by subtracting L* value of the paint on the black substrate (L*b) from L* value of the paint on white substrate (L*w). Δa* and Δb* were calculated in the same manner. Generally, smaller ΔL*Δa*Δb* indicates being closer to complete hiding[1].

1: Hiding power of a paint layer is the ability to cancel out optical characteristics, mainly color, of the underlying layer. To completely hide light reflection from the lower paint, light has to be all reflected or/and absorbed at the upper layer. A white layer hiding a layer underneath means hiding by light reflection. High hiding power by a colored layer can be achieved by the combination of light absorption and reflection. A black upper layer can hide the layer underneath by light absorption. Although both the blue and brown paints are highly translucent at certain wavelengths, the transparency was lost due to a large portion of the combined light absorption of the two paints. In this case, scattering ability changes as a result of saponification in a lower paint layer can be ignored as demonstrated. The color of an underpaint layer is important, especially when the upper paint is translucent with respect to the underlying paint.

Experiment 1: Saponification in a white paint

The standard paint consists of zinc white and barium sulfate in a one to one ratio in volume. Pigment volume concentration (PVC), which is the percentage of the total volume of pigments in a paint (pigments and binding media), was set at 30%, which is relatively low assuming an extreme case. Various paints with decreased amounts of zinc white were made by replacing zinc white with the same volume of zinc stearate (Table 3.8 for the detailed set up).

Table 3.8 Model paint formulations in Experiment 1

	Sample name	Zinc oxide	Zinc stearate	Barium sulfate	Oil
(1a)	ZnBy	0.56 g (0.1 cm^3)		15% (0.44g, 0.1cm^3)	70% (0.44g, 0.47cm^3)
		15%			
(1b)	ZnBySt-3	0.45 g (0.08 cm^3)	0.02 g (0.02 cm^3)		
		12%	3%		
(1c)	ZnBySt-6	0.34 g (0.06 cm^3)	0.04 g (0.04 cm^3)		
		9%	6%		
(1d)	ZnBySt-9	0.22 g (0.04 cm^3)	0.07 g (0.06 cm^3)		
		6%	9%		

Figure 3.17 Reconstructed image of the model paints. (1a) 15%, (1b) 12%, (1c) 9%, and (1d) 6% ZnO from Experiment 1. See Tables 3.8 and 3.9.

Table 3.9 L*a*b* data of the model paints in Experiment 1

Sample code	On white substrate			On black substrate			Δvalues (eg. ΔL*=L*w-L*b)		
	L*w	a*w	b*w	L*b	a*b	b*b	ΔL*	Δa*	Δb*
(1a)	88.76	-2.03	12.38	75.06	-2.57	-0.14	13.70	0.54	12.51
(1b)	88.72	-2.30	14.48	74.70	-2.84	0.97	14.02	0.54	13.52
(1c)	89.44	-2.58	14.58	73.04	-2.83	0.68	16.40	0.25	13.90
(1d)	89.31	-2.71	16.32	66.01	-2.66	-1.36	66.01	-2.66	-1.36

Visual observations and color measurement of the white paints demonstrated that conversion of zinc oxide to zinc stearate led to an increase of ΔL* indicating increased transparency, revealing the color of the underlayer (Table 3.9, Figure 3.17). Even though the transparency change in sample (1d) ZnBySt-9 is evident, when only the paints on the white substrate are compared, there is little difference in the reflectance. This confirms that transparency change of white paint on top of a light paint is small and may not be perceptible by the eye. In contrast, saponification of white pigments in the top layer over a dark underlayer might lead to a significant appearance change due to loss of hiding power.

Experiment 2: Translucent brown paint on saponified white paint

To verify the optical effects of saponification situated in lower paint layers, a translucent brown paint[2] was applied on the white paints from Experiment 1. Zinc stearate in the white paint hardly affects the appearance (Figure 3.18). ΔL* of the translucent brown paint directly applied on the black and white chart is shown in Table 3.10. The low reflectance on the black substrate is apparent indicating that the paint is rather translucent. The large value of ΔL* is however drastically diminished when the brown paint was applied on top of the white paints. The ΔL* from each brown surface is smaller than that of the corresponding paint in Experiment 1 (Table 3.10). This is because the original contrast between the black and white charts was already largely reduced by the white paints underneath. The results demonstrate that the top paint mostly determines the surface appearance if the underlayer is reasonably white regardless of reflectivity changes in the white underpaint. The hiding power of the top layer is therefore of key importance.

Table 3.10 L*a*b* data of the model paints in Experiment 2

Sample code	On white substrate			On black substrate			Δvalues (eg. ΔL*=L*w-L*b)		
	L*w	a*w	b*w	L*b	a*b	b*b	ΔL*	Δa*	Δb*
(2a)	58.34	17.20	52.49	46.07	15.58	43.41	12.26	1.62	9.08
(2b)	50.56	21.28	50.88	46.16	15.97	43.13	4.40	5.31	7.75
(2c)	55.06	19.54	52.96	49.14	12.53	41.82	5.93	7.01	11.14
(2d)	55.65	19.31	52.48	47.11	9.97	36.50	8.54	9.34	15.97
(e)	60.31	16.41	56.05	24.11	1.38	13.87	36.20	15.03	42.18

2: Formulation of translucent brown paint: refined linseed oil (Gamblin Artists Colors Co.) 1,40 g, Blanc fix (De Kat) 0,90g, Reseda Lemon 0,56g, Pompeii red 0,09g, and Gold ochre light 0,11g (Kremer Pigmente GmbH & Co. KG).

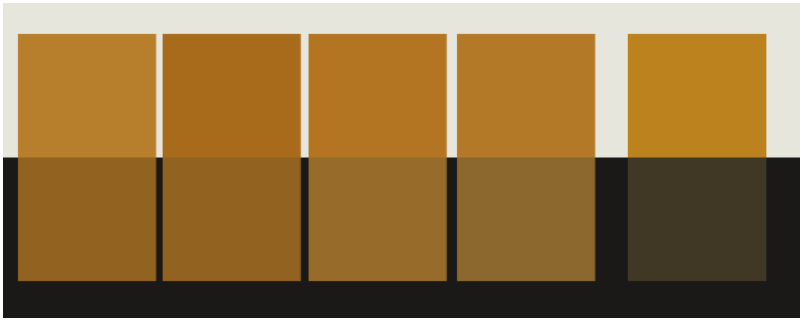

Figure 3.18 Reconstructed image of the model paints. (2a), (2b), (2c), and (2d) translucent brown paint on (1a), (1b), (1c), and (1d) of Experiment 1 respectively. (e) the translucent brown paint applied directly on black and white chart with 30 μm wet thickness. See Tables 3.8 and 3.10.

Experiment 3: Saponification in a blue paint

The optical effect of saponification of zinc white in a blue paint was studied also. Three pairs of blue paints with and without zinc stearate were made (Table 3.11). Within a pair, the paints contain the same volume of oil, synthetic ultramarine blue, and barium sulfate. The only difference is the ratio zinc white to zinc stearate. The PVC (zinc stearate as a pigment) was again 30%.

The appearance differences illustrated in Figure 3.19 are striking. A large shift in Δb* between samples (3j) ZnBy-blueC and (3k) ZnBySt-blueC (Table 3.12) indicates that the saponification in a colored layer would cause a significant color shift. A relatively large shift towards more intense blue on white substrate, indicated by b*w of

Table 3.11 Model paint formulations in Experiment 3

	Sample name	Zinc oxide	Zinc stearate	Ultramarine blue	Barium sulfate	Oil
(3f)	ZnBy03blue-A	0.55 g (0.098 cm^3)	0	0.005 g (0.002 cm^3)	0.44g (0.1cm^3) 15%	0.44g (0.47cm^3) 70%
		14.7%		0.3%		
(3g)	ZnBySt03blue-A	0.27 g (0.048 cm^3)	0.055 g (0.05cm^3)	0.005 g (0.002 cm^3)		
		7.2%	7.5%	0.3%		
(3h)	ZnBy03blue-B	0.50 g (0.09 cm^3)	0	0.023 g (0.01 cm^3)		
		13.5%		1.5%		
(3i)	ZnBySt03blue-B	0.22 g (0.04 cm^3)	0.055 g (0.05 cm^3)	0.023 g (0.01 cm^3)		
		6.0%	7.5%	1.5%		
(3j)	ZnBy03blue-C	0.45 g (0.08 cm^3)	0	0.047 g (0.02 cm^3)		
		12.0%		3.0%		
(3k)	ZnBySt03blue-C	0.17 g (0.03 cm^3)	0.055 g (0.05 cm^3)	0.047 g (0.02 cm^3)		
		4.5%	7.5%	3.0%		

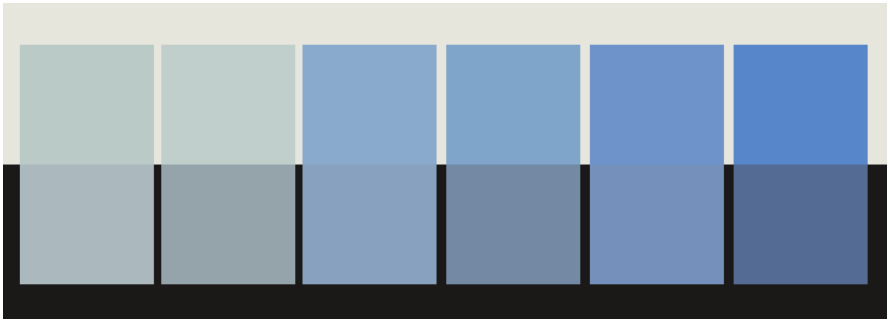

Figure 3.19 Reconstructed image of the model paint from Experiment 3. (3f) ZnBy-blueA, (3g) ZnBySt-blueA, (3h) ZnBy-blueB, (3i) ZnBySt-blueB, (3j) ZnBy-blueC, and (3k) ZnBySt-blueC. See Tables 3.11 and 3.12.

Table 3.12 L*a*b* data of the model paints in Experiment 3

Sample code	On white substrate			On black substrate			Δvalues (eg. ΔL*=L*w-L*b)		
	L*w	a*w	b*w	L*b	a*b	b*b	ΔL*	Δa*	Δb*
(3f)	80.20	-5.78	-0.89	73.85	-3.99	-4.35	12.26	-1.79	3.46
(3g)	81.67	-5.97	-0.83	65.43	-3.52	-6.38	16.24	-2.45	5.55
(3h)	67.79	-5.50	-21.34	65.35	-4.43	-18.11	2.44	-1.06	-3.22
(3i)	65.53	-6.69	-23.68	55.61	-3.62	-16.68	9.92	-3.07	-7.00
(3j)	60.44	-1.93	-33.71	57.49	-2.32	-25.39	2.95	0.39	-8.33
(3k)	56.32	-0.39	-41.09	45.39	-1.05	-24.48	10.92	0.66	-16.61

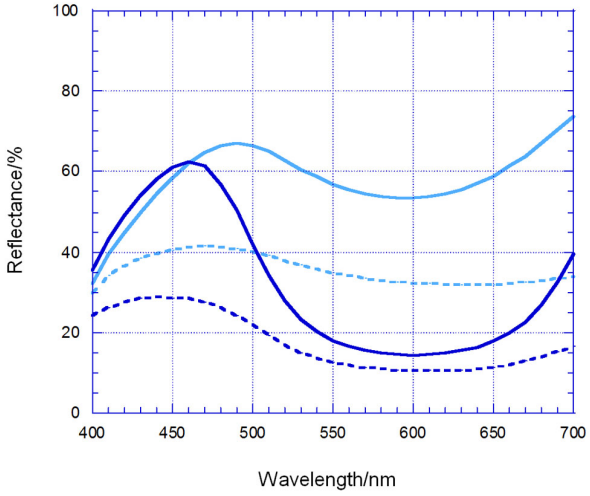

Figure 3.20 Light reflectance spectra of (3g) ZnBySt-blueA and (3k) ZnBySt-blueC
Light blue lines (3g) ZnBySt-blueA, blue lines (3k) ZnBySt-blueC
Solid lines: the blue paints on white substrate
Broken lines: the blue paints on black substrate

the pair C, suggests an appearance change even with a white underlayer. Focusing on transparency, despite the fact that the amount of zinc stearate in samples (3f) ZnBySt-blueA and 3k are equal, the sample 3f shows a higher transparency above 500 nm due to less light absorption in that spectral region (Figure 3.20). The ΔL* between the pair A is a little larger than that of the pair C also suggesting that the pair A is more translucent than the pair C. If only refractive indices are considered as a factor of transparency, this result would be a contradiction as the pair A contains more zinc oxide (RI 2.0) and less ultramarine blue (RI 1.5-1.6) than the pair C. Since absorption of light is much more effective on reaching high hiding [Stieg 1962; 1973], the whiter paint - pair A - that has less absorption appeared more translucent than the pair C. The pair A however shows the least difference in color shift. The results suggest that visual perception is more sensitive to color shift than transparency change and perceptible appearance change depends very much on the formulation of paint. The result also implies that color changes due to saponification in a colored layer situated below a translucent paint layer can't be neglected.

Experiment 4: Translucent brown paint on saponified blue paint

The translucent brown paint, which was used in Experiment 2, was applied on the blue paint from Experiment 3. The results are shown in Figure 3.21 and Table 3.13. As was observed in Experiment 2, the appearance difference within a pair in Experiment 3 was almost lost. This is because that the translucent brown paint absorbs light at shorter wavelengths where the blue paint reflects light (Figures 3.22, 3.23). The brown paint itself has a rather small scattering ability, therefore it has a light brown reflectance when it is present on a white substrate, but an extremely low reflectance on a black substrate. This means that the brown paint needs to be illuminated by non-blue-absorbing light, otherwise the blue light will be absorbed by the brown paint. However in Experiment

Figure 3.21 Reconstructed image of the model paint from Experiment 4. Brown paint on the blue paint from Experiment 3. (4f) ZnBy-blueA, (4g) ZnBySt-blueA, (4h) ZnBy-blueB, (4i) ZnBySt-blueB, (4j) ZnBy-blueC, and (4k) ZnBySt-blueC underneath. See Tables 3.8 and 3.13.

4, there is a blue paint underneath which absorbs light at longer wavelength. The characteristic blue light reflection appears at around 460 nm, which is still a light absorbing region of the upper brown paint. As a consequence, the light around this region has already partially been absorbed by the upper brown paint and does not reach the blue paint, therefore almost no blue light reflects. In the lower wavelength region, the opposite absorption and scattering of light occurs; the blue absorbs light so that there will be a small amount of light to reflect at the surface. This is evident in pairs of B (samples 4h and 4i) and C (samples 4j and 4k).

Table 3.13 L*a*b* data of the model paints in Experiment 4

Sample code	On white substrate			On black substrate			Δvalues (eg. ΔL*=L*w-L*b)		
	L*w	a*w	b*w	L*b	a*b	b*b	ΔL*	Δa*	Δb*
(4f)	53.79	13.22	41.31	48.50	13.41	36.33	5.29	-0.19	4.98
(4g)	49.40	17.35	39.15	44.09	11.40	30.53	5.31	5.94	8.62
(4h)	45.71	9.37	30.63	44.72	9.81	29.84	1.00	-0.44	0.79
(4i)	44.43	8.71	29.47	41.69	7.81	25.72	2.75	0.90	3.75
(4j)	42.71	6.65	25.84	41.65	7.73	24.79	1.06	-1.08	1.05
(4k)	38.85	7.12	23.46	37.58	6.35	21.48	1.27	0.78	1.97

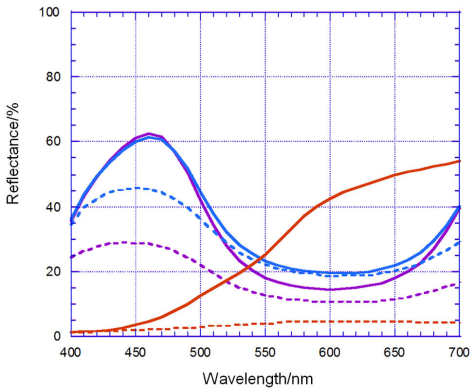

Figure 3.22 Reflectance spectra of independent paint samples
Blue lines: (3j) ZnBy-blueC paint
Violet lines: (3k) ZnBySt-blueC paint
Brown lines: (e) the translucent brown paint
Solid lines: each paint on white substrate
Broken lines: each paint on black substrate

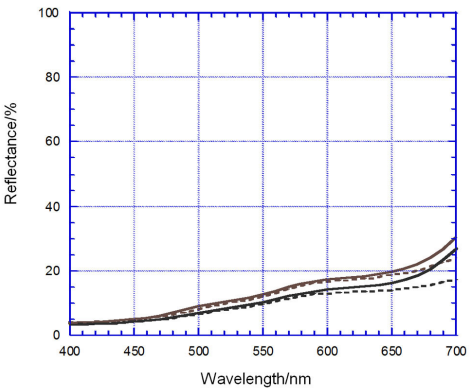

Figure 3.23 Reflectance spectra of (4j) the brown on ZnBy-blueC and (4k) the brown on ZnBySt-blueC
Gray lines: (4j) brown on ZnBy-blueC paint
Black lines: (4k) brown ZnBySt-blueC paint
Solid lines: each paint on white substrate
Broken lines: each paint on black substrate

3.5.4 Implications for the interpretation of appearance changes in '*The Doctor*'

The common practice of an artist working from a dark background to lighter objects in the foreground, followed here by Fildes, leads to the application of dark and translucent paints over the objects or background. This type of layer build-up was observed in both s3 and s12. In the case of s3, the saponified white layer was situated under light colored paints, which contain intact lead white. No obvious optical defects on the surface were visible to the eye.

In the case of s12 the saponified colored layers are situated below the translucent dark paints and the transparent resin layer, and on top of the white second ground. As Experiment 3 demonstrated, saponification of the white pigments in a colored paint layer will cause a relative darkening of the paint and may lead to a drastic appearance change. This result suggests that layer 3-5 will have a darker appearance. The resin layer 7 might function additionally as a yellow filter if the resin yellowed. Although it is unknown how effectively, it is suggested that more light could be absorbed by this layer which will contribute to making the surface appear even darker. Besides, the finely dispersed zinc in layer 9 suggests some degree of saponification and disintegration of zinc oxide particles, which contributes to a decrease in light reflection. Experiment 2 demonstrated that a surface paint has a strong effect determining a surface appearance, so a small change in the optical properties of the top paint layer should not be underestimated. The overall degree of appearance change is thus dependent on the paint build up, original formulation of paints and present color of the underlayers, and therefore not easy to derive. On the other hand, Experiment 4 demonstrated that paint layer build-up plays an important role in paint appearance. Even when an upper paint layer is highly translucent depending on the color of underlying paint layer, the opacity may be high due to a large amount of light absorption. At any rate, the whole paint system of s12 is developing towards conditions, where light absorption is increasing and light reflection is diminishing. Hence, the father figure in the painting is fading away.

3.6 Conclusions

Scientific examination of '*The Doctor*' has shown preferential saponification of zinc oxide over lead carbonate, in both dark and light paint samples. These areas correspond to the low electron reflective areas in the SEM-BSE images and close observation points out that pigment particles have indeed reacted away. Dispersed zinc distribution as detected by EDX also points to the formation of zinc soaps.

The resulting optical defects are less obvious in the light colored paint areas. In contrast, saponification of white pigments in a darker colored paint is leading to a darkening of the paint, which is resulted from a relative decrease in light reflection by the lowering of the refractive index via a change in composition of the white pigments.

Metal soap formation may easily be perceptible in appearance but depends on the color and hiding power of the paints below and on top. This however has a great impact on the appearance of the picture as seen by the eye. It is concluded that the "disappearing" of the father figure in *The Doctor* is predominantly caused by chemical and physical changes of zinc white on a microscopic level [Shimadzu *et al.* 2008].

References

Boon, J.J. and Van Och, J. 1996. A Mass Spectrometric Study of the Effect of Varnish Removal from a 19th Century Slovent-sensitive Wax Oil Painting. In: J. Bridgland, ed. *ICOM Committee for Conservation 11th Triennial Meeting, Preprints*. London: James & James, pp. 197-205.

Boon, J.J., Van der Weerd, J., Keune, K., Noble, P., Wadum, J. 2002. Mechanical and chemical changes in old master paintings: dissolution, metal soap formation and remineralization processes in lead pigmented ground/intermediate paint layers of 17th century paintings. In: R. Vontobel, ed. *ICOM Committee for Conservation 13th Triennial Meeting, Preprints*. London: James & James, pp. 401- 406.

Boon, J.J., Hoogland, F., and Keune, K. 2007. Chemical processes in aged oil paints affecting metal soap migration and aggregation. In: Parkin, H.M. ed. *AIC paintings specialty group postprints of the 19th annual meeting*. AIC, pp. 16-23.

Boon, J.J. and Van der Horst, J. 2008. Remarkably improved spatial resolution in SEM images of paint cross-sections after argon ion polishing. In: J.H. Townsend, T. Doherty, G. Heydenreich and J. Ridge eds. *Preparation for Painting: the Artist's Choice and its Consequences*. London: Archetype, pp. 42-49.

Heaton, N. 1928. *Outline of Paint Technology*. London: Charles Griffn & Co.

Holden, C. 1982. Luke Fildes R.A. 1844-1927 'The Doctor' 1890-91. In: *Completing the Picture: Materials and Techniques of twenty-six paintings in the Tate Gallery*. London: Tate Gallery, pp. 65-68.

Jacobsen, A.E. and Gardner, W.H. 1941. Zinc Soaps in Paints: zinc oleates. *Industrial and Engineering Chemistry*, 33, Oct., 1254-1256.

Keune, K. 2005. *Binding medium, pigments and metal soaps characterized and localized in paint cross-sections*. PhD Dissertation. University of Amsterdam, Amsterdam, The Netherlands.

Keune K. and Boon, J.J. 2007. Analytical Imaging Studies of Cross-Sections of Paintings Affected by Lead Soap Aggregate Formation. *Studies in Conservation*, 52, 161-176.

Kühn, H. 1986. Zinc white. In: R.L. Feller ed. *Artists' Pigments: a Handbook of their History and Characteristics vol. 1*. Washington DC: National Gallery of Art, pp. 169-186.

Noble, P., Wadum, J., Groen, K., Heeren, R., and Van den Berg, K.J. 1998. Aspects of 17th Century Binding Medium: Inclusions in Rembrandt's Anatomy Lesson of Dr Nicolaes Tulp. *Art et chimie, la couleur Actes du congrés*, 126-129.

O'Neill, and Brett, R.A. 1969. Chemical reactions in paint films. *Journal of the Oil and Colour Chemists' Association*, 52, 1054-1074.

Robinet, L. and Corbeil, M. 2003. The characterization of Metal Soaps. *Studies in Conservation*, 48, 23-40.

Shimadzu, Y., Keune, K., Van den Berg, K.J., Boon J.J., and Townsend, J.H. 2008. The effects of lead and zinc saponification on surface ap-pearance of paint. In: J. Bridgland, ed. *ICOM Committee for Conservation 15th Triennial Meeting, Preprints*. New Delhi: Allied Publishers Ltd., pp.626-632.

Stieg, F.B. 1962. The Geometry of White Hiding Power. *Official Digest*, 10, 1065-1079.

Stieg, F.B. 1973. Pigments/Binder Geometry; Interparticulate relationships. In: T.C. Patton, ed. *Pigment Handbook III: Characterization Physical Relationships*. Wiley, pp. 203-217.

Townsend, J.H. 1993. The refractive index of 19th-Century paint Media: A preliminary study. In: J. Bridgland, ed. *ICOM Committee for Conservation 10th Triennial Meeting, Preprints*. London: James & James, pp.586-592.

Van Bommel, M.R., Geldof, M., and Hendriks, E. 2005. An investigation of organic red lake pigments used by Vincent Van Gogh (November 1885 to February 1888). *Art Matters, Netherlands Technical Studies in Art*, 3, 111-137.

Van der Weerd, J., Boon, J.J., Geldof, M., Heeren, R.M.A., and Noble, P. 2002. Chemical Changes in Old Master Paintings—Dissolution, Metal Soap Formation and Remineralisation Processes in lead Pigmented Paint Layers of 17th Century Paintings. *Zeitschrift fur Kunsttechnologie und Konservierung*, 16, 36-51.

Van der Weerd, J., Geldof, M., Van der Loeff, L.S., Heeren, R.M.A., and Boon, J.J. 2003. Zinc Soap Aggregate Formation in 'Falling Leaves (Les Alyscamps)' by Vincent van Gogh. *Zeitschrift fur Kunsttechnologie und Konservierung*, 17(2), 407-416.

Van der Weerd, J., Van Loon, A., and Boon, J.J. 2005. FTIR Studies of the Effects of Pigments on the Aging of Oil. *Studies in Conservation*, 50, 3-22.

Chapter 4

Changing contrast in Verster's self-portrait (Stedelijk Museum De Lakenhal, S 766, 1921)

A self-portrait of F.H. Verster (Stedelijk Museum De Lakenhal, Leiden, The Netherlands, inventory no. S 766), which currently shows a somber appearance, was subjected to scientific investigation in order to find the reasons for its changed appearance. Close observation of the painting and existing black and white photographs mostly from the exhibition catalogues suggest that the painting has suffered severe contrast changes over time.

Evidence is found for a combination of two mechanisms, which change the appearance. Saponification of white pigments and the fading of a red lake are proposed to have distorted the original color contrast in several paint areas, resulting in the painting's somber appearance.

4.1 Introduction

Several paintings by Floris Hendrik Verster (1861-1927, Dutch) appear considerably dark and seem to have lost their color balance [De Wal 2002; Van den Berg *et al.* 2002]. The self-portrait of Verster painted in 1921 (Stedelijk Museum De Lakenhal, Leiden, The Netherlands, inventory no. S 766, catalogue no. 277a) (Figure 4.1) made available for our research must also have suffered considerable appearance changes. This was suggested by the current somber appearance and substantiated by photographs and prints of exhibition catalogues in black and white. According to the current appearance, our first hypothesis was that the saponification of white pigments was to blame for this appearance change, similar to the previous painting studies in Chapters 2 and 3.

In this chapter, a comparison of the various photos over a period of almost a century will be the first approach for determination of Verster's original intention. Then paint cross-sections will be investigated with light and electron microscopy and EDX; the binding media will be studied with mass spectrometric techniques in order to determine the binding medium. Paintouts were also made in order to visualize and support the hypothetical cause of the painting's contrast change.

4.2 Changes in photographs

4.2.1 Photographs and prints

The self-portrait was exhibited in public at an exhibition in 1927, which was dedicated to the artist [Utrechtsch Museum 1927]. The exhibition catalogue has a printed image of the self-portrait (image ID: PEC1927) (Figure 4.2, Table 4.1). In 1929, in another exhibition, the image of the self-portrait was laterally reversed in the catalogue (image ID: PEC1929) (Figure 4.3) [Den Haag 1929]. Two developed photographs of this painting have been stored in the Netherlands Institute for Art History (RKD: Rijksbureau voor Kunsthistorische Documentatie, The Hague). One of these (image ID: BWP-RKD, the photo is not shown) and the two prints of PEC1927 and PEC1929 completely match their outlines and shapes (group A) indicating that they are from a common negative.

Figure 4.1 *Self-portrait* by Floris Hendrik Verster painted in 1921, Stedelijk museum De Lakenhal, Leiden (Inventory no. S 766, and catalogue no. 277a: 405 × 305 mm) (Photo taken in 2013) ©Lakenhal 2015

Catalogues of other exhibitions in 1937 and 1941 also contain photographs of the painting (PEC1937 and PEC1941 respectively) (Figure 4.4) [Huinck and Scherjon 1937; De Wal 2002]. These prints look very similar and might have been printed from the same negative or photograph (group B). The two images are sharper and show stronger contrast with a larger number of light to dark steps than those of group A. This suggests a different negative for A and B, although this may have been the result of a modification of the contrast in the reproduction process.

The Museum de Lakenhal owns two developed photographs. One of the black and white photos has a note 'exhibition in 1952' (image ID: BWP1950s). It indeed matches a print in an exhibition catalogue of 1952 (image ID: PEC1952) [Stedelijk Museum 1952] (Figure 4.5). The main difference of these two (group C) with group B is the contrast difference at the right ear of Verster (see below).

Another photograph in the Museum de Lakenhal seems to be a black and white photograph, which was taken in 2002 when the color image (image ID: DCP2002) was also taken. The exhibition in 2002 was focused on Verster's works and the color photograph (DCP2002) was printed in the exhibition catalogue (Figure 4.6) [De Wal 2002]. Other color photographs were taken during our investigation in 2007 with a digital camera (image ID: DCP2007) (Figures 4.1, 4.6).

4.2.2 Comparison

There are some areas in the painting, the photographs and prints showing probable changes in contrast in the course of time. In order to compare color images to the other black and white photos, the color photos (DCP2002 and DCP2007) were converted into grayscale images (DCP2002bw and 2007bw respectively) with Photoshop® software (Figure 4.6).

Early photography was sensitive to light but not color [Eder and Epstean 1945: 457]. It was 1884 a color sensitive plate became commercially available called orthochromatic [ibid: 468-473]. This film was however insensitive to red (and orange) therefore red was reproduced dark in the photograph. On the other hand, the film was too sensitive to blue thus the blue was much lighter than red and orange. In 1920's, panchromatic film became universally available that was sensitive to all colors including red [Newhall 1949: 116].

The oldest photograph in this study, which was taken in between 1921 and 1927, was possibly reproduced from an orthochromatic film. Considering the characteristics of film, Verster's tie partially painted with blue must have reproduced light and fresh tone (eg. his right cheek) could have been darker, but they are not [Windisch 1956: 35-47]. Therefore it can be assumed that the oldest photo was reproduced from a panchromatic film though, the print PEC1927 is excluded for the contrast comparison in case the assumption was a mistake.

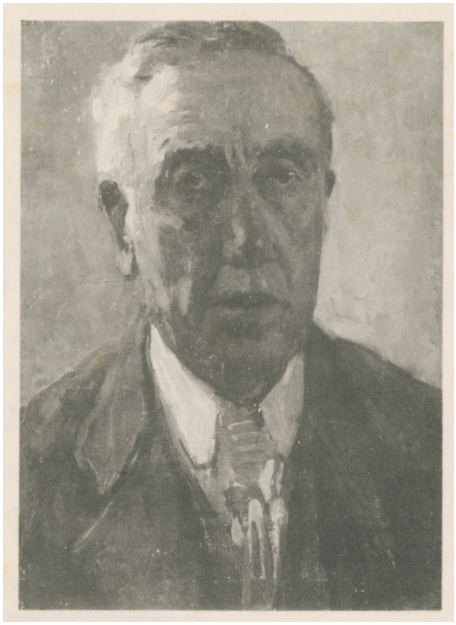

Figure 4.2 Printed black and white photograph in the exhibition catalogue of 1927 [Utrechtsche Museum] (PEC1927)

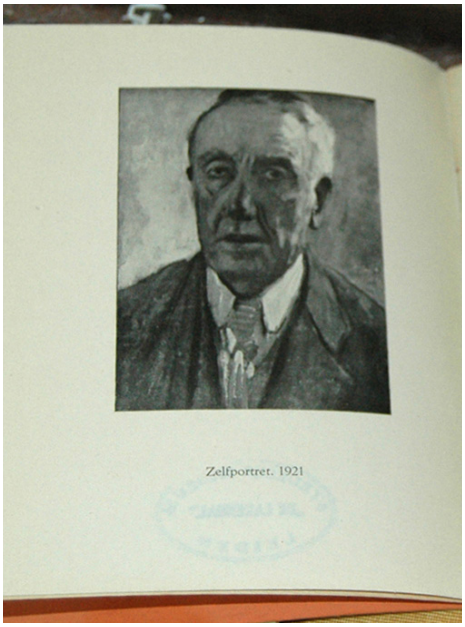

Figure 4.3 Laterally reversed black and white photograph in the exhibition catalogue of 1929 [Den Haag] (PEC1929)

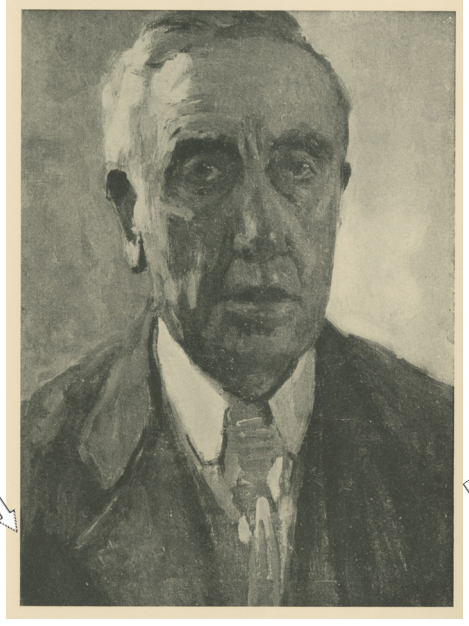

Figure 4.4 Printed black and white photograph in the exhibition catalogue of 1937 [Huinck and Scherjon] (PEC1937)

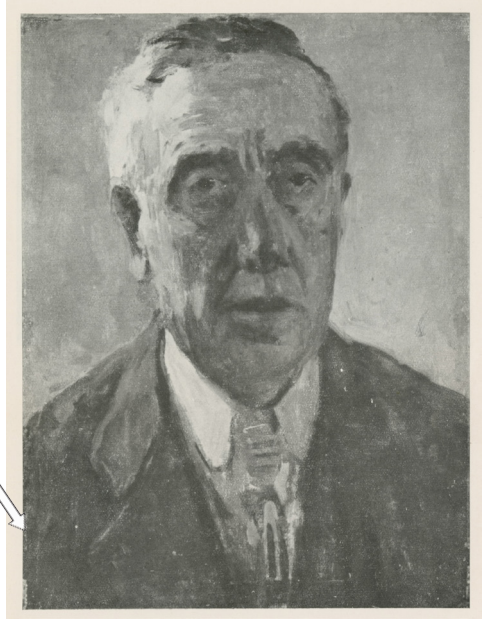

Figure 4.5 Printed black and white photograph in the exhibition catalogue of 1952 [Stedelijk Museum] (PEC1952)

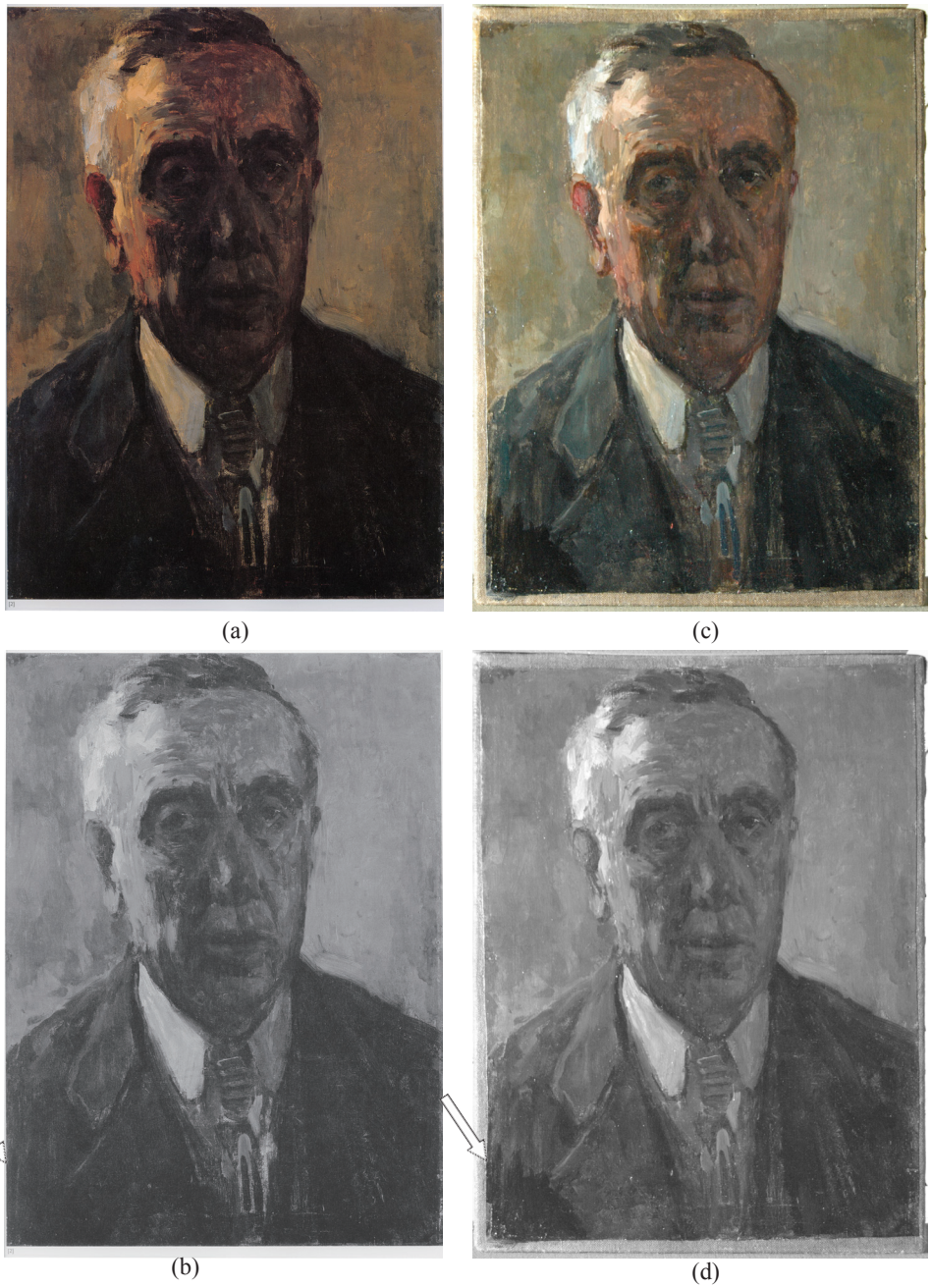

Figure 4.6 Color photographs taken in 2002 and 2007 and their grayscale images ©Lakenhal 2015
(a) color photograph taken in 2002 [De Wal] (DCP2002)
(b) grayscale image converted from (a)
(c) color photograph taken in 2007 (DCP2007)
(d) grayscale image converted from (c)

Table 4.1 List of photographs and printed images

ID name	Origin	Information	Group
BWP-RKD	Black and white photograph in RKD	with a frame	A
BWP1950s	Black and white photograph in Lakenhal	note 'tentoonst Lakenhal 1952'	C
BWP2002	Black and white photograph in Lakenhal	original photo of the exhibition catalogue of 2002	
PEC1927	Exhibition catalogue of 1927		A
PEC1929	Exhibition catalogue of 1929	Printed in mirror image	A
PEC1937	PEC1937Exhibition catalogue of 1937		B
PEC1941	Black and white image with caption 1941	re-printed in exhibition catalogue of 2002	B
PEC1952	Exhibition catalogue of 1952		C
DCP2002	Scanned color photo taken for exhibition catalogue of 2002 (color)		
DCP2007	Taken in 2007 (color)		

When the grayscale images converted from the above images that are in color, are compared to the image of PEC1937, the contrast at Verster's forehead was drastically increased and as a result it is now patchy. The color image of DCP2007 suggests that this patchy contrast is associated with the build-up of the layers. In the darker area in the black and white photos, there is a blue-violet paint beneath a brown surface paint layer (Figure 4.7). The surface color, of which the brown paint is directly on the white ground, is lighter as it can be seen in Figure 4.7.

Another area, which also indicates a possible contrast change, is around Verster's ears, especially his right ear. In PEC1937 for instance, the ear appears darker than its surroundings (Figure 4.8). On the other hand, DCP2007bw shows that the ear has become lighter, and the same trend is observed in DCP2002bw. Looking at PEC1952, the corresponding area is similar to that of the DCP2007 grayscale. In other words, his right ear was dark in grayscale image of PEC1937 but has become lighter in the images of after 1952. In the color image, the upper half of the right ear looks reddish gray, but according to the earlier photographs, the red color must have been more intense, which made the area darker in the black-and-white-photographs.

Furthermore, brushstrokes of the grayish paint in especially the right half of the face, are relatively predominant and make the contrast stronger. Similar grayish paint is seen at the eye white of right eye, which looks rather dark gray in DPE2007 that is not understandable as the artist's intention (Figure 4.7).

Contrary there is inconsistency in the contrast difference in the photographs and prints that are probably not an actual contrast change but can be a result of different conditions under which the photos were taken or of development of the negative and/or

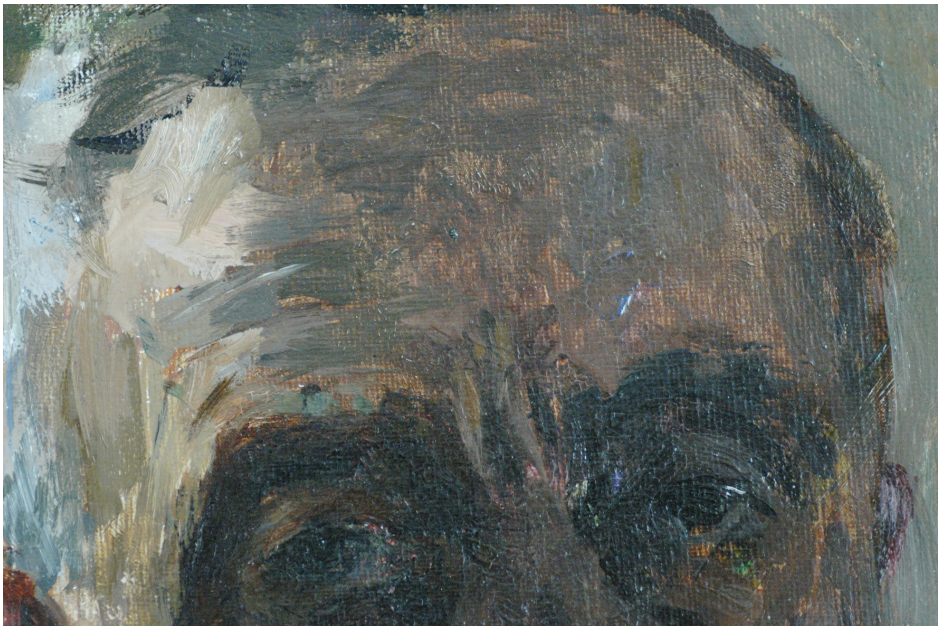

Figure 4.7 Detail of Verster's face depicted area. Underlying blue-violet paint is visible at his forehead. Eye white of the right eye is not white but grayish.

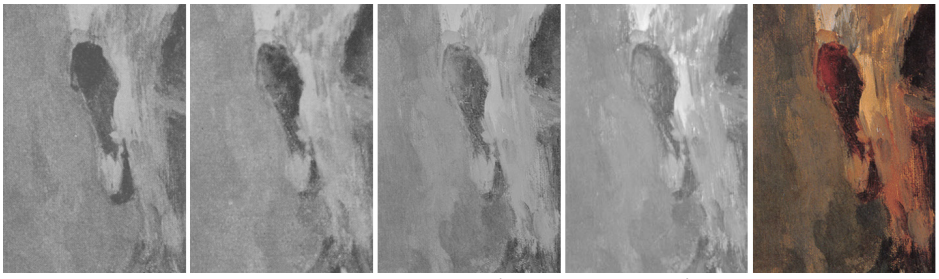

Figure 4.8 Contrast change at Verster's right ear depicted area in the prints and photographs

printing of the photograph, when a number of photographic papers made from different combinations of white pigment and extender for the backing layer, would have been available. The color information being recorded must have been influenced by different illumination conditions such as light intensity and direction. In addition, printing conditions may have been different. For instance, DCP2002 and DCP2007, both in the color images and their grayscale versions, their appearance differs extensively. It is however assumed that there are no obvious actual contrast changes between DCP2002 and DCP2007, considering they were taken within a relatively short time period.

The colorfulness of DCP2007 compared to DCP2002 is probably caused by a larger amount of light used for DCP2007. Another example where the use of photographs is problematic is Verster's black jacket of the left-bottom where a contrast difference is observed. In DCP2002 in grayscale (Figure 4.6 (b)), a slight contrast difference is observed at the left bottom corner, while DCP2007 in grayscale (Figure 4.6 (d)) shows a rather strong contrast in the corresponding area. On the black and white photograph of PEC1937, there is also a slight contrast difference (Figure 4.2). In PEC1952, however, almost no contrast difference is visible (Figure 4.5). The contrast scale in this area is not consistent. Regarding this area, it is concluded that there has been always a contrast difference after the completion of the work, but whether the degree of contrast changed or not is not known. A contrast ratio is determined photography conditions such as illumination, and could have been manipulated during the development. Therefore, determining a contrast change at such areas would be difficult on the basis of photo comparison alone.

The changes in contrast in the course of time are indicated by the black-and-white photographs and the recent color pictures as well as the current appearance of the painting itself giving strong support for the assumption that color changes have taken place leading to a changed appearance of Verster's Self-portrait.

4.3 Conservation history of the painting

4.3.1 Identification of the lining materials

The painting is lined but the date of the lining process is unknown. The lining materials were analysed with both direct temperature resolved mass spectrometry (DTMS) and thermally assisted hydrolysis and methylation gas chromatography/mass spectrometry in combination with Curie Point pyrolysis (Py-TMAH-GCMS). The sample (277a-02) was taken from the edge of the lined canvas with a scalpel (Figure 4.9, Table 4.2).

Characteristic ion fragments from colophony and beeswax were found in the DTMS chromatogram and spectrum (Figure 4.10). The indication of beeswax is the detection of ion fragments at *m/z* 592, 620, 648, 676, and 704 [Boon and Van Och 1996]. The presence of colophony was indicated by the detection of abietane related compounds. Ion fragments detected at *m/z* 239, 285, and 300 are assigned to dehydroabietic acid (DHA) formed by oxidation of abietane diterpenoid acids [Mills and White 1994: 98-99; Van den Berg *et al.* 1996]. Further oxidation of DHA leads to various oxo or hydroxy compounds. A mass peak at *m/z* 253 indicates the presence of 7-oxo-DHA. The ion fragment of *m/z* 315 is assigned to 15-hydroxy-7-oxo-DHA.

Furthermore, the presence of larixol and larixyl acetate was indicated with Py-TMAH- GCMS analysis pointing to the presence of Venetian turpentine (Figure 4.11) [Mills and White 1994: 100-102; Van den Berg *et al.* 2000].

Colophony, Venetian turpentine and beeswax were commonly used as lining

Figure 4.9 Sampling areas ©Lakenhal 2015

Table 4.2 Sample list

Sample no.	Sampling area	Surface appearance	Aims
277a-01	The edge of the painting on left-hand side	n/a	Varnish analysis
277a-02	The edge of the lined canvas	n/a	Lining material analysis
277a-03	Forehead	Brown	Paint compositions and layer build up
277a-04	The paint drip near one of pin holes at the right	Grayish brown and dull green	
277a-05	The background near his face	Bluish gray	
277a-06	The black jacket where a red paint drip was visible underneath	Black	
277a-07	Proper right collar of the shirt	Slightly bluish light gray	
277a-08	The black jacket at the bottom edge	Black	

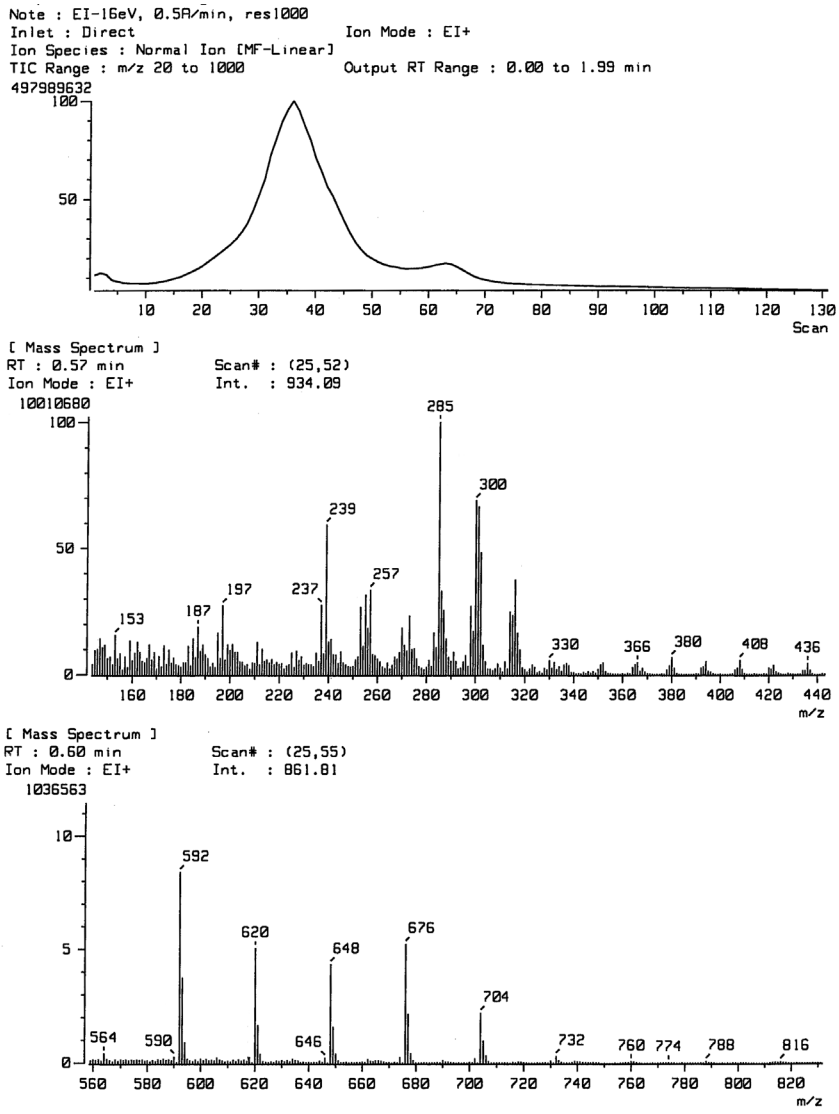

Figure 4.10 DTMS result of the lining materials (sample 277a-02): *Upper*; TIC (total ion current) chromatogram. Partial mass spectra of scans 25-52 showing volatile fractions: *middle*; ion fragments indicating colophony (*m/z* 239, 285, and 300), *lower*; ion fragments indicating beeswax (*m/z* 592 etc.).

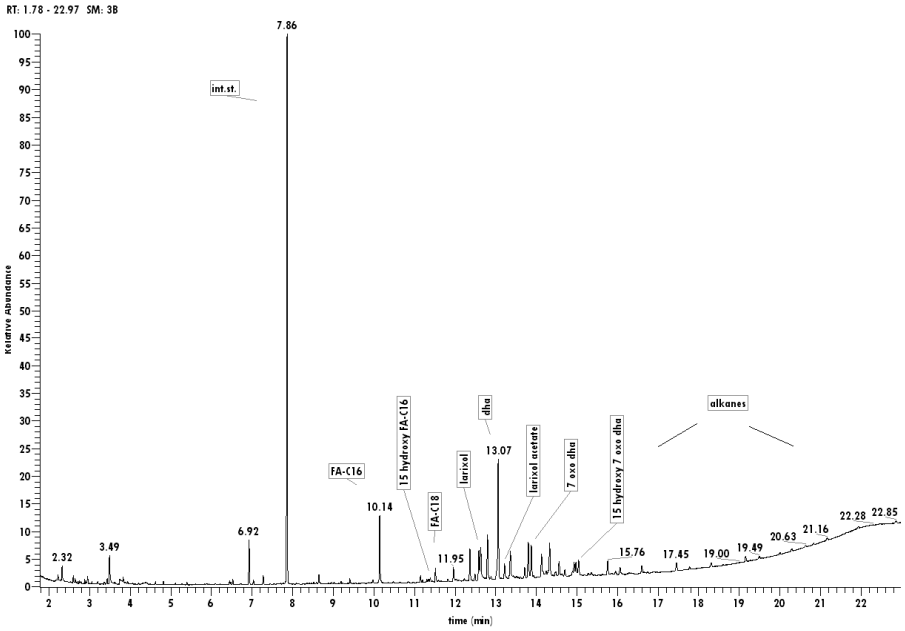

Figure 4.11 Py-TMAH-GCMS chromatogram of the lining materials

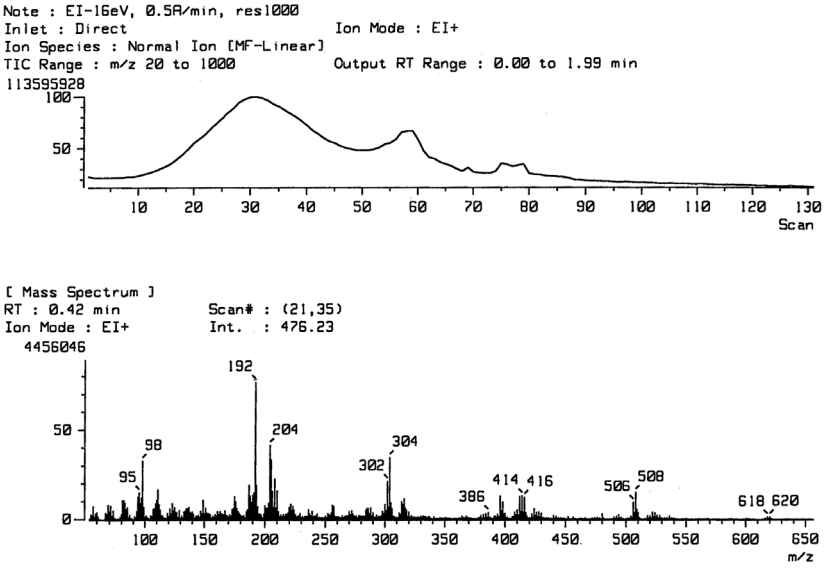

Figure 4.12 DTMS result of the varnish (sample 277a-01). *Upper*; TIC. *Lower*; partial mass spectra of scans 21-35. Ion fragments at *m/z* 98, 192, 204, 304 together with *m/z* 410, 510 and 620 indicate a cyclohexanon resin.

materials by Dutch conservators in the first half of the 20th Century [Hackney *et al.* 2013: 424-432; Van den Berg 2003].

4.3.2 Varnish

A sample for varnish analysis (277a-01) was taken from the edge of the painting on the left-hand side (Figure 4.9) where the paint appeared rather brownish. The varnish was extracted by cleaning the painting surface with a cotton swab wetted with iso-propanol. The brownish surface color was thought to be due to the yellowed varnish but while removing the varnish the paint color was that of the background.

Indications of natural resins were not found (Figure 4.12) but a cyclohexanone resin was confirmed by DTMS. Ion fragments detected at *m/z* 98, 192, 204, 304, and cluster ions at around *m/z* 410, 510, and 620 are indicative for a synthetic cyclohexanone type resin [Van der Doelen 1999: 49], likely Laropal K80 ketone [Boon and Van Och 1996]. The result suggests that the painting was treated between the 1950s and 1970s when ketone resins were widely used in The Netherlands.

4.4 Paint components

4.4.1 Samples

Paint samples were taken from six different places (Figure 4.9, Table 4.2). All samples were embedded for cross-sectional examination. The samples of 277a-03, -05, and -07 were divided into two parts, one for paint and one for ground analysis by mass spectrometry.

Sample 277a-03 was taken from Verster's forehead. The surface color is a dull reddish brown with blue violet paint is underneath. We considered it already too dark to serve as a flesh tone. This area is thought to be an area with increased contrast judging from the comparison of the black and white photographs and prints.

Sample 277a-04 was taken from a paint drip near one of pinholes at the right-hand side of the canvas edge. The surface appearance is a mixture of grayish browns and dull greens. The area sample 277a-05 with a surface appearance of bluish gray is also taken from the background near the face. These two samples were taken for identification of the pigments and also for examination of condition of the binding medium.

The area, where sample 277a-06 was taken, is Verster's black jacket where a red paint is visible underneath. This sample was taken for a comparison to sample 277a-08, which depicts the black jacket as well. The sample 277a-08 was taken from the bottom edge, and there is no red paint underneath. Sample 277a-07 was taken from the collar of his shirt on the right side. The surface color appearance is light bluish-gray and

suggest the use of a white pigment. This area was selected for identification of the white pigment and examination of its condition.

4.4.2 Organic components

DTMS analysis was performed on all paint samples (277a-03 to -08) and the results are listed in Table 4.3. The use of linseed oil as the main binding medium is suggested by a P/S ratios 1.7 to 2.2. Slightly higher P/S ratios in some samples might imply the use of other types of oil; it is possible that poppyseed oil was part of the medium (Van den Berg, Pers. Comm. 2014). The drying oil dried fully that is supported by near the absence of ion fragments from unsaturated fatty acids.

Beeswax found in most of the paint samples derive most likely from the lining process (see 4.3.1). The pine resin however was not found in those samples. Migration of beeswax into a paint layer is a common phenomenon in resin-wax lined paintings, while a lining resin usually does not penetrate the paint layers (Boon Pers. Comm. 2014). The beeswax may have been in the original paint as well asd it is a well-known addition to tube paints in the 19th and early 20th century [Carlyle 2001: 111-116; Hermens *et al.* 2002]. Some of the paint samples also show the features of the cyclohexanone varnish (see 4.3.2), which was not removed prior to analysis.

Table 4.3 Results of organic analysis with DTMS

Sample no.	277a-03		277a-04	277a-05		277a-06	277a-07		277a-08
Sample description	ground and paint	brown paint	gray paint	ground and yellow paint	gray and yellow paint	black and red paint	ground	gray paint	black paint
P/S ratio	1.7	2	2.2	2	2	(n.a.)	2.2	2.2	1.8
Beeswax	n.d.	n.d.	n.d.	+	+	++	trace	trace	n.d.
Cycrohexanone (Varnish)	+	+	+	n.d.	n.d.	n.d.	n.d.	n.d.	n.d.

n.d. not detected
(n.a.) very little *m/z* 284 was detected

4.4.3 The ground

The ground is made from two layers, as was confirmed in all samples except for 277a-07, which did not contain the lower ground. The lower ground is a little yellowish white by eye and rather high in transparency under light microscopic examination. It consists of a large amount of calcium carbonate and a relatively small amount of zinc

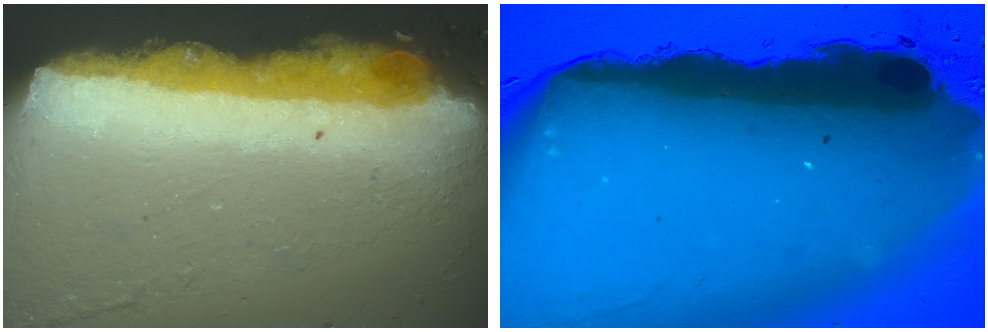

Figure 4.13 The first ground consisting of calcium carbonate and zinc oxide (277a-05 lower half) *Left*; VIS. *Right*; UVf.

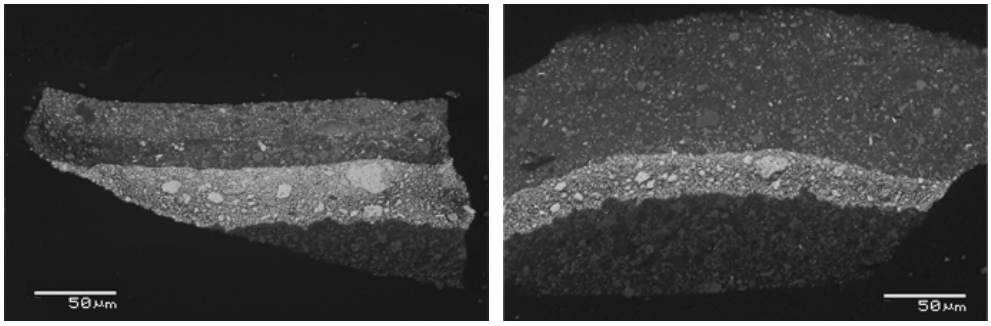

Figure 4.14 BSE images of the second ground consisting of lead white *Left*; 277a-03. *Right*; 277a-08 in the same scale

white indicated by EDX. The presence of zinc white is supported by the characteristic greenish UV fluorescence of zinc oxide (Figure 4.13). Lead was sparsely present in the lower ground, while the second ground consists of only lead white of which its layer thickness is about 20-30 µm (Figure 4.14).

4.4.4 The paints

The color photograph DCP2007 shows that the paint is inhomogeneous and the brushstrokes have a texture indicating that there is no clear and constant layer structure (Figures 4.1, 4.7). Information from cross-sections reveals that the paints in this painting are indeed often mixtures of several kinds of pigments. The results of EDX analysis and the interpretation of pigment types in each paint layer are listed in Table 4.4.

Three of the six paint samples, the background (277a-04 and -05) and the collar of Verster's shirt (277a-07) are an optical-gray made by mixing mainly lead white with colorful pigments (Figure 4.15). The artist used two types of pigment of the same hue, emerald green and viridian for green, yellow ocher and Indian yellow for yellow, red ocher and a red lake for red, and ultramarine blue and cobalt blue for blue. In addition,

Table 4.4 Pigment compositions (277a-03 to -08)

277a-03

Layer	Color in cross-section	EDX detection	Interpreted pigments	Notes
4	Brown	Pb	lead white	lead soap mass
		Zn		zinc soap, dispersed zinc
		Co, As	cobalt violet	
		Fe	red/yellow ochre	
		Ca, P	bone/ivory black	
		Cu, As	emerald green	
		Ba, S	barium sulfate	
		Cr	viridian	
			red lake	reddish UV fluorescence
3	Blue violet	Pb	lead white	no obvious lead soap
		Co, As	cobalt violet	
		Co, Al	cobalt blue	
		Zn, S	zinc sulfide	
		Ba, S	barium sulfate	
		Ca, P	bone/ivory black	
		Al, P	red lake	reddish UV fluorescence
2	White	Pb	lead white	
1	White	Ca	calcium carbonate	little Pb was found
		Zn	zinc oxide	greenish UV fluorescence

277a-04

Layer	Color in cross-section	EDX detection	Interpreted pigments	Notes
5				(Varnish layer)
4	Gray	Zn	zinc oxide	greenish UV fluorescence
		Sb		
		Ca, P	bone/ivory black	
3	Gray? partially greenish and brownish	Pb	lead white	
		Mg	Indian Yellow	yellow or orange UV fluorescence
		Cu, As	emerald green	
		Co, As	cobalt violet	
		Cr	viridian	
		Fe	red/yellow ochre	
			bone/ivory black	black particles
2	White			(2nd ground)
1	White			(1st ground)

277a-05

Layer	Color in cross-section	EDX detection	Interpreted pigments	Notes
5	Greenish gray	Pb	lead white	
		Fe	red/yellow ochre	
		Ca, P	bone/ivory black	
		Cu, As	emerald green	
4	Violet	Co, Al	cobalt blue	
		Co, As	cobalt violet	
		Zn, S	zinc sulfide	
		Ba, S	barium sulfate	
		Cr	viridian	
		Fe	red ochre	
		Al, P	red lake	reddish UV fluorescence
		Na, S, Al, Si	ultramarine blue	
		Pb	lead white	
3	Yellow	Fe	yellow ochre	
2	White			(2nd ground)
1	White			(1st ground)

277a-06

Layer	Color in cross-section	EDX detection	Interpreted pigments	Notes
5	Black	Ca, P	bone/ivory black	
		Co, Al	cobalt blue	
		Cr	viridian	
		Fe	red/yellow ochre	
		Na, S, Al, Si	ultramarine blue	
		Pb	drier or/and lead white	
4	Black	Ca, P	bone/ivory black	
		Co, As	cobalt violet	
		Cr	viridian	
		Fe	red/yellow ochre	
		Al, P	red lake	
		Pb	drier or/and lead white	
3	Red	Hg, S	vermilion	
2	White			(2nd ground)
1	White			(1st ground)

277a-07

Layer	Color in cross-section	EDX detection	Interpreted pigments	Notes
4	Gray	Zn	lead white	greenish UV fluorescence
		Ca, P	bone/ivory black	
3	Gray	Pb	lead white	
		Co, Al	cobalt blue	
		Cr	viridian	
		Cu, As	emerald green	
		Fe	red/yellow ochre	
		Al, P	red lake	no UV fluorescence
			bone/ivory black	
2	Pale grreen?	Pb	yellow ochre	
		Zn, S	zinc sulfide	
		Ba, S	barium sulfate	
			(viridian?)	green pigments
1	White			(2nd ground)

277a-08

Layer	Color in cross-section	EDX detection	Interpreted pigments	Notes
3	Black	Ca, P	bone/ivory black	
		Fe	yellow/red ochre	
		Cr	viridian	
		As	cobalt violet or and emerald green	
		Zn		
		Pb	lead white	
2	White			(2nd ground)
1	White			(1st ground)

cobalt violet was used to a relatively large extent that may be an indication of the artist's preference. Several achromatic pigments, lead white, zinc white, and lithopone, and bone/ivory black were found in the paints.

The presence of emerald green was indicated not only by EDX but also by DTMS. In the DTMS spectra, the detection of a peak at *m/z* 134 assigned to arsenic acetate (As: 75 amu and acetate: 59 amu) strongly suggests the use of emerald green.

Indian yellow is indicated by the feature that yellow particles strongly emit a yellow or orange UV fluorescence (Figures 4.16, 4.17). It was also supported by the detection of calcium and magnesium by EDX as these elements are counter ions to a euxanthin ion, which is the yellow component of Indian yellow [Baer *et al.* 1986].

Cobalt violet is a 19th century pigment invented in 1859. Two types, one with arsenate (III) and another one with phosphate are known [Corbeil *et al.* 2002]. The one found in the painting is the arsenate (III) type: $Co_3(AsO_4)_2$.

Slightly reddish particles with weak reddish UV fluorescence indicate the presence of a red lake (Figure 4.15). Reddish particles in sample 277a-07 were also thought to be a red lake. They did not show UV-fluorescence, but the particle color is pale red inside and red at the rim (Figure 4.18). The reddish particles with or without UV-fluorescence both contain aluminum and phosphorus detected by EDX. According to recipes on production of madder lakes in the 19th century, the lake was precipitated on alum, commonly with potassium or sodium carbonate, but also phosphate and calcium salts were used [Kirby *et al.* 2007; Schweppe and Winter 1997; Van Bommel *et al.* 2005]. High performance liquid chromatography (HPLC) analysis performed

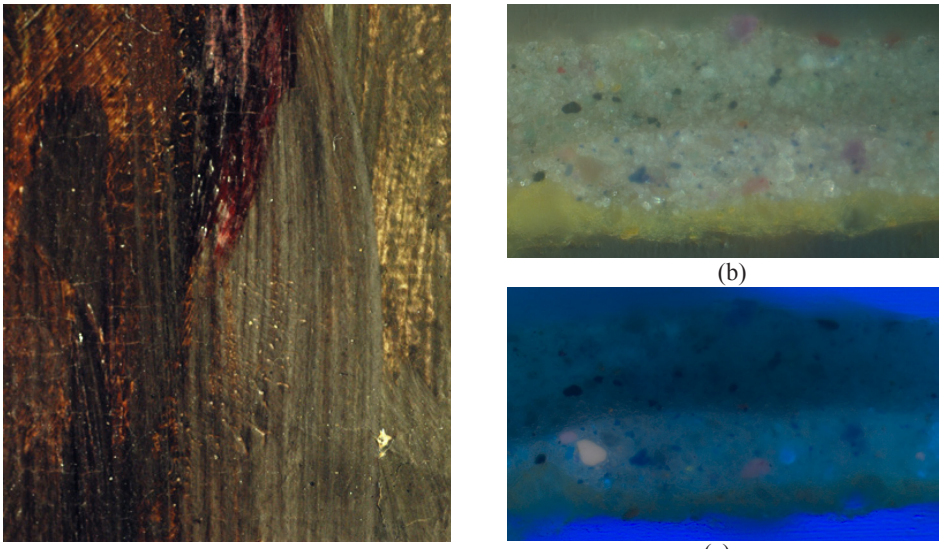

Figure 4.15 The surface of 277a-05 taken area and light microscopic images of the cross-section. (a) surface, (b) VIS (c) UVf, reddish UV-fluorescent particles in the middle layer

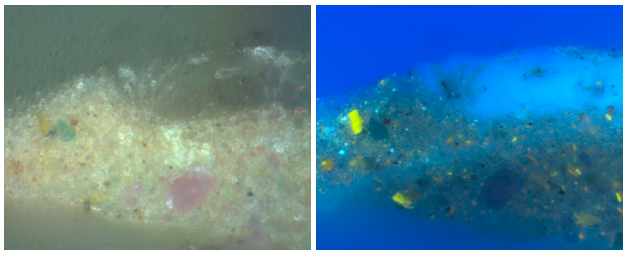

Figure 4.16 The use of Indian Yellow pigment in cross-secion 277a-04. *Left*; VIS, *Right*; UVf

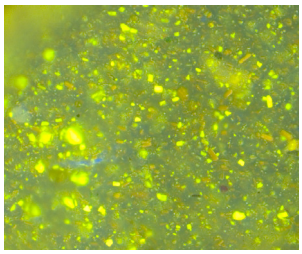

Figure 4.17 UVf of reference Indian Yellow

on sample 277a-07 for identification of the organic red component, detected alizarin. Absence of a purpurine component, which normally accompanies lakes on the basis of natural madder, suggests that the alizarin is synthetic [Hofenk de Graaff *et al.* 2004; 92-106]. Since alizarin does not have a response to UV light, the result matches 277a-07, but contradicts the observation of UV fluorescence in the other cross-sections. This might be an indication for e.g. madder lake, but unfortunately no additional analysis with HPLC could be done.

Zinc white was found in the top layers of 277a-04 and -07. The layers appear translucent white in cross-section and show the characteristic greenish UV fluorescence of zinc oxide (Figure 4.19) [Eastaugh *et al.* 2014]. Very little lead white was found in

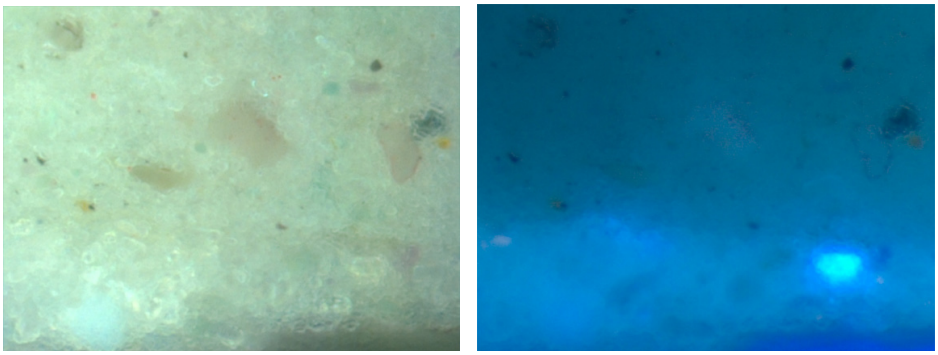

Figure 4.18 Indication of red lake particles in the lower paint layer in 277a-07: *Left*; VIS, *Right*; UVf

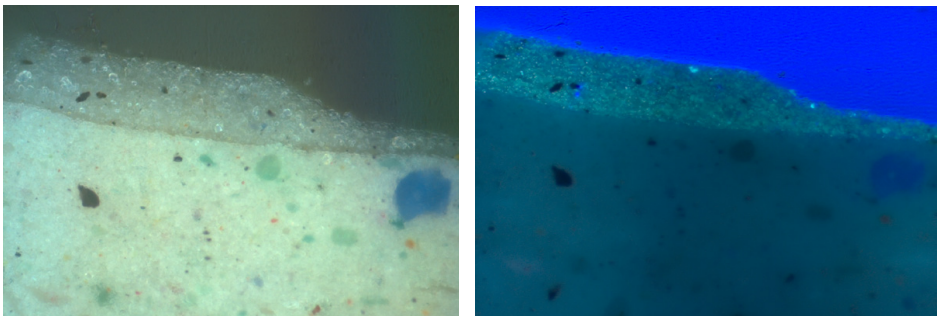

Figure 4.19 The independent use of zinc oxide in the top layer in 277a-07: *Left*; VIS. *Right*; UVf

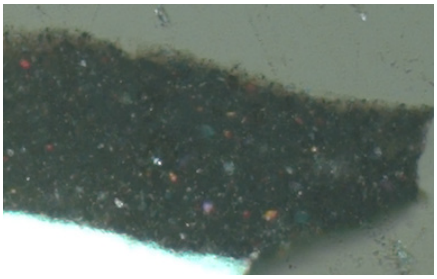

Figure 4.20
VIS of black paint in 277a-08

these layers suggesting that the artist used a pure zinc white paint tube. Zinc white was more widely used as an artists' pigment from the end of 19th century [Kühn 1986]. It was often used together with lead white in order to overcome its relatively lower hiding power. The use of the pigment as an alternative to lead white increased after improvement of the hiding power in the beginning of the 20th century.

Zinc sulfide and barium sulfate were found in the same paint layer indicating the use of lithopone, which is a two-component white pigment. Besides, independent use of ZnS as a pigment was rare before 1927 [Heaton 1928: 88-89].

The pigments found in the black paints of 277a-06 and -08 are similar to those found in the optical-gray paints (Figure 4.20). The non-black paints must have been added to moderate the strength of black color of bone/ivory black. In addition, they will improve the binding strength of the paints functioning as drier.

An intense red paint layer in 277a-06, which was taken from Verster's black jacket, is vermilion paint identified by DTMS and EDX. DTMS detected ion fragments at *m/z* 200 and 202 assigned to mercury. The detection of poly-sulfide at *m/z* 64, 96, 128, 160, 192, 224, and 256 (S_2, S_3, S_4, S_5, S_6, S_7, and S_8 respectively) indicates an abundance of sulfur. EDX indeed detected sulfur and mercury. The red paint is under the black paint but that does not correspond to the shape of jacket, neither to any figures in the painting. Moreover, vermilion was found only in this sample but the function of the red paint is not clear. It could indicate a *pentimento*.

The cross-sections of 277a-04 to -08 are not too informative for understanding the surface appearance. It was difficult to correlate the change in surface color with the observed colors in the cross-sections. The differences in the pigment compositions merely indicate the application of many paints with different tones.

The sample 277a-03 has a layer structure that likely corresponds to the surface appearance. The blue violet paint layer is situated between the white ground and the brown top paint layer, which is intended as a flesh tone. The blue violet paint consists of cobalt violet, cobalt blue, lithopone, a red lake, lead white and bone/ivory black. The presence of red lake is suggested by reddish UV fluorescence observed in cross-sections.

The brown paint consists of cobalt violet, red and yellow ochre, emerald green, viridian, a red lake, barium sulfates, and lead white. Among intact lead white particles, a cloudy area was observed in the SEM-BSE image (Figure 4.21). This area is presumably a lead soap mass as lead was mainly detected by EDX. The indication of lead azelate (*m/z* 350 along with an isotope at *m/z* 348) was detected with DTMS analysis. Zinc was also detected in this layer, but no obvious zinc containing particles were present. After polishing with an Argon ion cross-section polisher [Boon and Van der Horst 2008] a zinc-rich-mass was found, but the presence of intact zinc containing pigment in this layer was not confirmed in the EDX mapping (Figure 4.22).

The major source of lead soap must be lead white, while the source of zinc soap can be zinc oxide or zinc sulfide. The reactive nature of zinc oxide and the detection of formless zinc in 277a-03, makes it probable that zinc oxide was the original form

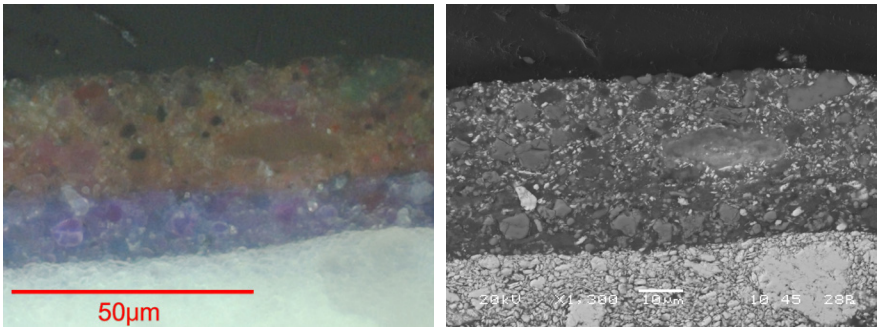

Figure 4.21 A lead soap mass observed in the top brown layer of 277a-03: *Left*; VIS. *Right*; BSE-image

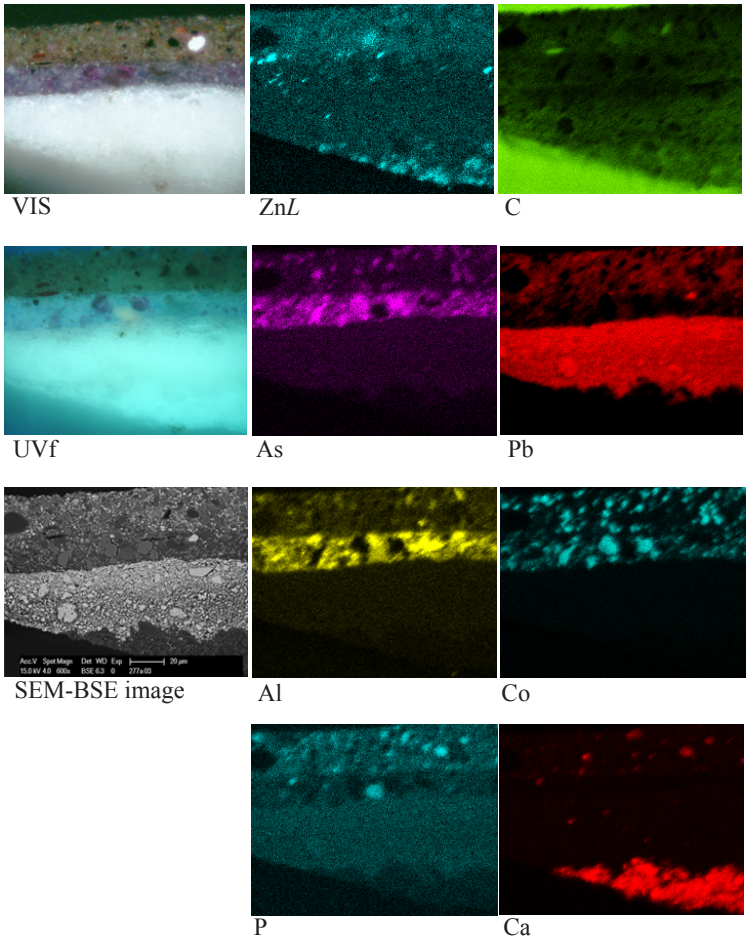

Figure 4.22 EDX mapping result of 277a-03 after polishing with a cross-section polisher.

[Heaton 1928: 84-89; Jacobsen and Gardner 1941; Morley-Smith 1958]. Although an obvious indication of zinc soap mass was not found in the zinc oxide layers of 277a-04 and -07 with the SEM-BSE, it could be matter of relative abundance. Zinc soap tends to be disperse and has a relatively low electron reflectivity [Van der Weerd *et al.* 2003; Osmond *et al.* 2005]. Imaging FTIR was not performed in this study because of unavailability of the instrument.

Zinc sulfide was found in the blue violet layer of 277a-03, the violet layer of 277a-05, and a pale greenish layer of 277a-07. The particles were intact and there was no indication of saponification such as hazy particle edges. Zinc sulfide seems to be stable and not likely the origin of zinc soaps in this painting.

4.5 Discussion and rationale for an experiment on the effect of light absorption on the opacity of paint

4.5.1 Metal soap formation and light absorption in paint opacity

The patchy contrast at Verster's forehead from a comparison of the recently taken photographs to the old photographs and prints corresponds to information from cross-sections where the presence or lack of a blue violet layer under a brown surface paint layer is evident (Figures 4.2, 4.4, 4.5 and 4.6). This change in contrast implies either a decrease of hiding power in the upper paint or an increase of light absorption in the lower paint. In this area the former was suggested by evidence for possible metal soap formation of both lead white and zinc white in the top paint layer of 277a-03 with light microscope and SEM (Figures 4.21, 4.22). Since the saponified areas are limited and there is also a reasonable amount of white pigment particles still intact, saponification alone may not sufficient explain the appearance change. On the other hand, it was demonstrated that even the loss of a small amount of white will affect the paint appearance depending on composition of the paint (as demonstrated in Chapters 1 and 3). Another argument for a decrease of the hiding power –the fading of red lakes– is suggested by Verster's use of red lakes indicated in the cross-sections of 277a-03 and -07 and the contrast changes seen at his right ear painted in red.

The light absorption in paint in general is a factor that affects the paints' opacity [Schäfer and Wallisch 1981; Camina 1968]. Any color pigment absorbs light at specific wavelengths. Therefore when there are light absorbing materials, namely colored pigments and media, in the same paint the relative degree of light absorption increases [Johnstone-Feller 2001: 128-144]. For instance a blue pigment absorbs yellow light significantly, while a red pigment absorbs green to blue light. Losing the light absorbers, such as a fading lake, can lead to a considerable decrease of light absorption resulting in a relative increase of light transmittance. Changing color appearance due to fading is a well-known phenomenon, but a relationship between opacity and color change has

received little attention [Van Bommel *et al.* 2005]. In this aspect, the following paint tests demonstrate the significance of light absorption in the transparency of paint in relation to light reflection (scattering) from white pigments.

4.5.2 Experiments on the effect of fading that affect transparency

As a red lake, eosin was selected for the experiments because the preparation method is relatively easy and it will fade rapidly. The experiment was not intended to be a study about kinetics nor fading mechanism. It was aimed to be a simple example to visualize a relation between fading and surface appearance.

The prepared paints (the details follow) were applied to a black and white chart (Byko-charts, BYK-Gardner GmbH) with a wet thickness 60 μm using the applicator described in chapter 1. The color was measured with a spectrophotometer (Minolta, CM-2600d, illuminant D65 and a 10° observer) after the paint dried. More than three spots were measured on each black and white substrate with the measuring apparatus 8 mm in diameter, and averaged.

The results are shown in CIELAB1976 (L*, a*, b*) color space and some with spectral reflectance graphs. The color images of Figures 4.23 and 4.25 are reconstructed using each mean L*a*b* data, both specular component and UV component of the illuminant excluded, with Photoshop® software. ΔL* was obtained by subtracting L* value of the paint on black substrate (L*b) from L* value of the paint on white substrate (L*w). Δa* and Δb* were calculated in the same manner. Generally, smaller ΔL*Δa*Δb* indicates closer to complete hiding.

Experiment 1: Effect of red lake fading on hiding power

Eosin was precipitated on aluminum trihydrate, $Al(OH)_3$ [Kirby 2005]. In order to imitate fading of the lake, $Al(OH)_3$ alone was also prepared. Pigment volume concentration (PVC) was set at 30%. Three different amounts of eosin containing paints were made by replacing eosin with the same volume of $Al(OH)_3$ (Table 4.5 for the detailed set up). Also two variations of zinc oxide containing paint were made for comparison.

Visual observations and color measurement of three eosin paint (ES-A to C) demonstrated that the fading of eosin would result in a slight increase of ΔL* (Table 4.6, Figure 4.23). Although the differences of ΔL* are not large, it is apparent that the reduction of blue to green light absorption led to a decrease in the hiding power (Figure 4.24).

The effect of zinc oxide to increase the hiding power is also shown in ES-D and ES-E as was already demonstrated in the previous Chapter 3. The redness (a*) of ES-D paint on the black substrate is higher than a* of ES-A paint (on the black substrate) despite of the fact that ES-A contains more Eosin. Because of the presence of good light reflectors in ES-D, multiple scattering is larger and much of the red light is reflected.

Table 4.5 Model paint formulations in Experiment 1

	Sample name	Eosin (on Al substrate)	Al substrate (without Eosin)	ZnO	Barium sulfate	Oil
(a)	ES-A	9 % [30%] (0.22 g)			21 % [70%] (0.92 g)	70% (0.65 g)
(b)	ES-B	6 % [20%] (0.14 g)	3 % [10%] (0.07 g)			
(c)	ES-C	3 % [10%] (0.07 g)	6 % [20%] (0.14 g)			
(d)	ES-D	6 % [20%] (0.14 g)		3 % [10%] (0.17 g)		
(e)	ES-E	9 % [30%] (0.22 g)		3 % [10%] (0.17 g)	18 % [60%] (0.79 g)	

%: volume% in total paint [%]: volume% within pigments

Table 4.6 L*a*b* data of the model paints in Experiment 1

Sample code	On white substrate			On black substrate			Δvalues (eg. ΔL*=L*w-L*b)		
	L*w	a*w	b*w	L*b	a*b	b*b	ΔL*	Δa*	Δb*
ES-A	62	59	31	31	25	2	31	34	29
ES-B	64	56	24	31	21	-1	33	35	35
ES-C	70	47	14	36	17	-4	34	30	18
ES-D	67	50	20	47	27	-2	20	23	22
ES-E	63	55	27	45	30	1	18	25	26

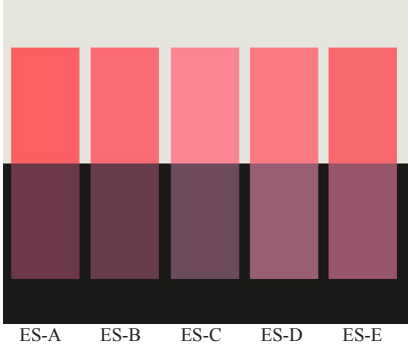

Figure 4.23 Reconstructed image of the model paints of ES-A to -E from Experiment 1. See Tables 4.5, 4.6

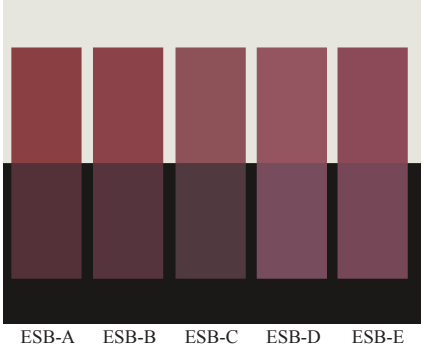

Figure 4.24 Reconstructed image of the model paints of ESB-A to -E from Experiment 1. See Tables 4.7, 4.8

This experiment indicates that the red lake alone has an ability to increase the hiding power due to the selective absorption, and this would be even more effective in the presence of a light reflecting white pigment.

Experiment 2: Effect of a small amount of light absorbers on hiding power

A small amount of bone black was added into the eosin containing paint in Experiment 1. The added amount was less than 1% in the total volume of paint and the same for all five paints (ESB-A to E; Table 4.7). Within the pigments, the volume concentration of bone black is 3%.

It is noted that a considerable decrease of ΔL* value in all paints compared to the ES paints (Table 4.8, Figure 4.25). Also L*a*b* values of each paint are lowered significantly. On the other hand, the trends due to a fading of the lake (shown in Experiment 1) were all observed to be the same, but the differences in a* and b* values became smaller. For instance, a difference ΔL* values of ES-A and ES-C is 3, and that of ESB-A and ESB-C is also 3. However, a difference Δa* values of ES-A and ES-C is

Table 4.7 Model paint formulations in Experiment 2

Sample name	Eosin (on Al substrate)	Al substrate (without Eosin)	ZnO	Barium sulfate	Bone black	Oil
(a) ESB-A	9 % [30%] (0.22 g)	—	—	21 % [70%] (0.92 g)	0.9 % [3%] (0.02 g)	69.1 % (0.65 g)
(b) ESB-B	6 % [20%] (0.14 g)	3 % [10%] (0.07 g)	—			
(c) ESB-C	3 % [10%] (0.07 g)	6 % [20%] (0.14 g)	—			
(d) ESB-D	6 % [20%] (0.14 g)	—	3 % [10%] (0.17 g)			
(e) ESB-E	9 % [30%] (0.22 g)	—	3 % [10%] (0.17 g)	18 % [60%] (0.79 g)		

%: volume% in total paint [%]: volume% within pigments

Table 4.8 L*a*b* data of the model paints in Experiment 2

Sample code	On white substrate			On black substrate			Δvalues (eg. ΔL*=L*w-L*b)		
	L*w	a*w	b*w	L*b	a*b	b*b	ΔL*	Δa*	Δb*
ESB-A	37	33	14	25	17	2	12	16	12
ESB-B	38	32	11	26	16	1	12	16	10
ESB-C	42	26	8	27	11	0	15	15	8
ESB-D	44	28	5	38	20	-2	6	8	7
ESB-E	40	29	5	36	22	-1	4	7	6

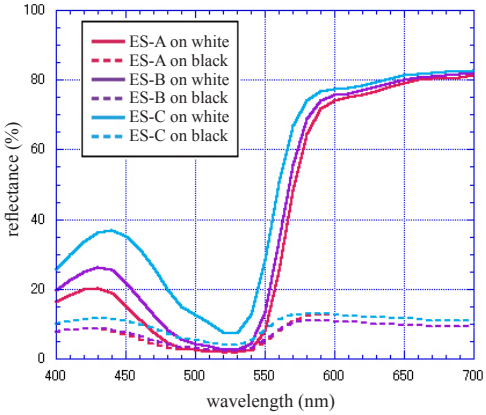

(a)

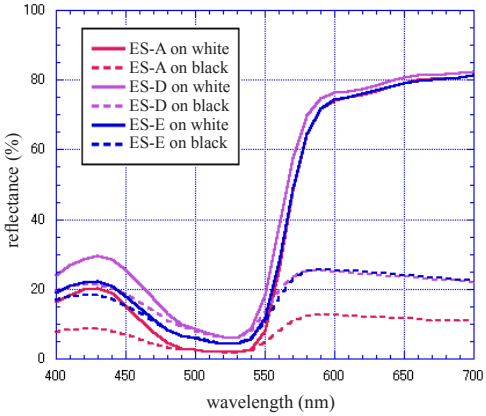

(b)

Figure 4.25 Colorimetric spectra of ES-A to E
(a) ES-A to C, (b) ES-A, -D, and -E

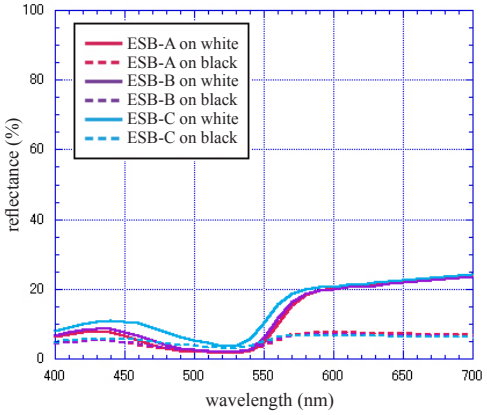

(a)

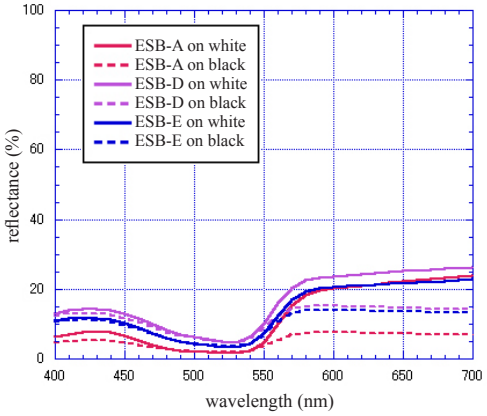

(b)

Figure 4.26 Colorimetric spectra of ESB-A to E
(a) ESB-A to C, (b) ESB-A, -D, and -E

4, while the difference in ESB is 1. This is because the presence of black pigment has already lowered the maximum reflectance at the longer wavelengths (Figure 4.26). It is demonstrated that the presence of strong light absorbers has a major impact on both hiding power and the surface reflectance.

4.6 Interpretation of appearance changes in *Self-portrait* by Verster

According to the layer build-up of 277a-03, the top paint layer is a brown layer made by mixing several pigments, mainly red ones (Table 4.4). EDX mapping shows that

aluminum and phosphorus are present throughout the layer. However, since only the lower areas show reddish UV fluorescence, the red lake in the upper paint layer is most likely faded away (Figures 4.18 and 4.27). The contrast change at Verster's right ear can be explained by red lake fading as the major cause. Although there is no sample from this area, the whitish surface of the red paint suggests that an increase of the relative lightness was caused by a considerable reduction of the red reflection.

In addition, the brown paint layer shows zinc and lead soap masses in the cross-sections. Although the amount is limited, it suggests that a certain degree of scattering from white pigments and thus light reflectivity of the layer must have been lost. In addition, the faded red lake has also caused an increase in light transmittance. In places where the blue-violet paint layer is present underneath, the transmitted light is largely absorbed by this lower paint. On the other hand, the transmitted light is reflected where the white ground is present under the brown paint. Therefore the contrast between the two areas theoretically would become larger.

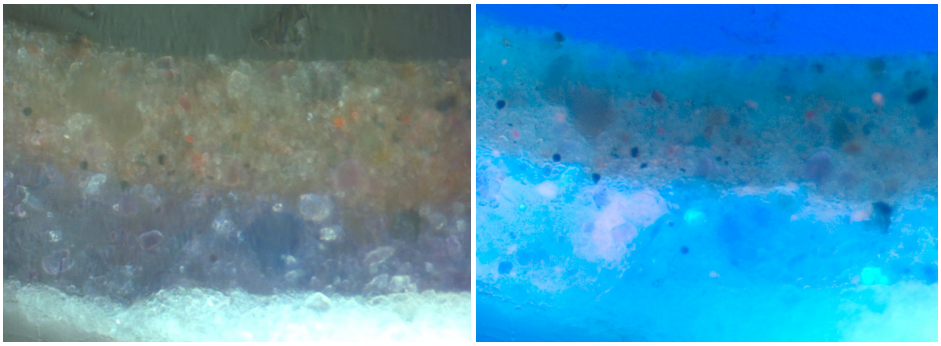

Figure 4.27 VIS of 277a-03: *Left*; VIS. *Right*; UVf; Reddish UV fluorescence indicating the presence of red lake in the upper layer

4.7 Conclusions

This chapter proposes that the current relatively dark appearance and contrast changes in the self-portrait by F.H. Verster have been caused by the combined changes in white pigments and red lakes. Saponification of lead white and zinc oxide has caused a decrease of the relative light reflection, whereas fading of the red lake resulted in a decrease of reflection of red light. Since both effects would reduce the surface reflection, their combination would result in the stronger final effect.

Considering the fact that the images of the painting in the exhibition catalogue of 1927 and 1952 show a contrast difference at Verster's right ear, the artist might have seen color changes of certain paints in his earlier works, and then he might have foreseen them in his later works. However, he could not possibly have known that it would affect the total balance of the painting even if there were already signs of color

changes. It would have been difficult also for us to reach our conclusion of changing contrast in this painting without the photographic documentation. Since Verster used commercially available paints [Van de Laar and Burnstock 1997], similar phenomena might have happened in his other works at this time as many of his works indeed have a fairly dark appearance [De Wal 2002].

References

Baer, N.S., Joel, A., Feller, R.L., and Indictor, N. 1986. Indian Yellow. In: R.L. Feller ed. *Artists' Pigments: a Handbook of their History and Characteristics, vol. 1*. Washington DC: National Gallery of Art, pp. 17-36.

Boon, J.J. and Van Och, J. 1996. A Mass Spectrometric Study of the Effect of Varnish Removal from a 19th Century Solvent-sensitive Wax Oil Painting. In: J. Bridgland, ed. *ICOM Committee for Conservation 11th Triennial Meeting, Preprints*. London: James & James, pp. 197-205.

Boon, J.J. and Van der Horst, J. 2008. Remarkably improved spatial resolution in SEM images of paint cross-sections after argon ion polishing, In: J.H. Townsend, T. Doherty, G. Heydenreich and J. Ridge eds. *Preparation for Painting: the Artist's Choice and its Consequences*. London: Archetype, pp. 42-49.

Camina, M. 1968. Measurements of the fading of pigments in relation to loss of opacity. *Journal of Oil and Colour Chemists' Association*, 51, 14-26.

Carlyle, L. 2001. *The Artist's Assistant*. Archetype Publications.

Corbeil, M., Charland, J., and Moffatt, E.A. 2002. The Characterization of Cobalt Violet Pigments. *Studies in Conservation*, 47, 237-249.

De Wal, J. 2002. *Floris Verster*. Stedelijk Museum De Lakenhal.

Den Haag. 1929. *Eere-tentoonstelling Floris Verster: 12 mei–4juni 1929*. Schilderkundig Genootschap Pulchri Studio, 's-Gravenhage.

Eastaugh, N., Nadolny, J., and Swiech, W. 2014. Interpretaioni of documentary sources for the industrial preparation of 'zinc white' in the 19th century. In: H. Dubois, J.H. Townsend, S. Eyb-Green, J. Nadolny, S. Neven and S. Kroustallis. Eds. *Making and transforming art: changes in artists' materials and practice*. London: Archetype, pp.102-108.

Eder, J.M., Epstean, E. 1945. *History of photography*, by Josef Maria Eder. Translated by Edward Epstean. New York: Columbia University press.

Hackney, S., Reifsnyder, J., te Marvelde, M., and Scharff M. 2013. Lining easel paintings, In: J.H. Stoner, R. Rushfield, eds. *Conservation of Easel Paintings*. Routledge, pp.415-452.

Heaton, N. 1928. *Outline of Paint Technology*. London: Charles Griffn & Co.

Hofenk de Graaff, J.H., Th Roelofs, W.G., and Van Bommel, M.R. 2004. *The Colourful Past:*

Origins, Chemistry and Identification of Natural Dyestuffs. London: Archetype.

Hermens, E., Kwakernaak, A., Van den Berg, K.J., and Geldof, M. 2002. A travel experience –The Corot Painting Box– Matthijs Maris and 19th century tube paints. *Art Matters, Netherlands Technical Studies in Art*, 1, 104-121.

Huinck & Scherjon. 1937. *Tentoonstelling van werken door Floris Verster, 1861-1927: 8 februari–6 maart 1937*. Amsterdam: Kunsthandel Huinck & Scherjon.

Jacobsen, A.E. and Gardner, W.H. 1941. Zinc Soaps in Paints: zinc oleates. *Industrial and Engineering Chemistry*, 33, Oct., 1254-1256.

Johnston-Feller, R. 2001. *Color Science in the Examination of Museum Objects: Nondestructive procedures, Tools for Conservation*. The J. Paul Getty Trust.

Kirby, J. 2005. The reconstruction of late 19th-century French red lake pigments. In: M. Clarke, J.H. Townsend and A. Stijnman, eds. *Art of the Past Sources and Reconstructions*. Archetype, pp. 69-77.

Kirby, J., Spring, M., and Higgitt, C. 2007. The Technology of Eighteenth- and Nineteenth-Century Red Lake Pigments. *National Gallery Technical Bulletin*, 28, 69-95.

Kühn, H. 1986. Zinc white. In: R.L. Feller ed. *Artists' Pigments: a Handbook of their History and Characteristics, vol. 1*. Washington DC: National Gallery of Art, pp. 169-186.

Mills, J. and White, R. 1994. *Organic Chemistry of Museum Objects*. 2nd edition. London: Butterworth-Heinemann.

Morley-Smith, C.T. 1958. Zinc oxide –A reactive pigment. *Journal of the Oil and Colour Chemists' Association*, 41, 85-97.

Newhall, B.1949. *The history of photography from 1839 to the present day*. New York: Museum of Modern Art.

Osmond, G., Keune, K., and Boon, J.J. 2005. A study of zinc soap aggregates in a late 19th century painting by R.G. Rivers at the Queensland Art Gallery. *AICCM Bulletin*, 29, 37-46.

Schäfer, H. and Wallisch, G. 1981. Obtaining opacity with organic pigments in paint. *Journal of Oil and Colour Chemists' Association*, 64, 405-414.

Schweppe, H. and Winter, J. 1997. Madder and Alizarin, In: E.W. FitzHugh, ed. *Artists' Pigments: a Handbook of their History and Characteristics, vol. 3*. Oxford University Press, pp.109-127.

Stedelijk Museum. 1952. *Floris Verster: voorjaar 1952: Stedelijk Museum de Lakenhal, Leiden*. Stedelijk Museum Amsterdam.

Utrechtsche Museum. 1927. *Tentoonsteling van werken door FLORIS VERSTER uit utrechtsch bezit in het Centraal Museum : 20 februari–24 maart 1927*. Utrechtsche Museum – Vereeniging voor Hedendaagsche Kunst.

Van Bommel, M.R., Geldof, M., and Hendriks, E. 2005. An investigation of organic red lake

pigments used by Vincent Van Gogh (November 1885 to February 1888). *Art Matters, Netherlands Technical Studies in Art*, 3, 111-137.

Van de Laar, M., and Burnstock, A. 1997. "With paint from Claus & Fritz": A study of an Amsterdam painting materials firm (1841-1931). *Journal of the American Institute for Conservation*, 36, 1-16.

Van den Berg, K.J., Boon, J.J., Pastorova, I., and Spetter, L.F.M. 2000. Mass spectrometric methodology for the analysis of highly oxidized diterpenoid acids in Old Master paintings. *Journal of Mass Spectrometry,* 35, 512-533.

Van den Berg, K.J., Geldof, M., De Groot, S., and Van Keulen, H. 2002. Darkening and surface degradation in 19th- and early 20th-century paintings: an analytical study. In: R. Vontobel, ed. *ICOM Committee for Conservation 13th Triennial Meeting, Preprints*. London: James & James, pp. 464-472.

Van den Berg, K.J., 2003. Mass spectrometric methodology for the analysis of highly oxidised diterpenoid acids in Old Master paintings. Part 2. LCMS and DTMS studies. Index for the Degree of Oxidation. In: *Analysis of diterpenoid resins and polymers in paint media and varnishes, with an atlas of mass spectra* (MOLART Report 10). Amsterdam: FOM Institute AMOLF, pp. 33-48 (only available as a PDF, last accessed on 26-Aug-2014: http://wiki.collectiewijzer.nl/images/8/84/Molart_Report_10.pdf).

Van der Doelen, G.A. 1999. *Molecular Studies of Fresh and Aged Triterpenoid Varnishes*. PhD dissertation, University of Amsterdam.

Van der Weerd, J., Geldof, M., Van der Loeff, L.S., Heeren, R.M.A., and Boon, J.J. 2003. Zinc Soap Aggregate Formation in 'Falling Leaves (Les Alyscamps)' by Vincent van Gogh. *Zeitschrift fur Kunsttechnologie und Konservierung*, 17(2), 407-416.

Windisch, H. 1956. *The manual of modern photography*. Heering Publications.

Appendix to chapter 4

Arsenic phosphide (As_nP_m) cluster generation from 19th C oil paint on the Pt/Rh analytical filament in direct temperature resolved mass spectrometry

4A.1 Introduction

The elements sulphur, phosphorus, and arsenic are known to bond readily to themselves, forming, for instance, S_2, P_2, and As_2, which can be detected by mass spectrometry [Kelly 1978; Šedo 2004; Špalt 2005]. It is known that arsenic sulphide (AsS) can be thermally generated in mass spectrometry [Kelly 1978]. Syntheses of phosphorus-sulphur clusters (P_nS_m) by laser ablation in connection with time-of-flight (TOF) mass spectrometry has been reported [Šedo 2004; Špalt 2005]. Generation of independent phosphorus, sulphur, and arsenic clusters has been seen in the analysis of painted materials in artistic works with temperature resolved mass spectrometry (DTMS) [Boon 1992]. This technique is generally used for organic component analysis but it is also useful to detect certain metals [Boon et al. 1995]. Earlier, reduced antimony clusters Sb_x (x=1-4) had been observed in tempera paint dosimeters containing Naples yellow ($Pb_2Sb_2O_7$), which were analysed with DTMS [Van den Brink 2001: 79-85]. We saw that phosphorus and arsenic can thermally generate arsenic phosphide (As_nP_m) under certain conditions with DTMS. Arsenic phosphide clusters were observed in an old oil paint with phosphate, arsenate, and arsenate (III) containing pigments. The generation of arsenic phosphide clusters was confirmed by high resolution mass spectrometry, and the reaction is reproducible using bone black and arsenate under reducing conditions with DTMS.

4A.2 Analytical method

The samples were measured using a JEOL JMS-SX/SX102A tandem mass spectrometer with B/E/B/E geometry. An ethanolic suspension of the sample was deposited on the platinum/rhodium (9:1) filament of a direct insertion probe. After evaporation of the ethanol, the probe was inserted directly into the ion source of the mass spectrometer, which was kept at 190 ºC. The filament was resistively heated by ramping the current at a rate of 0.5A min^{-1}. Using this ramp the temperature was linearly increased from ambient to approximately 800 ºC in two minutes. Desorbed and pyrolysed material was ionized by low energy (16eV) electron impact and accelerated to 8 kV. The mass spectrometer was scanned over a *m/z* range of 20-1000 using a 1s cycle time. The mass resolution was set to 1000.

Higher resolution mass spectrometric data was acquired on the same instrument using the similar sample introduction and ionization conditions. In this case the mass spectrometer was scanned over a *m/z* range of 20-400 using a 1.1s cycle time and the resolution was set to 5000.

4A.3 Determination of arsenic phosphide in the old oil paint sample

The paint sample was a black paint fragment taken from '*Selfportrait*' (1921) painted by F.H. Verster (Stedelijk Museum De Lakenhal, Leiden, The Netherlands). The black paint formulation was investigated by using a scanning microscope with energy dispersive X-ray spectrometry. Arsenic and phosphorus containing components found are bone black (calcium phosphate, $Ca_3(PO_4)_2$), cobalt violet (cobalt arsenate, $Co_3(AsO_4)_2.8H_2O$) [Corbeil *et al*. 2002], and emerald green (copper acetoarsenite, $3Cu(AsO_2)_2.Cu(CH_3COO)_2$) [Fiedler and Bayard 1997]. The DTMS spectrum is shown in Figure 4A.1 as a summarised scan from the last part of the total ion current trace of the analysis, implying that the reactions occurred at high temperature (above 650 celsius). Since reduction of phosphorus and arsenic in an old oil paint and thermal generation of their clusters had been seen before during DTMS studies of paint at AMOLF, the peaks at *m/z* 62, 93, 124, 150, 225, and 300 were assigned to P_2, P_3, P_4, As_2, As_3, and As_4 respectively. Note that both P and As have only one stable isotope. Other peaks at *m/z* 106, 137, 168, 181, 212, and 256 were assigned to clusters of phosphorus and arsenic, AsP, AsP_2, AsP_3, As_2P, As_2P_2, and As_3P (calculated mass 105.89, 136.86, 167.83, 180.81, 211.78, and 255.73, respectively) (Table 4A.1). Although these assignments to arsenic phosphide clusters are reasonable, high resolution mass spectrometry was performed for confirmation. The result of the high resolution mass spectrometry is shown in Table 4A.1. Close data analysis reveals that arsenic reduction starts before phosphorus reduction (Figure 4A.2). When phosphorus reduction starts, arsenic phosphide clusters also become detectable. The dominant form of reduced arsenic detected is the As_4 cluster at *m/z* 299.693. *M/z* 149.827 assigned to the As_2 cluster is also prominent. Reduced mono-arsenic As at *m/z* 74.904 and tri-arsenic As_4 at *m/z* 224.764 can be found, although their relative intensity is rather low compared to $As_2$and As_4. Among the phosphorus clusters, di-phosphorus molecule P_2 is the main form detected at *m/z* 61.940. Although other forms of phosphorus, P at *m/z* 30.966, P_3 at *m/z* 92.904, and P_4 at *m/z* 123.889, can be found, their relative intensities are very low. The result indicates that arsenic prefers As_4 and also As_2 clusters while P_2 cluster is favoured in reduced phosphorus. The most intense arsenic-phosphide clusters detected are AsP cluster at *m/z* 105.889 and As_2P_2 at *m/z* 211.775. Generation of *m/z* 167.838 of AsP_3 and *m/z* 255.734 of As_3P are fair but not intense. Two three-atom clusters, which are AsP_2 at *m/z* 136.856 and As_2P at *m/z* 180.810 are detected in low intensity.

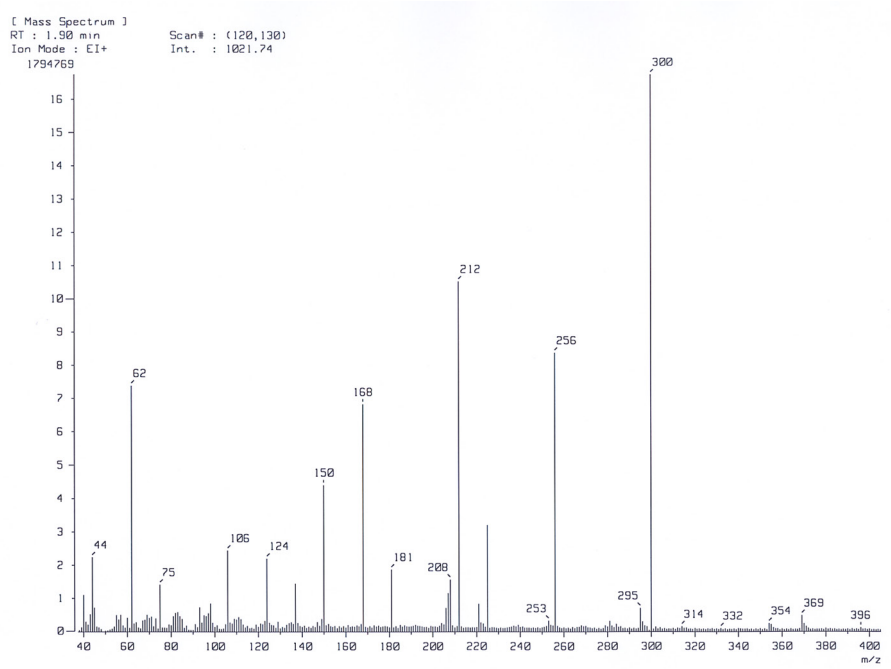

Figure 4A.1 Partial DTMS spectrum in the high temperature region (scan 120-130) of black paint sample from the *Selfportrait* by Verster.

Table 4A.1 List of As_n, P_m, and As_nP_m species generated on the Pt/Rh probe of DTMS and identified from mass spectra

Cluster type	Cluster	Theoretical *m/z*	Observed *m/z*	Confirmed *m/z* with DT high resolution MS
P_m clusters	P	30.97	31	30.966
	P_2	61.94	62	61.940
	P_3	92.91	93	92.904
	P_4	123.88	124	123.889
As_n clusters	As	74.92	75	74.904
	As_2	149.84	150	149.827
	As_3	224.76	225	224.764
	As_4	299.68	299 or 300	299.693
As_nP_m	AsP	105.89	106	105.889
cluster	AsP_2	136.86	137	136.856
	AsP_3	167.83	168	167.838
	As_2P	180.81	181	180.810
	As_2P_2	211.78	212	211.775
	As_3P	255.73	256	255.734
As_nO_x	As_3O_4	288.76	288 or 289	288.734
	As_4O_6	395.68	395 or 396	395.642

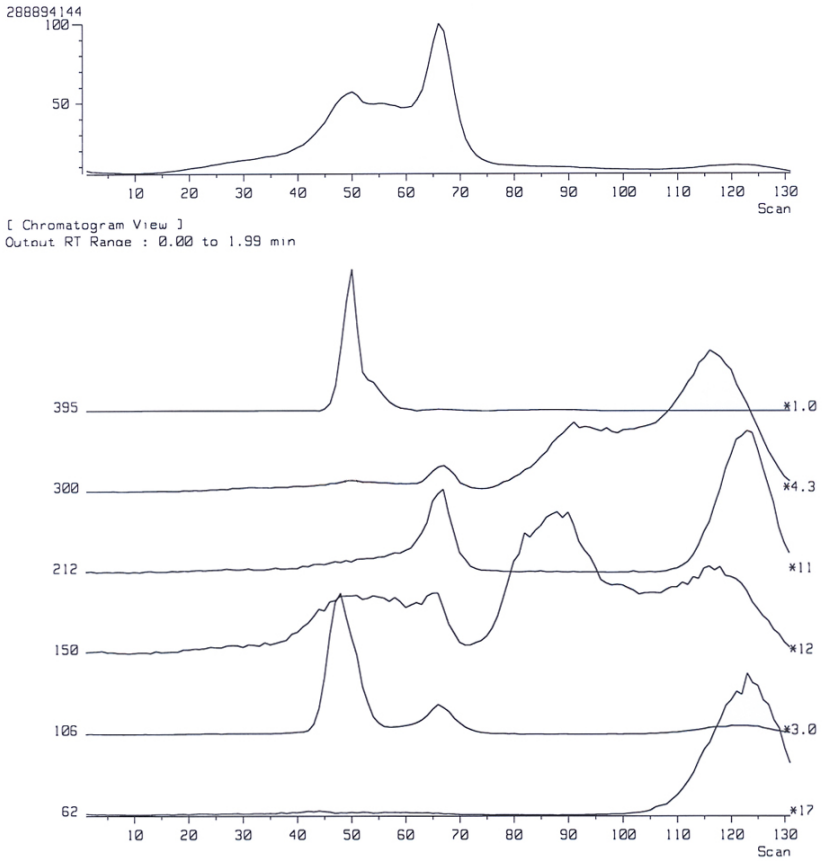

Figure 4A.2 Mass thermograms of reduced phosphorus (*m/z* 62; P_2), reduced arsenic (*m/z* 150; As_2 and *m/z* 300; As_4), arsenic oxide (*m/z* 395; As_4O_6), and arsenic phosphide (*m/z* 106; AsP and *m/z* 212; As_2P_2) in DTMS data of black paint sample from the *selfportrait*.

4A.4 Generation of arsenic phosphide clusters

It was a challenge to verify whether these reactions on the filament probe could be reproduced with pure laboratory substances. Copper acetoarsenite was made available from the historical pigments collection of ICN (now RCE). Arsenic and copper contents were confirmed by energy dispersive X-ray spectrometry in an SEM and the FTIR spectrum of the pigment matched a reference spectrum [Fiedler and Bayard 1997]. Since arsenate type cobalt violet was not available during this study, it was decided to use a chemically prepared arsenate reagent instead. Sodium arsenate dibasic heptahydrate [Na_2HAsO_4. $7H_2O$] (Sigma-Aldrich) was used. As a phosphate compound, calcium phosphate ($Ca_3(PO_4)_2$, Fluka), and later a bone black containing hydroxyapatite

(Kremer Pigmente GmbH & Co. KG) was used.

Generation of reduced arsenic and phosphorus in independent experiments was demonstrated prior to an attempt to generate arsenic phosphide clusters. Detection of reduced arsenic in copper acetoarsenite and sodium arsenate samples was easily achieved by adding amorphous carbon black (lamp black, Kremer). Crystalline carbon black was first used for the analysis but its contribution to the reduction reaction was unsatisfactory. On the other hand, reduced phosphorus from calcium phosphate was not detected even with amorphous carbon. Possible explanations for the negative results were that contact between lamp black and calcium phosphate was inadequate to enable the reduction reaction or that the calcium phosphate is far more stable than the calcium phosphate form ($Ca_{10}(PO_4)_6(OH)_2$) in bone black. In order to overcome these two factors, bone black containing oil paint (linseed oil was used) was prepared. To improve the contact between phosphate and carbon, lamp black was added to this paint. When this bone black paint was analysed by DTMS, a reduced phosphorus cluster P_2 was finally generated.

Subsequently, bone black paint mixed with copper acetoarsenite (1) and with sodium arsenate (2) was analysed. In both cases, arsenic phosphide clusters were generated with slightly different intensities in some clusters. Also peaks at *m/z* 395 or 396 and *m/z* 288 or 289 assigned to the arsenate (III) species As_4O_6 and As_3O_4, with

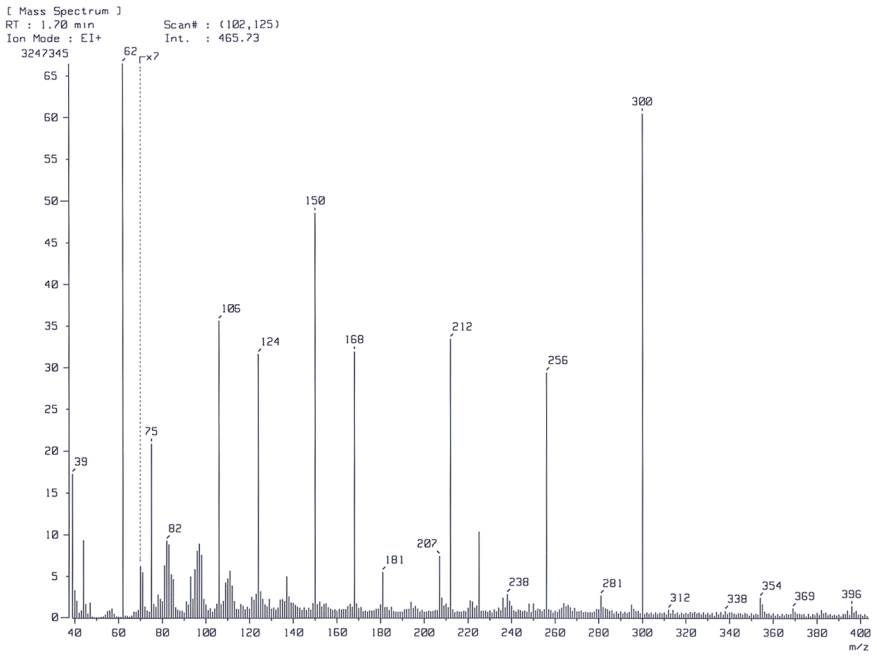

Figure 4A.3 Partial DTMS spectrum in the high temperature region (scan 102-125) of Sample (2); linseed oil paint containing bone black and carbon black with sodium arsenate.

calculated masses of *m/z* 395,68 and 288,76 respectively were detected. These species are detectable at much lower temperature compared to the detection of reduced arsenic, which appears at high temperature.

The large relative amount of arsenate (III) at the lower temperature in sample (1) suggests that the remaining amount of arsenate (III) must be relatively low. In that case, the dominant reduced arsenic cluster is di-arsenic (As_2) and not tetra-arsenic (As_4). Reduced phosphorus, as di-phosphorus (P_2), was detected at higher temperature than reduced arsenic. Although two arsenic phosphide clusters AsP and As_2P_2 were clearly detected, other clusters detected in the painting sample were not generated with the same intensity as seen in the paint sample.

In sample (2), arsenate (III) (As^{3+}) species are also detected, but no arsenate (As^{5+}) species like AsO_4 (calculated mass 138,92). Generation of As_4O_6 and As_3O_4(arsenate (As^{3+}) clusters) from arsenates (As^{5+} oxoanion) suggests that arsenate species are easily reduced and generate As^{3+} oxoanions. The main reduced form of phosphorus is the di-phosphorus P_2 as in sample (1). All of AsnPm clusters, which have been seen in the painting sample were also detected in this case (Figure 4A.3). Arsenic in arsenate and phosphorus in phosphate are both pentavalent. It is probable that the reduction reaction of both elements occurs more or less on the same time scale. This makes it possible to generate arsenic phosphide clusters. Each independent element cluster with the highest intensity is di-phosphorus (P_2, *m/z* 64) and tetra-arsenic (As_4, *m/z* 299 or 300). The combination of these two clusters As_4P_2 (calculated mass 361.62) however was not generated. A larger than four-atom clusters was not observed in this study, although arsenic can form larger cluster ions such as As^{5+} or As^{7+} [Špalt 2005]. This suggests that maximum numbers of atoms in a cluster AsnPm is four (n+m=4) under our analytical conditions. The low relative intensity of the peaks at *m/z* 137 and 181 corresponding to AsP_2 and As_2P, clearly the same tendency observed in the painting sample, indicates that odd number clusters (n+m=3) are difficult to generate. This appears also true for the pure atomic arsenic and phosphorus clusters As_3 and P_3. Whereas four-atom clusters containing three of atoms of phosphorus or arsenic, like AsP_3 and As_3P, have reasonable intensities and are easily detected.

4A.5 Conclusion

It is demonstrated that reduction of both arsenate and phosphate occurs at high temperature on the Pt/Rh probe of DTMS generates arsenic phosphide clusters. A forced reduction reaction by adding amorphous carbon is necessary, especially for generation of reduced phosphorus. Both arsenate (III)-phosphate and arsenate-phosphate combinations can generate arsenic phosphide clusters. Ion yield of each cluster is concentration dependent and depends on the available relative amount of reduced arsenic in the presence of reduced phosphorus.

References

Boon, J.J. 1992. Analytical pyrolysis mass spectrometry: new vistas opened by temperature-resolved in-source PYMS. *International Journal of Mass Spectrometry and Ion Processes*, 118/119, 755-787.

Boon, J.J., Pureveen, J., Rainford, D., and Townsend, J.H. 1995. The opening of the Wallhalla, 1842': Studies on the molecular signature of Turener's paint by direct temperature-resolved mass spectrometry (DTMS). In: J.H. Townsend, Ed. *Turner's Painting Techniques in Context 1995*. London: IIC, pp.35-45.

Corbeil, M., Charland, J., and Moffatt, E.A. 2002. The Characterization of Cobalt Violet Pigments. *Studies in Conservation*, 47, 237-249.

Fiedler, I. and Bayard, M.A. 1997. Emerald green and Scheele's green. In: E.W. FitzHugh, ed. *Artists' Pigments: a Handbook of their History and Characteristics, vol. 3*. Oxford University Press, pp. 219-271.

Kelly, W.R., Tera, F. and Wasserburg, G.J. 1978. Isotopic determination of silver in picomole quantities by surface ionization mass spectrometry. *Analytical Chemistry*, 50 (9), 1279-1286.

Šedo, O., Voráč, Z., Alberti, M., and Havel, J. 2004. Laser ablation synthesis of new phosphorus and phosphorus-sulfur clusters and their TOF mass spectrometric identification. *Polyhedron*, 23(7), 1199-1206.

Špalt, Z., Alberti, M., Peña-Měndez, E., Havel, J. 2005. Laser ablation synthesis of arsenic and arsenic sulphide clusters. *Polyhedron*, 24, 1417-1424.

Van den Brink, O.F. 2001. *Molecular changes in egg tempera paint dosimeters as tools to monitor the museum environment*. PhD dissertation (Molart Report 4), University of Amsterdam.

Chapter 5

Chemical changes and decrease of light reflected in '*La Descente des Vaches*' by Théodore Rousseau (The Mesdag Collection, HWM286, 1834-35)

An early painting by Théodore Rousseau 'La Descente des Vaches' shows severe surface deformation and extremely dark appearance, as previously described by van den Berg et al. [2002]. Use of bituminous materials, which was recorded by the artist's friend, was not found however, instead decomposition of emerald green pigment is indicated. Chemical changes in other pigments; saponification of lead white and fading of lakes are also suggested in other pigments. Along with Rousseau's painting technique, superimposing several glaze-like paint layers, the color balance of the painting, which deep green and/or brown must have been base colors, has been distorted unpredictably.

5.1 Introduction

5.1.1 The painting's condition

The painting *La Descente des Vaches* (Inv. Nr. HWM 286, The Mesdag Collection, The Hague, The Netherlands) (Figure 5.1a) shows two major paint defects: surface deformation and an extremely dark appearance [Van den Berg *et al.* 2002]. Théodore Rousseau (1812-1867) painted the work in 1835-36 for the Salon exhibition of 1836 [Leeman and Pennock 1996: 380-384].[1] Presently, the defects seriously hamper observation of the composition, which is a view of a herd of cattle being taken from the pastures in the mountains down to the valley. The surface shows many small and relatively large drying cracks, so-called 'alligator cracks', especially in the dark painted

1: The painting's full title is: «*La Descente des vaches, dans les montagnes du haut Jura. Portant au cou de pesants grelots, elles regagnent, sous la conduite des bergers, les pâturages d'automne. On voit étinceler à l'horizon, à travers les sapins, la neige des glaciers* ».

areas (Figure 5.2). The upper paints have become islands of paint resulting from contraction of surface paint layers (Figure 5.3). The large cracks in particularly expose the colors of underlying paints, and seriously change the tonality, the color harmony and the composition (Figure 5.4). This type of cracking is not observed in the sky area of the background, the light colored area of the cows, and the thinly painted area in the middle ground (Figure 5.5).

Along with the painting of this version, which was shown at the Salon, both an oil sketch (1834-35, Inv. Nr. HWM 287, The Mesdag Collection) and an *ébauche* (ca. 1835-36, Inve. Nr. 4371 Musée de Picardie, Amiens, France) for the painting have survived, and interestingly they do have not such severe defects (Figure 5.1) [Schulman *et al.* 1999:143-144]. A distinctive difference between the Salon version and the other two paintings is the thickness of the paint. In general, application of the paints in the Salon version is much thicker, and the stratigraphy seems to be much more complicated compared to the sketch and the *ébauche* version. This, however, is not the result of a

(a) (b) (c)

Figure 5.1 *La Descente des Vaches* by Théodore Rousseau
(a) *The descent of the cattle in the High Jura mountains,* Salon version, 1835-36, 259 × 162 cm, HWM 286, The Mesdag Collection, The Hague, The Netherlands. ©The Mesdag Collection, The Hague
(b) *ébauche* version, ca. 1835, 258.8 × 166 cm, Inv. nr. 4371, Musée de Picardie, Amiens, France. Musée de Picardie, Amiens. Inv. Nr. 4371. Canvas, 258,8 x 166 cm. (This painting was closely observed in one of the galleries of the museum in March 2000 by René Boitelle.)
(c) *The descent of the cattle in the Jura mountains (sketch)*, 1834-1835, 114 × 59.8 cm, HWM 287, The Mesdag Collection. ©The Mesdag Collection, The Hague

Figure 5.2 Severely cracked dark paint of the wood in the background, at center and close to the upper edge.
©R. Boitelle, Van Gogh Museum/The Mesdag Collection 2015

Figure 5.3 Detailed surface of the brown paint where paint islands have occurred at the middle of right side background.
©R. Boitelle, Van Gogh Museum/The Mesdag Collection 2015

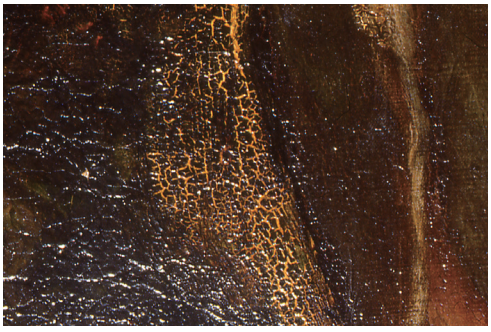

Figure 5.4 Cracks reveal colour of the underlying paintat the left side of foreground.
©R. Boitelle, Van Gogh Museum/The Mesdag Collection 2015

Figure 5.5 Sky area showing limited deformation.
©R. Boitelle, Van Gogh Museum/The Mesdag Collection 2015

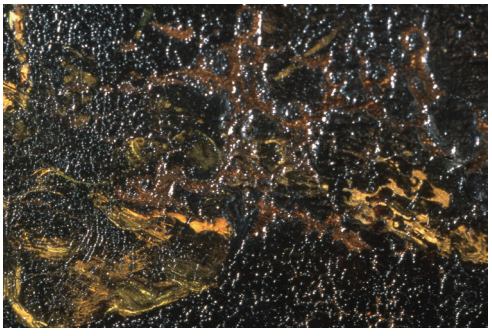

Figure 5.6 Muddy deep green paint over yellow and brown paint layers at around the middle of foreground where wild plants depicted area.
©R. Boitelle, Van Gogh Museum/The Mesdag Collection 2015

compositional change during the painting process, but may be related to Rousseau's concerns and dissatisfaction with the desired appearance of the painting [Boitelle *et al.* 2001].

The occurrence of cracks to such a large extent only in the Salon version clearly indicates poor drying of the paint materials perhaps due to improper technique or poor choices or combination of paint media by the artist. In addition, another major defect is the extremely dark brown and black appearance of the surface of the Salon version, which is suspected to be a result of a color change in the paints.

5.1.2 Possible reasons for the changed appearance of *La Descente des Vaches*

The appearance of the painting must have changed, leading to the composition becoming less visible, early in its existence. The deteriorated state of the Salon version was mentioned in Rousseau's biography *Souvenirs sur Th. Rousseau* written by his friend Alfred Sensier in 1872, although he did not specify the defects [Sensier 1872: 77-80]. It is also unknown when these defects appeared or were first recognized. In 1855, however, the critic G. Planche praised the painting, which suggests there were no severe cracks or color changes yet [Leeman and Pennock 1996: 380-384].

Sensier claimed that the materials used by the artist had caused the poor condition, especially the use of bituminous (= asphalt) or mummy materials used with drying oil called 'huile grasse' (boiled oil with a drier) and a resin varnish called 'vernis double' (presumably mastic varnish) [White *et al.* 1998]. Cracking problems due to slow drying and darkening in paint were often considered to be connected to the use of bituminous materials in the nineteenth century [Languri and Boon 2005; Erhardt *et al.* 1990; Willoughby 1987; White 1986; Stoner 1990; Child 1995]. Indeed, the *ébauche* was once thought to have been damaged due to darkening of bitumen reported in 1868. However it seems to be the yellowed varnish that caused the *ébauche* to look darkened [Leeman and Pennock 1996: 380-384].

In the Salon version, some areas are clearly affected by the yellowed varnish and also the extensive deformation of the surface [Jones 1990; Carlyle and Southall 1993], however they can't fully explain the current dark appearance. Muddy green and brown paints, for instance observed over the light paint in the foreground (Figure 5.6), are more likely responsible for the dark appearance. This is obviously not the artist's original intention nor the result of a compositional change during the painting process, as the Salon version and two preparatory paintings are almost identical.

A preliminary study proposed that the causes of the surface deformation and the dark appearance are not the presence of asphalt pigment as had been proposed by Sensier [Languri 2004:160-166]. If any was used, the amount of these materials should have been very small, therefore it was ruled out as the main cause of the drying cracks. Moreover, the reconstruction experiment in the preliminary study also showed that

when properly prepared asphalt[2] is not an anti-oxidant, although non-treated asphalt has an anti-oxidant effect [Languri *et al.* 2005].

An indication of lignite, which is a characteristic components of Kassel earth type pigments, were found in both the Salon version and the oil sketch [Languri 2004:160-166]. Although Kassel earth was another suspected anti-oxidant, the experimental study by Languri demonstrated that Kassel earth does not have an anti-oxidant effect on the drying of linseed oil.

The presence of other non-drying materials such as beeswax and vermilion are instead suggested as the real cause of the disastrous condition, but reasons for the dark appearance remained unclear. The analytical results showed no significant material differences in either pigments or binding media between the oil sketch and the Salon version. This suggests that a specific material is not the most significant cause of the defects, making it more likely that Rousseau's painting technique could also be responsible for the painting defects that developed.

The present study refers to a paper by Boitelle *et al.* [2001], which describes the history of the three paintings and a description of the condition of *La Descente des Vaches* in more detail. Recently, the decomposition of emerald green pigment was shown to be an important cause for the painting's dark appearance [Keune *et al.* 2012]. In this study, aspects of chemical and physical states of the paints of the Salon painting were reinvestigated in more detail in order to obtain a better insight into possible causes of the remarkable appearance. The chemical composition of the paint and distribution of the paint materials in the multi-layered paint system have been studied by using various imaging analytical techniques. The results of the analyses are combined with optical theory to discuss relations between the current appearance of the painting and the chemistry of the paints.

5.2 Painting study

5.2.1 Color appearance and paint conditions

5.2.1.1 Surface appearance and the samples

In the middle-ground and background the woods around the cows and cowherd are mostly brown and currently these areas are too dark to see any details. In the foreground, some green and other colors are still recognizable on close observation. However, these differences are not clear if you view the painting from the typical viewing distance of a few meters. This suggests that there must be differences in the paint composition or painting technique that created a distinctive color appearance in each area.

2: Most of recipes for preparing ahphalt involve headting (slow fire) and/or mixing with drying oil or resin [Carlyle 2001: 403-407], and the details of preparation methods in the experiments are descrived elsewhere [Languri 2004: 120-124].

Figure 5.7 Sampling areas ©The Mesdag Collection, The Hague 2015

In order to investigate these aspects, samples were taken from twelve different areas where are mostly close to the edges. The sample locations are shown in Figure 5.7 and the samples are given unique names from 286A to L (Table 5.1).

Samples 286A and C were taken from cracks close to the left corner in the foreground. This area is painted with a green paint, which looks almost black on the surface. The upper paint layers, which include the green paint are broken and show the reddish brown paint underneath (Figure 5.8). Remarkably, the underlying paint has not cracked. Sample 286A before embedding appears as a brown mass in which it is hard to see other colors, while in 286C the green color is visible where the upper paint layers are thin (Figure 5.9). Samples 286B, H, and I were taken from along the left edge. The surface colors of 286H and I are too dark to see details. The 286D, E, and I are brown paint fragments taken from the area of depicted woods. The upper brown paints near where 286D was taken contracted and have become islands of paint (Figure 5.3). Samples from light colored areas are 286F, G, and L. The 286F was taken from the sky in the background, while 286G, L, and K were taken from the foreground where relatively light colors of paint are visible.

The 286J was taken near the left edge in the middle-ground for a varnish analysis. The sample was removed with solvent on a cotton swab.

The eight samples 286A-H were divided and analysed with mass spectrometric

Table 5.1 Sample list

Sample name	Surface color	Description of the location
286A	Deep green (visually close to black)	Green can be recognised although the area is very deep dark green
286B	Deep green (visually close to black)	Left-hand side, bottom corner
286C	Deep green (visually close to black)	Close to the 286A was taken
286D	Brown	From the brown background where is the brown paint islands have occurred
286E	Brown	In the foliage, left from a tree truck
286F	Off-white, gray, including a bit of green	Sky paint, as a representative for light coloured areas
286G	Yellow	Relatively light coloured area from the foreground
286H	Very dark, visually black	Left-hand side, where very little colours are observable
286I	Brown	From a tree trunk where the brown paint islands have occurred
286J	(Varnish)	(Removed by a swab with ethanol)
286K	Green over white paint, with varnish	From a boarder between the back of cow and the brown background, where the green is visible
286L	Thin layers of green and brown, and cream-yellow	Green paint stroke in the foreground

and microscopic techniques. The other three samples, 286I, K, and L were made into cross-sections for microscopic investigation. The layer structure was examined to investigate the correlation with the current appearance as well as the surface deformations. The original materials used and chemical conditions of the paint were examined mostly by imaging FTIR and SEM-EDX. Organic components were analysed by Py-TMAH-GCMS, DTMS, and examined with imaging FTIR.

5.2.1.2 Paint layer build-up

The original color appearance of the dark paints is not clear. The cross-sections of the dark paint that show no clear color and a very complex layer buildup. The many superimposed paint layers resulted in an unusually thick paint system, point to the time consuming working methods of the artist. Observation with UV, SEM-BSE and element distribution by EDX were indispensable to distinguish these layers.

Sample 286A is a key cross-section, which includes a whole sequence of paints from the ground layer to the varnish layer although it is parted in two pieces (Figure 5.10). The total thickness of the paints, excluding the ground and varnish layers, is estimated to be 400 µm based on common layers in both pieces. The upper paint layers show no apparent layer structure in the visible light images due to poor light reflection (Figure 5.11). Layers 9 and 10 are only distinguishable based on differences in the electron back scattering in the SEM. Layer 9 is more electron reflective than layer 10 due to a higher relative amount of the lead. In contrast, layers 10 and 11 show little

Figure 5.8 Area where samples A and C were taken. The reddish brown paint underneath is exposed through the cracks of the upper green paint layer. ©R. Boitelle, Van Gogh Museum/The Mesdag Collection 2015

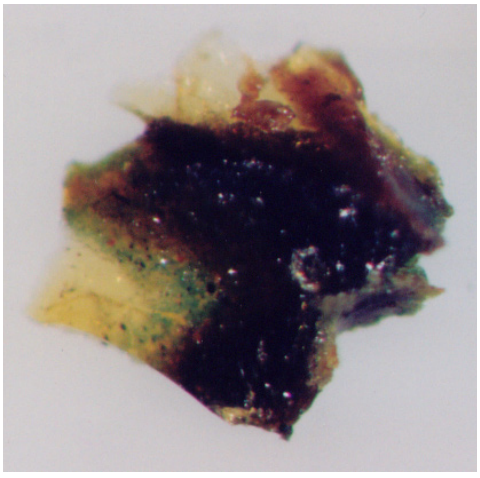

Figure 5.9 Sample C before embedding. The green color is visible where the paint is thin. ©R. Boitelle, Van Gogh Museum/The Mesdag Collection 2015

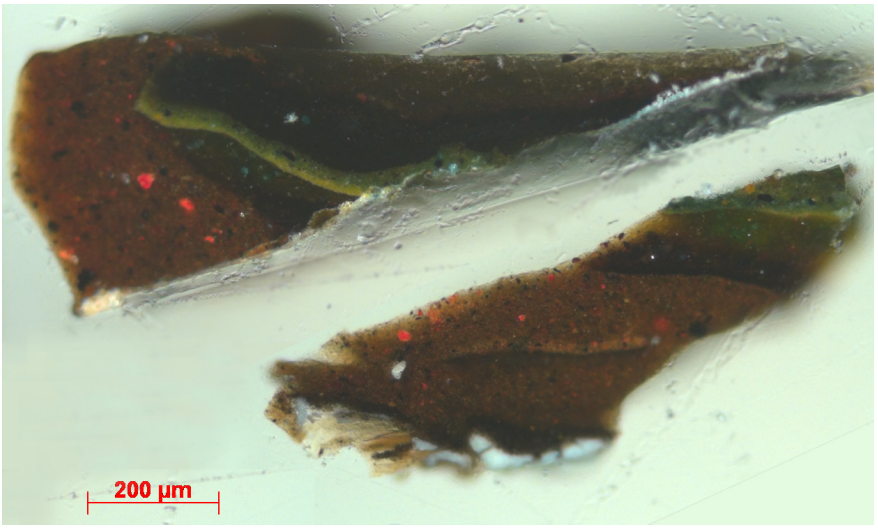

Figure 5.11 Visible light microscopic image (VIS) of 286A in cross-section.

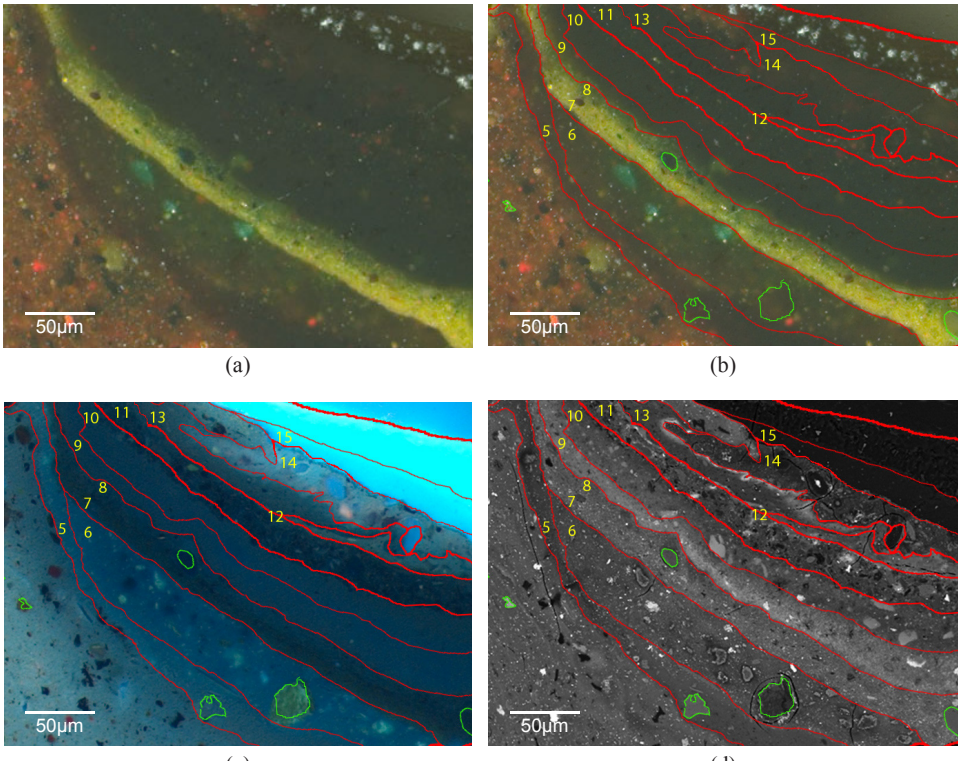

Figure 5.10 Paint layer build-up of cross-section 286A, upper paint layers: (a) VIS, (b) VIS with the outlines of each layer indicated, (c) with ultra violet light (UVf), (d) SEM backscattered (BSE) image.

contrast difference in the BSE image, however, they do show different responses to UV-light. Layers 11 to 13 can be distinguished based on their element distributions. Layer 14 shows a slight UV fluorescence and is also confirmed to be an independent paint layer by SEM.

The upper paint layers of 286B and C consist of translucent green and brown paints (Figures 5.12 and 5.13). Some paint layers show a similar electron reflectivity in their SEM-BSE images to that of the upper paint layers of 286A. In the paints a small number of particles were observable (Figure 5.14) and the sizes of these particles are less than 2 µm, indicating a glaze-like nature, and even some layers with an amorphous texture resulting in a cloudy appearance. In some cases, discernable particles are less electron reflective than the amorphous areas. The particle sizes are important for the surface appearance because small particles which are less than half of the wavelength of the incident light will not have the ability to scatter light [Stieg 1962].

Sample 286D consists of thirteen paint layers with a total thickness of c. 260 µm (Figure 5.15). Only the second paint layer looks green, the other layers are extremely light absorptive.

The paint sample 286H also appears very dark and the colors of paints are hardly observable in cross-section. Both 286D and H were also prepared as thin sections and studied on a white substrate in reflection mode, which was necessary to be able to observe the colors of the individual layers. For instance, the lower layer of 286H, which looks visually black in the cross-section, is actually green in the thin section (Figure 5.16). The results indicate that paint layers in both paint samples are highly light absorptive but less reflective.

Sample 286E, which was taken from the foliage area in the background, contained few light colored paint layers. The thickness of all paint layers is c. 200 µm; no white ground was included in the cross-section. The presence of several paints was shown by variations in UV fluorescence, and by inhomogeneous contrast in the BSE image (Figure 5.17). The sample looks dark brown in the middle layers, and no clear layer structure is observed due to a lack of light reflected. Both wet-in-wet and incomplete paint mixing on a

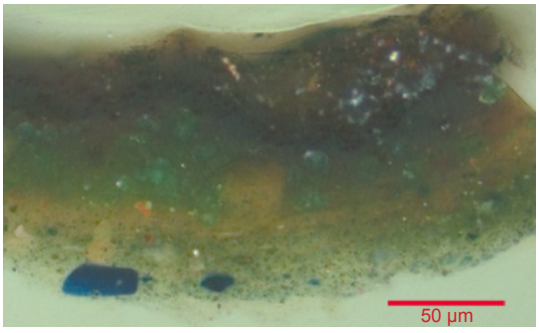

Figure 5.12 VIS of 286B in cross-section

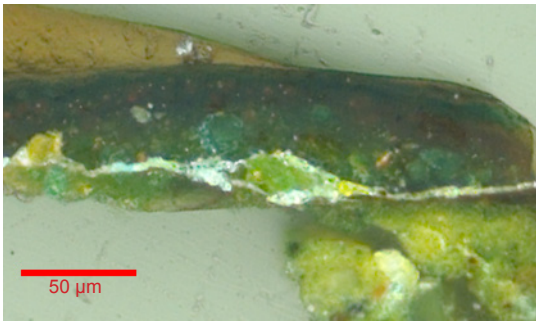

Figure 5.13 VIS of 286C in cross-section

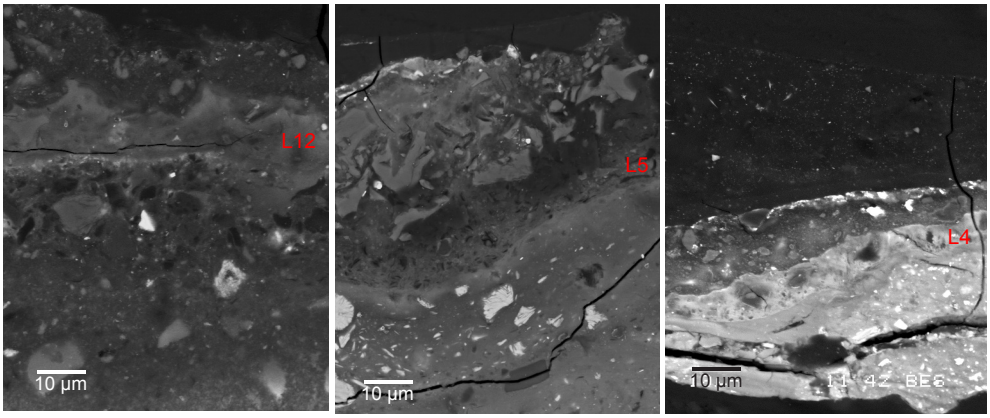

286A 286B 286C

Figure 5.14 BSE images of 286A, B, and C at the same magnification. Layers with marks of L12 in 286A, L5 in 286B, L4 in 286C show little particles and the amorphous feature.

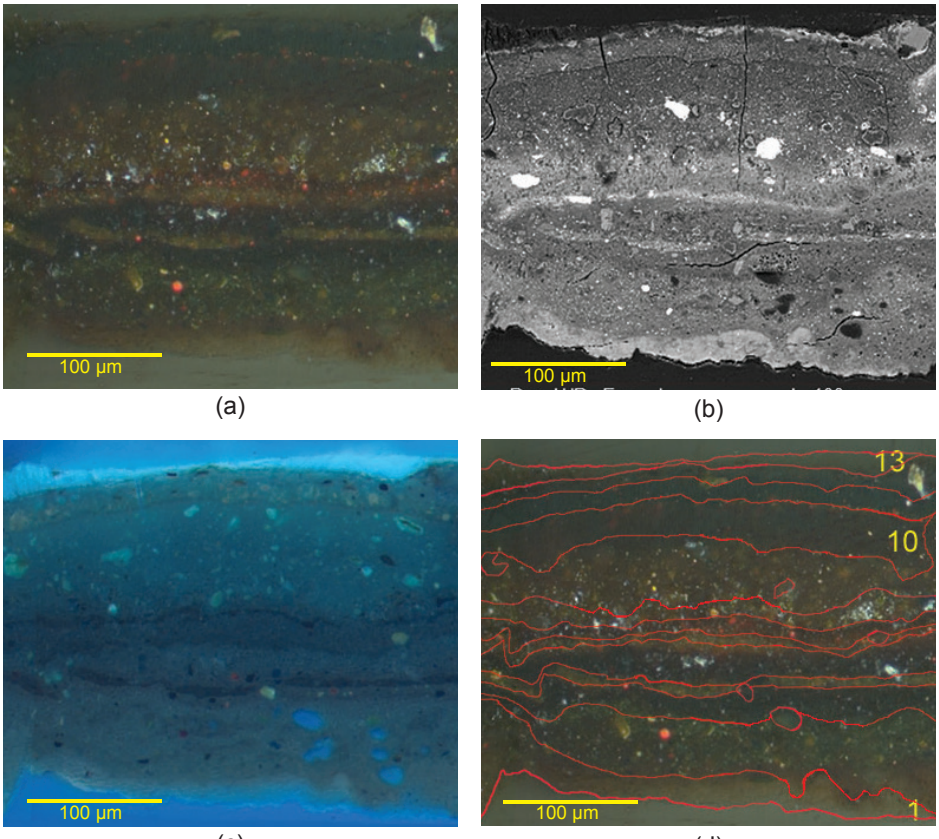

Figure 5.15 286B (a) VIS, (b) BSE image, (c) UVf, and (d) layer build-up with outlines based on interpretation of (a) to (c)

palette or even on the canvas are possible explanations for this type of layer structure.

In contrast, the colors and layer structure were easily observed in 286F, which is the only sample taken from a light area. In this case the paints contain some of white pigments ensuring sufficient light reflection (Figure 5.18). Three pale blue paint layers 1-3 in the lower part are presumably the base color of the sky. On top of the blue, more colors e.g. red (layer 6), white (layer 8), yellow (layer 9), and green (layer 10) were applied.

Samples 286G, K, and L also contain relatively light colored paints. In 286K, white paint layer 1 makes an optical contribution to a green paint layer right above

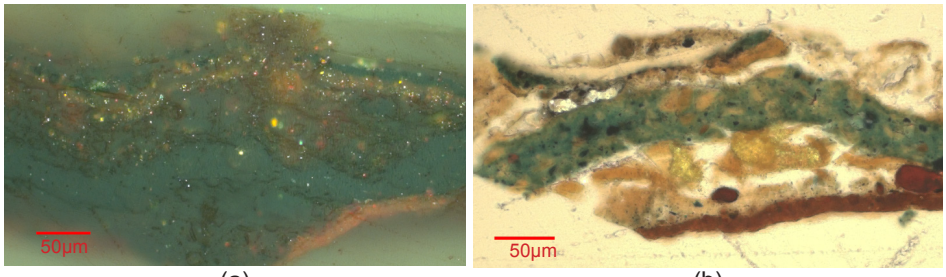

(a) (b)

Figure 5.16 VIS of 286H: (a) cross-section, (b) thin-section with a white substrate in reflection mode.

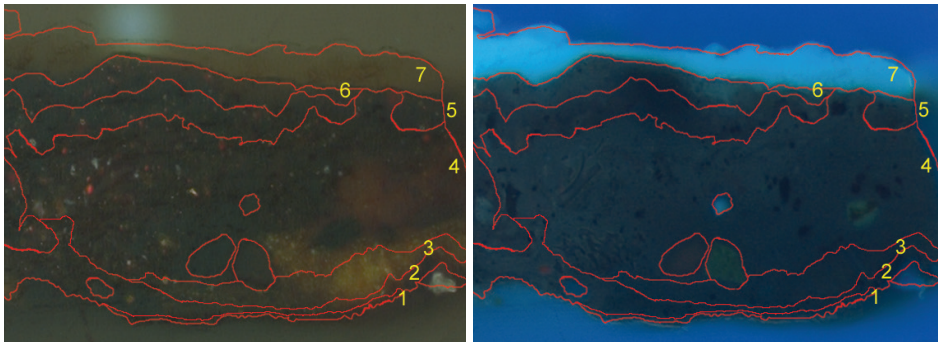

(a) (b)

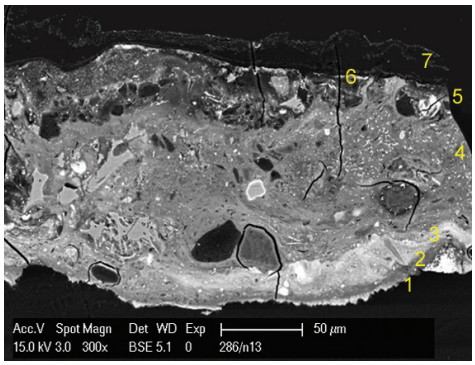

(c)

Figure 5.17 286H in cross-section: (a) VIS, (b) UVf, (c) BSE image.

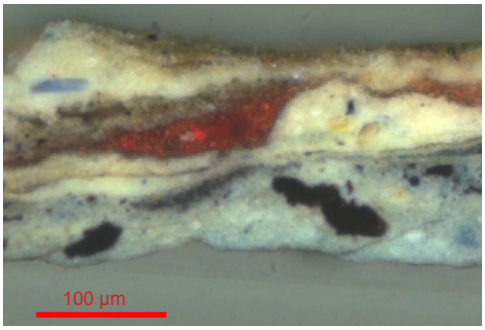

Figure 5.18 VIS of 286F taken from the sky depicted area

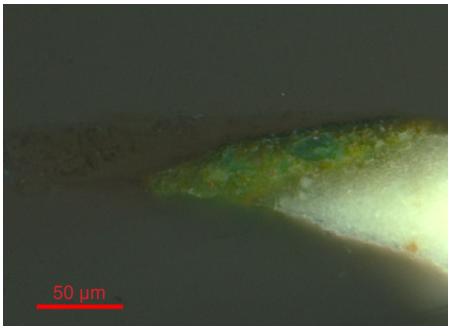

Figure 5.19 VIS of 286K

it (Figure 5.19). The green color must be either translucent or light absorbing as it is recognizable from surface examination only when it is illuminated by high intensity light. Since there is a brown paint layer on top of this paint, the green color could have been toned down at the surface, in addition to the aged varnish layers. Although the areas in the foreground where these samples originate are not remarkably light in appearance, they are still lighter due to the reflection from the light paint of lower layers compared to the other dark areas such as where 286A was taken.

In summary, the very limited color information in the cross-sections is due to strong light absorption in combination with the presence of none or limited amounts of white and/or light colored pigments. The chemical and optical changes, which could explain these phenomena will be discussed below.

5.2.1.3 Paint deformation

Paint cracks consistently appear in the dark areas where the paints were thickly applied. In many cases, only upper paint layers are cracked thus exposing the underlying paints. For instance, the contours of the cowherd in the middle of foreground are still visible through the cracked upper paint layers (Figure 5.20). The brown glaze-like paints, which were assumed to be applied for

Figure 5.20
Details of the cowherd in the center of the painting observable contours implying that the paint layers of pictorial composition is not cracked. [©R. Boitelle, Van Gogh Museum/The Mesdag Collection]

giving depth and shadow effects, are cracked, but paint of his figure, such as the arm, face, and hat, is not broken. This indicates that the lower paints are the least cracked, while the upper brown and green paints, which are fairly translucent, are severely cracked.

The cross-sections also show that the upper paint layers are more deformed than the lower paint layers. An extreme case is observed in 286H, which is strongly cracked and even protruded through the varnish layers as if the paint erupted (see Figure 5.16). This sample clearly demonstrates that the upper paints including the varnish layer hardened before the lower paint did. The upper paint layers could not bear the physical stress due to the mobility of the lower softer paints.

Samples 286A, B, D, E and I show wavy and uneven borders between two paint layers or the paint/varnish interface indicating paint shrinkage (Figure 5.21). In 286I, a wavy interface is observed between the paint and the varnish layers that are contrasted by the smoother surface of the varnish (Figure 5.22). In 286A some perpendicular cracks are observed through the layers possibly due to shrinkage of the paint.

These paint conditions on a microscopic level, such as the cracks and shrinkage, indicate that the upper paint and varnish layers are relatively harder than the lower paint layers. The condition matches the causes of alligatoring cracks. Such severe cracks must have been caused by application of a thick paint layer or a subsequent layer over an inadequately dried paint [Thompson 1915]. The surface dries earlier and will prevent the underlying paint layer from oxidative cross-linking, thus slowing the drying rate of the underpaints. Considering it was not uncommon for Rousseau to take years to complete a painting [Thomas 1999], this painting was rather rapidly finished over a period of less than two years to be in time for submission to the Salon in 1836 [Leeman and Pennock 1996: 380-384]. The presence of so many paint layers, which must have been applied over a short period, would suggest that the lower paint layers did not sufficiently dry, which would explain the surface deformation.

Cracks and wrinkles also influence the surface appearance. The deformed surface

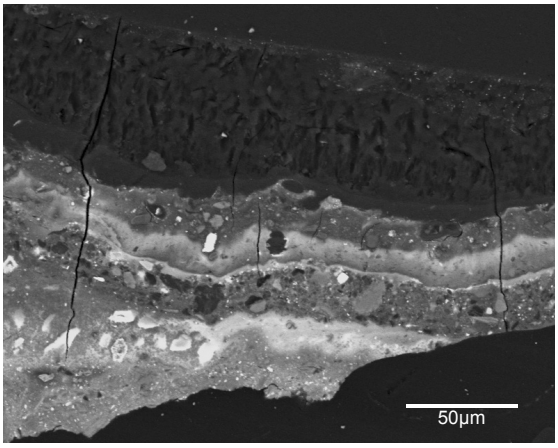

Figure 5.21
Wavy borders of the upper paint layers in 286A (BSE image)

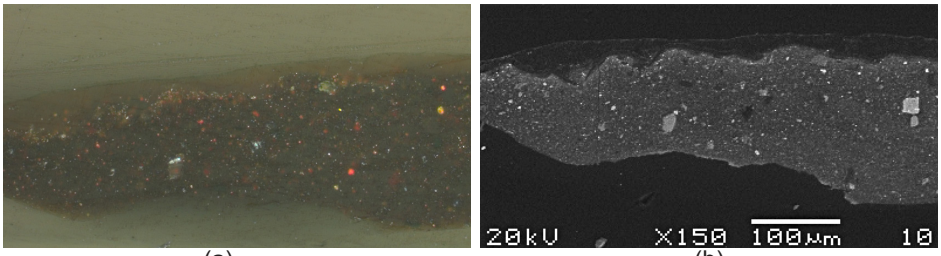

Figure 5.22 A wavy border of the top paint layer and varnish layer, and relatively smoother surface in 286I, (a) VIS, (b) BSE image.

reflects light diffusely, which leads to a relative decrease of light transmission into the paint, with the consequence of less color information from the paint. Furthermore, the edges of the cracks stand out disturbing the viewing of the painting.

5.2.2 Pigment Identification

The paint analysis indicates that the artist used many types of pigments together, which makes each area of paint unique and complex. It also suggests that some pigments have been involved in chemical reactions in the course of time making the situation even more complex. A summary of the pigment identification results including the alteration products is presented in Tables 5.2-5.12. The pigment identification and some specific features observed during the examination are discussed below.

5.2.2.1 Yellow

The presence of an organic yellow pigment was noted both through the identification of their aluminum substrates in many cross-sections and with mass spectrometric analysis. Yellow ochre and chrome yellow were also found in the cross-sections by the use of optical microscopy and SEM-EDX analysis.

The most noticeable layer containing yellow ochre is found in 286A (layer 7). Semi-transparent particles in this layer were found to be silica and alkali aluminum silicate, which are commonly found in natural ochre [Helwig 2007]. IR absorptions at around 1036 and 1086 cm^{-1} for aluminum silicate are clearly shown in the FTIR image.

Chrome yellow (lead chromate) was found in 286A, B, C, F, H, and L. Although the amount was rather small, strong light reflection in the VIS images and detection of lead and chromium in these particles indicated the use of the pigment.

Another type of yellow was a lake suggested by a yellow UV fluorescence and the detection of an aluminum substrate with EDX analysis. Relatively large particles of potassium aluminum sulfate ($KAl(SO_4)_2$) were found in 286C, D, E, H, and L. Smaller particles containing aluminum were also found in 286A and B. The yellow lake was

used not only for making the yellow-brown color, but also for a green color in mixtures with Prussian blue.

A few relatively large yellow UV fluorescent particles in 286A, B, and D may point to a specific type of yellow lake. The EDX mapping shows that its particles are carbon-rich; no other specific elements were detected, so the presence of genuine Indian yellow, a magnesium or calcium salt of euxanthic acid, was ruled out. This result implies that the particles are from an organic yellow dye that does not require a substrate, such as a flavonoid.

The presence of Indian yellow was demonstrated in 286D and H using mass spectrometric techniques (see below). Due to the nature of these techniques, the layer(s) in which the pigment was present could not be discerned. In principle, Indian yellow can be identified on the basis of its characteristic acicular shape and/or with UV fluorescence of yellow to orange [Baer *et al.* 1986], however this could not be confirmed for 286D and H, probably due to the low concentration of the yellow or the quenching of UV fluorescence.

Indian yellow in mass spectrometry

Indian Yellow is a yellow dye used probably since the fifteenth century. However this dye was not used in Europe before the late eighteenth century. Genuine Indian Yellow was manufactured from the urine of cows fed almost exclusively on mango leaves. As the production was banned sometime in the first half of the twentieth century, Indian yellow is not commercially available nowadays.

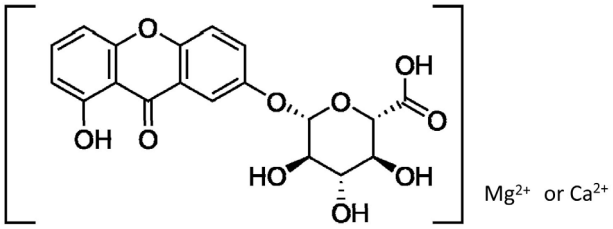

(1) Euxanthine

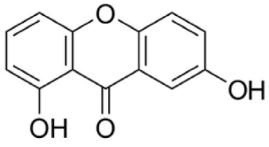

(2) Euxanthone

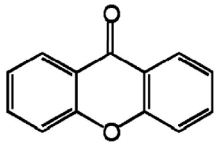

(3) Xanthone

Figure 5.23 Chemical structures of euxanthine and its related compounds

The molecular ion of euxanthone, which is a part of the main component in Indian yellow pigment, was detected with DTMS and Py-TMAH-GCMS (analytical conditions are described in Appendix). The main component of Indian yellow is magnesium or calcium euxanthate called euxanthin (Figure 5.23). Euxanthin is a glycoside of euxanthone (1,7-dihydroxyxanthone), which is a hydroxyl derivative of xanthone and naturally occurs in the leaves of *Mangifera indica* L., the Indian mango tree [Raistrick *et al.* 1936].

DTMS results

The peak at *m/z* 228 with an exceptionally high intensity is detected in the samples 286D and H. This peak was attributed to the euxanthone fragment ion. Possible euxanthone related fragment ions other than *m/z* 228 were not confirmed in any spectra. This implies that the euxanthone moiety in Indian yellow is rather stable using this analytical method.

In order to confirm that the peak at *m/z* 228 is indeed from Indian yellow, a genuine Indian yellow was analysed (reference collection of ICN, now RCE). Its identity was confirmed by ATR-FTIR and SEM-EDX.

The peak at *m/z* 228 was detected in a scan range around 65-75 seconds. This result strongly supports that the peak at *m/z* 228 in the oil paint samples can be attributed to euxanthone.

Py-TMAH-GCMS results

The euxanthone moiety was also found in the Py-TMAH-GCMS results. A total ion current (TIC) chromatogram of 286H is shown in Figure 5.24. In addition to these peaks, a peak with relatively high intensity was detected at retention time near 37 minutes. The peak is not attributable to a drying oil nor another possible component derived from binding media. The mass spectrum of this peak is shown in Figure 5.25. The peak at *m/z* 227 is assigned to a deprotonated euxanthone fragment ion. Euxanthone can easily be released by hydrolysis of the glycoside bond of Indian yellow. The peak at *m/z* 256 was attributed to di-methoxy euxanthone formed by the methylation procedure. Two hydroxyl groups at the 1 and 7 position are methylated. The peak at *m/z* 241 with rather low intensity is assigned to mono-methoxy euthanthone of which either one of the hydroxyl groups at the 1 or 7 position is methylated. The peak appearing at *m/z* 210 is derived from dehydroxylated euxanthone.

Genuine Indian yellow paint was also analysed in order to obtain reference mass data. The sample was an oil paint made of Indian yellow and a commercial linseed oil. All the earlier assigned peaks at *m/z* 227, 256, 241, and 210 were confirmed in the mass spectral data.

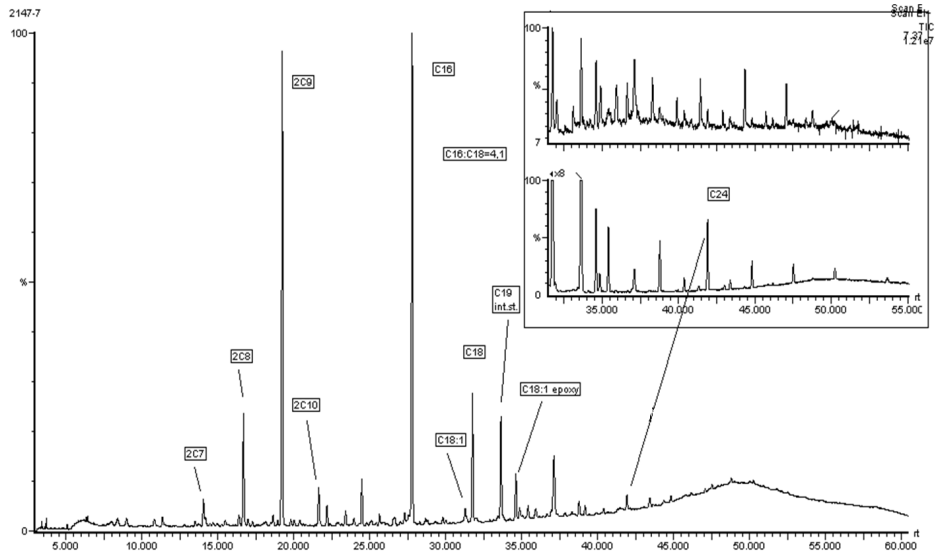

Figure 5.24 Py-TMAH-GCMS chromatogram of 286H

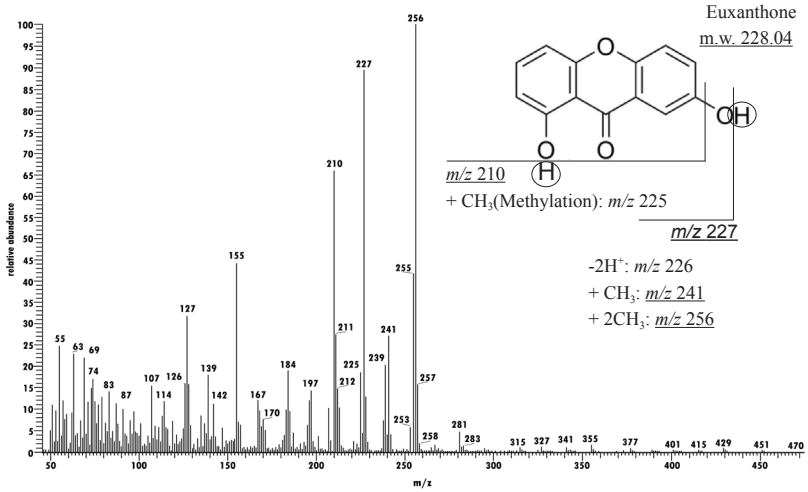

Figure 5.25 Mass spectrum of the euxanthone peak at retention time 37 minutes of Figure 5. 24 and assignment of the major ion fragments.

5.2.2.2 Prussian blue

Prussian blue was detected with FTIR through its typical cyanide bond absorption at around 2100 cm^{-1} (Figure 5.26). This absorption was observed in the relatively large dark particles in 286B, C and H (Tables 5.3, 5.4 and 5.9). EDX detected elemental aluminum in these particles in addition to iron, suggesting the presence of an aluminum (Al) compound combined with Prussian blue. This can be a result of Al substitution

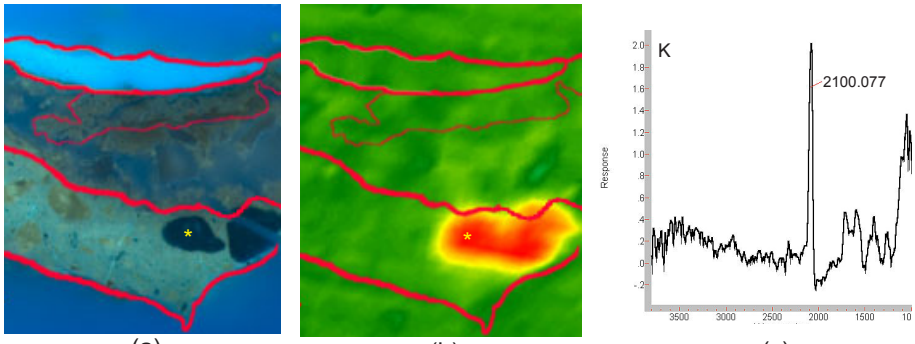

Figure 5.26 Prussian blue on aluminum compound: (a) UVf, (b) FTIR image of 2100 cm^{-1} absorption, (c) FTIR spectrum of the marked spot

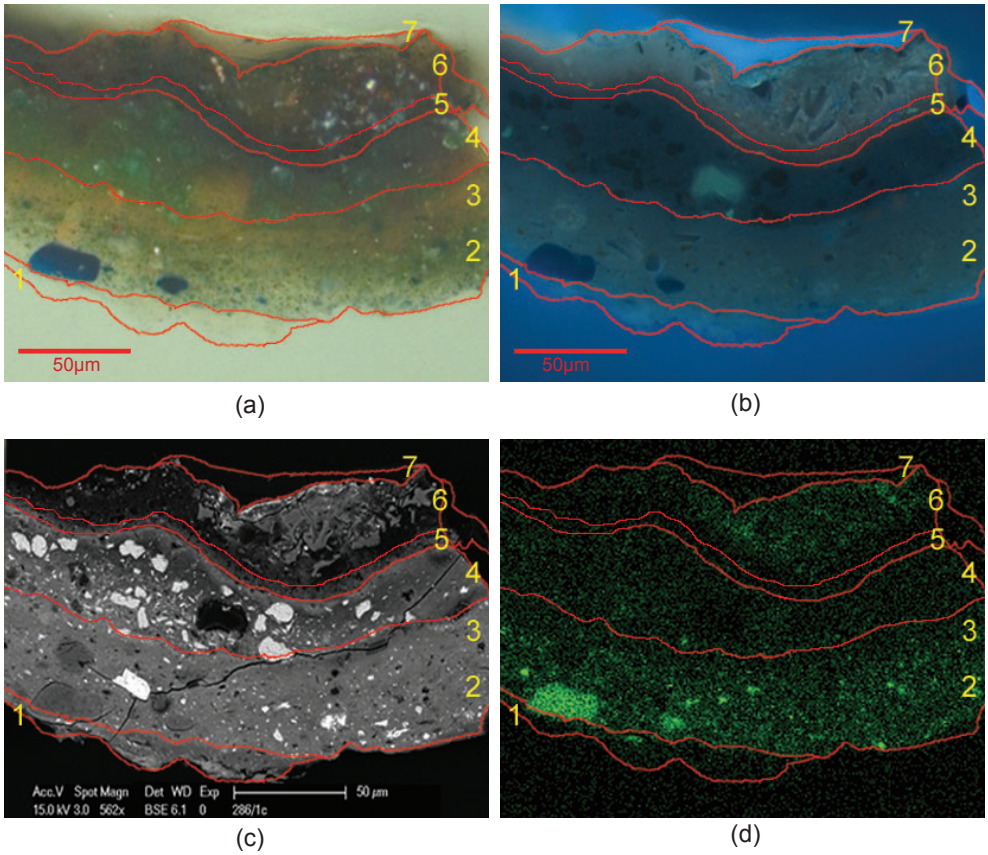

Figure 5.27 Cross-section images of 286B (a) VIS showing a green layer (2) and a yellow layer (3), (b) corresponding area of UVf, (c) BSE image, (d) iron (Fe) mapping of EDX

for the iron (Fe) or potassium (K) in Prussian blue that is often found in 19th century reference collections of the pigment (Townsend Pers. Comm. 2014). The pigment was also known to be difficult to wet with oil due to its low density, so this was facilitated by addition of alumina during the production process in contemporary 19th century paint industry, although this process might have not been introduced by Rousseau's time [Heaton 1928:157-159].

In other cases, the pigment was found in the form of fine particles with SEM-EDX, for example in the mixed green second paint layer in 286B. Because of the strong tinting strength of Prussian blue, little is necessary for a green color, which explains the similarity in contrast and elemental distributions in SEM-EDX results to the yellow third paint layer right above (Figure 5.27).

5.2.2.3 Earth pigments

The use of ochre pigments was indicated by the detection of iron with EDX in red or yellow particles. Silica and aluminum silicate were found together with the iron rich particles indicating the use of natural ochre pigments [Helwig 2007]. Representative layers containing red ochre are found in 286A and H. The reddish brown and oval-

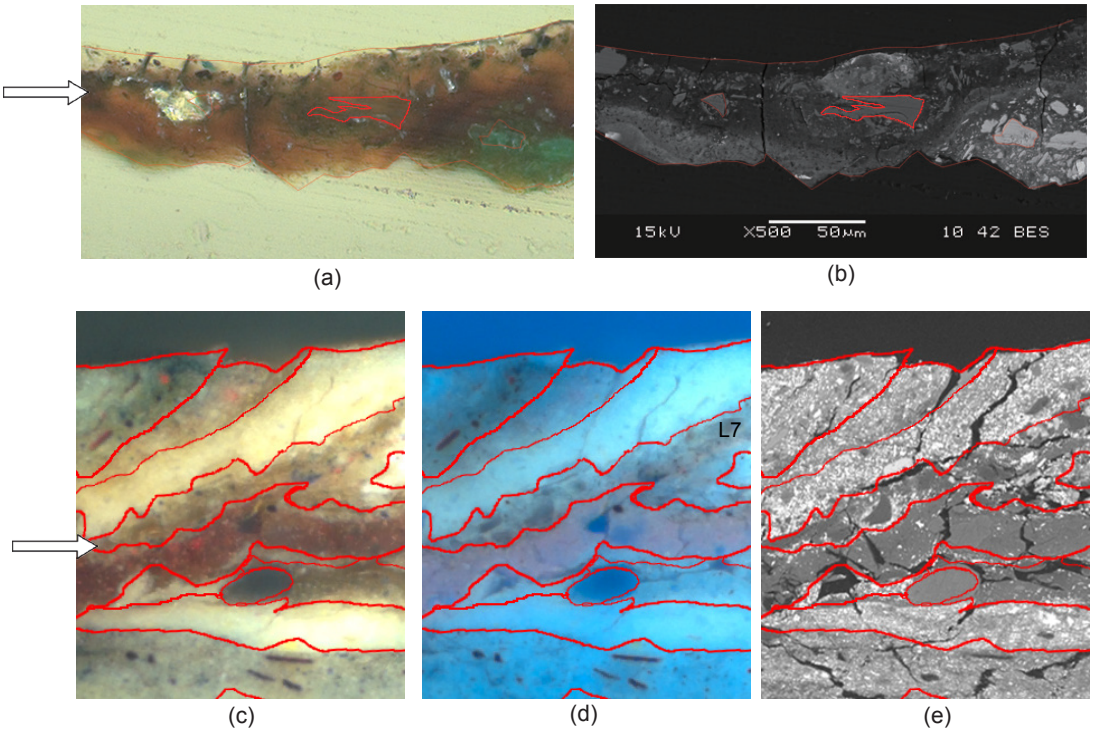

Figure 5.28 Translucent irregular-shaped particles in 286B and F layer 7 (indicated with arrows). (a) VIS of 286B, (b) 286B BSE image, (c) VIS of 286F, (d) 286F UVf (e) 286F BSE image

shaped particles are the characteristics of red ochre. The red paint layer of 286A situated right above the white ground may be intended to be a first paint layer used to tone down the white ground [Roy 1999].

Translucent irregular-shaped particles were found in 286B and D to H (Figure 5.28). They consist of sodium, aluminum, silicium, potassium, and small amounts of calcium and iron. The particles do not show UV fluorescence. Aluminum-silicate absorption at 1000-1050 cm^{-1} is observed by imaging FTIR suggesting the presence of an earth pigment. According to the color they differ from that of the other ochre containing layers, but could be green earth.

Green earth is normally defined by the presence of celadonite ($K(Mg, Fe^{2+})(Fe^{3+}, Al)[Si_4O_{10}](OH)_2$) or glauconite ($(K, Na)(Fe^{3+}, Al, Mg)_2(Si, Al)_4O_{10}(OH)_4$). Although the presence of magnesium was not confirmed in these particles, it is not necessarily a requirement as any greenish sand could have been called green earth [Grissom 1986]. It is also possible to be a part of low iron content ochre.

5.2.2.4 Copper arsenate green

Detection of copper and arsenic elements with EDX in green particles in 286A, B, C, and K suggested the use of Scheele's green or/and emerald green (the latter is called *vert Véronèse* in French). Scheele's green first became available in the late 18th century. It is a copper arsenate with an undermined chemical formula [Fiedler and Bayard 1997]. Emerald green was synthesized in 1814 and the chemical formula is most likely copper acetoarsenate ($Cu(CH_3CO_2)_2.3Cu(AsO_2)_2$). Scheele's green seems to have been replaced soon by emerald green since it was considered inferior. However, Scheele's green was still available when Rousseau created the painting [Constantin 2001].

The flower-like round shape of particles, which is a characteristic feature of emerald green [Fiedler and Bayard 1997] is observed in 286A, B, C, G and K. Very fine, and occasionally small oblong-shaped, copper arsenate particles were also found in 286B, C, and I. Emerald green has copper carboxylate absorption at around 1560 and 1470 cm^{-1} owing to copper acetate, which were detected in 286C and G (Figure 5.29). Raman spectroscopy eventually could show that only emerald green is present in the paints [Keune *et al.* 2012].

The presence of arsenic compounds was demonstrated also by the detection of poly-arsenide and arsenate (III) ion fragments in DTMS analysis (Appendix to Chapter 4). These ion fragments were detected mostly in the dark paint samples. The results of 286B and C for instance show high intensity peaks at *m/z* 289, 300, and 395 (Figure 5.30), which were attributed to arsenic tetraoxide (As_3O_4), tetraarsenic (As_4), and arsenic hexoxide (As_4O_6) respectively (Table 5.13, and see also Table 5.14 in later section). A detected ion fragment of *m/z* 134 in 286B was assigned to arsenic acetate ($AsCH_3COO$, calculated mass 133.96), which is a positive indication of the presence of emerald green. It was thermally generated with a reduced mono-arsenic and an acetate ion during the analysis.

The detection of the arsenate clusters; As_nO_m can be explained by polymerisation

tendency of the arsenate ion $[AsO_2]^-$ [Lee and Harrison 2004]. The As_4O_6 arsenate cluster is preferred under the analytical conditions. The tendency of XO_4 to become poly-atomic clusters in elements of the nitrogen group (phosphorus, arsenic, and antimony) and sulfur under certain conditions is known [Boon *et al.* 1995; Lau *et al.* 1982; Špalt *et al.* 2005].

The mass spectrum of 286A differs from the above mentioned samples since the reduced tetra-arsenic cluster at *m/z* 300 was found without detection of arsenate clusters. An almost complete absence of the arsenates is remarkable since the arsenate clusters are detectable at lower a temperature than that of the reduced arsenic clusters (Figure 5.31). It was thought to be an indication that arsenic sulfide pigments known as orpiment and realgar, which do not possess an arsenate group, were used. An analysis of an orpiment reference however excluded this possibility. Arsenic-sulfur bonding is strong enough to resist the thermal dissociation during the analysis. Therefore if intact orpiment was present in the sample, arsenic-sulfur clusters should have been detected. It is more likely that the detection of high intensity of poly-arsenic ions in 286A points to elemental arsenic as a possible degradation product in the paint.

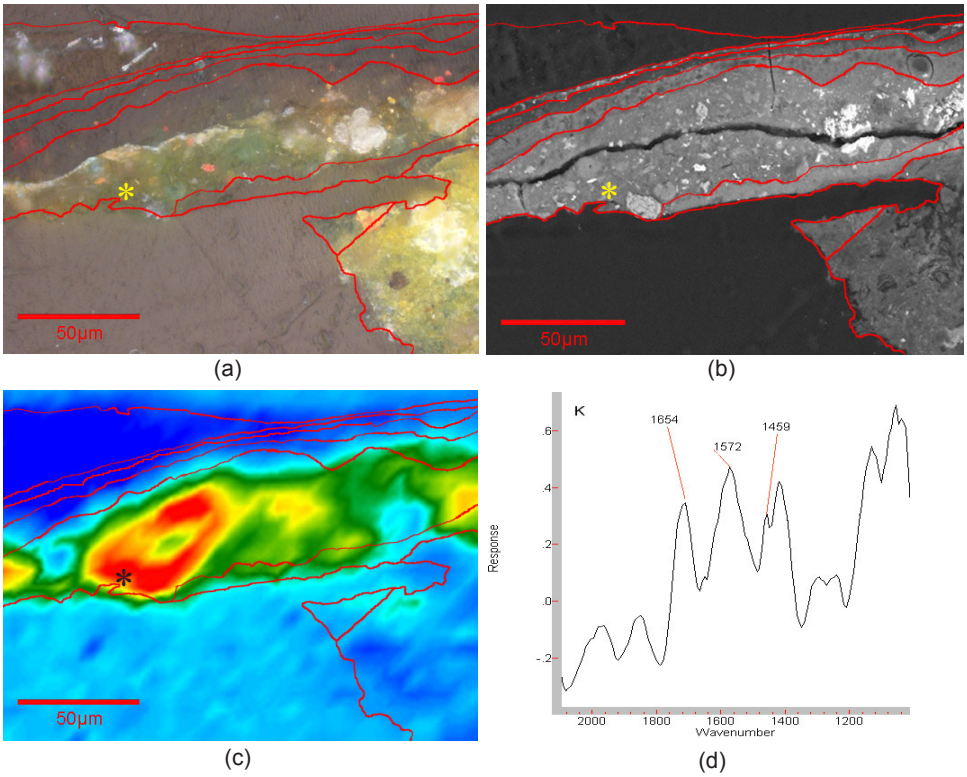

Figure 5.29 Emerald green in 286C layer 4: (a) VIS of 286C, (b) BSE image correspoinding to (a), (c) FTIR image of absorption at 1572cm^{-1}, (d) FTIR spectrum of the copper carboxylate absorptions indicated area with '*'.

Table 5.13 Arsenic related ion fragments

Ion fragments	Calculated mass *m/z*	Detected *m/z*
As	74.92	-
As_2	149.84	150
As_3	224.76	225
As_4	299.68	299 or 300
As_3O_4	288.76	288 or 289
As_4O_6	395.68	395
As-CH_3COO	133.92	134

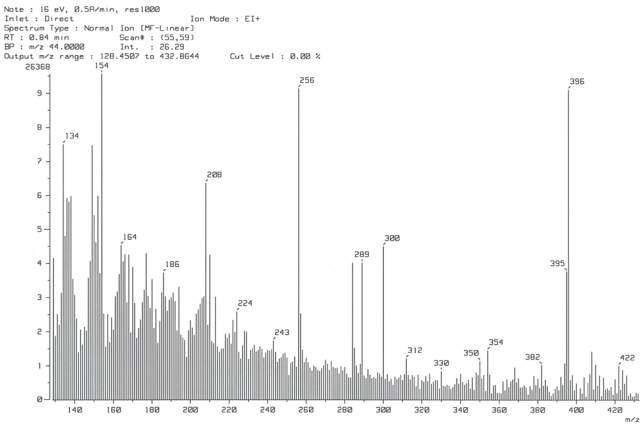

Figure 5.30 DTMS spectrum of 286B

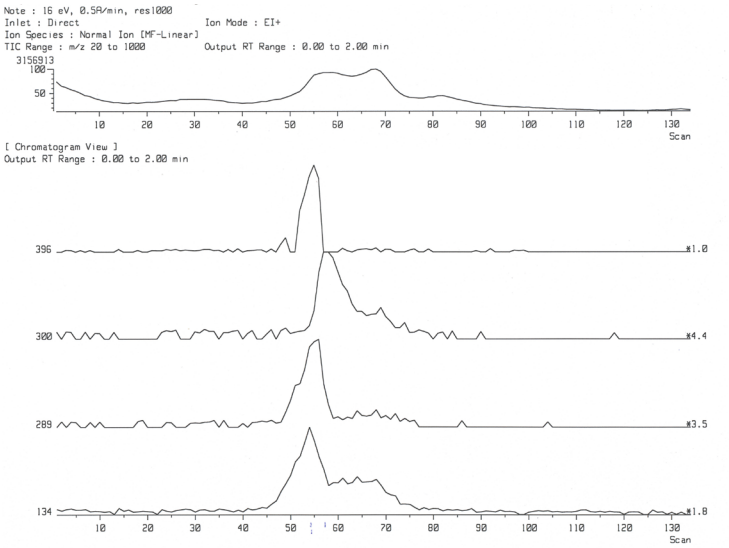

Figure 5.31 Thermal profile of arsenic components in DTMS Figure. 5.30

5.2.2.5 Other pigments and extenders

Carbon-rich brown particles were found by combined light microscopic examination and EDX analysis. The particles show a characteristic structure observed in the SEM-BSE image of 286A-layer 11 (Figure 5.32) suggesting that the particle is a Kassel earth type pigment. The use of Kassel earth was also suggested by the mass spectrometric analysis (see 5.2.3.3).

Vermilion was also found in many layers. No indication was found for blackening on the surface of this pigment [Plesters *et al.* 1982; Keune and Boon 2005] as a cause for the dark appearance.

As a white pigment, lead white was used. In the 1830's, this pigment was still the only white pigment used in oil painting [Kühn 1986: 170-172; Eastaugh *et al.* 2014]. Lead white was found in limited amounts in samples, which contain light paint; in 286F, G, K and L. Elemental lead was detected in all dark paint samples, but rarely as visible lead white particles. The significance of dispersed lead will be addressed later in 5.3.2.

Calcium sulfate was found mostly in the top paint layers of 286A, B, D, E, and L. Calcium sulfate might have been used as a substrate of organic yellow. Barium sulfate was found mainly in lower layers: 286A to E, K, and L. Both calcium sulfate and barium sulfate have low scattering ability in oil and were used as extenders.

The 286F-layer 4 is a blue paint layer consisting of cobalt blue and probably synthetic ultramarine blue. Modern cobalt blue consists of cobalt aluminum oxide. The cobalt blue particles contain phosphorus as revealed by EDX. Elemental phosphorus indicates the presence of cobalt phosphate, which is a contamination present as part of the production process in the early period of its production [Roy 2007].

The presence of chrome yellow was demonstrated with EDX. The use of chrome yellow as a pigment started in the early nineteenth century [Kühn and Curran 1986]. Together with other pigments such as cobalt blue introduced in 1802 and emerald green available after 1814, it shows that the artist used the most modern pigments at that time, in addition to more traditional pigments. These pigments are not uncommon in Barbizon or other 19th century paintings [Roy 1999; Burmester and Denk 1999, Townsend 1993].

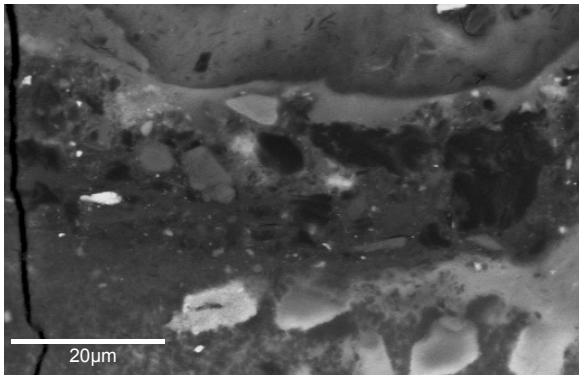

Figure 5.32
BSE image of 286A, carbon rich (Kassel earth?) particles containing layers 10, 11, and 12.

Table 5.2 286A

	Light microscopy (LM) VIS/ UVf	Thick-ness	Detected elements (EDX)	FTIR	Interpretaion from DTMS, LM, SEM-EDX, FTIR, (Raman)	Special features
L16	Translucent light brown	10-50	S		Varnish	
L15	Translucent light brown	20	N, S, As	1658 1538	Protein varnish	Migrated As
L14	No colour information obtained due to low amount of light reflection	20-30	Na, Al, Si, S, Cl, K, Ca, Fe, Cu, As, Sn, Hg, Pb		Vermilion, red lake (Al), ochre, silica, alkali alumina silicate, calcium sulphate, starch particles, lake (Sn)	As/Pb/S particle (20:10:2)(As/Pb/S) with (Sn, Ca)
L13		10-20	P, K, Ca, Fe, Cu, As, Pb	2102	Prussian blue, bone black, lakes (Sn and Ca)	Dispersed (Cu), As, Pb Relatively carbon rich
L12		10-15	Al, Si, S, K, Ca, Cu, As, Hg, Pb		Vermilion, alumina silicate	Dispersed Cu, As, Pb
L11		10-20	Al, Si, S, Cl, K, Ca, Cr, Fe, Cu, As, Ba, Pb		Prussian blue, silica, chrome yellow, Kassel earth, barium sulfate, yellow lake (Al), organic yellow	Dispersed Cu, As, Pb Pb/K particle Relatively carbon rich
L10		20-30	S, K, Cu, As, Pb		Cu carboxylate	Dispersed Cu, As, Pb Cu/Pb/As containing particles
L9		10-30	Si, S, Cl, Ca, Cu, As, Pb	1598 1430 1415	Cu carboxylate	K-containing particle Pb/K/S particles Cu/As/Pb particle (1:1:1)
L8	Green	10	Al, Si, S, Cl, K, Ca, Fe, Cu, As, Pb		Yellow ochre, Prussian blue, silica, alumina silicate	Dispersed Cu, As
L7	Yellow	10	Al, Si, P, S, K, Ca, Fe, Cu, As, Ba, Hg, Pb	1036 1086	Yellow ochre, vermilion, silica, carbon brown	
L6	Translucent green brown, yellow UV fluorescence particles	30-40	Al, S, K, Ca, Cr, Cu, As, Ba, Pb	1598 1430 1415	Emerald green, yellow lake (Al/S/K), copper carboxylate, chrome yellow, barium sulfate, lead white/drier	Dispersed Cu, As, Pb Relatively carbon rich
L5	Dark brown, no UV fluorescence	20-50	Al, Si, S, K, Fe, Cu, As, Pb		Alkali alumina silicate, lead white/drier	Dispersed Cu, As, Pb Relatively carbon rich
L4	Dark brown	10-30	Si, S, K, Ca, Fe, Hg, Pb		Alkali alumina silicate, carbon brown, yellow ochre, vermilion	Dispersed Pb Relatively carbon rich
L3	Reddish brown, matrix; whitish UV fluorescence	>80	Na, Al, Si, P, S, K, Ca, Fe, Hg, Cu, As, Pb	1708	Vermilion, yellow and red ochre, lead white/drier, carbon black and brown, red lake (Al/S), silica, alkali alumina silicate, bone black, starch Particles, ultramarine blue	Dispersed As P/K/S particles Relatively carbon rich
L2	Dark brown	20-25	Al, Si, P, Ca, Fe, Pb		Red ochre, bone black, lead white	
L1	White	>25	Pb		Lead white	

Table 5.3 286B

	LM VIS/ UVf	Thick-ness	Detected elements (EDX)	FTIR	Interpretaion from DTMS, LM, SEM-EDX, FTIR	Special features
L7	Bluish white uv-fluorescence	10-50	S, As		Varnish	Tiny particles
	Green	< 1	S, Cl, As, Pb		Green sediment?	
L6	No colour inforamtion	20-30	Na, Al, Si, S, Cl, K, Ca, Fe, Cu, As, Hg, Pb		Vermilion, Calcium sulphate, yellow lake (Al/S/K), alkali alumina silicate, silica, yellow ochre	As/Pb rich band Pb/Si/Cl-containing particles
L5	Translucent brown layer	5	S, Al, K, Pb		Yellow lake (Al/S/K)	Dispersed Pb Relatively carbon rich Yellow uv fluorescing particles
L4	Green	20-50	Al, S, Cl, K, Ca, Cu, As, Pb		Emerald green, yellow lake (Al/S), barium sulfate	Al/S substrate with As Many tiny oblong-shaped copper arsenate particles One large carbon-rich particle (with yellow UV fluorescence)
L3	Orange-yellow layer with red particles	10	Al, Si, S, K, Ca, Cr, Cu, As, Ba, Pb		Yellow lake (Al), calcium sulphate, silica, barium sulfate, chrome yellow, yellow ochre, lead white	Low electron reflective particles
L2	Green, overall whitish UV fluorescence	30-50	Al, Si, S, K, Ca, Cr, Fe, Cu, As, Ba, Pb		Prussain blue, yellow ochre, barium sulfate, lead white, calcium sulphate, silica, alumina silicate, chrome yellow	
L1	Slightly brownish translucent layer	10-15	Pb		Lead white	

Table 5.4 286C

	LM VIS/ UVf	Thick-ness	Detected elements (EDX)	FTIR	Interpretaion from DTMS, LM, SEM-EDX, FTIR	Special features
L7	Translucent brown with strong UV fluorescence	10-20	n.a.		Varnish	
L6	Translucent light brown, cleamy blue UV fluorescence	5-10	n.a.	1654 1522	Protein varnish	
	Green	1-3	Mg, Al, S, K, Ca, Fe, As, Pb		Calcium sulphate	Pb, As crust, sediment?
L5	Translucent brown	5-10	Mg, Al, Si, S, K, Ca, Fe, (As), (Pb)	1683	Yellow lake (Al/S/K), Prussian blue	
L4	Brown	2-10	Al, Si, Ca, Cu, As, Pb		Copper arsenate green, lead drier/white	Low electron reflective particles spread in Pb dispersed matrix, As>Cu (comparing to emerald green particles)
L3	Green	10-30	Ca, Cu, As, Pb	1572 1457 1394	Copper arsenate green, lead white	Dispersed Pb
L2	Translucent green	5-15	Cu, As, Pb	1635	Copper arsenate green, lead white/drier	Dispersed Pb
L1	Yellowish green	> 15	Mg, Al, Si, S, K, Ca, Cu, Fe, As, Ba, Hg, Pb	1259	Yellow and red ochre, Prussian blue, alumina silicate, silica, lead white, vermilion, barium sulfate, copper arsenate green	

Table 5.5 286D

	LM VIS/ UVf	Thick-ness	Detected elements (EDX)	FTIR	Interpretaion from DTMS, LM, SEM-EDX, FTIR	Special features
L13	Translucent brown, UV fluorescence	< 20	n.a.		Varnish	
L12	Translucent brown, slight UV fluorescence	10	Na, Si, S, K, Ca, Fe, As, Pb		Calcium sulphate, silica	Dispersed As, Pb Relatively C rich
L11	Green, yellow UV fluorescence particles	15	Na, Al, K, Fe, As, Pb	1696 1434	Yellow lake (Al/S/K), Prussian blue	Dispersed As
L10	Translucent yellow, yellow UV fluorescence particles	30	Al, S, K, Pb	1696 1434	Yellow lake (Al/S/K)	Relatively C rich
L9	Yellow, yellow UV fluorescence particles	40	Al, Si, S, K, Cu, Ba, Pb	1696 1434	Yellow lake (Al/S/K), barium sulfate, silica (few)	Dispersed Cu (emerald green particles were once observed)
L8	Yellow	20	Al, Si, S, K, Fe, Cu, Ba, Pb	1696 1434	Yellow ochre, barium sulfate, silica, yellow lake (Al/S/K), lead white	Dispersed Cu
L7	Reddish brown	15	S, Cu, Hg	1696 1434	Vermilion	Dispersed Cu Relatively C rich
L6	Yellow	5	Al, Si, Fe, Pb	1696 1434	Yellow ochre, lead white	
L5	Translucent brown	20-30	Na, Al, Si, K, Cu	1696 1650 1434	Alkali alumina silicate, silica, yellow lake (Al/S/K)	Dispersed Cu Relatively C rich
L4	Yellow	5	Al, Fe, Pb	1650	Yellow ochre, lead white	
L3	Translucent brown	20-30	Al, Si, Ca, Pb	1650	Yellow lake (Al/S/K), calcium sulphate	Dispersed Pb Relatively C rich
L2	Dull green	30-50	Al, Si, S, Ca, Fe, As, Hg, Pb		Prussian blue, Yellow ochre, vermilion, alkali alumina silicate, starch particle	
L1	Translucent light brown	20	Pb		Lead white	

Table 5.6 286E

	LM VIS/ UVf	Thick-ness	Detected elements (EDX)	FTIR	Interpretaion from DTMS, LM, SEM-EDX, FTIR	Special features
L7	Translucent brown, UV fluorescence	10-20	n.a.			Tiny particles
L6	Brown	10-20	Al, Si, S, Ca, Cu, As, Pb	1598	Calcium sulphate, alkali aumina silicate	Dispersed Cu, As
L5	Brown	20	Al, Si, S, Fe, Cu, As, Ba	2937	Barium sulfate, ochre, alkali alumina silicate, vermilion	Dispersed Cu as a spot
L4	Dark brown	80-100	Na, Al, Si, P, S, Cl, K, Ca, Fe, Cu, As, Pb	2937 1375	Red lake, bone black, ochre, carbon rich particles, vermilion, yellow lake (Al/ S/K), alkali alumina silicate	Ca/P particle with UV fluorescence Cu is localized at the lower area
L3	Yellow	10-20	Al, Si, K, Fe, Cu, As, Pb	2937	Yellow ochre, lead white, alkali alumina silicate	Dispersed Cu, As
L2	Brown	5-15	Al, Si, Fe, Cu, Pb	2937	Ochre, lead white, alkali alumina silicate, silica, starch particle	
L1	Light brown	2-3	Pb		Lead white	

Table 5.7 286F

	VIS/ UVf	Thick-ness	Detected elements (EDX)	FTIR	Interpretaion from DTMS, LM, SEM-EDX, FTIR	Special features
L10	Green	<30	Na, Al, Si, S, K, Ca, Fe, Cu, As, Hg, Pb	1543 1509 1393	Prussian blue, yellow ochre, vermilion, copper arsenate green, ultramarine blue, silica, calcium carbonate, lead white, lead carboxylate	
L9	Orange-yellow	20	Na, Al, Si, P, S, Ca, Fe, Hg, Pb	1543 1509 1393	Lead white, vermilion, yellow ochre, ultramarine blue, bone black, lead carboxylate	
L8	White	20-30	Si, S, Ba, Pb	1543 1509 1393	Lead white, silica, barium sulfate, lead carboxylate	
L7	Translucent	10	Na, Al, Si, P, S, K, Ca, Fe	1063	Alkali alumina silicate, bone black, silica	
L6	Red	20-30	Al, P, S, Co, Sn, Pb	1063	Red lake (Al and Sn), cobalt blue (Co, Al, P), lead white	
L5	White	5	Pb		Lead white, carbon black	
L4	Translucent blue	15-20	Na, Al, Si, P, S, K, Co, Pb		Cobalt blue (Co, Al, P), ultramarine blue	Relatively C rich
L3	White	10-20	Si, S, Cr, Hg, Pb	2931 1515 1509 1393	Lead white, chrome yellow, vermilion, lead carboxylate	
L2	Blue	20-30	Al, Si, S, K, Ca, Pb	2931 1515 1509 1393	Lead white, carbon black, ultramarine blue, lead carboxylate	Relatively C rich
L1	White with fine green, red/ brown, blue and black particles	20-60	Al, Si, P, Ca, Co, Cu, As, Sn, Pb	2931 1515 1509 1393	Lead white, silica, bone black, cobalt blue (Co, Al, P), lakes (Al and Sn), carbon brown,emerald green, lead carboxylate	

Table 5.8 286G

	LM VIS/ UVf	Thick-ness	Detected elements (EDX)	FTIR	Interpretaion from DTMS, LM, SEM-EDX, FTIR	Special features
L8	Translucent light brown	2-40	n.a.	2936 1509 1397		
L7	Pale yellow	20-30	Al, Si, Fe, Pb	1573 1464 1074	Lead white, yellow ochre, lead carboxylate	
L6	Yellow, green, red particles mixture	10-25	Al, Si, S, Fe, Cu, As, Hg, Pb	2936 1575 1617	Emerald green, yellow/red ochre, vermilion, yellow lake, lead white	
L5	Brownish green	10	Al, K, Ca, Cu, As, Pb	2936 1575 1617	Copper arsenate green	Dispersed Pb, Cu, As
L4	Light brown	20-30	Na, Al, Si, K, Fe, Pb	2936 1575 1617	Alkali alumina silicate	
L3	Dark brown with reddish UV fluorescence	5-10	Na, Al, Si, S, K, Ca, Cu, As, Pb	2936 1575 1617	Red and yellow lakes, calcium carbonate, carbon black or brown	
L2	Brown with red particles	15-70	Al, K, S, Cu, As, Hg, Pb	2936 1575 1617 1397	Lead white, vermilion, yellow lake, copper arsenate green, lead carboxylate	Dispersed Pb, Cu, As
L1	Green	10	n.a.	2936 1575 1617		

Table 5.9 286H

	LM VIS/ UVf	Thick-ness	Detected elements (EDX)	FTIR	Interpretaion from DTMS, LM, SEM-EDX, FTIR	Special features
L9	Bluish UV fluorescence	5-10	n.a.	1649 1540	Protein varnish	
L8	Translucent green	10	Si, S, Ca, Cr, Cu, As, Hg, Pb		Vermilion, chrome yellow, Prussian blue, yellow lake	Sediment? Difficult distingush from L7 due to the terribly damaged paint layers Dispersed Cu, As, Pb
L7	Translucent yellow	10-15	Si, S, Ca, Cr, Cu, As, Hg, Pb		Vermilion, chrome yellow, Prussian blue, yellow lake	Dispersed Cu, As, Pb
L6	Ttranslucent light brown	50-70	Na, Al, Si, K, Fe		Alkali alumina silicate	Very Si rich
L5	Green	20-40	Al, Si, S, K, Ca, Fe	2098 1601 1464 1411	Yellow lake (Al/S/K), Prussian blue	
L4	Yellow	50	Al, Si, S, K, Ca, Cr, Pb, Mg/As		Yellow lake, chrome yellow, starch particles	
L3	Green	20	n.a.			
L2	Red	10	Fe, Pb		Lead white, red ochre	
L1	Translucent light brown	15	n.a.			

Table 5.10 286I

	LM VIS/ UVf	Thick-ness	Detected elements (EDX)	FTIR	Interpretaion from DTMS, LM, SEM-EDX, FTIR	Special features
L2	Bluish UV fluorescence	10-15	n.a.		Varnish	
L1	Brown	70	Na, Al, Si, P, S, Cl, K, Ca, Fe, Hg		Vermilion, ochre, barium sulfate, copper arsenate green, carbon brown, bone black, ultramarine blue	

Table 5.11 286K

	LM VIS/ UVf	Thick-ness	Detected elements (EDX)	FTIR	Interpretaion from DTMS, LM, SEM-EDX, FTIR	Special features
L5	Bluish UV fluorescence	5-20	n.a.		Varnish	
L4	Green	3	Al, Si, K, Ca, Fe, Cu, As, Pb		Prussian blue, copper arsenate green	Very thin, sediment?
L3	Brown (right side only)	10	n.a.			
L2	Yellowish green	< 25	Al, Si, S, Ca, Fe, Cu, As, Ba, Pb		Emerald green, lead white, barium sulfate, yellow ochre	
L1	White	100	n.a.		Lead white	

Table 5.12 286L

	LM VIS/ UVf	Thick-ness	Detected elements (EDX)	FTIR	Interpretaion from DTMS, LM, SEM-EDX, FTIR	Special features
L5	Bluish UV fluorescence	20	n.a.		Varnish	
		2-5	S, Ca		Calcium sufate	sediment?
L4	Translucent green; with yellow UV fluorescence particles	10-25	Al, Si, S, K, Ca, Fe		Yellow lake (Al/S/K), Prussian blue	
L3	Translucent brown	10	Na, Al, Si, S, K, Ca, Fe, Cu, As, Pb		Lead white, ochre, emerald green, barium sulfate	
L2	Yellow	30-200	Al, Si, S, Fe, Cr, Hg, Pb		Lead white, chrome yellow, vermilion, ochre	
L1	Translucent brown	15	n.a.			

5.2.3 Binders and other organic components

5.2.3.1 General features of the oil paint fraction

The DTMS results of all analyses are given in Table 5.14 and the mass spectra of sample 286D and 286F are shown in Figures 5.33 and 5.34. Sample 286D was taken from the area depicting the woods at the light side of middle-ground. Whether darkening could have taken place in the area is hard to determine but the surface deformation is evident. Sample 286F is a paint sample from the sky with no particular darkening nor surface deformation. The former sample is taken as representative of the darker paints and the latter is considered to be representative of the light paints in the picture. Comparing both spectra, 286D shows a broad range of mass peaks indicative of the presence of a high relative abundance of organic components of higher volatility. On the other hand, 286F shows a markedly plain spectrum, which is a common DTMS spectrum from an aged lead white oil paint [Boon *et al.* 1995, Boon and Van Och 1996]. The total ion current (TIC) chromatogram of each sample are inserted in Figures 5.33 and 5.34 respectively. Low molecular and volatile fractions are detectable at lower temperature (scans 20-50). The detection of high ion currents at lower temperature in the TIC of 286D supports the conclusion that the dark paint contains a relatively large amount of volatile organic components.

The saturated monocarboxylic fatty acids of palmitic (C16) and stearic acid (C18) observed in DTMS as *m/z* 256 and 284 respectively are present in all analysed samples. Besides the molecular ions of these saturated fatty acids, electron ionisation mass fragments at *m/z* 60, 73, 129, 171, 185 and 213 from these fatty acids are found with DTMS. The ratio of palmitic to stearic acids (P/S ratio) varies from less than 1 to more than 4 in different samples (Table 5.14). Some samples with a P/S ratio higher than 4 strongly suggest the usage of poppyseed oil [Mills and White 1994: 171-172]. The diverse values however indicate the presence of other types of oil: both linseed and walnut oil are possible, but other oils are also used in the 19th century [Carlyle 2001: 101-140]. The use of poppyseed oil for light areas was recommended as it was known that linseed oil would yellow and change the tone of light colored paints [Carlyle 2001: 23-26]. This practice was confirmed in paintings of the Barbizon school [Roy 1999]. For this painting, the P/S ratios of 286F (from the sky) are 2.5 with DTMS and 3.7 with Py-TMAH-GCMS suggest the use of non-yellowing oil for light colored paint. Note however that palmitic acid moieties can be derived from beeswax (which is present, see 5.2.3.3) when analysed Py-TMAH-GCMS, which affects the P/S ratio. The multiple layered paint build-up in this painting (see 5.2.1.2) makes it difficult to draw any conclusions about the oil composition of the individual paints used.

Diacylglycerol molecular fragments are seen in 286D and were detected in some other dark paint samples. The ions with *m/z* 550, 578, and 606 are assigned to saturated diacylglycerol molecules with the fatty acyl combinations of C16/C16, C16/C18, and C18/C18 respectively [Boon *et al.* 1995]. Thermal fragments from cross-linked oil residues that are formed at high temperature evidenced by alkyl-benzenes appear at *m/z*

Table 5.14 DTMS and Py-TMAH-GCMS reuslts

		P/S	bees-wax	oxo-DTP	TTP	Protein	Kassel earth	Pb	Pb source	HgS	As	Indian Yellow	special features
286A	DTMS	2,3- 4	+ (+oxo)		+	?	+	+		+	+	+	high in 2C9, *m/z* 280, DG; *m/z* 578, 606
	GCMS	4									n/a		C18:1
286B	DTMS	2-4	+ (+oxo)	---	+		+	+		---	++	+	DG; *m/z* 551, 578, 606
	GCMS	3									n/a		
286C	DTMS	0,7-2,2	---	trace	+	?	---	+		---	++	+	
	GCMS	3-4									n/a		C18:1
286D	DTMS	2	+ (+little oxo)	---	+	+ (glair?!)	---	+		---	+ (*m/z* 150, 300, 134, no AsO_x)	++	*m/z* 280, 292, high in 2C9, DG; *m/z* 550, 578, 606
	GCMS	4,1	*	---							n/a	+	high in 2C9, C18:1
286E	DTMS	2,7	+ (+oxo)	+	+ (M)		---	+		---	---	+	high in 2C9, *m/z* 280, no SO_2, DG; *m/z* 550, 576, 578, 606
	GCMS	2,4	---	---	---						n/a	---	
286F	DTMS	2,5	---	trace	+		---	+++	lead white	---	---	---	K
	GCMS	3,7	---	---							n/a		high in 2C9
286G	DTMS	2,9	trace	---	+		---	++	lead white	---	+ (*m/z* 134, 395, but no *m/z* 300)	---	K, little SO_2 at late stage
	GCMS										n/a		linseed/walnut oil, good drying of oil, no lignites?, alkanes
286H	DTMS	2,9-4	+ (+trace of oxo)	---	+ (M)	?	---	+	drier (and lead white?)	---	+ (no AsO_x)	+++	high K (Prussian blue), *m/z* 280
	GCMS	4,1	+	---							n/a	+	C18:1, high in 2C9
286I	DTMS	2	---	+	+ (M)		---	+		---	---	trace	high in 2C9, (trace SO_2)
	GCMS			---							n/a	---	Fatty acids, C16 and C18
286J	GCMS	3,4	---	colo-phony	M						n/a	---	

DTP: diterpenoid resins, TTP: Triterpenoid resins, M: Mastic resin
oxo-: oxidized beeswax componets, AsO_x: arsenic oxide

91 and 105 in all DTMS data [Van den Berg 2002: 118].

A fragment ion at *m/z* 152 attributed to azelaic acid (2C9) was detected by DTMS with relatively high intensity in many of the analysed samples. Py-TMAH-GCMS results also support this observation. This suggests that the oil was highly autoxidized in the course of time. High relative intensities of other diacids; sebacic acid (2C10), suberic acid (2C8), and pimelic acid (2C7) detected with Py-TMAH-GCMS in 286D, H, and J suggest that a pre-polymerised oil was used [Mills and White 1999: 171-172]. *M/z* 280 assigned to an octadecadienoic acid molecular ion, which possibly formed by retro-Diels-Alder reaction from cyclisized (poly)unsaturated fatty acid moieties, is observed in DTMS mass spectra of dark paint samples. This mass peak together with those at *m/z* 278 and 292 is thought to be an indication of a strong heat treatment of the oil [Theodorakopoulos 2005; Burnstock *et al.* 2006]. These results suggest the use of thermally pre-polymerised oil by Rousseau. So-called '*huile grasse*' is a heat-bodied oil treated with lead or manganese drier in the nineteenth century in France [White *et al.* 1998]. This oil is mentioned in Rousseau's biography.

The peak at *m/z* 264 in DTMS of some dark paint samples is assigned to an acylium ion from the monounsaturated fatty acid, oleic acid (C18:1) ($C_{17}H_{31}COOH$). The corresponding compound was also detected with Py-TMAH-GCMS. Unsaturated fatty acids are usually not observed in aged oil paint since unsaturated bonds usually have reacted away to azelaic acid or have become part of oil paint networks. The presence of this peak points to protection of the double bond by anti-oxidant agents in this painting or to sequestering by sulfur compounds [Sinninghe Damste and De Leeuw 1990] in the dark paints (see Table 5.14).

5.2.3.2 Resin components in the paint layers

Both diterpenoid and triterpenoid resins were also detected in paint samples using DTMS, but not with Py-TMAH-GCMS analysis except for the varnish sample (Note: Py-TMAH-GCMS has a tendency to underestimate triterpenoids). Identification of diterpenoid resins with DTMS corresponds to the detection of *m/z* 315 from 15-hydroxy-7-oxo-dehydroabietic acid, which is an oxidized component of colophonium [Van den Berg *et al.* 2000]. This *m/z* peak was found in DTMS results of 286-C, E, F, and I in rather low intensity.

The identification of mastic and dammar resins with DTMS was made on the basis of a series of ions in region between *m/z* 400-470 which is indication of a triterpenoid resin. Both resins give a broad profile of terpenoid hydrocarbon fragments in the mass range from *m/z* 107-320 but these are not so discriminating [Van der Doelen 1999: 62-63]. Upon oxidation dammar resin often develops a relative high concentration of ocotillone with a typical high intensity fragment ion at *m/z* 143. The detection of *m/z* 163 from moronic acid strongly supports the presence of oxidized mastic resin. The ion series of triterpenoids were detected in all samples and the indicator mass at *m/z* 163 of mastic resin was found only in 286-E, H, and I. The *m/z* 143 was never a prominent feature in the data, which implies that dammar is either not there or present as a minor

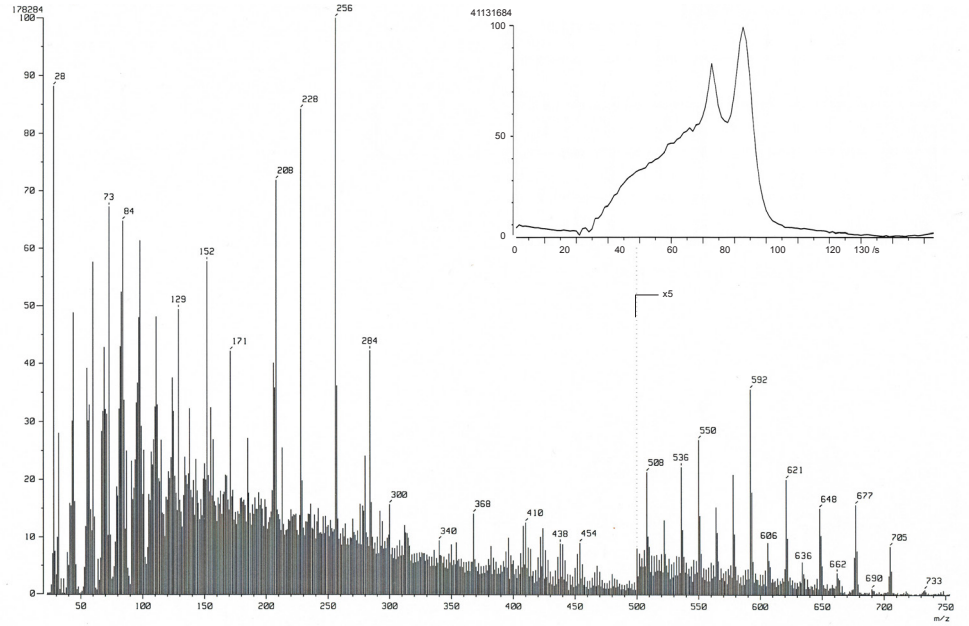

Figure 5.33 DTMS spectrum of 286D with TIC inserted

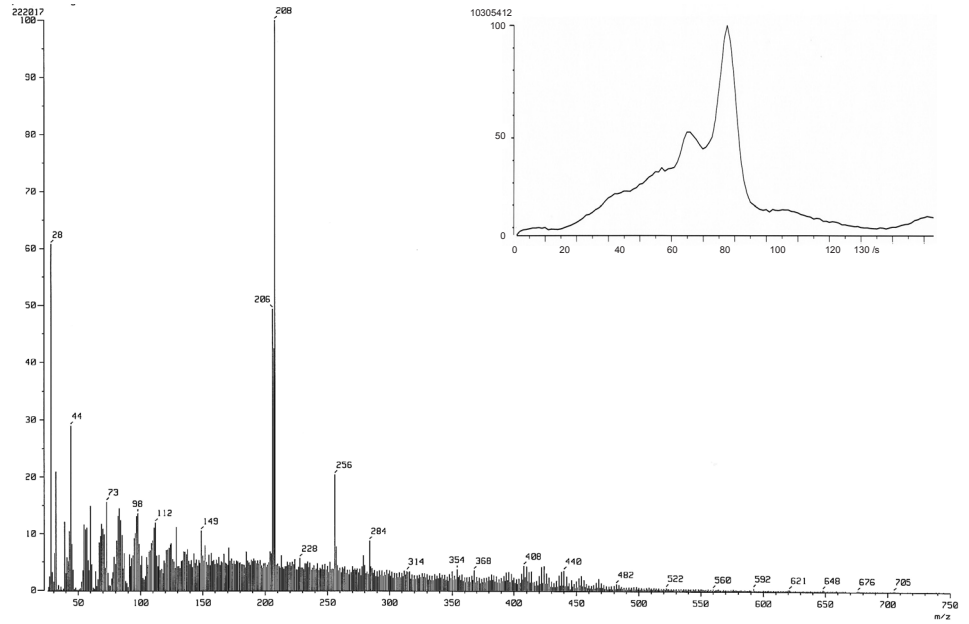

Figure 5.34 DTMS spectrum of 286F with TIC inserted

component. All DTMS and Py-TMAH-GCMS results suggest that the resin content in the paints is low. The presence of mastic resin in the varnish sample makes it difficult to say whether the paint itself contains mastic resin, for example in the form of megilp, which is a combination of mastic resin-based varnish and prepolymerised oils.

5.2.3.3 Long-chain components

Beeswax was detected with DTMS in most of the dark paint samples. A series of palmitoyl wax esters with *m/z* 592 (C40), 620 (C42), 648 (C44), 676 (C46), 704 (C48), and 732 (C50), their fragment ion *m/z* 257 and the free tetracosanoic fatty acid with molecular ion at *m/z* 368 are DTMS indicator mass peaks of beeswax. Corresponding oxidized beeswax esters formed by insertion of oxygen via peroxidation leading to a stable keto group gives *m/z* 606, 634, 662, and 690 detected in most of the dark samples. Oxidized beeswax components marked as 'oxo' in Table 5.14 are relatively prominently present in sample 286A, B, D and E. These fragments are usually not detected in fresh beeswax but have been observed before in aged beeswax in paintings (Boon Pers. Comm. 2012). Some components (for example reactive metals acting as catalysts) in the painting might be responsible for their formation. Formation of free radicals catalyzed by metals such as copper could be an explanation. The detection of oxidized beeswax fragments indicates that some parts of the paint system are detrimental for the preservation of organic compounds.

In addition to the long chain components from beeswax, ions at *m/z* 760, 788, 816, 844, and 872 were detected with DTMS in 286A, B and D (Figure 5.35). These mass fragments correspond to C52 to C60 wax ester respectively indicating the presence of long chain hydrocarbon-like compounds other than beeswax. Further detection of long chain fatty acids with molecular ions *m/z* 396, 410, 424, 452, 480, and 508 corresponding to C26 to C34 fatty acids respectively, and phenolic compounds suggest the presence of so-called brown coal type materials which are known as Kassel earth or/and Van Dyke brown [Languri 2004: 76-89]. Because these components were only found in the upper paint samples A and D that were removed from the surface with solvents, such a brown pigment must have been used to give a warmer tone to the upper surface layers.

5.2.4 Varnish layers

A brownish tone contribution by the surface varnish layers is evident from the visual observation. Relatively thick varnish layers are present in certain areas. In the cross-sections, sample 286A, C, and G show such thick varnish layers. Py-TMAH-GCMS analysis of 286J for varnish identification shows the presence of prepolymerised oil, mastic resin, and colophony (Figure 5.36). Dehydroabietic acid (DHA), 7-oxo-DHA, and 15-hydroxy-7-oxo-DHA as indicators of oxidized abietic acid are present in colophony which is obtained from Pinaceae trees [Van den Berg *et al.* 2000]. The

abietic acid carbon skeleton is relatively resistant to degradation.

The presence of mastic resin was indicated by the detection of gas chromatographic peaks from methylated moronic acid and oleanolic acid. Mastic resin was a common type of triterpenoid resin used in the early nineteenth century in

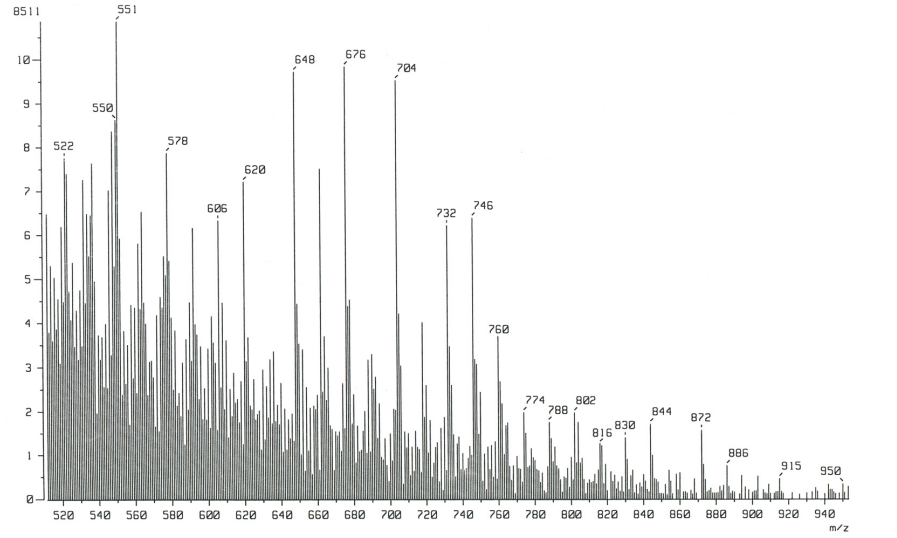

Figure 5.35 DTMS spectrum of 286B showing the long chain components related to beeswax

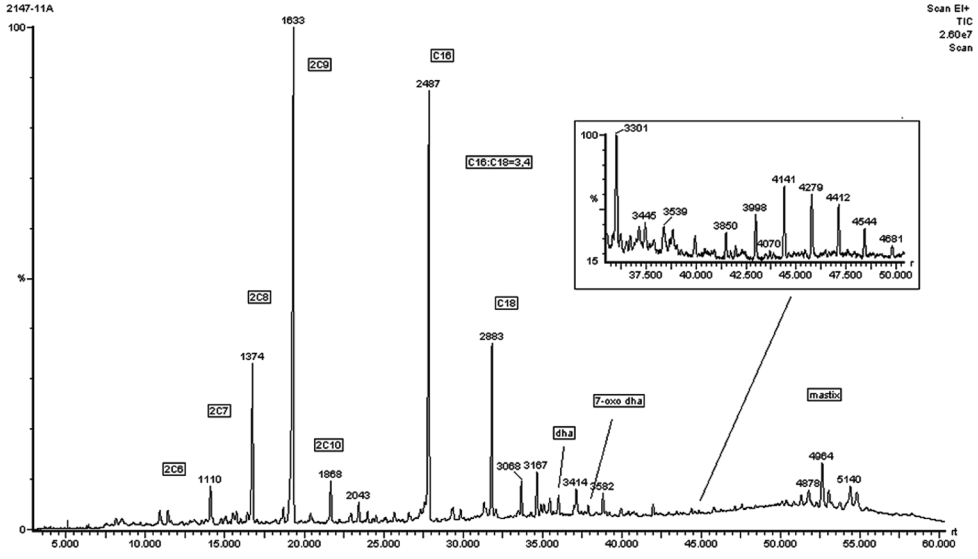

Figure 5.36 Py-TMAH-GCMS chromatogram of 286J (varnish sample)

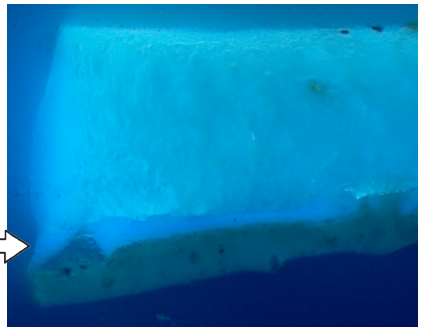

Figure 5.37 Two varnish layers with different responces to UV-light, sample 286C. The arrow indicates the lower one.

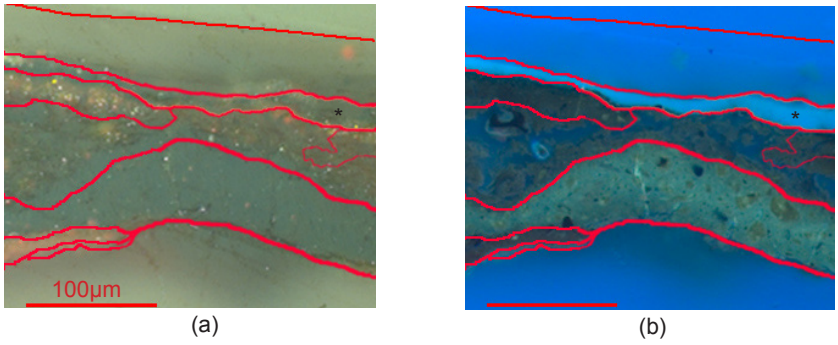

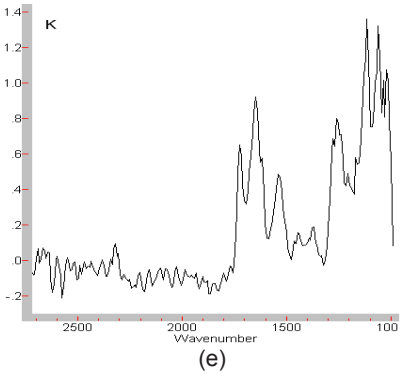

Figure 5.38 FTIR result of 286H: (a) VIS, (b) UVf, (c) FTIR image at 1649 cm^{-1} (amide I absorption) (d) FTIR image at 1540 cm^{-1} (amide II absorption) , (e) FTIR spectrum of protein varnish (analysed on the spot with '*')

paintings as varnish and also is a component of a megilp type binding medium [Carlyle 2001: 101-106; White and Kirby 2001]. Dammar resin, which is another triterpenoid type resin does not seem to have been used in this painting as suggested by a rather low relative concentration of dammar resin indicators such as hydroxy-dammaran derivatives [Van der Doelen *et al.* 1998]. Furthermore, drying oil components were detected such as the saturated fatty acids (C16 and C18), and the diacids 2C6 (adipic acid), 2C7, 2C8, 2C9, and 2C10. It is not clear whether the oil derived components are from the paint or originally present in the varnish, since the varnish could not be fully separated from the paint layers.

Using optical microscopy, two varnish layers were confirmed in 286A, C, and K. Milky bluish UV fluorescence was observed from the lower varnish layers (Figure 5.37). In addition, the presence of a proteinaceous varnish was indicated with the imaging FTIR analysis in 286A and H (Figure 5.38). Clear amide absorptions at around 1650 and 1530 cm^{-1} are observed. EDX analysis detected nitrogen in the lower varnish layer of 286A supporting the result. These could indicate the presence of an egg white varnish, which was a common temporary varnish in the nineteenth century according to English documentary sources [Carlyle 1990].

It was found that some components migrated into the varnish layers. In case of sample 286A and B, sulfur and arsenic were detected with EDX. It is obvious that arsenic had migrated from the paint. In the 286A, C, D, and E, fine particles containing lead (Pb*M*)/sulfur (S*K*) and potassium (K) are found. The source components must have been derived from either the atmosphere or the paint layers. The minute particles reasonably reflect electrons in the SEM-BSE image. Development of lead-potassium-sulfur particles has been reported in seventeenth century paintings [Van Loon 2008: 16, 111; Boon and Oberthaler 2013]. In the case of the Vermeer painting it was proposed to have formed due to the German lining method and the extended exposure to moisture of the painting. The sulfates in *La Descente des Vaches* could be attributed to atmospheric SO_2 pollution from coal burning stoves in the galleries or even external pollutants arising from animal dung, perhaps from horse-drawn transport.

5.3 Discussion –appearance changes implied by alterations in the paint layers

5.3.1 Decomposition of emerald green

5.3.1.1 Isolation of arsenic and copper ions

We suggested that copper arsenate has decomposed and arsenic components have migrated to the other layers [Keune *et al.* 2012] as evidence was found that showed some particles of copper arsenate show low electron-reflective rims around them (Figure 5.39). The EDX spot analyses indicated that the detection intensity of copper differs on the inside of particle and its circumference. Relatively higher intensity of copper

than that of arsenic was noted in the low electron-reflective areas. Inside the particles, arsenic and copper were both detected strongly. This suggested that either the copper was released, or arsenic had left the particles. It is more likely to be the latter case because arsenic was detected in the upper paint layers without the pigment particles, and it also corresponds with very low amounts of copper in EDX examination.

It was shown in 286A, D, and E that the copper distribution did not completely overlap with the arsenic distribution. In 286A, arsenic was detected in the upper layers (12 and 14) in addition to in the middle layers (6, 9 and 10). The detection intensity of copper in the upper layers is considerably less compared to the middle layers that contain copper arsenate green (Figure 5.40). In 286D, arsenic is dispersed throughout the layer 11, while the copper is relatively concentrated in the middle layers (layer 5 to 8) (Figure 5.41). In the case of 286E copper was detected in a certain spot in layer 6, while arsenic was found throughout the layer.

Furthermore, arsenic was often detected along with elements other than copper. Lead is one of these observed as associated with arsenic. For instance, dispersed arsenic was detected with lead and concentrated at the interface between the top paint layer and the varnish in 286D (Figure 5.42). The cross-sections of 286C (layer 6) and B (layer 6) show a similar result: a very thin line containing arsenic, lead (or sulfur), and chlorine. Copper was almost not detected in this area. Also arsenic and lead were detected in oval shaped particles with blue UV fluorescence found in 286A, D, E, and H (Figure 5.43). In other cases, arsenic was detected associated with tin (Sn) in 286A, or was adsorbed to aluminum substrates of lake pigments. Finding arsenic with the other metallic elements suggests certain affinity between arsenic and these elements [Vaughan 2006]. A recent study by Keune and Boon [2011] suggests that arsenic trioxide, which is known as a degradation product of arsenic containing pigments, is mobile in the presence of moisture. This can explain the different distribution of copper and arsenic and also arsenic migration to the other layers.

Copper ions seem to have reacted with fatty acid components forming copper soaps. Although there are other pigments containing copper such as verdigris (copper

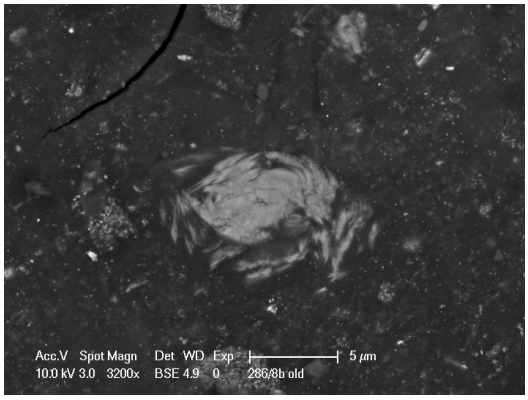

Figure 5.39
BSE image of copper arsenate (III) pigment with low electron reflective rim.

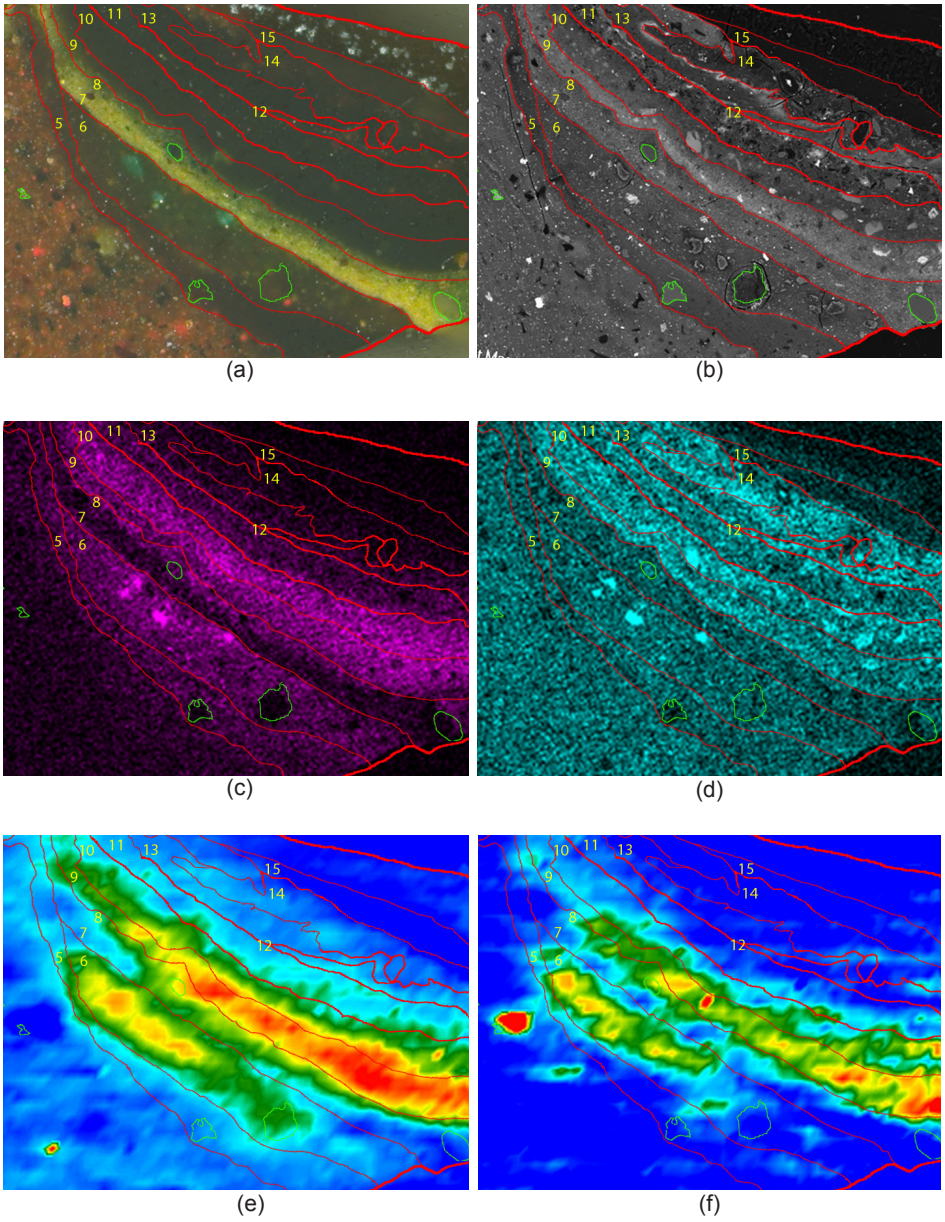

Figure 5.40 Result of the imaging FTIR and EDX mapping of 286A. (a) VIS, (b) BSE image, (c) copper mapping, (d) arsenic mapping, (e) FTIR image at 1600 cm^{-1}, (f) FTIR image at 1415 cm^{-1}.

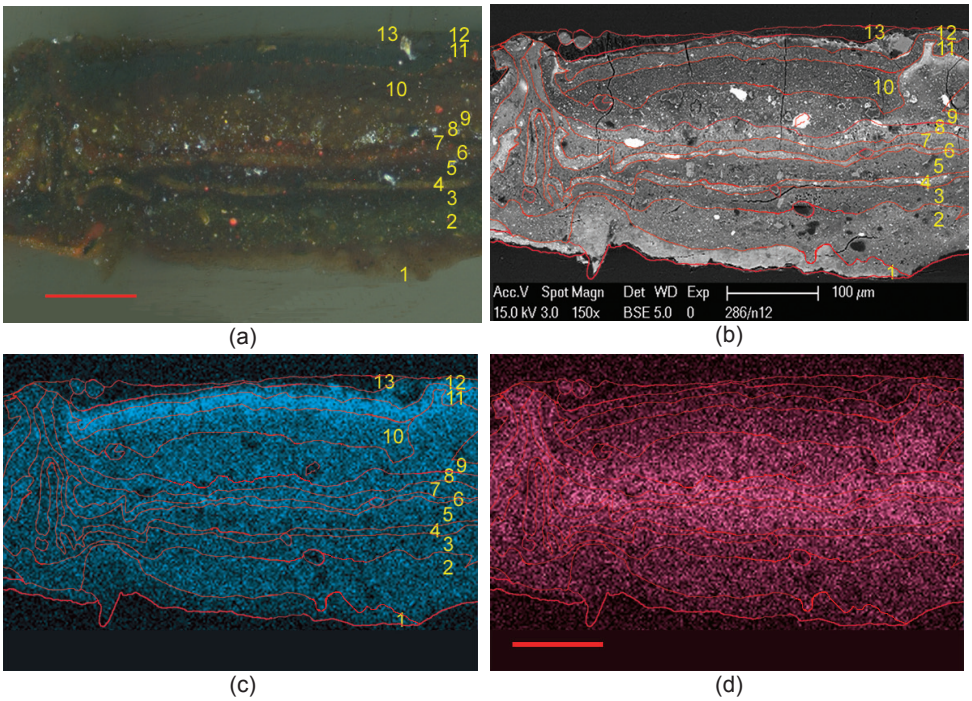

Figure 5.41 Result of EDX mapping of 286D. (a) VIS, (b) BSE image, (c) arsenic mapping, (d) copper mapping

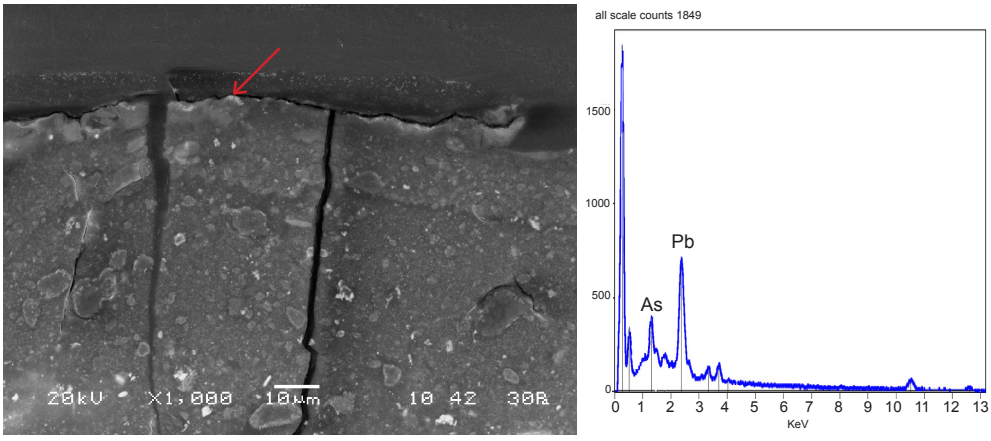

Figure 5.42 Result of EDX spot analysis at the thin interface layer in 286D, which lays down between the top paint layer and the first varnish layer. *Left*: analysed point indicated in the BSE image. *Right*: EDX spectrum of the highlight in the BSE image.

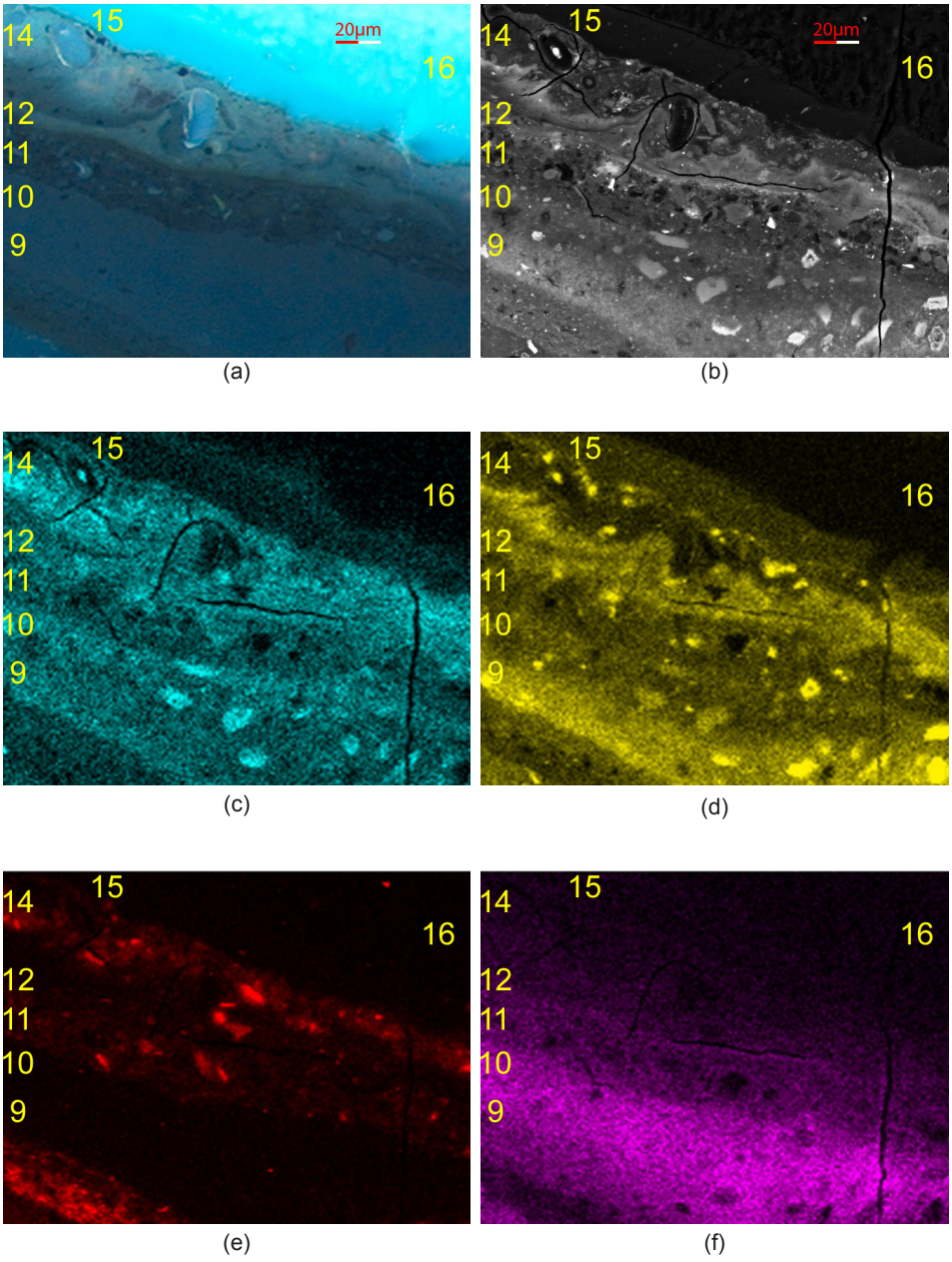

Figure 5.43 Result of EDX mapping of the upper layers of 286A. Arsenic was detected with lead and aluminum rather than copper. (a) UVf, (b) BSE image, and elemental distribution of (c) arsenic, (d) lead, (e) aluminum, (f) copper.

acetate), no indications were found for their-use in this painting. Considering the instability of copper arsenate pigments [Keune *et al.* 2012], the source of copper is likely to be emerald green. In 286A, IR absorptions at around 1600 cm^{-1} and 1415 cm^{-1} were observed throughout the middle layers (6 to 9) of 286A, which are assigned to copper carboxylate (see Figure 5.40). The absorption at 1600 cm^{-1} corresponds to asymmetric stretching vibration and 1415 cm^{-1} corresponds to the symmetric vibration of copper carboxylate bonding. In 286A, emerald green particles were observed in layer 6, while only dispersed copper was detected in layers 9 and 10. Similarly, dispersed copper was noted in some layers of 286D and E (Tables 5.4 and 5.6). This "dispersed" copper is a common feature that can be found easily in the cross-sections of the dark paints.

5.3.1.2 Contribution of copper arsenate decomposition to the dark appearance

Disintegration or decomposition of emerald green is evident in the data. From the optical point of view, such changes lead to a decrease in the amount of green light reflected. Reduction of the particle size furthermore lowers the green saturation and increases light scattering, until a certain size is reached, but further reduction in size leads to a loss of scattering power of the particles. Therefore the disintegration of the copper arsenate lowers the saturation of the green at the early stage but subsequently leads to an increase of the light absorption. The amount of light reflected eventually decreases and the green would therefore deepen in color.

The presence of copper soaps suggests that the green pigments no longer retain copper ions. This will cause a decrease of the green color as a result of the particle losing its color center. It may not have a significant effect on the appearance since copper carboxylate does not have a strong light absorbing or scattering capability. The reaction with the oil binding components, however, will dissolve the pigment/binder boundaries, which would cause a large decrease of the yield of reflected light.

Copper ions or copper soaps may react further and form light absorptive compounds such as black copper oxide (CuO), dark brown red copper oxide (Cu_2O), or black copper sulfide (CuS) [Banik *et al.* 1981; 1982]. The occurrence of these phases is expected to distort the color balance and drastically change the original color especially when the paint reflects light to a reasonable extent. Browning of emerald green has been observed in a water color painting by Cezanne [Zieske 1995]. Color alteration of the pigment in an oil paint was reported by Feller [1967; Johnston-Feller 2001: 98-100]. In Persian manuscripts, verdigris has changed its color from green to brown, which was a result of formation of Cu_2O [Barkeshli 1999]. Although chemical aspects were not investigated in this study, formation of such light absorbing compounds even in small amounts might have a significant effect on appearance (Appendix to Chapter 1).

5.3.2 Lead in the paint layers

5.3.2.1 Lead soap in paint layers

The presence of lead soap in 286F and 286G was indicated by imaging FTIR. Both samples were taken from the relatively light colored areas that contain a rather large amount of lead white. Apparent IR absorptions of carboxylate were only detected in the layers of containing intact lead white pigment.

A rather dark paint layer of 286G contains a relatively large white chunk. This was a lead white agglomerate surrounded by lead carboxylate supported by IR absorptions of carbonate at around 1400 cm^{-1} and of carboxylate at 1509 cm^{-1} (Figure 5.44). The carboxylate indicated area appears with a hazy gray tone in the SEM-BSE image showing less electron reflected than intact lead white. This type of appearance in an SEM-BSE image with dispersed lead in between the particles is assumed to be a lead-saponified area [Keune and Boon 2007; Keune *et al.* 2011]. However, no carboxylate indication was found in the rest of the layer, although lead was detected by EDX.

The other dark paint layers also contain lead detected by EDX but lead containing particles were hardly observed. Mostly lead was dispersed and sometimes it was observed as amorphous electron reflective areas in the SEM-BSE images. This lead is assumed to be in carboxylate form.

5.3.2.2 Source of lead soap and corresponding appearance changes

Lead white in particle form with reasonable size (ca. 1-5 μm) was found mostly only in the light colored paint samples. However lead was detected in the dark paint layers, and its presence was also indicated in all samples analyzed by DTMS [Boon *et al.* 1995; Boon and Van Och 1996]. The relative intensity was low in the dark paint samples, which suggest the use of a lead based drier. Lead white is also a possible source since both lead white and lead driers could react away and form lead soaps.

The optical effects when both would change from their original state to soap forms are considered. A drier can be added by a paint maker during the manufacturing and/or by artists during the painting process to improve the drying rate of paint. In the early 19th century, the most common driers were zinc sulfate, litharge, and sugar of lead (lead acetate) [Carlyle 2001: 41-54]. The use of zinc sulfate in this painting is excluded since no zinc was detected. Not many records of artists that added a litharge dryer by themselves have been discovered and reported, the English artist Reynolds (died 1792) being an exception [Jones *et al*. 1999]. Lead acetate, which was commercially available in bladders is the most likely lead compound to have been added by artists [Carlyle 2001; 42-46]. As lead acetate is colorless, there is no fear of that it would tint a paint and further appearance change is also least expected (see Appendix to Chapter 1). *Huile grasse* (a heat-bodied oil treated with a lead or manganese drier) is another possible source of lead (see 5.2.3.1). Changes in optical aspects due to addition of driers have

rarely been cited an issue in the literature hitherto.

On the other hand, saponification of lead white is expected to cause changes of appearance, because unaltered lead white is a good light reflector. According to the model paint experiment in Chapter 3, saponification of lead white in a paint, which contains a relatively large amount of intact lead white would not affect the appearance. However, if the amount of lead white is relatively small, the saponification may have a crucial effect on changing the appearance (see Appendix to Chapter 1). It is also logical that Rousseau used the least amount of lead white possible for the glaze-like paints, in order to obtain suitable depth and transparency. Addition of a small amount of white pigment would contribute significantly to an increase in light reflection that could be beneficial for gaining an appropriate appearance, whereas a large amount of lead white makes paint opaque.

The green and possible orange upper paint layers of 286B, C, E, and H are assumed to be glazing layers considering that a relatively small amount of pigment particles were found in the paints. Because the two paints are close to being complementary colors, a large amount of light must have been absorbed, which is a possible cause of an unintended dark appearance. If lead white had been present in these

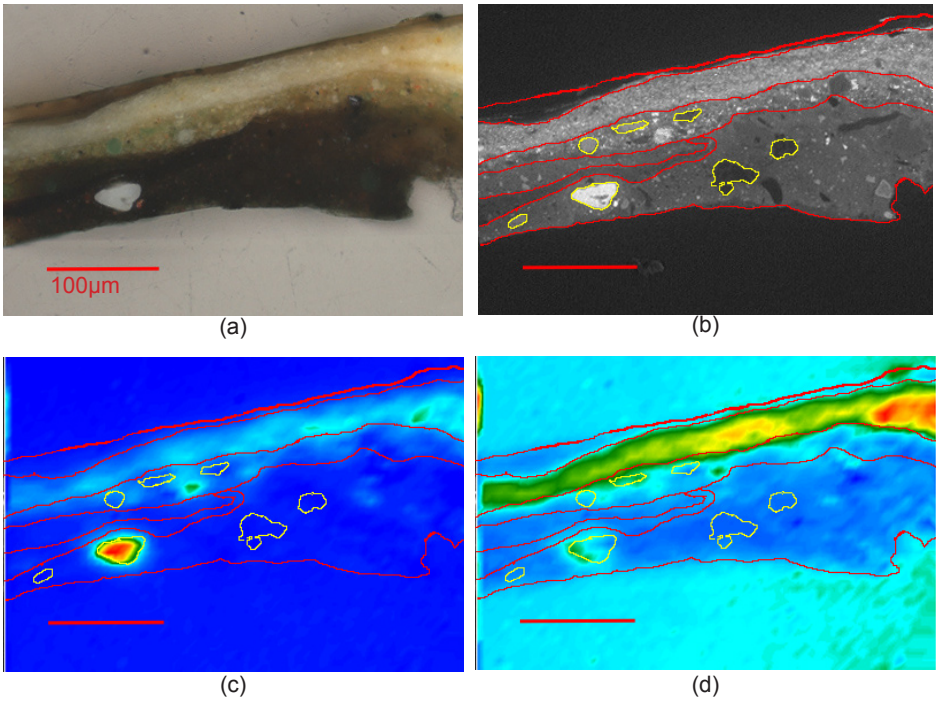

Figure 5.44 Lead soap indication in 286G. (a) VIS, (b) BSE image, (c) FTIR image at 1397cm^{-1} (carbonate absorption), (d) FTIR image at 1509cm^{-1} (lead carboxylate absorption).

layers, the upper paint layers would be a little more light reflective, thus making the appearance lighter. Suppose that such a small amount of lead white would saponify or disintegrate for some reason, then these paint layers would lose their scattering power to quite an extent. At the same time, the relative absorption would increase and the paint appearance after some time would be very dark.

Glazing is an effective way to achieve high saturation when it is applied over a reasonably light-reflective underlayer. It has been shown that where such translucent paint is present, it acts as a key factor for the appearance (Appendix to Chapter 1). However, a translucent layer is not only easily influenced by other (underlying) paints but also sensitive to the scattering factors in itself.

5.3.3 Effects of lake pigments

The use of a large amount of yellow lakes is evident from this examination (see 5.2.2.1). The presence of red lakes was also indicated in a few paint layers (Tables 5.2-5.12). These lake pigments may have faded and this would also have caused color changes (See Chapter 4.5) [Saunders and Kirby 1994; Kirsh and Levenson 2000: 161-167]. Another drawback of the fading is reduction of light reflection at certain wavelength. This will caused a decrease in the saturation. At the same time the decrease of selective absorption leads to an increase in light transmission since absorption greatly contributes to an increase in opacity [Johnstone-Feller 2001: 128-144; Camina 1968]. The transparency change can be overlooked when the underlying layer is reasonably light reflective. However, if the color of the underlying layer is dark or a complementary color to the faded layer, there will be a considerable change in appearance.

The paints contain a relatively large amount of potassium aluminum sulfate (alum) as a substrate compound for the unidentified yellow lake. This might have contributed to poor drying condition of oil components. Potassium aluminum sulfate has a characteristic feature of releasing protons by hydrolysis. This makes the paint system more acidic. Normally oil paint has an ability to compensate for the acidity by binding available metal ions [Boon 2006]. Considering that the paint –especially the dark paint– in this painting contains a fairly low amount of pigments, it would be difficult to maintain the pH because of a shortage of metal ions.

5.3.4 Changes in varnish layer and its optical effects on the surface

The severe cracks of the varnish and paint layers reflect light diffusely at the surface, which is one of the main reasons for the disruption of legibility [Carlyle and Southall 1993, Kirsh and Levenson 2000: 218]. This is because a relatively large amount of incident light reflects at the surface and less light would be available for the characteristic light absorption (and reflection) in the paint layers [De la Rie 1987].

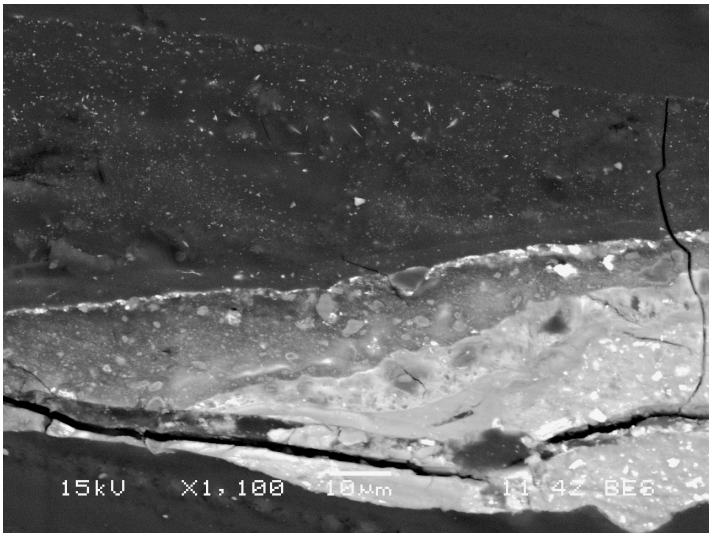

Figure 5.45 Particles occurred in the varnish layers in 286C (BSE-image).

Blanching, efflorescence, and re-crystallization or the occurrence of new compounds on and in a varnish layer has a similar effect. The presence of fine particles in the varnish layers seen in 286A and C is probably one of the causes of the muddy and whitish surface appearance (Figure 5.45). The cracked and deformed varnish as well as the fine particles causes the incident light to reflect before reaching the paint layers, in other words, an increase of surface reflection and a relative decrease of light transmission results.

Yellowing of varnish would be another obstacle to the light path as it absorbs more light than non-discolored varnish. Therefore, the yellowed varnish diminishes the light reflection by absorbing the light before reaching the paint layers and also after reflecting back toward the surface. Furthermore, the yellowness would be enhanced if any of light scattering particles are in the varnish layer [Butler 1962].

5.4 Conclusions

The present study supports the previous suggestion the dark appearance of *La Descente des Vaches* is strongly associated with the changes of the chemical and physical condition of the painting's constituents over time. The manifestation and distribution of copper, arsenic and lead and the small amount of lead white are keys to explain its extremely dark and illegible appearance. The most remarkable change affecting the dark appearance turns out to be the decomposition of emerald green pigment. Two main elements; copper and arsenic, both present in emerald green, have distinct behaviors.

Copper was found to have altered to copper carboxylates, likely remained in the original paint layers. In contrast, arsenic was often found in the upper layers of the paints, suggesting that the arsenic component is much more mobile. The loss of either arsenate (III) units or copper (II) ions from the molecular structure of emerald green causes a loss of the green color. The distribution of the two elements suggests that the original form consisting of particles is no longer maintained within the stratigraphy. Since the pigment emerald green is functional both in reflection and absorption, its loss would lead to a diminishing of the green color, browning and a reduction of scattering power.

Saponification or/and disintegration of a small amount of light reflecting lead white in the paint are suggested to be primarily responsible for the dark appearance. Saponification of lead white was confirmed in the light color paints, while dispersed lead was detected by EDX in the dark paints. Assuming that the original form of lead was lead white, the dissolution would lead to reduction in the amount of light reflected.

The yellow lakes might have faded and changed the tonality of the paint by losing their yellowness. Furthermore, an increased yellowed varnish will be contributing to further toning down of the appearance. The severe cracks and the particles occurring in the varnish layers are barrier for light transmission into the paint.

These chemical and physical changes must have totally distorted the color balance of the painting. Rousseau's painting techniques are partly responsible, although for him to predict these changes would not have been possible. Considering his desire for achieving depth and high saturation, he must have used paints, which reflect the required amount of light but without considering the possible consequences of his technique. His technique here also implied the use of a relatively large amount of yellow lakes and Prussian blue, but less lead white or any other light color pigments. Superimposing such translucent paint layers must have made the painting at first rich in color and depth. However, loss of the limited light reflective components and color changes due to chemical reactions within the paint have made the paint system gradually becoming extraordinarily absorbing for light.

References

Baer, N.S., Joel, A., Feller, R.L., and Indictor, N. 1986. Indian Yellow. In: R.L. Feller ed. *Artists' Pigments: a Handbook of their History and Characteristics, vol. 1*. Washington DC: National Gallery of Art, pp. 17-36.

Banik, G., Stachelberger, H., Mairinger, F., Vendl, A., and Ponahlo, J. 1981. Analytical investigations of the problem of "Kupferfraß" in illuminated manuscripts. *Microchimica Acta*, 75 (1-2), 49-55.

Banik, G., Stachelberger, H. and Wächter, O. 1982. Investigation of the destructive action

of copper pigments on paper and consequences for conservation. In: *Science and Technology in the Service of Conservation*. London: IIC, pp. 75-78.

Barkeshli, M. 1999. The presence of saffron in Persian miniature paintings and its use as an inhibitor for the destructive effect of verdigris. In: J. Bridgland, ed. *ICOM Committee for Conservation 12th Triennial Meeting, Preprints*. London: James & James, pp. 489-494.

Boitelle, R., Van den Berg, K.J., Geldof, M. & Languri, G. 2001. Descending into the details of Th. Rousseau's '*La descente des vaches*' (The Mesdag Collection, The Hague) - Technical Research of a Darkened Painting. In: A. Phenix, ed. *A joint meeting of ICOM-CC Working Groups Paintings 1 & 2 and The Paintings Section*. London: UKIC, pp. 27-31.

Boon, J.J., Pureveen, J., Rainford, D., and Townsend, J.H. 1995. The opening of the Wallhalla, 1842': Studies on the molecular signature of Turner's paint by direct temperature-resolved mass spectrometry (DTMS). In: J.H. Townsend, Ed. *Turner's Painting Techniques in Context 1995*. London: IIC, pp.35-45.

Boon, J.J. and Van Och, J. 1996. A Mass Spectrometric Study of the Effect of Varnish Removal from a 19th Century Solvent-sensitive Wax Oil Painting. In: J. Bridgland, ed. *ICOM Committee for Conservation 11th Triennial Meeting, Preprints*. London: James & James, pp. 197-205.

Boon, J.J. 2006. Processes inside paintings that affect the picture: chemical changes at, near and underneath the paint surface. In: J.J. Boon and E.S.B. Ferreira, eds. *Reporting Highlights of the De Mayerne Program*. The Hague: NWO, pp.21-32.

Boon, J.J. and Oberthaler, E. 2013. Mechanical Wakness and Chemical Reactivity Observed in the Paint Structure and Surface of The Art of Painting by Vermeer. In: J.H. Stoner, R. Rushfield, eds. *Conservation of Easel Paintings*. Routledge, pp. 328-335.

Burmester, A., Denk, C. 1999. Blue, Yellow and Green on the Barbizon Palette. *Zeitschrift fur Kunsttechnologie und Konservierung*, 13 (1), 79-87.

Burnstock, A., Van den Berg, K.J., De Groot, S., and Wijnberg, L. 2006. An Investigation of Water-Sensitive Oil Paints in Twentieth-Century Paintings. In: *Modern Paints Uncovered*. Los Angeles: The Getty Conservation Institute, pp.177-187.

Butler, W.L. 1962. Absorption of Light by Turbid Materials. *Journal of the Optical Society of America*, 52 (3), 292-299.

Camina, M. 1968. Measurements of the fading of pigments in relation to loss of opacity. *Journal of Oil and Colour Chemists' Association*, 51, 14-26.

Carlyle, L. 1990. British nineteenth-century oil painting instruction books: a survey of their recommendations for vehicles, varnishes and methods of paint application. In: J.S. Mills and P. Smith, eds. *Cleaning, Retouching and Coatings: Technology and Practice for Easel Paintings and Polychrome Sculpture*. London: IIC, pp. 76-80.

Carlyle, L. and Southall, A. 1993. No Short Mechanic Road to Fame -The Implications of Certain Artists' Materials for the Durability of British Painting: 1770-1840. In: *Robert Vernon's Gift: British Art for the Nation 1847*. London: Tate Gallery, pp. 21-26.

Carlyle, L. 2001. *The Artist's Assistant*. Archetype Publications.

Child, R.E. 1995. Pitch, Tar, Bitumen and Asphalt? A Sticky Problem. In: *Resins, Ancient and Modern*. Edinburgh: SSCR, pp. 111-113.

Constantin, S. 2001. The Barbizon painters: A guide to their suppliers. *Studies in Conservation*, 46, 49-67.

De la Rie, R. 1987. The Influence of Varnishes on the Appearance of Paintings. *Studies in Conservation*, 32, 1-13.

Eastaugh, N., Nadolny, J., and Swiech, W. 2014. Interpretaioni of documentary sources for the industrial preparation of 'zinc white' in the 19th century. In: H. Dubois, J.H. Townsend, S. Eyb-Green, J. Nadolny, S. Neven and S. Kroustallis. Eds. *Making and transforming art: changes in artists' materials and practice*. London: Archetype, pp.102-108.

Erhardt, D., Von Endt, D., and Tsang, J. 1990. Condition, Change, and Complexity: The Media of Albert Pinkham Ryder. In: *Postprints of The Paintings Specialty Group Annual Meeting 1990*. AIC, pp. 28-35.

Feller, R.L. 1967. Problems in Spectrophotometry. In: *Conference on Museum Climatology*. London: IIC, pp. 257-269.

Fiedler, I. and Bayard, M.A. 1997. Emerald green and Scheele's green. In: E.W. FitzHugh, ed. *Artists' Pigments: a Handbook of their History and Characteristics, vol. 3*. Oxford University Press, pp. 219-271.

Grissom, C.A. 1986. Green earth. In: R.L. Feller ed. *Artists' Pigments: a Handbook of their History and Characteristics, vol. 1*. National Gallery of Art, pp. 141-167.

Heaton, N. 1928. *Outline of paint technology*. London: Charles Griffn & Co.

Helwig, K. 2007. Iron oxide pigments: Natural and synthetic. In: B.H. Berrie, ed. *Artists' Pigments: a Handbook of their History and Characteristics, vol. 4*. London: Archetype Publications, pp. 59-63.

Johnston-Feller, R. 2001. *Color Science in the Examination of Museum Objects: Nondestructive procedures, Tools for Conservation*. The J. Paul Getty Trust.

Jones, R. 1990. Drying crackle in early and mid eighteenth century British painting. In: *Appearance, Opinion, Change: Evaluating the Look of Paintings*. London: United Kingdom Institute for Conservation, pp. 50-52.

Keune, K. and Boon, J.J. 2005. Analytical Imaging Studies Clarifying the Process of the Darkening of Vermilion in Paintings. *Analytical Chemistry*, 77 (15), 4742–4750.

Keune K. and Boon, J.J. 2007. Analytical Imaging Studies of Cross-Sections of Paintings Affected by Lead Soap Aggregate Formation. *Studies in Conservation*, 52, 161-176.

Keune, K. and Boon, J.J. 2011. 'Can dispersed and migrated arsenic from degraded pigments in paintings be a marker for water-linked transport processes?'. In: J. Bridgland, ed. *ICOM Committee for Conservation 16th Triennial Meeting, Preprints*. London: James & James, pp. 1609 1–7.

Keune, K., van Loon, A., and Boon, J.J. 2011. SEM backscattered-electron images of paint cross sections as information source for the presence of the lead white pigment and lead-related degradation and migration phenomena in oil paintings. *Microscopy and Microanalysis*, 17 (05), 696-701.

Keune, K., Boon, J.J., Boitelle, R., and Shimadzu, Y. 2012. Degradation of Emerald green in oil paint and its contribution to the rapid change in colour of the Descente des vaches (1834–1835) painted by Théodore Rousseau. *Studies in Conservation*, 58 (3), 199-210.

Kirsh, A., and Levenson, R. S. 2000. *Seeing through Paintings: Physical Examination in Art Historical Studies Vol. 1*. Yale University Press.

Kühn, H. 1986. Zinc white. In: R.L. Feller, ed. *Artists' Pigments: a Handbook of their History and Characteristics, vol. 1*. Washington DC: National Gallery of Art, pp. 169-186.

Kühn, H. and Curran, M. 1986. Chrome Yellow and Other Chromate Pigments. In: R.L. Feller, ed. *Artists' Pigments: a Handbook of their History and Characteristics, vol. 1*. Washington DC: National Gallery of Art, pp.188-189.

Languri, G.M, Boon, J.J. 2005. Between Myth and Reality: Mummy Pigment from the Hafkenscheid Collection. *Studies in Conservation*, 50 (3), pp. 161-178.

Languri, G.M, Boon, J.J., and Boitelle, R. 2005. Changing properties of the asphalt- and oil-derived components in asphalt-oil paints prepared according to 19th century recipes. In: I. Verger, ed. *ICOM Committee for Conservation 14th Triennial Meeting, Preprints*. London: James & James, pp. 489-494.

Languri, G.M. 2004. *Molecular studies of asphalt, Mummy and Kassel earth pigments: their characterisation, identification and effect on the drying of traditional oil paint*. PhD dissertation (MolArt report no. 9), University van Amsterdam.

Lau, K.H., Brittaiin, R.D., and Hildenbrand, D.L. 1982. Vaporization of arsenic trisulfide and the dissociation energy of arsenic sulfide. *Journal of Physics and Chemistry*, 86, 4429-4432.

Lee, C. and Harrison, W.T.A. 2004. The catena-arsenite chain anion, $[AsO_2]_n^{n-}$:

$(H_3NCH_2CH_2NH_3)_{0.5}$ $[AsO_2]$ and $NsAsO_2$ (revisited). *Acta Crystallographica*, C60, m21-m218.

Leeman, F., and Pennock, H. 1996. Théodore Rousseau, In: *Museum Mesdag: Catalogue of Paintings and Drawings*. Zwolle: Waanders Publishers, pp. 380-384.

Mills, J. and White, R. 1994. *Organic Chemistry of Museum Objects*, 2nd edition. London: Butterworth-Heinemann.

Plesters, J., Roy, A., and Bomford, D. 1982. Interpretation of the magnified image of paint surfaces and samples in terms of condition and appearance of the picture. In: N.S. Brommelle and G. Thomson, eds. *Science and Technology in the Service of Conservation*. London: IIC, pp. 169-176.

Raistrick, H., Robinson, R., and White, D.E. 1936. CLXXXVII. Studies in the biochemistry of micro-organisms. L. Ravenelin (3-Methyl-1:4:8-tryhydroxyxanthone), a new metabolic product of Helminthosporium Ravenelii curtis and of H. Turcicum Passerini. *Biochemical Journal*, 30(8), 1303-1314.

Roy, A. 1999. Barbizon Painters: Tradition and Innovation in Artists' Materials. In: A. Burmester, C.H. Heilmann, and F. Michael, eds. *Barbizon: Malerei Der Natur, Natur Der Malerei*. München: Klinkhardt & Biermann, pp. 330-342.

Roy, A. 2007. Cobalt blue. In: B.H. Berrie, ed. *Artists' Pigments: a Handbook of their History and Characteristics, vol. 4*. London: Archetype Publications, pp.151-177.

Saunders, D. and Kirby, J. 1994. Light-induced Colour Changes in Red and Yellow Lake Pigment. *National Gallery Technical Bulletin*, 15, 79-97.

Schulman, M., Bataillès, M., and Sérafino, V. 1999. *Théodore Rousseau, 1812-1867: catalogue raisonné de l'œuvre peint*. L'Amateur.

Sensier, A. 1872. *Souvenirs sur Th. Rousseau*. Leon Techener.

Sinninghe Damste, J.S., and De Leeuw, J.W. 1990. Analysis, structure and geochemical significance of organically-bound sulphur in the geosphre: State of the art and future research. *Organic Geochemistry*, 16 (4-6), 1077-1101.

Špalt, Z., Alberti, M., Peña-Měndez, E., Havel, J. 2005. Laser ablation synthesis of arsenic and arsenic sulphide clusters. *Polyhedron*, 24, 1417-1424.

Stieg, F.B. 1962. The Geometry of White Hiding Power. *Official Digest*, 10, 1065-1079.

Stoner, J.H. 1990. Washington Allston: Poems, Veils, and "Titian's dirt". *Journal of the American Institute for Conservation*, 29 (1), 1-12.

Theodorakopoulos, C. 2005. *The excimer laser ablation of picture varnishes: an evaluation with reference to light-induced deterioration*. PhD dissertation Royal College of Art, RCA/V&A Conservation.

Thomas, G.M. 1999. The practice of »Naturalism« : The Working Methods of Théodore Rousseau. In: A. Burmester, C.H. Heilmann, and F. Michael, eds. *Barbizon: Malerei Der Natur, Natur Der Malerei*. München: Klinkhardt & Biermann, pp.139-152.

Thompson, G.W. 1915. Painting defects: Their causes and prevention. *The Journal of Industrial and Engineering Chemistry*, 7 (2), 136-145.

Van den Berg, *J.D.J. 2002. Analytical chemical studies on traditional linseed oil paints*. PhD dissertation, University of Amsterdam.

Van den Berg, K.J., Boon, J.J., Pastorova, I., and Spetter, L.F.M. 2000. Mass spectrometric methodology for the analysis of highly oxidized diterpenoid acids in Old Master paintings. *Journal of Mass Spectrometry*, 35, 512-533.

Van den Berg, K.J., Geldof, M., De Groot, S., and Van Keulen, H. 2002. Darkening and surface degradation in 19th- and early 20th-century paintings: an analytical study. In: R. Vontobel, ed. *ICOM Committee for Conservation 13th Triennial Meeting, Preprints*. London: James & James, pp. 464-472.

Van der Doelen, G.A. 1999. *Molecular Studies of Fresh and Aged Triterpenoid Varnishes*. PhD dissertation, University of Amsterdam.

Van der Doelen, G.A., van den Berg, K.J. and Boon, J.J. 1998. Comparative chromatographic and mass-spectrometric studies of triterpenoid varnishes: fresh material and aged samples from paintings. *Studies in Conservation*, 43, 249-264.

Van Loon., A. 2008. *Color changes and chemical reactivity in seventeenth-century oil paintings*. PhD dissertation, University of Amsterdam.

Vaughan, D.J. 2006. Arsenic. *Elements*, 2 (2), 71-75.

White, R. 1986. Brown and Black Organic Glazes, Pigments and Paints. *National Gallery Technical Bulletin*, 10, 58-71.

White, R. and Kirby, J. 2001. A Survey of Nineteenth- and Early Twentieth-Century Varnish Compositions found on a Selection of Paintings in the National Gallery Collection. *National Gallery Technical Bulletin*, 22, 64-84.

White, R., Pilc, J., and Kirby, J. 1998. Analyses of Paint Media. *National Gallery Technical Bulletin*, 19, 74-95.

Willoughby, C 1987. Search for Permanence—Materials and Methods of G.F. Watts, In: *Das 19, Janhrhundert und die Restaurierung; Beiträge zur Malerei, Maltechnik und Konservierung*. Heinz Althöfer (Hrsg.), pp. 203-216.

Zieske, F. 1995. An investigation of Paul Cézanne's watercolors with emphasis on emerald green. In: *AIC The book and paper group, annual meeting preprints, 14*. pp. 105-115.

Appendix
Analytical Instrumentation

A. Light microscope (LM)

ZEISS Axioplan 2 polarized light microscope (reflected/transmitted light)

B. Scanning electron microscopy and energy dispersive X-ray spectroscopy (SEM-EDX)

B-1 ICN (now RCE)

Instrument: JSM-5910LV (JEOL)
Accelerating voltage: 15 keV or 20 keV
EDX: ThermoNoran operated by the Vantage software

B-2 AMOLF

Instrument: XL30 SFEG high vacuum electron microscope (FEI, Eindhoven).
Accelerating voltage: 15 keV
EDX: EDAX (Tilburg, The Netherlands).

C. Cross-section polisher

Instrument: Cross-section Polisher (CP®) (JEOL Ltd., Tokyo, Japan)
Gas: Argon
Ion accelerating voltage: 4-7 keV

D. Direct Temperature resolved mass spectrometry (DTMS)

Instrument: JMS-SX/SX 102A four-sector double-focusing mass spectrometer (JEOL-Europe, Schiphol-Rijk, The Netherlands)
Direct insertion probe: platinum/rhodium; Pt/Rh (9/1) filament (diameter 100 um) (Drijfhout, The Netherlands)
Filament temperature: a rate of 0.5 A/min to about 800 °C
Ionisation: EI 16 eV (chamber temperature kept at 180 °C)
Mass range: m/z 20-1000 with 1 second cycle time
Data process: JEOL MP-7000 data system.

Procedure:

The sample was made into a suspension with about 2-5 µl of ethanol. About 1-2.5 µl of the sample suspension were deposited on the filament.

E. Thermally assisted hydrolysis and methylation gas chromatography/mass spectrometry in combination with Curie Point pyrolysis (Py-TMAH-GCMS)

Methylation reagent: tetramethylammonium hydroxide (TMAH)

GC Instrument: Thermo Quest GC8000Top Voyager Gas Chromatograph
Pyrolysis temperature: 610°C (pyrolysis unit: 290°C)
Column: ZB5 (0,25 mm id., 0,1 um film thickness, 15 meters length)
Carrier gas: Helium (He)
Flow rate: 0.8 ml/min
Oven temperature: starting with 45˚C, then increase with a rate 50˚C /min till 100 ˚C and a rate 6˚C/min till 310˚C retained for 8 min.

MS Instrument: VoyagerPlus Mass Spectrometer
GC/MS interface temperature: 240˚C,
Ion source temperature: 220˚C.
MS: a linear quandrupole then accelerated to 3 kV, mass separated and post-accelerated to 10 kV before detection.
Ionization: EI, 70eV.
Mass range: *m/z* 45-480

GC Condition 2 (Chapter 4: used for Indian Yellow reference sample analysis)
Column: SLB5 ms (20 meters length, 0.18 mm internal diameter, and 0.18 µm film thickness) (Supelco)
Carrier gas: Helium (He)
Flow rate: 0.8 ml/min
pyrolysis temperature: 625°C (pyrolysis unit: 290°C)
Oven temperature: starting with 35˚C (for 1 min.), then increase with a rate 60˚C /min till 110 ˚C and a rate 14˚C/min till 240˚C and a rate 5˚C/min till 315˚C retained for 2 min.

F. Fourier Transfer Infrared spectroscopy (FTIR)

F-1 ICN (RCE) (ATR method)

Instrument: Perkin Elmer Spectrum 1000 FTIR with ATR (Graseby Specac Inc.)
Scanned: 40 times
Resolution: 8 cm^{-1}
IR range: 4000-600 cm^{-1}

F-2 AMOLF (Imaging technique)

Instrument: Bio-Rad FTS-6000 FTIR spectrometer connected to an IR microscope Bio-Rad UMA-500 (Bio-Rad, Cambridge, MA)
Imaging System; 64 x 64 mercury-cadmium telluride (MCT) focal plane array camera
Resolution: 16 cm^{-1}

G. HPLC-PDA (High Performance Liquid Chromatography- Photo Diode Array)

Column Luna C18, 150x2 mm id. 3 um.
PDA: 200-800 nm. Fluorescence with 510 excitation and 580 nm emission, with addition of 0.1 M Aluminum nitrate in 20% methanol / water as fluorescence enhancer.

Summary

The appearance of paintings changes for various reasons in the course of time as a result of aging of the materials chosen or employed by the artist. Extensive studies on painting materials and their chemistry in the last fifteen years have revealed that saponification of basic pigments often occurs in oil paintings. This saponification reaction is a "natural" characteristic of oil paint systems, but in some cases the effects can become so visible at the surface that they will disturb the esthetic quality of the painting. In most cases the painting's appearance will darken because of a decrease of reflected light due to dissolution of light reflecting pigment particles. This thesis contributes to a deeper understanding of appearance changes due to saponification especially of white pigments such as lead white and zinc white, with notes on how to recognize the phenomenon. In addition, other color change phenomena with an impact on appearance, such the effect of discoloration of lakes, the decomposition of pigments, and in general a change in transparency of paint layers were studied from a chemical and optical point of view. Paint stratigraphy in affected paintings, reconstructions and experiments with paint composition and paint layering were used to understand the loss of contrast and change in color.

General optical theories about appearance and their determining factors are presented in chapter 1 including a few brief reviews on light behavior in oil paint systems. Appearance is largely determined by light reflecting from a painting, which is a result of many interactions between light and paint constituents. The light reflection from the paint, which is a result of scattering and absorption in the paint, is governed by optical characteristics of paints, for instance the refractive indices of pigments and binding media, the paint stratigraphy, and the particle sizes and particle distributions within the paint layers. The paint color is greatly dependent on the kind of colorant used. Binding media or a varnish layer are linked to glossiness of the surface and/or saturation of the color but they can also influence the paint color depending on their degree of yellowing. Layer build-up is another important factor that affects the appearance since many paint layers are partially translucent and receive reflected light from the lower layers. For this reason glaze-like translucent paint layers are more sensitive to changes in light scattering and absorption.

Following theoretical discussions to clarify the factors determining appearance in a paint system, the optical effects of saponification are addressed. Saponification, soap aggregation and protrusions were demonstrated analytically in paint layers in the late 20th century, although saponification of lead white was already suggested in the early part of the 20th century in relation to transparency changes of oil paint. It was one of the theoretically possible three explanations for the notion of 'transparency of oil paint increasing in course of time'. The most widespread explanation among them

however, was an increase of refractive index (RI) of the oil binding media leading to a decrease of RI differences between the binding media and pigment. It is presently understood that oil paint media change from a cross-linked viscous state into a metal ion coordinated saponified state as time progresses. The experiments with reconstructed paints applied over black and white substrates suggest that an optical effect of an RI change in oil binding media is limited and is not effective enough for the human eye to see it as an appearance change (see Appendix to Chapter 1). Other experiments with paint reconstructions emphasize that light scattering is a key factor for seeing the appearance of paints, and the effect of size and distributions of colorant particles are very determining.

The painting studies in chapters 2 to 5 describe the investigation of a possible correlation between the appearance of a painting, and the chemical and physical condition of the paints. Four oil paintings painted in the 19th and the early 20th century, with a dark appearance were selected for an investigation of the current appearance. Their appearances are sufficiently changed that they do not convey the artists' intention anymore, especially in the dark passages where many details are now lost.

The examination of paint cross-sections and compositional analyses clarified the chemical conditions of the paint, especially the darkened paint. Chemical and physical changes on the microscopic level were employed to explain the dark appearance. Comparison of the light and dark paint revealed differences in light reflecting components and stratigraphic conditions that illustrate the conditions when appearance changes can become visible.

An example is provided by a late 19th century painting '*Speak! Speak!*' by J.E. Millais (1829-1896) whose darkened appearance is due mainly to increased transparency by zinc soap formation (Chapter 2). The light colored paint layer was suspected to have become much more translucent than the original paint. Because this layer is painted over the dark paint layer, this area gives the impression of partial darkening. Scientific examination of the paint sample from this area revealed that the paint contains zinc soaps. Finding non-affected zinc oxide in the same paint layer indicated that zinc oxide was the original material form. When the pigment has saponified, the morphology of the particles is destroyed. Since light scatters at the particles, loss of particles means that light has no chance to scatter anymore, which consequently leads to a quantitative reduction of reflected light. The remaining light would reach the underlying paint layer and will be reflected upwards in case the layer underneath is light reflective. On the other hand, when the underlying paint is light absorptive, not much reflected light is expected. Thus, a paint layer with an increasing transparency by itself, may lose even more reflected light because of the reflecting properties of lower layers.

Chapter 3 is second case study that links metal soap formation and appearance. The painting '*The Doctor*' by L. Fildes (1843-1927) gives the impression that the human figure in the background has almost disappeared. The paint sample from this area indeed contains zinc soaps. Interestingly, zinc soaps were found not only in the area of the figure disappearing but also in areas where no appearance changes are observed.

In both areas, saponification was confirmed in the upper paint layers. In the sample from the figure, there is a brown paint layer underneath the saponified paint layer. Contrary, a white paint was found below the layer from the area where appearance changes are absent.

Judging from results of these two paintings, a decrease of lightness i.e. darkening due to the saponification can be recognized when there is a dark paint underneath. This explains why we see the appearance changes only in certain areas. These results also initiated the experiments using reconstructed paint to visualize optical effects of the saponification in oil paint. An increase of transparency was demonstrated as a decrease of the hiding power when zinc oxide was replaced with the corresponding zinc soap. Since the opacity of a white paint is based on scattering power of the pigment, saponification of white pigment leads to an increase of transmission. The transmitted light is either reflected or absorbed by the underlying paint. When the light is reflected enough, the saponification of white pigments would not have a strong optical effect on the appearance. In contrast, when the underlying paint is dark colored the light will be largely absorbed resulting in a dark appearance. Such paint experiments show the effect of the layer build-up of paints i.e. whether the saponified paint layer is situated above or below, and whether the underlying paint is dark or light colored.

The study of an oil painting '*Self-Portrait*' of the Dutch painter F.H. Verster (1861-1927) painted in the early 20th century shows unreasonably strong contrasts suggesting a severe change in contrast in time (Chapter 4). Close observation of some photographs both in color and black-and-white, and also prints in exhibition catalogues over a period of about a century reinforced this impression. A strong color contrast is observed at Verster's forehead depicted area and in a paint sample taken from the dark paint stroke saponification of both lead white and zinc oxide could be shown. This confirms that there is certain loss of light scattering. The same paint layer contains a red lake that is discolored to some extent, which indicates that red reflection is reduced.

The effect of combined saponification of white pigments and discoloration of red lake was investigated with experiments on eosin lake containing paints. Adding a white pigment that increased the hiding power of the paint at the same time, caused an enhancement of the redness of the eosin paint. Because of these two chemical changes in the self-portrait painting of Verster, the balance of light scattering and absorption that painter once set, is now disturbed.

'*La Descente des Vaches*' by Th. Rousseau (1812-1867), painted in 1834-35, has an extremely dark appearance and also shows severe surface deformation (Chapter 5). According to the artist's biography, bitumen and the type of binding media that Rousseau employed were the cause of these defects. A preliminary study of the painting found little evidence for the use of bitumen. Furthermore the darkness of the paints seems to be too strong to be considered only a result of the yellowing of the binder and varnish. A sketch and an *ébauche* made by Rousseau as preliminary studies of the final painting, showed the true color scheme intended by the artist. Examination of the paint cross-sections of the darkened foliage in the painting revealed that emerald green

pigment decomposed to form copper carboxylates thus releasing the arsenic component from the copper-arsenate coordination compound that constitutes the pigment. The optical effect is a loss of scattering due to the disappearance of particles. Most of the lush green color disappeared leaving a dark brown paint.

The paints of Rousseau's painting contain very fine grained particles and are remarkably medium rich. In addition he used very limited amounts of white-pigmented paints and light colored paints. Considering that lead was often detected dispersed in the dark paints, lead white might have been used more often than is present in the paints now. From observation of the cross-sections it appears that most of the dark paints are strongly light absorptive because of a shortage of light reflectors. It is known from historical sources that Rousseau wanted to achieve deep, saturated but clear colors, especially green color. Therefore, he possibly avoided opaque paints and sparsely used light reflecting pigments. Darkening oil media and resins, yellowing varnishes and discoloration of organic Indian yellow in combination with the loss of the relatively light reflective emerald green pigment and possibly lead white, left a darkened painting with mainly light absorbing components.

The case studies of the four paintings demonstrate the importance of light scattering for their appearance. Changes in both light scattering properties of the paints and light absorption can strongly affect the transparency of the paints. Changes on the molecular level in an aging paint may irreversibly alter the color balance and harmony configured by paint combinations that are an essential part of the painting's appearance as intended by the artist.

Samenvatting

Het uiterlijk van schilderijen verandert in de loop van de tijd door verschillende oorzaken maar met name door de veroudering van de door de kunstenaar toegepaste materialen. Onderzoek naar de chemie van verfmaterialen heeft in de laatste vijftien jaar uitgewezen dat verzeping van alkalische pigmenten vaak optreedt in olieverfschilderijen. Deze verzepingsreactie is een inherente karakteristiek van olieverfsystemen, waarbij de effecten in sommige gevallen zo zichtbaar worden aan het oppervlak dat ze de esthetische kwaliteit van het schilderij aantasten. In de meeste gevallen zal dit leiden tot een verdonkering van het object door het 'oplossen' van de lichtreflecterende pigmentdeeltjes.

Dit proefschrift tracht bij te dragen aan een beter inzicht in verandering in de verschijningsvorm en dus het uiterlijk van schilderijen door verzeping van met name witte pigmenten als loodwit en zinkwit, waarbij aanwijzingen zijn gegeven over de manier waarop het fenomeen kan worden herkend. Hiernaast zijn kleurveranderingen in pigmenten die invloed hebben op de uiterlijke verschijningsvorm van het schilderij bestudeerd, zoals het effect van het verbleken van organische (lak)pigmenten, en de ontleding van pigmenten. In het algemeen zijn veranderingen in transparantie beschouwd vanuit een chemisch en een optisch uitgangspunt. De samenstelling en laagopbouw in de schilderijen werd bestudeerd en vergeleken met verfreconstructies met verschillende verfsamenstellingen en laagopbouw, teneinde veranderingen in contrast en kleur beter te begrijpen.

Optische theorieën over verschijningsvormen en de onderliggende factoren worden geïntroduceerd in hoofdstuk 1, waarbij ook een kort overzicht wordt gegeven over het gedrag van licht in olieverfsystemen. Het uiterlijk van een schilderij wordt in hoge mate bepaald door het licht dat gereflecteerd als gevolg van vele interacties tussen licht en verf. De kleur van de verf wordt primair bepaald door de gebruikte pigmenten. De lichtreflectie is een gevolg is van verstrooiing en absorptie in de verf en wordt bepaald door optische kenmerken van de verf, zoals de brekingsindices van pigmenten en bindmiddelen, de verfstratigrafie, de deeltjesgrootte en -verdeling binnen de verflagen. Bindmiddelen of vernislagen bepalen de glans van het oppervlak en verzadiging van de kleuren maar kunnen ook de verfkleur mede bepalen, afhankelijk van de mate waarin zij vergeeld zijn. De laagopbouw is een andere belangrijke factor die het schilderijuiterlijk beïnvloedt aangezien veel verflagen gedeeltelijk transparant zijn en gereflecteerd licht uit verschillende verflagen komt. Hierdoor zijn glacerende/doorschijnende verflagen meer gevoelig voor veranderingen in de lichtverstrooiing en -absorptie.

In aanvulling op theoretische discussies worden de optische effecten van verzeping besproken. Terwijl verzeping, aggregatie van zepen en uitbarsten van

deze aggregaten door het verfoppervlak (protrusies) in oude Meesters pas werden gedetecteerd en beschreven aan het eind van de 20ste eeuw, is de mogelijke verzeping van loodwit al geponeerd aan het begin van de 20e eeuw als één van de drie theoretische verklaringen voor de waargenomen toename van transparantie in olieverf in de loop van de tijd. De meest voorkomende verklaring in die tijd was echter dat een stijging van de brekingsindex van de oliebindmiddelen verantwoordelijk was, door een daling van de brekingsindex¬verschillen tussen bindmiddel en pigment. Verouderingsexperimenten met olieverfsystemen op zwart-witte ondergronden suggereren dat een optisch effect van een verandering van de RI in oliebindmiddelen niet effectief genoeg is om waar te nemen met het menselijk oog en dus beperkt is (zie appendix bij hoofdstuk 1). Andere experimenten met verfreconstructies benadrukken dat lichtverstrooiing alsmede het effect van grootte en verdeling van kleurstofdeeltjes bepalend zijn voor de verschijning van verven.

De schilderijstudies in hoofdstuk 2 tot en met 5 beschrijven het onderzoek naar een mogelijk verband tussen het uiterlijk van de schilderijen en de chemische en fysische toestand van de verf. Vier olieverfschilderijen geschilderd in de 19e en de vroege 20e eeuw met een bijzonder donkere uitstraling werden onderzocht; hun uiterlijk is zodanig veranderd dat ze er niet meer het uitzien zoals de kunstenaars het oorspronkelijk hadden bedoeld. Dit geldt met name voor de donkere passages waar veel details niet meer zichtbaar zijn. Onderzoek aan verfdwarsdoorsneden en chemische analyses in dit proefschrift gaven meer inzicht in de chemische toestand, met name van de verdonkerde verven. Chemische en fysische veranderingen op microscopisch niveau werden gebruikt om de donkere verschijning van de schilderijen te verklaren. Vergelijking van de lichte en donkere verf toonde verschillen in lichtreflecterende componenten en stratigrafie die de voorwaarden illustreren waaronder uiterlijke veranderingen zichtbaar kunnen worden.

In hoofdstuk 2 wordt een voorbeeld besproken van het eind-19de eeuwse schilderij '*Speak! Speak!*' van J.E. Millais (1829-1896) waarin de verdonkering met name wordt veroorzaakt door toename van transparantie door vorming van zinkzepen. Bij lichte verflagen, geschilderd over donkere, geeft dit een indruk van gedeeltelijke verdonkering. Analyse van de verfmonsters uit dit gebied gaf aan dat de verf zinkzepen bevat. De aanwezigheid van zinkoxide in dezelfde laag verf wees erop dat dit pigment oorspronkelijk aanwezig was. Bij verzeping van het pigment gaat de morfologie van de deeltjes verloren. Aangezien licht op de deeltjes verstrooit, betekent verlies hiervan dat licht geen kans meer heeft om te verstrooien en leidt tot een vermindering van gereflecteerd licht. Als de onderliggende verf lichtabsorberend is, zal dit leiden tot verdonkering.

Hoofdstuk 3 beschrijft tweede case studie die metaalzeepvorming verbindt met het veranderde uiterlijk. Het schilderij '*The Doctor*' door L. Fildes (1843-1927) wekt de indruk dat de menselijke figuur in de achtergrond bijna is verdwenen. Ook in dit gebied bevat een monster van de verf zinkzepen. Zink zepen bleken niet alleen in de verf van de verdwijnende figuur voor te komen, maar ook in gebieden waar geen duidelijke

veranderingen werden waargenomen. In beide gebieden, werd verzeping bevestigd in de bovenste verf lagen, maar werd in het niet-veranderde gebied een witte verf gevonden onder de verzeepte laag.

De resultaten van beide schilderijen geven aan dat verdonkering kan worden verwacht in het geval van een lichte toplaag waarin verzeping plaatsvindt, in combinatie met een donkere laag daaronder. Deze resultaten werden bevestigd door reconstructie-experimenten met verfsystemen met verschillende laagopbouw waarin lagen met zinkoxide en lagen met zinkzepen om het effect van de verzeping van het zinkwit te visualiseren. Aangezien de dekking van een witte verf is gebaseerd op de verstrooiing van het pigment, leidt verzeping van het pigment tot een toename van transmissie. Het doorvallende licht wordt ofwel gereflecteerd, of geabsorbeerd door de onderliggende verflaag. Als de onderliggende laag wit is en niet verzeept en het licht intens genoeg is, zou de verzeping van de witte pigmenten geen sterk optisch effect op het uiterlijk hebben. Aan de andere kant, als de onderliggende verf donker gekleurd is zal het doorvallend licht grotendeels geabsorbeerd worden, resulterend in een donkerder kleur. Deze experimenten tonen het effect van de verfopbouw aan bijvoorbeeld doordat de verzeepte verflaag boven of onder ligt of doordat de onderliggende laag donker of licht gekleurd is.

De studie van het olieverfschilderij '*Zelfportret*' van de Nederlandse schilder F.H. Verster (1861-1927), geschilderd in de vroege 20e eeuw, toont zeer sterke licht- en donker contrasten die een ernstige verandering van het uiterlijk in de loop van de tijd doen vermoeden. Deze indruk wordt versterkt bij het bekijken van zowel kleur als zwart/wit foto's onder meer in tentoonstellingscatalogi over een periode van bijna een eeuw. Verster's voorhoofd representeert een gebied waar in het huidige schilderij een sterk kleurcontrast wordt waargenomen. Met analyse van verf uit een donkere verfstreek kon verzeping van loodwit en zinkoxide worden aangetoond. Dit bevestigt dat er een verlies van lichtverstrooiing is opgetreden. Dezelfde laag bevat een rode lakpigment dat is deels is ontkleurd, waardoor de reflectie van licht van het rode deel van het spectrum is verminderd. Het verlies van het reflecterende wit en doorschijnend rood heeft een kleurverandering veroorzaakt die het contrast sterk heeft versterkt.

Het effect van gecombineerde verzeping van wit pigmenten en het verbleken van rode lak werd onderzocht met experimenten op eosine lakverf. Het toevoegen van een wit pigment dat de dekkingskracht van de verf verhoogt, veroorzaakt een verhoging van de roodheid van de verf. Vanwege de twee chemische veranderingen in het zelfportret van Verster, de verzeping en de verbleking, is het saldo van de verstrooiing van licht en absorptie dat schilder had ingesteld, nu verstoord.

'*La Descente des Vaches*' van Th. Rousseau (1812-1867), geschilderd in 1834-35, heeft een zeer donkere uitstraling en vertoont daarnaast ernstige vervorming van het oppervlak (hoofdstuk 5). Volgens de biografie van de kunstenaar waren bitumen en het type bindmiddel die Rousseau gebruikte de oorzaak van deze defecten. In een eerdere analytische studie van het schilderij werd echter maar weinig bewijs voor het gebruik van bitumen gevonden. Daarnaast leek de verdonkering van de verf te sterk

om te worden beschouwd als alleen het resultaat van de vergeling van het bindmiddel en vernis. Een schets en een zogenaamde *ébauche* gemaakt als voorstudies voor het schilderij, toonden het door de kunstenaar bedoelde kleurenschema. Analytisch onderzoek van de verfdwarsdoorsneden van het verdonkerde gebladerte in het schilderij liet zien dat ontleding had plaatsgevonden van smaragdgroene pigmentdeeltjes waarbij koperzepen werden gevormd en de arseencomponent van het koper-arsenaat pigment vrijkwam. Het optisch effect hiervan is een verlies van verstrooiing en toename van transparantie als gevolg van het verdwijnen van deeltjes. Op het schilderij laat zich dit zien als een verlies van de weelderige groene kleur tot een donkerbruine verf.

De verven van Rousseau's schilderij zijn zeer fijn-korrelig qua pigmentatie en opmerkelijk bindmiddelrijk. Daarnaast zijn maar zeer beperkte hoeveelheid wit-gepigmenteerde en andere licht gekleurde verven aanwezig. Gezien het feit dat in de donkere verf vaak lood werd gedetecteerd in opgeloste toestand, is het zeer waarschijnlijk dat Rousseau vaker loodwit heeft gebruikt dan nu in de verf aanwezig is. Uit bestudering van de dwarsdoorsneden blijkt dat de meeste van de donkere verflagen sterk licht absorberend zijn door het tekort aan licht reflectoren. Het is bekend uit historische bronnen dat Rousseau diepe, verzadigde maar heldere kleuren wilde bereiken, met name bij groene kleuren. Daarom vermeed hij mogelijk het gebruik van dekkende verven en gebruikte lichtreflecterende pigmenten maar spaarzaam. Sterk verdonkerde olie- en harsbindmiddelen in verf en vernis, verbleking van Indiaas geel (*Indian Yellow*) in combinatie met het verlies van het relatief sterk lichtreflecterende smaragdgroene pigment, en mogelijk loodwit, hebben geleid tot een donker schilderij met hoofdzakelijk licht absorberende componenten.

De *case studies* van de vier schilderijen tonen het belang en de invloed van verstrooiing van licht van pigmenten aan voor hun verschijning. Veranderingen in zowel lichtverstrooiingseigenschappen als lichtabsorptie van de verf kunnen de doorzichtigheid van de verf sterk beïnvloeden. De kleurbalans en harmonie, zijn een essentieel onderdeel van het oorspronkelijk uiterlijk van het schilderij en een uiting van het talent van de kunstenaar. Veranderingen op moleculair niveau in een verouderende verf kunnen hierop een grote negatieve invloed hebben.

要旨 (Summary in Japanese)

絵画の見た目は、時間の経過にともない経年劣化や作者が選択した絵画材料の劣化といったさまざまな理由や要因により変化する。ここ 15 年間に実施された克明な絵画材料とその化学状態に関する調査研究により、油彩画において、塩基性の顔料は比較的容易に金属石鹸化することが明らかにされた。この反応は材料が持つ化学的性質に起因する自然な反応であるが、場合によっては絵画の見た目を変化させ、作者の意図した表現をも歪曲しうる。多くの場合、この現象は見た目の暗色化として表れる。顔料粒子は、本来光を反射することで色や形といった図像を作り出しているが、乾性油成分と反応し金属石鹸化すると、粒子の形状が失われ、それにともない光の反射も減少するためである。本研究ではこの現象に着目し、白色顔料、とくに鉛白（塩基性炭酸鉛）と亜鉛華（酸化亜鉛）の金属石鹸化による油彩画の見た目の変化について、実際に目視できるかといった検討も含めた調査研究をおこなった。さらに、有機質顔料の退色や顔料の分解などの絵画材料の化学変化が絵画の見た目に及ぼす影響についても取り上げる。このような化学変化と絵画層の透明度の関係性を明らかにするため、光学的な考察を取り入れた。また、絵画層中に生じる化学変化がもたらす絵画の見た目上の変色やコントラストの変化をより深く理解することを目的とし、すでに暗色化が観察される絵画を対象とした絵画層の重なり状態の分析、あるいは調製した絵画層を用いた実験などを実施した。

第1章では、一般的な光学理論により、絵画あるいは絵画層の見た目や色調を決定する要素について説明する。また、絵画層内での光の挙動についても概観する。我々が見ているもの＝「見た目」は、物体からの光、すなわち反射光を認知することで決められる。絵画では、絵画層からの反射光とは、層内での光の拡散反射や吸収といった絵画材料と光の相互作用の結果といえる。この反射光の性質は、絵画層の光学的性質、たとえば、顔料や展色材の屈折率、絵画層の積層状態、顔料粒子の大きさや分布状態などに依存している。絵画層の色は、色材の種類によって決定されることがほとんどであり、展色材やワニスは、表面の光沢や彩度に大きく関与している。展色材やワニスの黄色化は、変色の度合いや色材の色によっては、絵画層や絵画全体の色調を変化させることもある。また、絵画層は、その薄さゆえにたいていは半透明であり、複数の絵画層が重なっている場合、相互に光学的影響を及ぼしている。そのため、重ね塗りの状態も絵画の見た目に影響を与える重要な要素のひとつであるといえる。たとえば、透明度の高いグレーズ層のような絵画層では、色材の含有量の多い絵画層よりも光の拡散や吸収の変化による影響を受けやすい。

光学理論により、油彩画の絵画層内における見た目に影響を及ぼす要素を概観したのち、顔料の金属石鹸化による光学的な効果について述べる。鉛白の金属石鹸化とそれに関連した油彩絵画層の透明性への影響については、20 世紀初頭に言及されていたが、絵画層内での金属石鹸の生成については、20 世紀後半になって分析により確認された。油彩画の絵画層は経年とともに絵画層の透明性が増すといわれており、この通説について、3つの自然科学的な説明が知られている。鉛白の金属石鹸化は、この説明のひとつであるが、もっともよく知られている説明は、展色材である乾性油の屈折率が増大することにより、顔料と乾性油の屈折率の差が減少することによるという説である。現在、油性展色材は、

重合反応によるクロスリンク状態から、時間の経過とともに金属イオンを取り込んだ錯イオン状態を形成していると考えられている。また、絵画層の透明性を隠ぺい力として評価する実験（適宜調製した絵具を隠ぺい力試験用のモノクロ用紙に塗布）によれば、乾性油の屈折率の増大による絵画層の透明度への影響は、人間の目で容易に目視できるほどではなく、限定的であると考えられる（第1章付録参照）。一方、その他の絵具の塗布実験により、絵画層内での光の拡散反射の方が、絵画層の見た目への影響が大きく、色材の粒子の大きさや分布状態がきわめて重要であることを示した。

第2章から第5章では、絵画の見た目と絵画層内の化学状態および物理状態の関係性についての調査事例を報告する。19 世紀から 20 世紀初頭に描かれた油彩画4作品を選び、現在の全体に暗い印象の見た目の要因を明らかにすることを目的とした。この調査は、現状の暗い色調のために部分的に絵画の詳細が見えにくい状態であり、画家が本来意図したものではないとの推察に基づいている。

調査では、絵画層の組成分析、クロスセクション（断面試料）による層構造の観察などをおこない、とくに暗色部分の絵画層の化学状態を分析した。加えて、各種の顕微鏡を利用して粒子の分散状態などの物理状態を観察し、暗色を呈した絵画層についての化学および物理状態を明らかにした。暗色化箇所の絵画層と明色箇所の絵画層を比較し、光の反射要因である粒子の分布状態や塗り重ねの状態などに認められる差異を示し、暗色化が目視される条件を提案した。

第2章では、19 世紀末に描かれたジョン・エヴァレット・ミレイ（1829–1896 年）作「スピーク！スピーク！（Speak! Speak!）」の調査について報告する。ここでは、金属石鹸化による見た目の変化事例として、亜鉛華の金属石鹸化を主要因とする暗色化が認められた。これは、比較的明るいベージュ色の絵画層が、元の状態よりも透明性を増したためと推察した。つまり、明色の絵具が暗茶褐色の絵画層の上層に塗られたために、部分的な暗色化がみられるものと考えられる。この部分の絵画層を分析したところ、実際に亜鉛石鹸の存在が確認された。同じ絵画層中に、酸化亜鉛の粒子が確認できたことから、亜鉛石鹸は酸化亜鉛から生成したものと考えられた。酸化亜鉛の金属石鹸化にともない、粒子の形状は失われる。顔料粒子は光を反射するので、粒子形状の消失は、光の反射要因がなくなり反射光量の減少につながる。反射されない光は、そのまま下層に達し、下層の絵画層が明色の場合、ここで十分に光は反射する。しかしながら、下層の絵画層が光を吸収する場合、反射する光量は限られる。したがって、絵画層の透明性が増した場合、その層からの光の反射量が減少することに加えて、下層からの反射光量の影響も受けやすくなるため、下層の絵画層が暗色であれば、最終的に表面に達する光量がより減少することとなる。

第3章では、第2章と同様に、絵画層内での金属石鹸の生成が見た目の変化をもたらした事例を報告する。調査作品は、ルーク・フィルズ（1843–1927 年）作「医師（The Doctor）」である。この作品では、画面の上部に描かれた人物像が消えかかっているように見えることに着目した。

実際に、ここでも絵画層内には亜鉛石鹸の存在が認められた。興味深いことに、亜鉛石鹸は見た目上に変化のない絵画層内にも生成していることが明らかとなった。クロスセクション観察によれば、いずれの場合も、複数の絵画層のうち、表面に近い絵画層内に亜鉛石鹸が生成していた。消えかけている人物像は、暗色の背景色を塗ったのちに描かれていることから、人物像を描いた絵画層の下層には暗茶色の絵画層がある。他方、見た目上の変化が認められない箇所では、下層に白色の絵画層が存在していることが明らかとなった。

以上、2つの作品の調査結果から、金属石鹸の生成による絵画表面の明度の減少、すなわち暗色化は、下層の絵画層が暗色の絵画層である場合に認められているといえる。この結果は、見た目の変化が局所的にみられる理由を示している。さらに、この結果に基づき、金属石鹸を含む絵画層を実験的に作製し、見た目に及ぼす影響の可視化を試みた。実験では、絵画層の透明度は隠ぺい力として評価することとし、白色顔料（酸化亜鉛を使用）の一部を、金属元素量で相当量の金属石鹸に置き換えた絵画層を作製した。白色絵画層の隠ぺい力は、白色顔料の反射率に依存するため、予測通り金属石鹸量の増加にともない隠ぺい力は著しく低下した。絵画層を透過した光は、下層の絵画層において反射あるいは吸収される。仮に、下層からの光の反射が十分な場合には、上層の絵画層において金属石鹸が生成したとしても、見た目上の影響はほとんど確認できない。他方、下層に暗色の層がある場合、透過光は下層に吸収され、見た目の暗色化を引き起こす。以上の実験により、絵画層の重ね塗りの状態、つまり、金属石鹸を生じている絵画層が表面近くにあるか、あるいは、下層に暗色、明色どちらの絵画層があるかといったことにより、見た目の変化への影響が異なることが示された。

次いで、20 世紀初頭に描かれたフロリス・ヘンドリック・フェステル（1861–1927 年）による自画像の調査結果を報告する（第4章）。本作品では、とくに顔の描画部分において色のコントラストが強く、全体の色調に過度の斑があるような印象を与えている。カラー写真およびモノクロ写真、これまでに開催された展覧会カタログに掲載された写真を比較したところ、コントラストが経年により変化していると推察された。フェステルの額を描いた部分において、コントラストが強調されており、この部分から採取した絵画試料中に鉛と亜鉛を含む金属石鹸の存在が示唆された。このことから、絵画層からの拡散光量が減少しているものと考えられる。同じ絵画層内では、赤色レーキの退色も確認され、赤色の反射光の減少も示された。

同一の絵画層内での白色顔料の金属石鹸化と赤色レーキの退色がもたらす見た目への影響について、エオシンレーキを用いた実験をおこなった。赤色のエオシン絵具に白色顔料を加えると、白色顔料の多重拡散により隠ぺい力が増大すると同時に、エオシンの赤色も強調されることが示された。よって、白色顔料の金属石鹸化と赤色レーキの退色という2つの化学変化により、フェステルが意図した色調のバランスは大きく変わってしまっているものと推察される。

テオドール・ルソー（1812–1867 年）作「La Descente des Vaches」（制作年 1834–35）は、全体にきわめて暗い画面を呈しており、また、亀裂などの絵画表面の損傷も著しい（第5章）。ルソーの伝記によれば、作者がビチュメン（瀝青：天然アスファルト）を使用したため、あるいは用いた展色材の性質のために、暗色化や亀裂が生じたと記されている。しかしながら、絵画層の詳細な化学分析をおこなった先行研究の結果からは、ビチュメンの使用は確認されていない。展色材の経年劣化による黄色化なども多少暗色化に寄与している可能性はあるものの、描画のほとんどが観察できないほどの暗色化を引き起こしている主原因とは考えにくい。さらに同時期に描かれたカラースケッチやエボーシュ（一種の習作）では、現在でも十分な色情報がみてとれる。絵画層の化学分析および顕微鏡による観察の結果、顔料であるエメラルドグリーンが分解しており、成分元素のヒ素は顔料粒子から遊離し、銅はカルボン酸銅（銅石鹸）として存在することが明らかとなった。エメラルドグリーンが分解したために、顔料粒子が消失したことで拡散反射が減少、さらに、緑色が失われ暗茶色の絵画層が残っている状態と考えられる。

本作品の絵画層には、きわめて微細な粒子が含まれており、メディウム（マトリックス）部分が多い。加えて、明色の絵画層や絵画層中の白色顔料の含有量がきわめて少ないことも特徴的である。多くの絵画層内において鉛白粒子は確認できなかったものの、鉛元素が検出されていることを考慮すると、もともとは現在よりも多くの鉛白顔料粒子が存在していた可能性が高い。絵画層の顕微鏡観察でも、暗色の絵画層には光を反射するような粒子はほとんど存在せず、光が吸収されてしまう状態が確認できる。残された記録から、ルソーが彩度の高い、奥行きのある緑色の表現を求めていたことが知られている。このことから、絵画層を不透明にする白色顔料の使用を最少量に抑えていたと考えられる。乾性油や樹脂の変色、ワニスの黄色化、インディアン・イエローの退色などに、エメラルドグリーンの分解や、おそらく鉛白の金属石鹸化といった現象が同時に起こり、絵画層全体の光の反射量が著しく低下したことが、本作品の画面が暗色化している原因と考えられる。

以上、4作品の調査分析を通して、絵画層からの光の反射が絵画の見た目においてきわめて重要な要素であることを示した。絵画層の透明度は、層内における光の拡散反射ならびに吸収に大きく依存している。絵画層内で生じる化学変化により、作者が意図した絵画表現を作り出している微妙な色調のバランスや調和が崩れると、絵画全体の見た目を変化させうるといえよう。

Acknowledgements: 謝辞

I would like to express my deepest appreciation to my supervisors Prof. dr. Jaap J. Boon and Dr. Klaas Jan van den Berg. There are so many things I would like to thank you both for, but probably firstly for your long time support for the completion of this volume. I am very happy that this day has finally come thanks to your guidance.

When I started this program I almost had no knowledge about oil painting. Thank you Jaap, what you taught me is not only chemistry of oil painting but also how I would find research issues and approach them scientifically. I have admired your intelligence and am fortunate to have had the opportunity to carry out research under your mentorship.

Thank you Klaas Jan, you have been very kind and supportive. It would not have been possible for me to finish this work without your support. I am also grateful to you for your caring guidance, your help in arranging all aspects relating to my research, introducing me to people, and so on.

Next, my special thanks goes to researchers at ICN (now RCE) during my stay; Frank Ligterink, Muriel Geldof, Ineke Joosten, Suzan de Groot, IJsbrand Hummelen, Henk van Keulen, Maarten van Bommel, Hayo de Boer, Birgit Reißland, Karin Groen, Thea van Oosten, Luc Megens, Agnes Brokerhof, Han Neevel, Ad Stijnman, Matthijs de Keijzer, Bart Ankersmit, Peter Hallebeek, Bill Wei, Alberto de Tagle, Leslie Carlyle, Maartje Witlox, Gisela van der Doelen, Eva Goetz, Kathrin Pilz. It was a great time working with all of you. Frank, thank you very much for teaching me optical theories and answering all my questions. Thanks to Muriel, Ineke, Gisela, Eva and Suzan I have learnt a lot about how to examine oil paint samples. IJsbrand, for me it was first time working with an art historian, so I was probably very reserved. Nevertheless you have cared about me and gave a lot of information. I am grateful to you for broadening my perspective. Thank you Leslie, Maartje, and Kathrin showing and teaching me how I was supposed to handle oil paints. It was also an amazing experience to see your work backed with your skills and knowledge. Henk and Maarten, thank you for performing the analysis. Birgit, Han, Luk, Hayo, Thea, Agnes, Ad, Matthijs, Bart, Peter, Bill, and Alberto, it was fun to talk with you. Thanks to all of you my stay at ICN was very pleasant.

I also would like to thank Nel Oversteegen, Kirsten van Meer for administrative work, and Julian van den Berg, Roland, Huguenin, and Cor Mulders for supporting the bibliographic search.

There were times that I worked at AMOLF. It was great time especially for having discussions with people in the painting research group; Katrien Keune, Ester Ferreira, Frank Hoogland, Annelies van Loon, and Beatrice Marino. Thank you all for helping with my analytical work. I am very grateful to Jerre van der Horst for his support with analysis and assistance.

I am grateful to Dr. Joyce H. Townsend (Tate, UK), René Boitelle (Van Gogh Museum, Amsterdam) and, Rob Wolthoorn (Museum De Lakenhal, Leiden) for access to the paintings, provision of samples and related information. Thank you very much Joyce for giving useful advice through the program, guiding me how to examine painting samples when we visited Tate, and extensive writing instructions.

I also would like to thank Luuk van der Loeff (Kröller-Müller Museum, Otterlo) and Aviva Burnstock (Courtauld Institute of Art, UK) for their helpful discussions.

I gratefully acknowledge financial support from NWO, and permission for use of the painting images from Tate, De Lakenhal, and Van Gogh Museum Enterprises B. V. for The Mesdag Collection.

I would like to thank my friend Sunita Changoe who was kindly shared her flat throughout my stay in the Netherlands. At the beginning I was nervous because it was first time for me being abroad without any relatives or even friends. She treated me like I was a family member, taking me to her parent's house, introducing her friends and colleagues and spending a lot of time with me. Thank you Sunita, I enjoyed being with you a lot and my private time was very fruitful thanks to you.

I am grateful to Yoko Taniguchi who urged me to study abroad and helped me to undertake this opportunity. Thank you Yoko, it took me a really long time but finally I reached this day.

I would like to thank all my friends who encouraged me to continue writing up when I had a hard time finding the spirit to continue. It was not only one time but many times that I was close to giving up. At those times, I was asked how my writing was going on and you always said 'don't give up'. Although we all have different specialties, talking with you was always fun and gave me energy to start writing again.

I finally would like to thank my parents and younger sister for supporting my studying in the Netherlands. 最後に、長らくご支援くださった両親と妹に心より感謝いたします。

2014年 12月 吉日

島津 美子

Yoshiko Shimadzu

About the Author

Yoshiko Shimazu was born in 1976 in Yamanashi, Japan. In 1999 she obtained her BSc. in chemistry at Kanazawa University. She studied conservation science in the graduate school of Tokyo GEIJUTSU DAIGAKU (Tokyo University of the Arts). From 2001 to 2002, she worked as an assistant research scientist, in the Department of Restoration Techniques, National Research Institute for Cultural Properties, Tokyo. After a one-year stay in Malta studying conservation of stone monuments and performing research on color alteration of ni-nuri (a traditional coating method in Japanese wooden buildings with red lead and animal glue paint).

She worked at ICN (now RCE) on the NWO supported MM19 project of a framework of the De Mayerne program from 2004-2008. The results are mostly presented in this PhD thesis.

After her stay in the Netherlands, she worked in Japan Center for International Cooperation in Conservation, National Research Institute for Cultural Properties, Tokyo (-2013). The center was conducting several conservation projects for wall painting conservation in the Central Eurasia region. She was involved in projects in Tajikistan and India.

Currently she works for the National Museum of Japanese History and is conducting a collaborative research project for understanding modern paint materials in Japan.